

KANDAGATLA, SUNEEL KUMAR, Ph.D. Effects of Açai Berry (*Euterpe oleracea*) Extracts on Human Antioxidant Systems and Drug Metabolism. (2015)
Directed by Dr. Gregory M. Raner. 187 pp.

The source and sink of reactive oxygen species are diverse and so are the control mechanisms to counteract them. Sources may be exogenous or endogenous from normal metabolic pathways. Similarly, the sink could be a simple radical scavenging event by small molecule antioxidants and antioxidant enzymes or complex events involving cellular signaling processes. The effects of reactive oxygen species may precipitate cellular dysfunction from its toxicity, protect from invading microorganisms or perform essential functions through regulation of cell signaling pathways. Excessive Reactive oxygen species leads to oxidative stress which mediates cellular damage and is implicated in several pathological conditions. The current research addresses biological systems that may effect redox balance in humans.

One goal of the current research was to establish structure activity relationship for substrate binding to several human drug metabolizing enzymes implicated in reactive oxygen species generation, namely CYP2A6 and CYP2E1. The substrate dynamics of these two enzymes were studied by probing the active site with a series of small chain saturated and 2,3-unsaturated aldehydes using human liver microsomes. The study demonstrated that the aldehydes inhibited both the enzymes in competitive manner with unsaturated aldehydes being more potent than their saturated counterparts. The potential for π -stacking interactions between the phenylalanine rich active site of these enzymes and the double bond at 2-position in unsaturated aldehydes conferred high affinity for

these aldehydes. It also confirmed an earlier findings that the active site of CYP2A6 is rigid where as CYP2E1 is flexible due to the presence of extended π -system allowing the expansion of its active site.

Another goal was to examine the possible interactions between human cytochrome P450 enzymes of pharmacological and toxicological importance with a natural product called açai. Açai (*Euterpe oleracea*) is a Brazilian palm tree that has emerged from traditional medicinal plant to a recent super-fruit status. The assumption that it is safe to consume açai currently lacks evidence from its interactions with drug metabolizing cytochrome P450 enzymes. The interaction between the crude extracts of açai and major cytochrome P450 enzymes involved in drug metabolism and toxicology demonstrated the potential for chloroform extract to inhibit the isoforms CYP1A1, CYP2B6 and CYP2C8. The Michaelis-Menten Kinetics studies indicated mixed mode of inhibition of these enzymes by crude chloroform extract of açai with low K_I and K_I' values for CYP2C8 followed by CYP2B6 and CYP1A1. In addition, the study was extended to identification of inhibitors for toxicologically important CYP2A6 and CYP2E1 using a collaborative bioassay-guided fractionation approach. Although the crude chloroform extract of açai showed considerable inhibition of these enzymes, specific inhibitors were not identified.

Finally, the regulation of a signal transduction pathway namely Nrf2/ARE signaling pathway by açai constituents was also studied as a potential strategy to prevent oxidative damage. The nuclear factor erythroid 2-related factor 2 (Nrf2)-antioxidant

response element (ARE) pathway is a cellular defense to counteract oxidative stress.

Activation of this pathway increases the expression of a battery of antioxidant genes. This was achieved by monitoring the activation of a *cis*-acting DNA sequence referred to as Antioxidant Response Element (ARE) contained in a luciferase-containing promoter vector in cultured HepG2 cells. A high-throughput analysis of fractions generated using bioassay-guided fractionation of açai has resulted in the identification of a class of compounds known as Pheophorbides as the inducers of ARE-luciferase. Dose response analysis using pure compounds demonstrated significant induction of ARE-luciferase at concentrations as low as 8.2 μM and 16.9 μM for Pheophorbide a methyl ester and Pheophorbide a, respectively.

EFFECTS OF AÇAÍ BERRY (*EUTERPE OLERACEA*) EXTRACTS ON HUMAN
ANTIOXIDANT SYSTEMS AND DRUG METABOLISM

by

Suneel Kumar Kandagatla

A Dissertation Submitted to
the Faculty of The Graduate School at
The University of North Carolina at Greensboro
in Partial Fulfillment
of the Requirements for the Degree
Doctor of Philosophy

Greensboro
2015

Approved by

Committee Chair

To my Mother, Father, Wife, Family and Friends,
Without your love, support and encouragement this would not have been possible.
Thank you all.

APPROVAL PAGE

This dissertation written by Suneel Kumar Kandagatla has been approved by the following committee of the Faculty of Graduate School at The University of North Carolina at Greensboro

Committee Chair _____
Gregory M. Raner

Committee Members _____
Nicholas Oberlies

Will Taylor

Vincent Henrich

George Loo

Zhenquan Jia

Date of Acceptance by Committee

Date of Final Oral Examination

ACKNOWLEDGEMENTS

I would like to express my deepest gratitude to my mentor, Dr Gregory M. Raner for his guidance, support and for providing me with excellent atmosphere for conducting my research at UNCG. I would like to thank my committee members Dr Nicholas Oberlies, Dr Will Taylor, Dr Vincent Henrich, Dr George Loo and Dr Zhenquan Jia for their valuable suggestions and assistance through my graduate work. I would also like to thank all the Professors who have helped me professionally and also as a student at UNCG. I would like to thank all my lab mates and my fellow graduate students for their support.

I would have never been able to come this far, without the support of my family and friends. I would like to thank my parents Bhaskar and Sharada for being supportive in every aspect of my life. I would like to thank my brother Rajesh, sister Sunanda and brother-in-law Satyaprakash for their love and encouragement. I would like to thank my nieces Anshika and Mahanvi for their love. I would also like to thank my friends Sridhar, Prashanth, Anil and Asritha for being there when I needed them and for being great friends. Finally, I would like to thank my wife Bhavana for her love, understanding, patience, support and encouragement, and most of all for having faith in me.

TABLE OF CONTENTS

	Page
LIST OF TABLES	ix
LIST OF FIGURES	x
LIST OF SCHEMES.....	xvi
CHAPTER	
I. INTRODUCTION TO ANTIOXIDANT RESEARCH, HUMAN ANTIOXIDANT SYSTEMS AND DRUG METABOLISM.....	1
1.1. Introduction.....	1
1.1.1. Oxygen Evolution and Emergence of Life.....	1
1.1.2. Reactive Oxygen Species	2
1.1.3. Sources of Reactive Oxygen Species	3
1.1.4. Functions of Reactive Oxygen Species	5
1.1.5. Redox Homeostasis	5
1.1.6. Redox Regulation	6
1.1.7. Dysregulation of Redox Homeostasis and Oxidative Stress	8
1.1.8. Oxidative Stress Paradigm and its Relevance to Health and Disease.....	9
1.1.9. Cellular Signaling and Adaptation	12
1.1.10. Oxidative Stress and Toxicology	13
1.1.11. Natural Products as Therapeutic Agents	13
1.1.12. The Açai Berry	15
1.1.13. Target-based Identification of Bioactive Constituents of Açai	17
1.2. Hypothesis and Aims	18
II. INHIBITION OF HUMAN CYTOCHROME P450 2E1 AND 2A6 BY ALDEHYDES: STRUCTURE AND ACTIVITY RELATIONSHIPS.....	20
2.1. Introduction.....	20
2.2. Materials and Methods.....	22
2.2.1. Chemicals	22
2.2.2. Enzymatic Assays: P450 _{2E1}	22
2.2.3. Inhibition of P450 _{2E1}	23
2.2.4. Enzymatic Assays: P450 _{2A6}	23

2.2.5. Inhibition of P450 _{2A6}	24
2.2.6. Reversibility Studies.....	25
2.2.7. Aldehyde Oxidation by Human P450 Enzymes.....	25
2.2.8. Analysis of Kinetic Data	26
2.2.9. Graphical Images of P450 Active Sites.....	26
2.3. Results.....	27
2.3.1. Inhibition of P450 _{2E1} by Alkanals and Alkenals	27
2.3.2. Effects of Branching on Inhibition of 2E1	29
2.3.3. Effects of Aldehyde Function.....	32
2.3.4. Inhibition of P450 _{2A6} by Alkanals and Alkenals.....	33
2.3.5. Other Structural Determinants for P450 _{2A6} Inhibition by Aldehydes	35
2.3.6. Oxidation of Aldehydes by Human S9 Fractions and Expressed Cytochrome P450 _{2E1} and P450 _{2A6}	35
2.4. Discussion	36
2.5. Conclusions.....	42

III. IDENTIFICATION OF INHIBITORS OF HUMAN CYTOCHROME P450 ENZYMES INVOLVED IN DRUG METABOLISM AND TOXICOLOGY BY AÇAÍ EXTRACTS.....43

3.1. Introduction.....	43
3.1.1. Cytochrome P450 Catalytic Cycle	46
3.1.2. Cytochrome P450 Mediated Reactive Oxygen Species Generation	47
3.1.3. Cytochrome P450 2A6	51
3.1.4. Cytochrome P450 2E1.....	52
3.1.5. The Açai Berry	54
3.2. Materials and Methods.....	57
3.2.1. Chemicals and Reagents.....	57
3.2.2. Human Liver Microsomes and cDNA Expressed ⁰ Supersomes.....	58
3.2.3. Açai Berry Extracts	58
3.2.4. Bioassay-guided Fractionation of Açai	59
3.2.5. Preparation of Crude Açai Berry Extracts.....	60
3.2.6. Sample Preparation of Açai for CYP Inhibition	62
3.2.7. Cytochrome P450 Assays.....	62
3.2.8. Michaelis-Menten Model of Enzyme Kinetics	63
3.2.9. Screening of Açai Extracts	64
3.2.10. Determination of Inhibition Constant (K _I).....	65
3.2.11. Isoform Specific Assay Conditions and Modes of Analyses	66
3.2.12. Data Analysis	71

3.3. Results.....	71
3.3.1. <i>In vitro</i> Inhibition of cDNA Expressed Cytochrome P450 Enzymes	72
3.3.2. CYP1A1 Assay.....	73
3.3.3. CYP1A2 Assay.....	74
3.3.4. CYP2A6 Assay.....	76
3.3.5. CYP2B6 Assay.....	78
3.3.6. CYP2C8 Assay.....	80
3.3.7. CYP2C9 Assay.....	82
3.3.8. CYP2D6 Assay.....	84
3.3.9. CYP2E1 Assay	85
3.3.10. CYP3A4 Assay.....	87
3.3.11. Screening of Crude Açai Berry Extracts for <i>In vitro</i> 0 Inhibition of cDNA Expressed Cytochrome P450 Enzymes	89
3.3.12. <i>In vitro</i> Inhibition of CYP2A6 and CYP2E1 using Human Liver Microsomes.....	94
3.3.13. Bioassay-guided Fractionation of Açai Berry Extracts for CYP2A6 Inhibition <i>In vitro</i> using Human Liver Microsomes	96
3.3.14. Summary of CYP2A6 Inhibition.....	116
3.3.15. Bioassay-guided Fractionation of Açai Berry Extracts for CYP2E1 Inhibition <i>In vitro</i> using Human Liver Microsomes	117
3.3.16. Summary of CYP2E1 Inhibition	130
3.4. Discussion.....	131

IV. INDUCTION OF ARE-DEPENDENT GENE EXPRESSION IN CULTURED HEPG2 CELLS BY CONSTITUENTS OF AÇAÍ.....135

4.1. Introduction.....	135
4.1.1. The Nrf2/ARE Signaling Pathway	136
4.1.2. Açai Berries in Relation to Nrf2 Antioxidant Pathway.....	139
4.2. Materials and Methods.....	141
4.2.1. Chemicals and Reagents.....	141
4.2.2. Cell Culture	141
4.2.3. Oligonucleotides, Vectors and Enzymes.....	142
4.2.4. Construction of ARE Reporter Vectors.....	142
4.2.5. Bioassay-guided Fractionation of Açai	144
4.2.6. Sample Preparation of Açai.....	144
4.2.7. Induction of ARE-luciferase	145
4.2.8. Transfection.....	146

4.2.9. Treatment.....	146
4.2.10. Measurement of ARE-luciferase Activity	147
4.3. Results	149
4.4. Discussion.....	177
REFERENCES	180

LIST OF TABLES

	Page
Table 2.1 Experimentally Determined Inhibition Constants (K_I) for the Inhibition of Human Cytochrome P4502A6 by Straight Chain Saturated and Unsaturated Aldehydes Ranging in Size from 5 to 12 Carbons.	34
Table 3.1 Activity Assay Parameters for CYP isoforms	68
Table 3.2 Chromatographic Separation Parameters of CYP Activity Assays	69
Table 3.3 Detection Parameters of CYP Activity Assays.....	70
Table 3.4 Inhibition constants, K_I and K_I' for inhibition of CYP1A1, CYP2B6 and CYP2C8 by crude chloroform extract of açai at 10 μ g/ml concentration.....	93
Table 4.1 Chemical Structure of Pheophorbide-a Derivatives	174

LIST OF FIGURES

	Page
Figure 1.1 Oxidative Phosphorylation	2
Figure 1.2 Generation of Reactive Oxygen Species	4
Figure 1.3 Redox Regulation of Reactive Oxygen Species	7
Figure 1.4 Role of Reactive Oxygen Species in Regulation and Dysregulation of Cellular Homeostasis	9
Figure 1.5 Açai Berry Fruit.....	16
Figure 2.1 Effects of Saturated and 2-Unsaturated Aldehydes on P450 _{2E1} Activity	28
Figure 2.2 Structure and Measured Inhibition Constants for Branched Saturated and Unsaturated Aldehydes, Citral, Citronellal, and the Corresponding Linear, Saturated and Unsaturated 10 Carbon Aldehydes, Decanal and Trans-2-Decenal.....	31
Figure 2.3 Key Residues in the Active Site Structure of Human Cytochrome P450 2A6 with the Substrate Coumarin Bound.....	32
Figure 2.4 Active Site Structure of P450 2E1 Showing the Position of Key Phe Residues in the Presence of the Substrates (A) Pilocarpine (PDB: 3T3Z), (B) Indazole (PDB: 3E6I) and (C) Imidazolyl- -Dodecanoic Acid (PDB: 3LC4).....	41
Figure 3.1 Schematic of Cytochrome P450 Mediated Xenobiotic Metabolism	44
Figure 3.2 Distribution of the Metabolism of the Xenobiotics by Various Metabolizing Enzymes.....	45
Figure 3.3 Distribution of the Metabolism of the Xenobiotics across Various CYP Isoforms and Factors Affecting their Expression.....	46
Figure 3.4 Schematic Representation of Cytochrome P450 Catalytic Cycle	47
Figure 3.5 Schematic Representation of P450 Mediated Production of Reactive Oxygen Species.....	48

Figure 3.6 Contributions towards the Generation of Reactive Species by Various Human Enzymes (A).....	50
Figure 3.7 Schematic Representation of Bioassay-Guided Fractionation Approach	59
Figure 3.8 A Typical Michaelis-Menten Plot illustrating the Relationship between the Substrate Concentration [S] and the Reaction Rate V and Predicted K_m and V_{max}	64
Figure 3.9 A Typical Michaelis-Menten Kinetics Plot illustrating the Concentrations suitable for Inhibition Studies.....	65
Figure 3.10 CYP1A1 Mediated Catalysis of 7-Ethoxycoumarin to 7-Hydroxycoumarin.....	73
Figure 3.11 Michaelis-Menten Kinetics Plot for O-Demethylation of 7-Ethoxycoumarin by CYP1A1 Supersomes.....	74
Figure 3.12 CYP1A2 Mediated Hydroxylation of Naphthalene to 1-Naphthol	75
Figure 3.13 Michaelis-Menten Kinetics Plot for Hydroxylation of Naphthalene to 1-Naphthol by CYP1A2 Supersomes	76
Figure 3.14 CYP2A6 Mediated Hydroxylation of Coumarin to 7-Hydroxycoumarin.....	77
Figure 3.15 Michaelis-Menten Kinetics Plot for Hydroxylation of Coumarin to 7-Hydroxycoumarin by CYP2A6 Supersomes.....	78
Figure 3.16 CYP2B6 Mediated Catalysis of Bupropion to (2S,3S)-Hydroxybupropion	79
Figure 3.17 Michaelis-Menten Kinetics Plot for Hydroxylation of Bupropion to (2S,3S)-Hydroxybupropion by CYP2B6 Supersomes.....	80
Figure 3.18 CYP2C8 Mediated N-Deethylation of Amodiaquine to N-Desethylamodiaquine	81
Figure 3.19 Michaelis-Menten Kinetics Plot for N-Deethylation of Amodiaquine to N-Desethylamodiaquine by CYP2C8 Supersomes.....	82
Figure 3.20 CYP2C9 Mediated Catalysis of Diclofenac to 4'-Hydroxydiclofenac	83

Figure 3.21 Michaelis-Menten Kinetics Plot for Hydroxylation of Diclofenac to 4'-Hydroxydiclofenac by CYP2C9 Supersomes.....	83
Figure 3.22 CYP2D6 Mediated O-Demethylation of Dextromethorphan to Dextrorphan	84
Figure 3.23 Michaelis-Menten Kinetics Plot for O-Demethylation of Dextromethorphan to Dextrorphan by CYP2D6 Supersomes	85
Figure 3.24 CYP2E1 Mediated Hydroxylation of <i>p</i> -Nitrophenol to <i>p</i> -Nitrocatechol	86
Figure 3.25 Michaelis-Menten Kinetics Plot for Hydroxylation of <i>p</i> -Nitrophenol to <i>p</i> -Nitrocatechol by CYP2E1 Supersomes.....	87
Figure 3.26 CYP3A4 Mediated Oxidation of Nifedipine to Dehydronifedipine.....	88
Figure 3.27 Michaelis-Menten Kinetics Plot for Conversion of Nifedipine to Dehydronifedipine by CYP3A4 Supersomes	89
Figure 3.28 Inhibition of Various cDNA Expressed Cytochrome P450 Enzymes by Açai Crude Extracts.....	91
Figure 3.29 Dose Response Relationship for the Inhibition of Various cDNA Expressed Cytochrome P450 Enzymes by Açai Crude Chloroform Extract.....	92
Figure 3.30 Michaelis-Menten Kinetics Plot for Hydroxylation of Coumarin to 7-Hydroxycoumarin by CYP2A6 Enzymes in Human Liver S9 Fraction	97
Figure 3.31 Inhibition of Human CYP2A6 by Açai Crude Extracts	99
Figure 3.32 Inhibition of Human CYP2A6 by Açai-34-Series.....	101
Figure 3.33 Inhibition of Human CYP2A6 by Açai-38-Series.....	103
Figure 3.34 Inhibition of Human CYP2A6 by Açai-61-Series.....	105
Figure 3.35 Inhibition of Human CYP2A6 by Açai-62-Series.....	106
Figure 3.36 Inhibition of Human CYP2A6 by Açai-63-Series.....	107
Figure 3.37 Inhibition of Human CYP2A6 by Açai-64-Series.....	107

Figure 3.38 Inhibition of Human CYP2A6 by Açai-78-Series.....	110
Figure 3.39 Inhibition of Human CYP2A6 by Açai-82-Series.....	111
Figure 3.40 Inhibition of Human CYP2A6 by Açai-94-Series.....	112
Figure 3.41 Inhibition of Human CYP2A6 by Açai-76-Series.....	113
Figure 3.42 Inhibition of Human CYP2A6 by Açai-97-Series.....	115
Figure 3.43 Inhibition of Human CYP2A6 by Açai-98-Series.....	116
Figure 3.44 Michaelis-Menten Kinetics Plot for Hydroxylation of <i>p</i> -Nitrophenol to <i>p</i> -Nitrocatechol by CYP2E1 Enzymes in Human Liver S9 Fractions.....	118
Figure 3.45 Inhibition of Human CYP2E1 by Açai Crude Extracts.....	119
Figure 3.46 Inhibition of Human CYP2E1 by Açai-34-Series	120
Figure 3.47 Inhibition of Human CYP2E1 by Açai-38-Series	121
Figure 3.48 Inhibition of Human CYP2E1 by Açai-61-Series	122
Figure 3.49 Inhibition of Human CYP2E1 by Açai-62-Series	123
Figure 3.50 Inhibition of Human CYP2E1 by Açai-63-Series	124
Figure 3.51 Inhibition of Human CYP2E1 by Açai-64-Series	125
Figure 3.52 Inhibition of Human CYP2E1 by Açai-78-Series	126
Figure 3.53 Inhibition of Human CYP2E1 by Açai-82-Series	127
Figure 3.54 Inhibition of Human CYP2E1 by Açai-94-Series	128
Figure 3.55 Inhibition of Human CYP2E1 by Açai-76-Series	129
Figure 3.56 Inhibition of Human CYP2E1 by Açai-97-Series	130
Figure 4.1 Nrf2/ARE Signaling Pathway	138

Figure 4.2 Schematic Illustration of Promoter Region of pGL3 Plasmid Vector, Wild-Type and Mutant ARE Constructs.....	143
Figure 4.3 Construction of ARE-luciferase containing Plasmid Vectors.....	144
Figure 4.4 Schematic Illustration of ARE-luciferase Induction by Açai Berry in Cultured HepG2 Cells.....	145
Figure 4.5 Bioluminescence Reactions Catalyzed by Firefly and Renilla Luciferases	148
Figure 4.6 Induction of ARE-driven Luciferase Expression pGL3, pGL3- <i>wt</i> ARE and pGL3- <i>m</i> ARE containing Plasmids in Cultured HepG2 Cells by <i>t</i> -Butylhydroquinone	151
Figure 4.7 Induction of ARE-driven Luciferase Expression in Cultured HepG2 Cells by Crude Açai Berry Extracts.....	152
Figure 4.8 Induction of ARE-driven Luciferase Expression in Cultured HepG2 Cells by Crude Chloroform Extract Of Açai	153
Figure 4.9 Induction of ARE-driven Luciferase Expression in Cultured HepG2 Cells by Açai-34-Series	155
Figure 4.10 Induction of ARE-driven Luciferase Expression in Cultured HepG2 Cells by Açai-38-Series	156
Figure 4.11 Induction of ARE-driven Luciferase Expression in Cultured HepG2 Cells by Açai-86-Series	158
Figure 4.12 Induction of ARE-driven Luciferase Expression in Cultured HepG2 Cells by Açai-61-Series	160
Figure 4.13 Induction of ARE-driven Luciferase Expression in Cultured HepG2 Cells by Açai-62-Series	161
Figure 4.14 Induction of ARE-driven Luciferase Expression in Cultured HepG2 Cells by Açai-63-Series	162
Figure 4.15 Induction of ARE-driven Luciferase Expression in Cultured HepG2 Cells by Açai-64-Series	163

Figure 4.16 Induction of ARE-driven Luciferase Expression in Cultured HepG2 Cells by Açai-94-Series	165
Figure 4.17 Induction of ARE-driven Luciferase Expression in Cultured HepG2 Cells by Açai-76-Series	166
Figure 4.18 Induction of ARE-driven Luciferase Expression in Cultured HepG2 Cells by Açai-98-Series	168
Figure 4.19 Induction of ARE-driven Luciferase Expression in Cultured HepG2 Cells by Açai-92-Series	169
Figure 4.20 Induction of ARE-driven Luciferase Expression in Cultured HepG2 Cells by Açai-78-Series	171
Figure 4.21 Induction of ARE-driven Luciferase Expression in Cultured HepG2 Cells by Açai-97-Series	173
Figure 4.22 Chemical Structure of Pheophorbide-A Derivatives	174
Figure 4.23 Induction of ARE-driven Luciferase Expression in Cultured HepG2 Cells by Pheophorbide-a Methyl Ester and Pheophorbide-a	175
Figure 4.24 Induction of ARE-driven Luciferase Expression in Cultured HepG2 Cells by Açai-82-Series	176

LIST OF SCHEMES

	Page
Scheme 1. Bioassay-guided Fractionation of Freeze-dried Açai Berry Powder.	61
Scheme 2. Initial Crude Extracts of Açai Berry	98
Scheme 3. Fractionation of Crude Chloroform Extract of Açai (Açai-31-2)	100
Scheme 4. Fractionation of Açai-34-8	102
Scheme 5. Fractionation of Açai-38-1, Açai-38-2, Açai-38-3 and Açai-38-4.....	104
Scheme 6. Fractionation of Açai-62-2, Açai-62-3, Açai-63-4 and Açai-64-3.....	109
Scheme 7. Fractionation of Açai-78-H, Açai-76-A and Açai-76-B	114
Scheme 8. Bioassay-guided Fractionation of Açai-31-2 and Açai-34-8	154
Scheme 9. Fractionation of Pooled Extracts Açai-38-6, Açai-38-7 and Açai-38-8.....	157
Scheme 10. Fractionation of Açai-38-1, Açai-38-2, Açai-38-3 and Açai-38-4.....	159
Scheme 11. Fractionation of Açai-63-4	164
Scheme 12. Fractionation of Açai-64-3	166
Scheme 13. Fractionation of Açai-76-A and Açai-76-B	167
Scheme 14. Fractionation of Açai-62-2	170
Scheme 15. Fractionation of Açai-78-H	172
Scheme 16. Fractionation of Açai-62-3	176

CHAPTER I
INTRODUCTION TO ANTIOXIDANT RESEARCH, HUMAN ANTIOXIDANT
SYSTEMS AND DRUG METABOLISM

1.1. Introduction

1.1.1. Oxygen Evolution and Emergence of Life

Life on Earth can be distinguished into three distinct landmarks in time based on the emergence of various life forms^{1, 2}. Early life began with the evolution of organisms such as bacteria capable of performing anoxygenic photosynthesis. These organisms developed systems that use hydrogen and sulfur for energy metabolism. The ensuing years saw the advent of oxygenic photosynthesis utilizing carbon dioxide and water, and the evolution of oxygen as a by-product of the reaction. Light from solar energy served as a driving force of oxygenic photosynthesis and is efficiently transformed into chemical energy of carbon bonds in glucose. The prosperity of oxygenic photosynthesis resulted in the accumulation of atmospheric oxygen. The increase of atmospheric oxygen led to the third landmark, the appearance of aerobic life on Earth, beginning with the appearance of the eukaryotic organisms and subsequent evolution of metazoan organisms. These organisms completed the energy cycle by oxidizing glucose to carbon dioxide and water. Just as the prior establishment of photosynthesis is responsible for the emergence of eukaryotes, the evolution of metazoans is dependent on the development of highly

efficient energy recovery system, oxidative phosphorylation. The recovery of energy contained in the chemical bonds of glucose through oxidative phosphorylation in metazoans is much more efficient than glycolysis.

Oxygen is therefore vital for the survival of all metazoan organisms, as it is utilized as a substrate for the generation of energy through oxidative phosphorylation in the mitochondrial respiratory chain, where it is completely reduced to water. Oxygen serves as a terminal electron acceptor. The electrons transferred from NADH in mitochondrial respiratory chain ultimately react with oxygen through complete reduction to form water. (Figure 1.1).

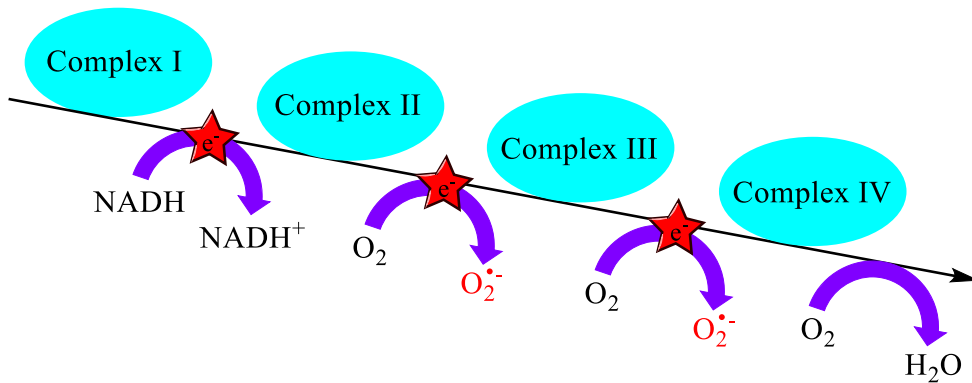


Figure 1.1 Oxidative Phosphorylation

1.1.2. Reactive Oxygen Species

Cells often produce partially reduced oxygen, termed reactive oxygen species (ROS), as products of normal cellular metabolism³. Reactive oxygen species are often referred as free radicals and other non-reactive species derived from oxygen. Precisely, reactive oxygen species can be defined as molecules or molecular fragments containing

one or more unpaired electrons in the outer atomic or molecular orbitals involving oxygen molecules. Reactive oxygen species represent the most important class of radical species generated in biological systems and is characterized by their short half-life, instability and the tendency to react with other molecules in order to achieve stability⁴.

1.1.3. Sources of Reactive Oxygen Species

A vast majority of reactive oxygen species are generated through electron transfer reactions in biological milieu. In an aerobic environment, reactive oxygen species are constantly generated in the power plants of the cell, mitochondria, as oxygen is reduced along the electron transport chain during normal cellular respiration. Addition of an electron to the molecular oxygen in the mitochondrial respiratory chain results in the formation of superoxide anion radical ($O_2^{\bullet-}$) and subsequent addition of another electron in a controlled manner reduces superoxide anion to form water. The process of conversion of molecular oxygen to water is extremely efficient in providing the energy required for the existence of higher organisms. However, a significant portion of electrons escape the mitochondrial respiratory chain and reacts with oxygen prematurely resulting in the production of oxygen free radical, superoxide anion ($O_2^{\bullet-}$)⁵. Superoxide anion is considered as the primary reactive oxygen species because of its propensity to react with the other molecules to generate secondary reactive oxygen species including neutral forms such as hydroxyl ($\bullet OH$), hydroperoxy (HO_2^{\bullet}) and peroxy (RO_2^{\bullet}) radicals. Certain nonradical oxidizing agents such as hydrogen peroxide (H_2O_2) contribute to the generation of reactive oxygen species when the peroxisomes that produced them are

damaged. Therefore, reactive oxygen species are formed as indispensable byproducts of cellular respiration⁶ (Figure 1.2).

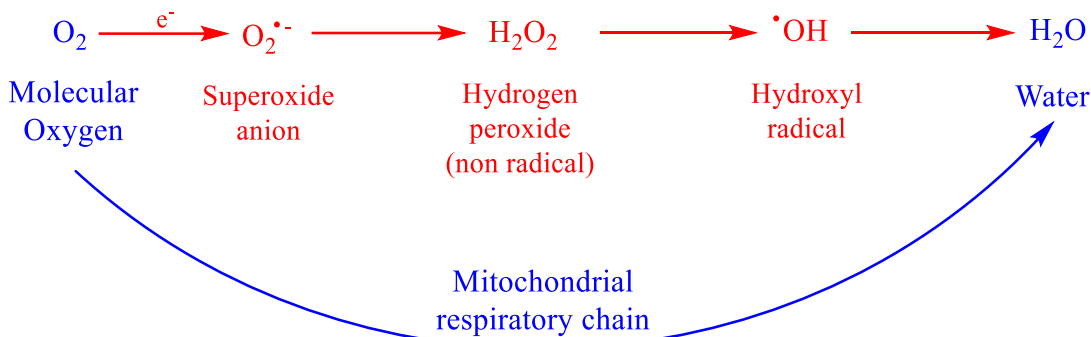


Figure 1.2 Generation of Reactive Oxygen Species

In addition, reactive oxygen species are also generated endogenously as necessary intermediates in a variety of oxidative enzyme catalyzed reactions⁶. Uncoupling of the oxygen reduction from the substrate oxidation during the catalytic cycle of certain monooxygenase reactions results in the leakage of reactive oxygen species. For example, the drug metabolizing cytochrome P450 enzymes (CYPs) and enzymes dedicated for phagocytosis such as NADPH oxidase and myeloperoxidase in phagocytic cells, neutrophils and macrophages can generate reactive oxygen species through this uncoupling pathway^{7, 8}. Virtually all the activities that involve oxygen consumption have the potential to produce reactive oxygen species during enzymatic catalysis.

Other sources of reactive oxygen species include the interaction of ionizing radiation or smoke and other environmental pollutants such as herbicides and pesticides with biological molecules. Certain therapeutic drugs with oxidizing effects also contribute toward the generation of reactive oxygen species.

1.1.4. Functions of Reactive Oxygen Species

Reactive oxygen species are critical for normal cell functions and cell signaling when the concentration is maintained within strict physiological limits^{9, 10}. Reactive oxygen species are indispensable intermediates essential for enzymatic reactions, signal transduction pathways, activation of nuclear transcription factors, gene expression and cellular defense mechanisms by macrophages and neutrophils against various pathogens, in addition to the mitochondrial electron transport chain critical for the cell survival. Historically, reactive oxygen species are regarded as purely harmful intermediates in physiological environment despite their utility in the normal function of the cell. This is largely, but loosely, based on the highly reactive nature of these species and overlooked is the fact that the deleterious effects are only precipitated by the exceedingly high concentrations of reactive species. Importantly, this mechanism is also employed as defense mechanism to fight against invading foreign organisms and even in the situations of clean-up of the damaged cells that appear to be irreparable.

1.1.5. Redox Homeostasis

Reactive oxygen species normally occur in the living cells at relatively low steady-state levels. Redox homeostasis refers to intracellular redox balance that can be defined as a delicate balance between the rates of production and clearance of reactive oxygen species. Intracellular redox homeostasis is being achieved by antioxidant defense systems comprising of low molecular weight antioxidants such as glutathione, in addition to the protein antioxidants such as enzymes that are capable of competing with substrates

susceptible to oxidation and thus delay the oxidation of these substrates. The complex web of antioxidant defense systems checks and maintains the concentration of reactive oxygen species at a steady level. Low molecular weight antioxidants such as ascorbate (vitamin C), α -tocopherol (vitamin E), β -carotene and glutathione are also present in millimolar concentrations within the cells. An array of antioxidant enzymes such as superoxide dismutase (SOD), glutathione peroxidase (GPx) and catalase have specific subcellular localizations and chemical reactivities. Enzymatic antioxidants are also a component of the cellular system involved in phase II drug metabolism; for example, glutathione transferases and sulfotransferases facilitate the removal of foreign chemicals after activation by phase I or cytochrome P450 enzymes.

1.1.6. Redox Regulation

Redox regulation is required to maintain oxidant-antioxidant balance. Cells essentially remain in a stable condition when the rates of production and elimination of reactive oxygen species are in equilibrium. A summary of events contributing to the generation and elimination of reactive species is depicted in figure 1.3. The basis of redox regulation is dependent on a regulatory process called redox signaling in which a controlled increase in the production of reactive oxygen species leads to a temporary imbalance. Redox regulation requires the steady state to be disturbed from either an increase in reactive oxygen species concentrations or a decrease in the activities of one or more antioxidant systems. Such an oxidative event is induced in a regulated manner in higher organisms. Cells have several mechanisms to re-establish the original redox state

after a transient exposure to the reactive oxygen species. A transient increase in reactive oxygen species at relatively small concentrations stimulates antioxidant response to produce an adaptive cellular response sufficient to compensate for the increase and reset original redox balance. At low concentrations, it helps the cell to activate signal transduction pathways capable of instituting an adaptive cellular response. Reactive oxygen species thus help the cell to take a preemptive action against the impending toxicities and ailments by serving itself as a stimulus for the induction of the enzymes responsible for their own elimination.



Figure 1.3 Redox Regulation of Reactive Oxygen Species

One main mechanism for this adaptation response is the induction of redox sensitive signal cascades leading to an increased expression of antioxidant enzymes or an increase in cysteine transport system facilitating an increase in intracellular glutathione¹⁰.¹¹. Many of the enzymes that are a part of this cascade have common characteristics such as coordinated induction by a broad range of chemical agents, including certain reactive oxygen species. Therefore, these enzymes are inducible and are redox regulated. In other

words, reactive oxygen species are capable of inducing the enzymes responsible for their own elimination.

1.1.7. Dysregulation of Redox Homeostasis and Oxidative Stress

A strong and persistent increase in reactive oxygen species production may often fail to elicit antioxidant response sufficient enough to reset redox homeostasis to basal level. It stems again from the highly unstable nature of reactive oxygen species that provides oxygen a two-faced character (Figure 1.4). Excessive levels of reactive oxygen species, if left uncontrolled damage the cellular structures associated with its production including lipids, membranes, proteins and nucleic acids. The magnitude and the duration of the dysregulation of reactive oxygen species can produce a chronic shift in redox homeostasis. However, dysregulation of reactive oxygen species may not be overt in appearance before it manifests into several pathological conditions. In fact, the normal process of aging is one such condition shown to be associated with oxidative state. Dysregulation of the redox balance towards the accumulation of reactive oxygen species refers to a condition called oxidative stress¹². The resultant manifestations of various physiological processes during oxidative stress conditions thereafter lead to several pathological conditions as a consequence. Disease conditions such as inflammation, carcinogenesis, degenerative neurologic diseases, reperfusion injury, atherosclerosis, drug toxicities are some of the conditions resulting from oxidative stress. Therefore, redox homeostasis is highly desirable for the salutary effects to be predominant and

therefore, survival of the cell. The irony is that the oxygen utilization critical for the survival of an organism is not without risk.



Figure 1.4 Role of Reactive Oxygen Species in Regulation and Dysregulation of Cellular Homeostasis

1.1.8. Oxidative Stress Paradigm and its Relevance to Health and Disease

Oxidative stress paradigm premises a plausible concept that there exists a subtle balance between oxidants such as reactive oxygen species and antioxidants in normal physiology. Perturbation of this delicate balance between oxidants and antioxidants causes oxidative damage in the cellular milieu resulting in a condition called oxidative stress. Oxidative stress awaits several possible undesirable outcomes as pathologies ensue when oxidants are produced in excess of the endogenous antioxidants. Reactive oxygen species produce deleterious effects on the cell through indiscriminate damage to the macromolecules such as carbohydrates, lipids, proteins and nucleic acids leading to

cellular dysfunction or death. Therefore, strategies to counteract this biological damage to macromolecules by the reactive oxygen species have emerged with a promise to minimize associated pathological conditions. These strategies are historically based on the presupposition that all reactive oxygen species share a very common feature of damaging biological systems and that all antioxidants will prevent or reverse the pathological conditions associated with oxidative stress without any regard to the mechanism. Furthermore, to a large extent they have relied on identification of direct acting antioxidants that react in a 1:1 stoichiometry with the reactive oxygen species.

For example, oxidative modifications of proteins by the products of lipid peroxidation by reactive oxygen species in disease conditions has been studied extensively with a focus on the development of therapeutic antioxidant compounds such as α -tocopherol (vitamin E), ascorbate (vitamin C), β -carotene and dietary polyphenolic compounds in an attempt to terminate lipid peroxidation. However, supplementation of antioxidants in many chronic diseases produced diffuse and nonspecific results in controlled clinical trials despite the evidences from basic research. Animal studies and epidemiological data collectively demonstrated oxidative damage of biomolecules by reactive oxygen species.

These results also indicate that these traditional antioxidants such as α -tocopherol and glutathione essentially act as insulators of redox signaling moieties and prevent the cross-talk inside the cell. Further, the extent of modifications of biomolecules by reactive oxygen species *in vivo* in oxidant-dependent pathologies is extremely low with an abundance of antioxidants present in the cells and tissues. Therefore, the endogenous

antioxidants act as redox insulators. For example, the concentrations of exogenous oxidants required to offset the redox balance *in vitro* or *in vivo* are in the orders of magnitude much greater than the levels that can be achieved in healthy or disease conditions. Such exogenous oxidants must break down the redox insulation to produce an effect and therefore requires high nonphysiological concentrations. These findings demonstrate that effective antioxidants must have a greater role of modulating much more complex networks controlling cell signaling pathways related to redox balance. It also requires a precise definition of the molecular targets and mechanisms.

Contrary to the corollary that all the reactive oxygen species are bad and antioxidants are good, reactive oxygen species such as hydrogen peroxide and nitric oxide are now established as important cell signaling molecules. This signals that reactive oxygen species plays an important role in biology and that antioxidants assume a regulatory function. For example, low levels of products from lipid peroxidation by enzymatic and nonenzymatic reactions accumulate over time and modify certain proteins in a specific manner to modulate protective cell signaling pathways. However, high levels result in the modifications of susceptible nucleophilic residues in a less specific manner leading to deleterious consequences if the subsequent repair or removal mechanisms fail to rescue the damage.

Therefore, redox homeostasis is incessantly critical for the survival of organisms and consequently organisms have developed intricate mechanisms that modulate complex networks controlling cell signaling and metabolism.

1.1.9. Cellular Signaling and Adaptation

Cell signaling can be thought of as a means of communication among the cells through biological mechanisms in response to extracellular stimuli. Transmission of the information from the outside of a cell to various functional elements inside the cell is referred to as signal transduction. Several stress responsive signaling pathways to the reactive oxygen species of endogenous or environmental origin have been identified¹⁰. The reactive oxygen species activate specific pathways in a controlled manner through the modifications of redox sensitive signaling proteins, thus eliciting downstream signal transduction pathways. This holds true with other reactive species including electrophiles resulting from oxidative reactions in cellular milieu. Further, the involvement of specific pathways and genes in response to reactive oxygen species demonstrates that the reactive oxygen species act as sub-cellular messengers in redox sensitive signal transduction. The signals are ultimately being transmitted to the transcriptional machinery in the nucleus responsible for gene regulation through a class of proteins called transcription factors. Binding of the transcription factors to the specific DNA sequences elicit transcription of target genes. Most of these pathways are characterized by response through localized receptors to specific stimulus modulating its function and therefore downstream effectors. These pathways are reversible, allowing the control and responsiveness to multiple stimuli. One of the most widely characterized signaling pathways that orchestrates with the dysregulation of redox homeostasis is Nrf2/ARE signaling pathway.

1.1.10. Oxidative Stress and Toxicology

The toxicities arising from the exposure to a toxicant may result from a cascade of events at the cellular and molecular level that may eventually culminate in a toxic endpoint. A toxicant may be a chemical with intrinsic toxicity or a chemical derived through a process called bioactivation or metabolic activation, which can be defined as a process of metabolic conversion of an innocuous chemical into a toxicant. Initiation of toxicity usually begins with the covalent interactions of toxicants with the cellular macromolecules.

Metabolic conversion of most of the xenobiotic is carried out by the cytochrome P450 enzymes transforming them into inactive and polar metabolites suitable for excretion. However, certain cytochrome P450 enzymes such as CYP1A1, CYP1A2, CYP2A6 and CYP2E1 have toxicological importance for their involvement in the bioactivation of xenobiotics, including drugs converting relatively inert chemical species into toxic products. In addition to bioactivation, the isoforms CYP2A6 and CYP2E1 with its leaky catalytic cycle also contributes to the generation of reactive oxygen species in the form of hydrogen peroxide or superoxide.

1.1.11. Natural Products as Therapeutic Agents

Natural products have been used for their medicinal properties over the millennia and are the single most productive source for the discovery of novel therapeutic agents. The inherent chemical diversity and chemical variations associated with natural products presumably makes them a very rich and viable source for the discovery and development

of new therapeutic and preventative agents for a variety of pathological conditions. This complexity presents itself as a limiting factor in the evaluation of the overall health benefits. Huge diversity among the natural products and low accessibility of the potentially bioactive constituents presents a major challenge that requires to be resolved to prove the concept that the bioactive constituents interact with their targets. Unraveling the complex composition of natural products through mechanistic studies and bioactivity guided fractionation has a huge potential to provide insights into target-ligand relationships. In addition, the pharmacokinetic and pharmacodynamic characteristics of natural products add even more complexity to these agents presenting several challenges in the understanding of mechanisms of action *in vitro* and *in vivo*. Despite the structural and functional complexity of the natural products, their screening for biological activity has proven to be an effective method for identifying potential therapeutic agents. Molecules with such exquisite complexities cannot be constructed easily by other means. Examples of plant-based molecules used in medicine dates back to more than 200 years where morphine stands as the first pharmacologically active pure compound isolated from *Papaver somniferum*. Examples of natural product based therapeutic agents includes antibiotics such as penicillin and tetracycline, antimalarials such as quinine and artemisinin, antiparasitics such as avermectin, antihyperlipidemics such as lovastatin, anticancer agents such as taxol, doxorubicin and immunosuppressants such as cyclosporine and rapamycin. In fact, natural products occupy a major share in the classes of antibacterial and anticancer agents. However, the repertoire of natural products has not been completely explored and only a small fraction of the chemical diversity present in

nature has been uncovered. It is therefore highly likely that nature will provide an abundant supply of the pharmaceutical agents in the years to come.

Several classes of compounds of natural product origin have been shown to inhibit the enzymes involved in the generation of reactive oxygen species and stimulate cellular pathways that function to minimize the toxic effects of reactive oxygen species ¹³. ¹⁴. Limiting the formation of reactive oxygen species inside a cell, as well as eliminating reactive oxygen species produced, using natural products represents a viable strategy to maintain a healthy redox balance. Thus, the use of natural products to maintain normal homeostasis of a cell presents a novel prophylactic strategy in preventing illnesses associated with oxidative stress.

1.1.12. The Açaí Berry

The Brazilian palm tree *Euterpe oleracea*, commonly known as açaí, belonging to the family Arecaceae, has been traditionally used as a medicinal plant in Brazil (Figure 1.5). Açaí has been widely acclaimed in recent years for its health-promoting effects and emerged as a novel nutraceutical in the United States. The high nutritive values of açaí surely places it to be a part of the healthy diet but açaí is yet to be qualified to have any significant health benefits. Açaí is found to be richer in antioxidants than similar fruits such as cranberries, strawberries, raspberries, blackberries or blueberries. Numerous studies have demonstrated the dietary intake of fruits and vegetables as a rich source of nutrients or phytochemicals in relation to health benefits. Açaí has been touted as a superfruit by its manufacturers claiming to have a lot of health benefits. A lot of

enthusiasm has been exercised by its manufacturers in the rising of açai as a commercially successful and viable product on market.



Figure 1.5 Açai Berry Fruit

Currently, there is inadequate scientific evidence on both the chemical composition of açai and its biological targets, both of which are decisive in our understanding of the purported health benefits of açai. There is also a clear lack of definitive scientific evidence from studies involving basic research, animal and human studies concerning molecular mechanisms associated with the use of this product. Therefore, açai is currently not qualified to be listed on the United States Food and Drug Administration (USFDA) Generally Regarded As Safe (GRAS) list for its intended use¹⁵. The benefits of açai have been linked to high levels of antioxidants including anthocyanins, proanthocyanidins, flavonoids and other polyphenolic compounds present in it. The reported benefits, for the most part, are based on its *in vitro* antioxidant capacity and radical scavenging ability in biological samples, however; the biological significance has not been established. In fact, the United States Department of Agriculture (USDA) invalidated the physiological significance of a once widely accepted antioxidant assay,

oxygen radical absorbance capacity (ORAC) due to lack of scientific evidence that the ORAC values have no relevance to the effects of specific bioactive compounds, including polyphenols on human health (<http://www.ars.usda.gov/services/docs.htm?docid=15866>). Furthermore, the scientific refutation of ORAC resulted in USDA's Nutrient Data Laboratory (NDL) removal of more than a decade-long web publication of ORAC database. Thus, the basis for the positive health effects of the açai berry attributed to the presence of radical scavenging antioxidants is of debate and remains currently unresolved. Therefore, the purported health benefits of açai are most likely the result of more complex interactions with biological targets, rather than direct radical scavenging effects. This clearly demonstrates the necessity to provide scientific evidence about the possible health benefits of açai relating specific bioactive constituents to specific targets and associated molecular mechanisms.

1.1.13. Target-based Identification of Bioactive Constituents of Açai

As with several other natural products, the diverse make-up of the açai berries and the added complexity of antioxidant defense system limited identification of bioactive constituents and their biological targets. Therefore, the promising antioxidant potential of the açai berry extracts needs to be deciphered down to individual bioactive constituents and their cellular targets to understand the associated mechanism of action conferring health benefits. Identifying açai berry constituents as inhibitors of enzymes contributing to ROS generation and as signaling molecules of various pathways resulting in ROS elimination through induction of phase II antioxidant enzymes would provide a basis for

explaining its antioxidant potential, and may lead to effective approaches to chemoprevention of ROS-linked diseases. The identification and isolation of the bioactive chemical species is as complicated as identifying a biochemical target. The current study aims at addressing both the challenges through better utilization of various chromatographic techniques.

1.2. Hypothesis and Aims

The primary focus of the current research is to understand the antioxidant properties of açai berries by identifying potential biological targets and to delineate the biochemical basis of action for better insights into observed effects. Restoring the homeostasis of the cell using natural products and dietary supplements has become an active area of research owing to the increasingly common use of these products in modern world. Recently, açai emerged as a superfruit and has been widely acknowledged to have high antioxidant potential. Although açai has been shown to exhibit many physiological effects, its active constituents, cellular targets and the precise molecular mechanisms conferring specific biological activity are yet to be defined. Therefore, it is worthwhile to pursue the antioxidant properties of açai as oxidative stress is the key determinant in the pathogenesis of a variety of human ailments.

The central hypothesis for this dissertation is that several classes of compounds present in açai may favorably interact with natural antioxidant defense system and cytochrome P450 enzymes to maintain and/or restore proper redox balance, thus preparing the cell to combat against oxidative stress. This leads to the broad objectives of

identifying the antioxidant constituents of açai modulating oxidative stress, and their biological targets. The rationale for carrying out the present work is that a detailed understanding of the underlying mechanisms by which the açai constituents restore or maintain proper redox balance within the cell is essential for its effective prophylactic use. Moreover, it may form basis for development of strategies utilizing açai as a potential therapeutic agent in treating or preventing oxidative stress-related diseases.

CHAPTER II

**INHIBITION OF HUMAN CYTOCHROME P450 2E1 AND 2A6 BY
ALDEHYDES: STRUCTURE AND ACTIVITY RELATIONSHIPS**

2.1. Introduction

The function of microsomal cytochrome P450 enzymes is generally a protective one, where foreign chemicals entering the body can be oxidized in a way that makes them more readily excreted. However, the human microsomal cytochrome P450 isoforms 2E1 and 2A6 have been implicated in the deleterious effects of a variety of drugs and environmental agents, including acetaminophen, nitrosamines, and carbon tetrachloride, to name a few¹⁶⁻¹⁹. There is also evidence to suggest that the inhibition of these isoforms during times of exposure to these agents can provide a level of protection against the harmful effects²⁰⁻²². Consequently, identification of selective inhibitors of these isoforms and understanding the basis for selectivity has been the focus of a number of recent studies. It has been established through crystallographic analysis and binding studies that the active sites of these two isoforms are relatively small compared with other microsomal P450s, with the 2A6 isoform being the more sterically restricted²³⁻²⁵. Comparisons between the two enzymes suggest that 2A6 is more structurally rigid, whereas the 2E1 active site may have more flexibility, and can change in response to different substrates²⁶⁻²⁸. Indeed, active site volumes ranging from 190 Å³ to 470 Å³ have

been measured for 2E1 with different substrates bound²⁷. This is consistent with spectroscopic studies indicating that the active site of this isoform displays a significant level of compressibility under high pressure, whereas the 2A6 active site is considerably more unyielding^{29, 30}. Crystallographic and computational studies suggest that π -stacking interactions in the active site may facilitate the binding of planar low molecular weight molecules to both isoforms, and in 2E1, these interactions may be the basis for active site reorganization associated with observed substrate inhibition^{31, 32}.

The goal of the current study was to explore structure–activity relationships mediating the binding of a series of related aldehydes to human Cytochrome P450_{2E1} and P450_{2A6} in order to gain additional insight into the structural features contributing to selectivity of substrates and inhibitors toward these two isoforms, along with features that facilitate active site reorganization and expansion. In particular, factors such as chain length, branching in the 3-position and unsaturation in the 2-position were evaluated for their influence on K_i . Aldehydes were selected on the basis of prior studies involving rabbit liver cytochrome P450s identifying aldehydes as a class of P450 inhibitors, and the availability of a wide range of structurally related compounds belonging to this class³³. In addition, aldehydes of the type described in this study can be generated physiologically via lipid peroxidation, thus insight gained through this study may guide future studies related to toxicology and cellular oxidative stress.

2.2. Materials and Methods

2.2.1. Chemicals

The aldehyde compounds used in this study were purchased from Acros Organics. Coumarin, 7-hydroxycoumarin (umbelliferone), NADPH, *p*-nitrophenol and 4-nitrocatechol were from Sigma Chemical Co. Human liver S9 fractions were purchased from Moltox Inc., Asheville, NC.

2.2.2. Enzymatic Assays: P450_{2E1}

All assays for 2E1 (*p*-nitrophenol) were carried out according to published protocols with slight modifications³⁴. S9 fractions (0.5 mg) were incubated in 100 mM phosphate buffer (pH 7.4) in the presence of 20–100 μ M *p*-nitrophenol and 1.0 mM NADPH for a total of 30 min at 37 °C in a 0.5 mL total reaction volume. Reactions were terminated by addition of ice-cold 6% perchloric acid and incubation on ice for an additional 10 min, followed by centrifugation to remove precipitated protein. Cleared supernatant (50 μ L) was then analyzed by RP-HPLC on a 150 \times 4.6 C18 column with a mobile phase consisting of 35% acetonitrile, 64.5% H₂O, 0.5% acetic acid at a flow rate of 1.0 mL/min. Absorbance detection at 340 nm was used to quantify the 4-nitrocatechol product. A Shimadzu LC 20A Series HPLC system consisting of an SPD-20A UV/Vis detector, LC 20AT solvent delivery, and a Sil 20A autosampler was used for analysis of samples.

2.2.3. Inhibition of P450_{2E1}

All inhibitors, including the aldehydes and acids, were prepared as aqueous stocks by diluting 4.0 μg inhibitor into 100 mL DI H₂O immediately prior to their use. Initially, a dose–response curve was generated for each of the aldehydes with regard to their relative inhibitory effects on P450_{2E1}. Reactions contained 0.5 mg S9 fractions, 50 μM *p*-nitrophenol, 1.0 mM NADPH and aldehyde concentrations ranging from 5 μM to 370 μM in a 0.50 mL volume of 0.1 M phosphate buffer (pH 7.4). Samples were quenched and processed for HPLC analysis as described earlier. To obtain more detailed kinetic parameters, Michaelis–Menten kinetic experiments were then performed to probe the mode and potency of inhibition using inhibitor concentrations of either 30 μM or 60 μM . These concentrations were chosen based on the results of the screening experiments in which it was determined that this was the lowest concentration to produce measurable inhibition for all of the compounds being examined except for dodecyl aldehyde. The substrate concentrations were varied from 20.0 μM to 100 μM in a total reaction volume of 0.50 mL for 30 min, and reactions were processed as described above. A minimum of 4 independent trials were carried out for each experiment and the standard deviations are reported.

2.2.4. Enzymatic Assays: P450_{2A6}

The assay that was used to measure inhibition of 2A6 is one that utilizes the conversion of coumarin into 7-hydroxycoumarin. The procedure is modified from that of Waxman and Chang³⁵. Liver S9 fractions (0.50 mg) were incubated in a reaction mixture

containing 3.0 μM coumarin, 100 mM potassium phosphate buffer (pH 7.4) and 1.0 mM NADPH in a total volume of 0.50 mL. Following a 30 min incubation at 37 °C the protein was precipitated with 100 μL of 6% perchloric acid and placed on ice for 10 min. Samples were centrifuged at 13,500 rpm for 10 min and 40 μL of the cleared supernatant was injected onto a RP-C18 HPLC column with a mobile phase consisting of 59% DI water, 40% methanol, and 1% acetic acid, at a flow rate of 1.0 mL/min.

2.2.5. Inhibition of P450_{2A6}

Inhibitors were prepared as aqueous stock solutions by diluting 4.0 μg inhibitor into 100 mL DI H₂O immediately prior to their use. Dose–response curve was generated for each of the aldehydes with regard to their relative inhibitory effects on P450_{2A6}. Reactions contained 0.5 mg S9 protein, 3.0 μM coumarin, 1.0 mM NADPH and aldehyde concentrations ranging from 5 μM to 370 μM in a 0.50 mL volume of 0.1 M phosphate buffer (pH 7.4). Samples were quenched and processed for HPLC analysis as described in the previous sections. Michaelis–Menton kinetic experiments were then performed using inhibitor concentrations of either 30 μM or 60 μM . Again, these inhibitor concentrations were selected based on the results of the screening experiments, as with the 2E1 reactions. The substrate concentrations were varied from 0.5 μM to 6.0 μM in a total reaction volume of 0.50 mL for 30 min, and reactions were processed as described above. A minimum of 4 independent trials were carried out for each experiment and the standard deviations are reported.

2.2.6. Reversibility Studies

To determine whether the inhibition of each P450 isoform by the individual aldehydes was reversible or irreversible, microsomal samples were pre-incubated with (1) Buffer alone, (2) Buffer + Aldehyde and (3) Buffer + Aldehyde + NADPH, as described in previously by Raner et al.³³.

2.2.7. Aldehyde Oxidation by Human P450 Enzymes

Oxidation of *trans*-2-octenal was carried out in a total reaction volume of 200 μ L, and contained expressed human P450 (2E1 or 2A6 supersomes, Gentest, 50 nM final), 100 mM potassium phosphate buffer (pH 7.4), 100 μ M *trans*-2-octenal, and 1 mM NADPH. The reaction was quenched with 6% perchloric acid as described previously. A C18 RP HPLC column (4.6 \times 250 mm) from Phenomenex was used with a mobile phase consisting of 55% acetonitrile and 45% water, both containing 0.1% TFA at a flow rate of 1.4 mL/min and detection was at 230 nm. A sample of *trans*-2-octenoic acid was acquired from Sigma–Aldrich and used to generate a standard curve for quantification of product. The reactions with human 2E1 supersomes were linear for 45 min at 37 $^{\circ}$ C, so all additional reactions were carried out under these conditions. The 2A6 supersomes failed to produce NADPH-dependent acid product. The oxidation of *trans*-2-decenal, *trans*-2-nonenal, *trans*-2-octenal and *trans*-2-heptenal by the expressed cytochrome P450_{2E1} in supersomes was also carried out with each of the aldehydes present at the following concentrations: *trans*-2-decenal (110 μ M), *trans*-2-nonenal (120 μ M), *trans*-2-octenal (100 μ M) and *trans*-2-heptenal (110 μ M), along with 1.0 mM

NADPH in a 100 mM phosphate buffer at pH 7.4. Reactions were carried out for 45 min at 37 °C and quenched as described above. Control reactions without NADPH were carried out in parallel, and the reaction mixtures were analyzed using HPLC under the same conditions as described for *trans*-2-octenoic acid alone. The effects of ethanol (0.001%, 0.01%, 0.10% and 1.0%) on the activity in 2E1 supersomes was also monitored under identical conditions.

2.2.8. Analysis of Kinetic Data

Michaelis–Menten plots were prepared for each of the various activity data sets in the presence and absence of inhibitor. All data was fit using SlideWrite version 4.1 (Advanced Graphics Software Inc.) and the non-linear regression analysis function using the Michaelis–Menten equation. Based on Michaelis–Menten plots for each aldehyde, the inhibition could be described using the competitive model, so values for K_I were calculated using this model, where V_{\max} remains constant, α is defined as K_m^{app}/K_m and $K_I = [I]/(\alpha-1)$.

2.2.9. Graphical Images of P450 Active Sites

The active site images of the 2E1 and P450_{2A6} enzymes were generated using crystal structure coordinates deposited in the protein databank. The file PDB: [1Z10](#) was used for the image of P450_{2A6} with coumarin bound; PDB: [3T3Z](#) was used for P450_{2E1} with pilocarpine bound; PDB: [3E6I](#) was used to generate the P450_{2E1} image with indazole bound; and the PDB: [3LC4](#) coordinates were used for P450_{2E1} image with

imidazolyl-dodecanoic acid bound. RasWin 2.7.5.2 Molecular Graphics software was used to generate each of these images based on the respective PDB files.

2.3. Results

2.3.1. Inhibition of P450_{2E1} by Alkanals and Alkenals

Dose–response inhibition studies using *p*-nitrophenol oxidation as a measure for 2E1 activity were initially carried out using saturated straight-chain aldehydes ranging from 8 to 12 carbon atoms and 2-unsaturated aldehydes with 8-, 9- and 12-carbon atoms (Figure 2.1) at fixed inhibitor concentrations of 30 μ M and 230 μ M. Inhibition was observed for each aldehyde as a dose-dependent reduction in activity, relative to a control in which no aldehyde was present. The selection of these concentrations was based empirically on their ability to highlight the differences in potency among this group of aldehydes. Maximum inhibition was observed for the nonyl and decyl aldehydes, and unsaturation significantly increased the level of inhibition, suggesting the extended π -system of the unsaturated aldehydes leads to more favorable binding in the active site.

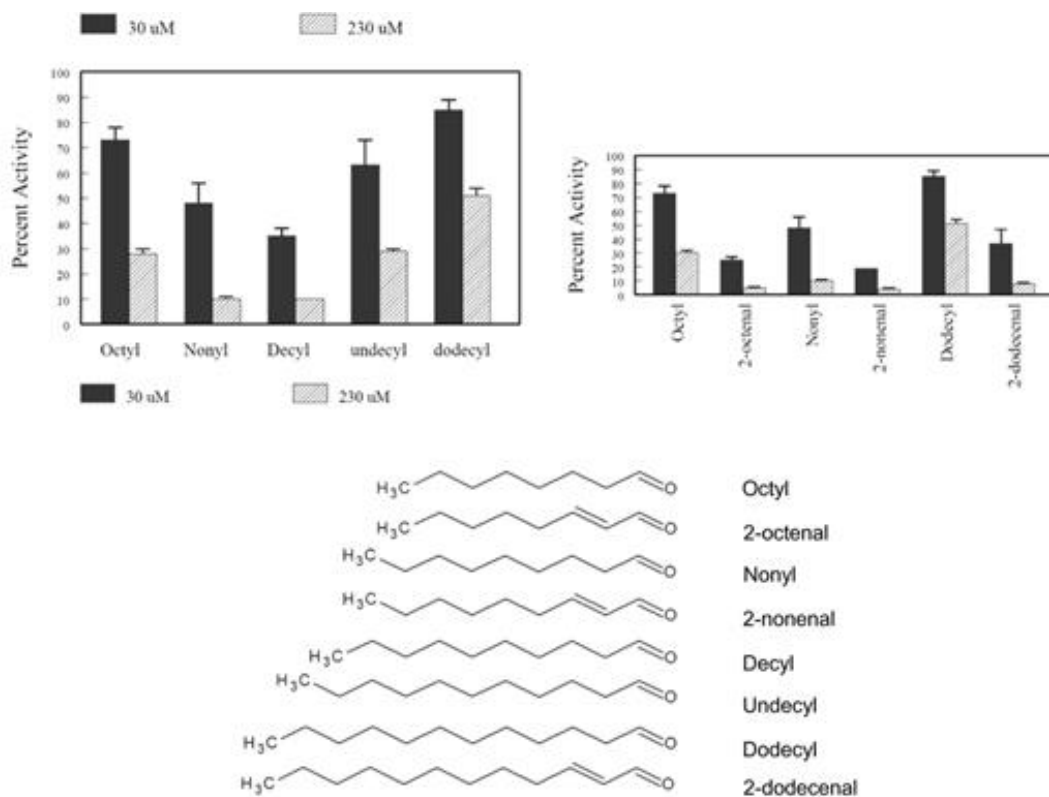


Figure 2.1. Effects of Saturated and 2-Unsaturated Aldehydes on P450_{2E1} Activity. (A) Effect of Chain Length on P450 Inhibition by Saturated Aldehydes at 30 And 230 mM Aldehyde Concentration. (B) Comparison of the Effects of Saturated vs 2-Unsaturated Aldehydes on P450_{2E1} Inhibition at 30 and 230 mM Aldehyde Concentration. (C) Structures of Aldehydes used for These Comparative Studies.

The reversibility of inhibition was examined for each of the aldehydes represented in figure 2.1 by pre-incubating the aldehydes with S9 fractions in the presence and absence of NADPH for 15 min at 37 °C. Dilution of the pre-incubation mixture resulted in complete restoration of the *p*-nitrophenol oxidation activity of the samples, thus all of these saturated and unsaturated aldehydes (data not shown) appeared to be reversible

inhibitors of 2E1 under the conditions used. As a positive control, the experiment was carried out using 11-undecylenic aldehyde at a concentration of 25 μM . Following a 15 min pre-incubation at 37 °C in the presence of 1 mM NADPH, a loss of ~50% of the activity of 2E1 was observed (data not shown). This compound possesses a terminal olefin group, which is known to cause irreversible damage to the heme³⁶⁻³⁸.

Detailed inhibition studies were subsequently carried out in which the inhibition constants (K_i) were calculated for the aldehydes, both saturated and unsaturated, with carbon chain lengths, between 5 and 12, using the standard Michaelis–Menten approach (Table 2.1). For all the aldehydes tested, V_{max} was unaltered, once again indicating competitive-reversible type inhibition, thus the competitive model of inhibition was applied for K_i determination. Consistent with the preliminary screening data, the K_i values indicate that the 9- and 10-carbon aldehydes, possessing a 2-double bond (nonenal and decenal) were the most potent inhibitors of the human 2E1 isoform. It is also worth noting that a strong dependence on chain length was observed for the saturated compounds, whereas less dependence on chain length was observed with unsaturated aldehydes. Furthermore, the unsaturated compounds were all much more potent than the respective saturated compounds, with K_i values as much as 30-fold lower in the case of the 11- and 12-carbon aldehydes.

2.3.2. Effects of Branching on Inhibition of 2E1

Additional aldehydes (citral and citronellal) with branching at the 3-position were evaluated for inhibitory potency against 2E1. Citral (3,7-dimethyl 2,6-octadienal) as

shown in figure 2.2, is a naturally occurring mixture of 2,3-unsaturated aldehyde isomers with branching methyl groups at carbon 3 and 7. Citronellal (3,7-dimethyl 6-octenal), shown in figure 2.3, also has a 3-methyl branch but does not have a double bond in the 2-position. Both aldehydes showed reversible competitive inhibition profiles when evaluated using the Michaelis–Menten model. K_I values were measured for both of these compounds and were compared with those of the linear 10-carbon saturated and unsaturated aldehydes. By comparing citral to citronellal it is clear that the double bond at the 2-position dramatically impacts inhibition; K_I values of 18.8 μM vs 57.8 μM , respectively. As for the effects of branching, both decanal and citronellal are saturated at the 2-position and possess 10 carbon atoms, like decanal. The K_I for Decanal, however, is about 8-fold lower than the branched citronellal (7.0 μM vs 57.8 μM). Likewise, a comparison between decanal and citral showed a 5-fold increase in K_I (3.3–15.7 μM) with the inclusion of a branching methyl at the 3-position of the aldehyde.

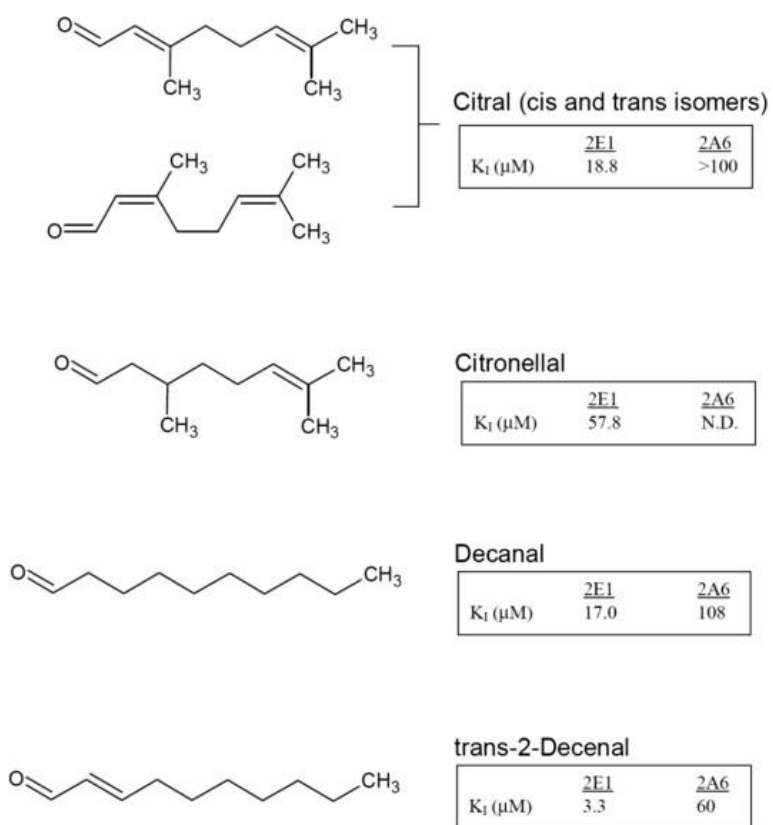


Figure 2.2. Structure and Measured Inhibition Constants for Branched Saturated and Unsaturated Aldehydes, Citral, Citronellal, and the Corresponding Linear, Saturated and Unsaturated 10 Carbon Aldehydes, Decanal and Trans-2-Decenal.

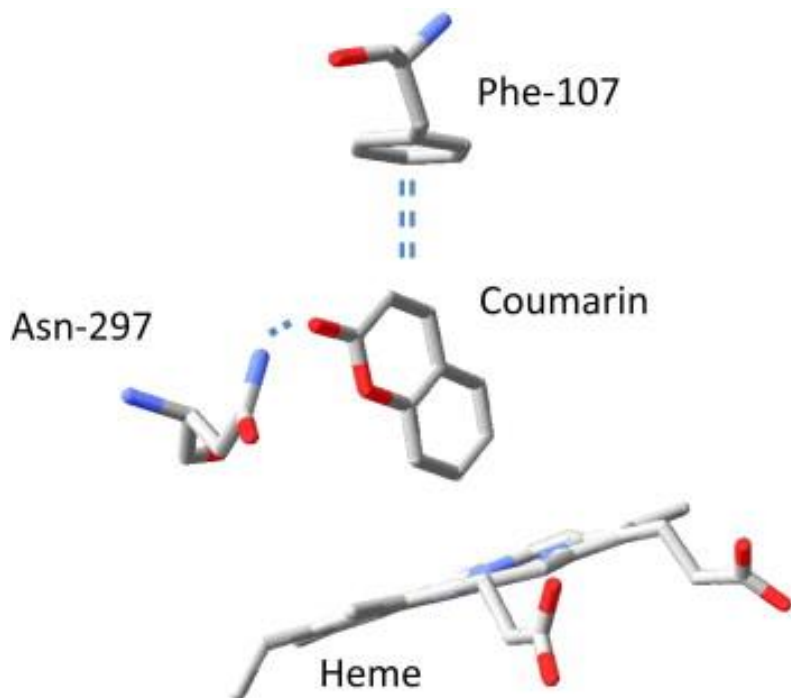


Figure 2.3. Key Residues in the Active Site Structure of Human Cytochrome P450 2A6 with the Substrate Coumarin Bound. Hydrogen Bond Interactions between the Carbonyl Oxygen on the Substrate and the Amide Group from Asn-297 and π - π Interactions between Phe-107 and the Aromatic Ring of Coumarin are shown (Generated using RasWin 2.7.5.2 and Coordinates from PDB: [1Z10](#)).

2.3.3. Effects of Aldehyde Function

The importance of the aldehyde group for inhibition was probed by monitoring 2E1 inhibition using the corresponding 8- to 12-carbon saturated carboxylic acids. Over a range of 1.0–100 μ M, only lauric acid inhibited 2E1 significantly (data not shown). At a concentration of 50 μ M, lauric acid reduced the activity of 2E1 by 50%, which is still

modest inhibition relative to the aldehydes. Due to the lack of observed inhibition at high concentrations of carboxylic acid, K_I values were not determined.

2.3.4. Inhibition of P450_{2A6} by Alkanals and Alkenals

As with the 2E1 isoform, all of the aldehydes tested, both saturated and unsaturated, inhibited coumarin hydroxylation via a reversible competitive mode. Values for K_I were determined for each of the saturated and unsaturated aldehydes used with 2E1, and these values are presented in table 2.1. A trend similar to that observed with 2E1 was also observed for 2A6. However, the optimal chain length appeared to be slightly shorter for 2A6, with a carbon chain length of 7–8 being most potent. Comparison of the saturated vs unsaturated aldehydes again suggested that the double bond in the 2-position improved the interaction with the active site, as indicated by a 2- to 3-fold decrease in K_I for the unsaturated aldehydes over nearly the entire range. It is worth pointing out that with 2A6 inhibition, dodecanal and undecanal appeared to be outliers in the general trends observed, as both of these saturated aldehydes inhibited more potently than the smaller decanal, and more potently than the corresponding unsaturated counterparts. Another clear distinction between the 2E1 and 2A6 data can be seen in the behavior of the unsaturated aldehydes. Where the 2E1 isoform appeared to be almost insensitive to chain length, the inhibitors of the 2A6 isoform had an optimal chain length of 7 or 8, and above or below this value the potency of inhibition decreased in a continuous manner, with the 2 notable exceptions previously pointed out.

Table 2.1. Experimentally Determined Inhibition Constants (K_I) for the Inhibition of Human Cytochrome P4502A6 by Straight Chain Saturated and Unsaturated Aldehydes Ranging in Size from 5 to 12 Carbons. K_I values were calculated using a competitive model for inhibition and a minimum of 3 trials were carried out for each aldehyde.

Aldehyde	P4502A6		P4502E1	
	K_I (μM) Saturated	K_I (μM) Unsaturated	K_I (μM) Saturated	K_I (μM) Unsaturated
Pentyl	126 ± 16	1270 ± 150	155 ± 13	13 ± 1
Hexyl	57 ± 7	33 ± 3	26 ± 2	6.7 ± 0.2
Heptyl	16 ± 1	9 ± 1	32 ± 1	5.6 ± 0.1
Octyl	25 ± 2	7 ± 1	13 ± 1	4.1 ± 0.1
Nonyl	55 ± 6	34 ± 3	8.0 ± 1	2.9 ± 0.2
Decyl	106 ± 29	59 ± 6	17 ± 1	3.3 ± 0.1
Undecyl	68 ± 7	103 ± 22	117 ± 15	3.4 ± 0.1
Dodecyl	48 ± 9	128 ± 35	85 ± 8	2.6 ± 0.1

2.3.5. Other Structural Determinants for P450_{2A6} Inhibition by Aldehydes

As with P450_{2E1}, saturated carboxylic acids were ineffective at inhibiting the 2A6 isoform at concentrations as high as 100 μ M, thus K_I values were not determined. Interestingly, branching in the aldehyde also resulted in a dramatic loss in potency as demonstrated by the use of citral and citronellal as inhibitors of 2A6. Only citral inhibited 2A6, and here the K_I was still >100 μ M (data not shown).

2.3.6. Oxidation of Aldehydes by Human S9 Fractions and Expressed Cytochrome P450_{2E1} and P450_{2A6}

To determine that the aldehyde function of each inhibitor was inside the active site, reactions involving 4 of the unsaturated aldehydes, *trans*-2-heptenal, *trans*-2-octenal, *trans*-2-nonenal and *trans*-2-decenal were evaluated for the formation of the corresponding carboxylic acid. The substrate *trans*-2-octenal was examined initially to establish linearity over time, and the effects of ascorbate and glutathione on the reaction. This aldehyde was selected on the basis of its ability to inhibit both 2A6 and 2E1 isoforms effectively. The reaction with 2E1 supersomes was linear for 45 min at 37 °C, and beyond 45 min a marked decrease in activity was observed. In addition, inclusion of either 1.0 mM ascorbate or 1.0 mM glutathione had no effect on the rate of acid formation. Furthermore, for the 2E1-dependent reaction, increasing concentrations of ethanol (a P450_{2E1} inhibitor), between 0.001% and 1.0% caused a dose-dependent decrease in acid formation, with $>80\%$ inhibition at 1% and 40% inhibition at 0.1%

ethanol. In contrast, 2A6 supersomes did not catalyze oxidation of *trans*-2-octenal. An additional experiment was carried out in which the four aldehydes; *trans*-2-heptenal, *trans*-2-octenal, *trans*-2-nonenal and *trans*-2-decenal were incubated with either expressed 2E1 or expressed 2A6, and the NADPH-dependent oxidation of each aldehyde was monitored. Supersomes containing expressed 2E1 were effective in the oxidation of all 4 aldehydes, while 2A6 supersomes again yielded no acid products.

2.4. Discussion

Prior studies involving rabbit cytochrome P450_{2B4} indicated that mammalian cytochrome P450s were susceptible to aldehyde-mediated irreversible mechanism-based inhibition³³ Mechanistically, the inactivation was the result of heme destruction and was correlated to the aldehyde deformylation reaction mechanism^{39, 40}. No prior studies have been reported involving interactions between aldehydes and the human isoforms, including 2E1 and 2A6, both of which are of considerable toxicological importance. In the current study, no evidence for irreversible inhibition was observed with any of the aldehydes or either cytochrome P450, rather, reversible competitive inhibition was observed. However, oxidation of the aldehyde function by the expressed 2E1 enzyme was observed indicating an “aldehyde in” binding orientation in the active site for these compounds. With 2A6, a different binding orientation must be envisioned based on the inability to oxidize the aldehyde function. It should be noted that in the rabbit liver study, aldehyde concentrations used to calculate inactivation rates were in the mM range, whereas in the current study, the highest aldehyde concentrations used were mostly

below 100 μM . It is conceivable that inactivation of the human P450s could occur at higher aldehyde concentrations.

All of the saturated aldehydes inhibited both P450 isoforms, with varying potency, as determined by measured K_I values. Several interesting trends were observed in this data. For both 2E1 and 2A6, there appeared to be an optimal carbon chain length as it related to inhibition potency. For 2E1, the nonyl and decyl aldehyde had the lowest measured K_I , whereas heptyl and octyl aldehydes were most effective against 2A6, and neither isoform was inhibited by corresponding carboxylic acids. Several recent comparative studies have been carried out concerning structural and activity relationships between the 2E1 and the 2A6 human P450 isoforms that support these experimental observations^{26, 27, 29}. Both enzymes have relatively small active sites, and therefore binding of larger molecules may be disfavored via steric interactions, consistent with the observed pattern of inhibition. The 2A6 active site has a slightly smaller volume than 2E1 based on crystal structures with the small molecule pilocarpine bound (280 \AA^3 vs 337 \AA^3), which is consistent with the smaller optimum chain length for inhibition of 2A6 (7–8 carbons for 2A6 vs 9–10 for 2E1)²⁸. In addition, DeVore et al., using both experimental and computational approaches showed that the 2E1 active site was slightly less polar than 2A6, however both contained a cluster of phenylalanine groups that appeared to define the active site boundaries²⁸. The reduced interaction of both isoforms with carboxylic acids relative to aldehydes is most easily justified by the less polar character of the aldehyde group. The crystal structure of 2A6 reveals an Asn side chain (Asn 297) that may help to stabilize the carbonyl group of the aldehydes via hydrogen

bonding. Indeed, the substrates pilocarpine and coumarin both have carbonyl oxygens that form H-bond interactions with Asn 297 (Figure 2.3 shows the structure of the 2A6 active site with coumarin bound).

The 2-unsaturated aldehydes were generally more potent inhibitors of both 2E1 and 2A6, with some K_I values nearly 10-fold lower than the corresponding saturated compounds. Computational studies by Xu et al. highlight the importance of π - π interactions in the binding of 4-(methylnitrosamino)-1-(3-pyridyl)-1-butanone (NNK) in the active site of 2A6, thus similar interactions with the planar π -system of the 2-unsaturated aldehydes could be envisioned as a basis for more efficient binding⁴¹. Furthermore, based on the crystal structure of the human 2A6 isoform with coumarin bound, the nature of this π - π interaction involves the perpendicular arrangement of the π -orbitals on the aromatic ring systems of coumarin with those on Phe107 ring. , it is reasonable to suggest that the π -system of the 2-unsaturated aldehyde interacts favorably with Phe-107 of 2A6 in an analogous fashion, which serves to orient the substrate and restrict its mobility⁴². Thus, increasing size would create steric interference in the rigid 2A6 active site, if these binding interactions were to be maintained²⁷. This binding mode can also be used to rationalize the lack of aldehyde oxidation, as the carbonyl group of the aldehyde would be hydrogen bonded to Asn-297, which is removed from the activated oxygen in the catalytic site. The increase in potency toward 2A6 for the undecanal and dodecanal, relative to the corresponding unsaturated compounds was noted, however, it is not clear what the molecular basis for this observation is. It is tempting to rationalize this based on the greater flexibility of the large saturated

aldehydes in the rigid active site. This does not account for the increased potency of these larger aldehydes relative to the smaller decanal, which should have less steric restrictions on binding. A more likely explanation is that given the hydrophobic nature of these compounds, disruption of the P450_{2A6}/P450-reductase complex may result in the more potent observed inhibitory action.

Interestingly, for the unsaturated aldehydes, the dependence on chain length was almost completely abolished in 2E1, with the aldehydes containing 7–12 carbon atoms all inhibiting with K_i in the 3–5 μM range. This is in stark contrast to the behavior of the unsaturated aldehydes with 2A6. Although the π -interactions appear to be strongly driving the binding of these aldehydes to both enzymes, the 2E1 active site appears to have the ability to accommodate larger molecules in response to the presence of the π -system of the unsaturated aldehydes. First, 2E1 lacks the H-bond donor to the carbonyl that is present in 2A6, as Asn-297 is replaced in 2E1 with Asp-295, which is excluded from the active site. According to DeVore et al. the substrate pilocarpine appears to adapt to the 2A6 active site upon binding, whereas the 2E1 active site may change topology in response to substrate binding²⁸. In support of this flexibility model, the 2E1 active site volume can expand to 420–470 \AA^3 in response to the binding of the large substrate imidazolyl-dodecanoic acid²⁵.

Figure 2.4 shows a comparison of the active site structure of P450_{2E1} with (A) pilocarpine (B) imidazolyl-dodecanoic acid and (C) indazole bound (substrate molecules are omitted from the structure). Although each of these substrates is structurally distinct

from the aldehydes used in the current study, what is apparent is that there are residues in the active site that can rearrange in response to substrate and/or inhibitor binding. Four Phe side chains (Phe 116, Phe 207, Phe 298 and Phe 478) that form the upper surface of the active site are shown in this figure. The most significant differences on substrate binding occur in the position of Phe 298 and Phe 478 with respect to the heme. For example, in panel A, Phe 298 and Phe 478 have moved up relative to the heme, creating a larger volume directly above the heme when the bulky pilocarpine molecule binds. With indazole bound (panel C) Phe 478 is angled down toward the heme, reducing the overall volume of this cavity. Panel B shows the additional movement of Phe 298 in response to binding imidazolyl-decanoic acid. This motion allows the acyl chain of the substrate to access a binding channel running parallel to the I-helix just above Phe 298, which presumably accounts for the larger active site volume in the presence of this substrate. It is conceivable that π -interactions between unsaturated aldehydes and the 2E1 active site may have an analogous effect on Phe 298, essentially holding this door open so that longer chain aldehydes can gain access to the more remote areas of the active site. Alternatively, computational studies by Li et al. suggest that the phenyl ring of Phe 478 can rotate to become almost perpendicular to the heme as a substrate binds to an “effector” site, which lies along the substrate access channel, directly above the γ -meso position on the heme³². This motion repositions both the active substrate and a key catalytic residue T303, resulting in negative cooperativity. Li et al. indicate the orientation of Phe 478 is significantly altered via π - π stacking interactions when an aromatic ligand occupies the effector site³². As the saturated aldehydes would not be

expected to bind to this effector site, it is also reasonable to suggest that the π -system of the 2-unsaturated aldehyde allows it to gain access to the effector site, thus increasing the available active site volume for unsaturated aldehydes. The lack of a hydrogen bonding group analogous to Asn-297 in 2A6 appears to allow the carbonyl group of the substrate more freedom to explore the active site, resulting in its oxidation by 2E1, but not 2A6.

P450_{2E1} active site

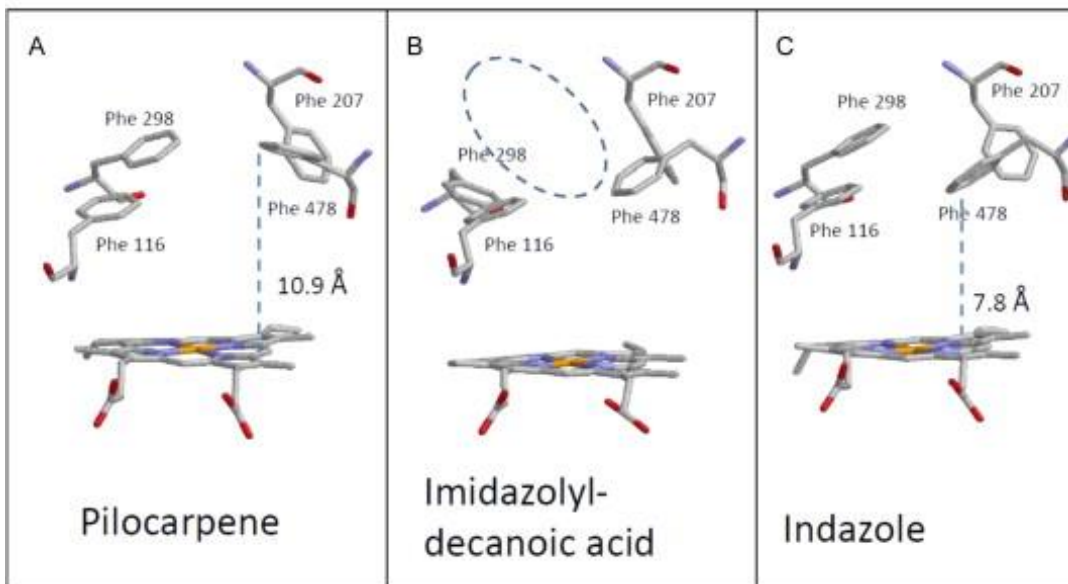


Figure 2.4 Active Site Structure of P450 2E1 Showing the Position of Key Phe Residues in the Presence of the Substrates (A) Pilocarpine (PDB: [3T3Z](#)), (B) Indazole (PDB: [3E6I](#)) and (C) Imidazolyl-dodecanoic Acid (PDB: [3LC4](#)). Images were prepared using RasWin 2.7.5.2 Molecular Graphics software.

2.5. Conclusions

In summary, the current work demonstrates that a series of saturated and unsaturated aliphatic aldehydes are effective competitive inhibitors of both human P450 2E1 and 2A6. The relatively small size of the 2E1 and 2A6 active sites result in a preference for binding the 7–10 carbon saturated aldehydes. In addition, 2-unsaturated aldehydes display 5 to 30-fold higher affinity for both human enzymes than their corresponding unsaturated counterparts, which is likely due to the potential for π -stacking interactions in Phenylalanine-rich active site of these enzymes. This study also provides direct experimental support for the flexibility model of substrate binding to 2E1, and suggests that an extended π -system may be a key determinant in active site expansion.

CHAPTER III
IDENTIFICATION OF INHIBITORS OF HUMAN CYTOCHROME P450
ENZYMES INVOLVED IN DRUG METABOLISM AND TOXICOLOGY BY
AÇAÍ EXTRACTS

3.1. Introduction

Cytochrome P450 enzymes belong to a superfamily of enzymes that are evolutionarily conserved across all the life forms. In mammals, cytochrome P450 enzymes are heme-containing microsomal monooxygenases found membrane bound to the endoplasmic reticulum of the cells. The enzymes are distributed across all the tissues with specialized functions but a substantial proportion is found in liver, the primary detoxifying organ. Cytochrome P450s catalyze a wide variety of metabolic and biosynthetic processes through oxidative metabolism of various endogenous and exogenous compounds including drugs, carcinogens and xenobiotics. It usually results in the addition of a hydroxyl moiety resulting in more polar metabolites that in some instances are predisposed to further metabolism by phase II enzymes. This process of conversion of foreign compounds into polar metabolites that can be readily excreted out of the body is called biotransformation. This is usually achieved by attaching a polar hydroxyl moiety to the xenobiotic (Figure 3.1). Cytochrome P450-dependent metabolism usually results in the formation of less toxic compounds. Cytochrome P450 enzymes

metabolize a wide range of structurally diverse compounds and are responsible for the elimination of a vast majority of exogenous compounds and xenobiotics ⁴³.

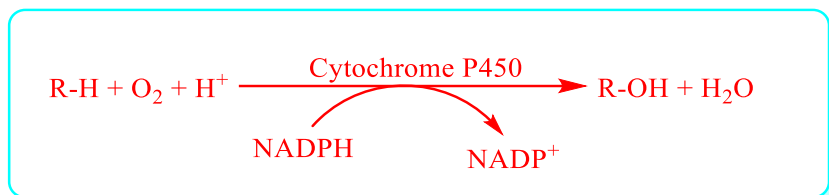


Figure 3.1 Schematic of Cytochrome P450 Mediated Xenobiotic Metabolism

In humans, a total of 57 genes coding Cytochrome P450 enzymes have been identified and conveniently categorized based on their sequence homology into 18 families and 44 subfamilies^{44, 45}. Enzymes that share more than 40% amino acid sequence identity are grouped into one family designated by an Arabic numeral. The members of a family sharing more than 55% sequence identity are assigned a letter. Members belonging to 1, 2 and 3 families metabolize a majority of xenobiotics. These enzymes are evolutionarily less conserved and exhibit polymorphism among individuals. They also have less affinity and therefore broader selectivity towards a wide range of foreign compounds. Among these CYP isoforms, CYP1A1, CYP1A2, CYP2A6, CYP2B6, CYP2C8, CYP2C9, CYP2D6, CYP2E1 and CYP3A4 share the metabolism of xenobiotics to a great extent.

Enzymes belonging to the family 4 participate in metabolism of fatty acids and related substrates and also some xenobiotics. The other isoforms belonging to the families 5 through 51 are highly conserved with a high affinity for endogenous substrates and therefore have specific endogenous functions such as biosynthesis of steroid

hormones, prostaglandins and bile acids. Despite the broader selectivity and the overlapping sensitivity of these enzymes towards various substrates, metabolism of two-thirds of foreign compounds that enter the human body including drugs, is carried out by one of these few enzymes as illustrated in figure 3.2 ⁴⁶.

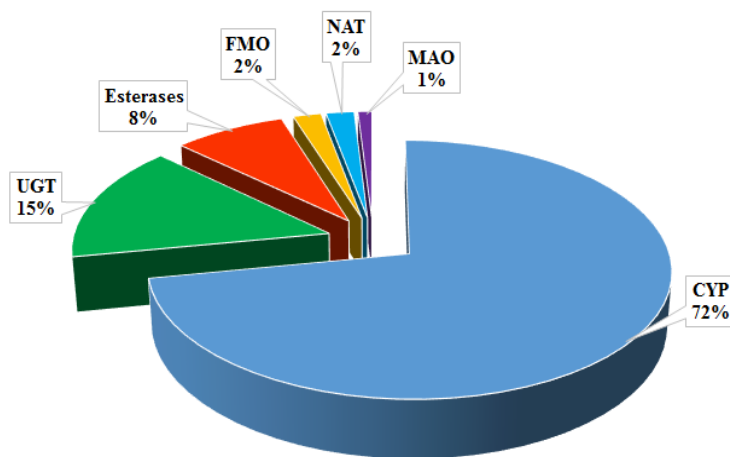


Figure 3.2. Distribution of the Metabolism of the Xenobiotics by Various Metabolizing Enzymes

An important feature of these enzymes is that their expression and function can be altered by a variety of intrinsic and extrinsic factors, including the presence of multiple drugs or xenobiotics (Figure 3.3)⁴⁷. Factors such as age, sex, polymorphism and concomitant disease conditions and several drugs alter the expression of these enzymes with possible consequences of increased or decreased clearance of drugs administered concurrently. An increasing use of natural products for treating various ailments also adds complexity to metabolism of various concurrently used medications. These factors are implicated in many off-target undesirable effects through their influence on the

biotransformation and bioactivation of xenobiotics when the metabolites formed are reactive oxygen metabolites, radicals and reactive electrophiles. Therefore, a thorough knowledge of the interactions between each of the CYP isoforms and all forms of xenobiotics, including natural products, is essential towards a better understanding of overall effects on human health. It is also vital for a careful assessment of safety and efficacy, and prediction of interactions among xenobiotics including natural products.

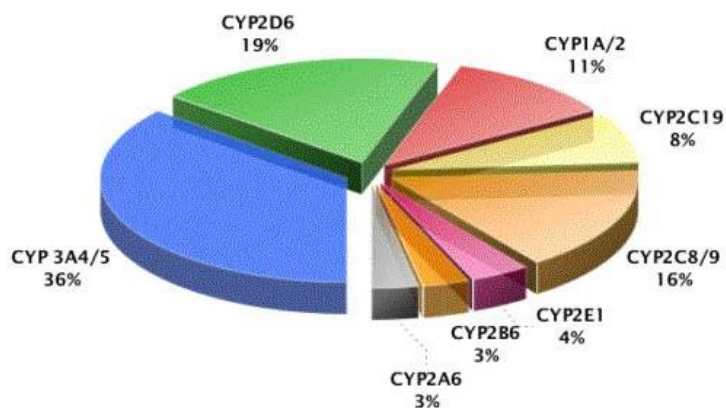


Figure 3.3. Distribution of the Metabolism of the Xenobiotics across Various CYP Isoforms and Factors Affecting their Expression

3.1.1. Cytochrome P450 Catalytic Cycle

Cytochrome P450 enzymes are metalloenzymes containing a heme iron center at the active site and are therefore termed as heme proteins. The heme iron in its native ferric state (Fe^{3+}) is stable and is bound by a protoporphyrin IX, along with a thiolate group arising from cysteine and water. Binding of the substrate to the low spin ferric state displaces the water molecule from the center and reduces iron to the ferrous state (Fe^{2+}).

Cytochrome P450 enzymes require activation of molecular oxygen for their catalytic activity. Binding of molecular oxygen to the heme center followed by subsequent reduction, protonation and heterolysis of heme bound oxygen results in the formation of iron-oxo state (Fe^{5+}) that oxidizes the substrate to the oxygenated product (Figure 3.4). The derivation of the name, P450 originates from the absorption maximum for the enzyme at 450nm, characteristic of the complex formed through the binding of carbon monoxide to the ferrous (Fe^{2+}) state⁴⁸.

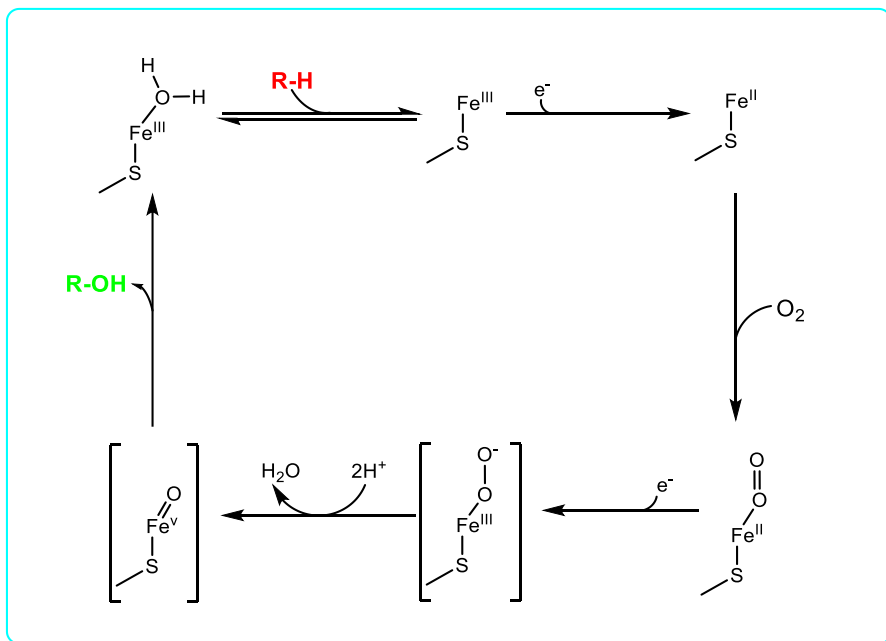


Figure 3.4 Schematic Representation of Cytochrome P450 Catalytic Cycle

3.1.2. Cytochrome P450 Mediated Reactive Oxygen Species Generation

Cytochrome P450 enzymes are also a major producer of the endogenous reactive oxygen species inside the cell. Inefficient coupling of the substrates to the cytochrome

Persistent production of reactive oxygen species by cytochrome P450 through NADPH consumption is an inevitable event in both the presence and absence of the substrates. Factors such as the type of substrate, pH, ionic strength and oxygen concentration also affect the production of reactive oxygen species by cytochrome P450 enzymes⁴⁹. In addition, certain CYPs catalyze some less favorable reactions including activation of xenobiotic substrates leading to the generation of highly reactive electrophilic species called reactive metabolites such as epoxides, carbonium and nitrenium ions that may result in toxicity^{50, 51}. This process of transformation of innocuous chemicals to a potentially deleterious metabolite is referred to as bioactivation or metabolic activation. The resultant products of bioactivation are not efficiently detoxified particularly when the balance between their production and elimination is disrupted. Therefore, bioactivation forms the basis for the toxicities associated with several innocuous xenobiotics. Furthermore, cytochrome P450 enzymes contribute towards the generation of approximately two-third of carcinogen activation. Therefore, the mechanisms of toxicity associated with the cytochrome P450 mediated generation of reactive oxygen species have significant toxicological consequences. The enzyme isoforms, particularly CYP1A1/2, CYP2A6 and CYP2E1, are noteworthy for their roles in this process⁵² (Figure 3.6).

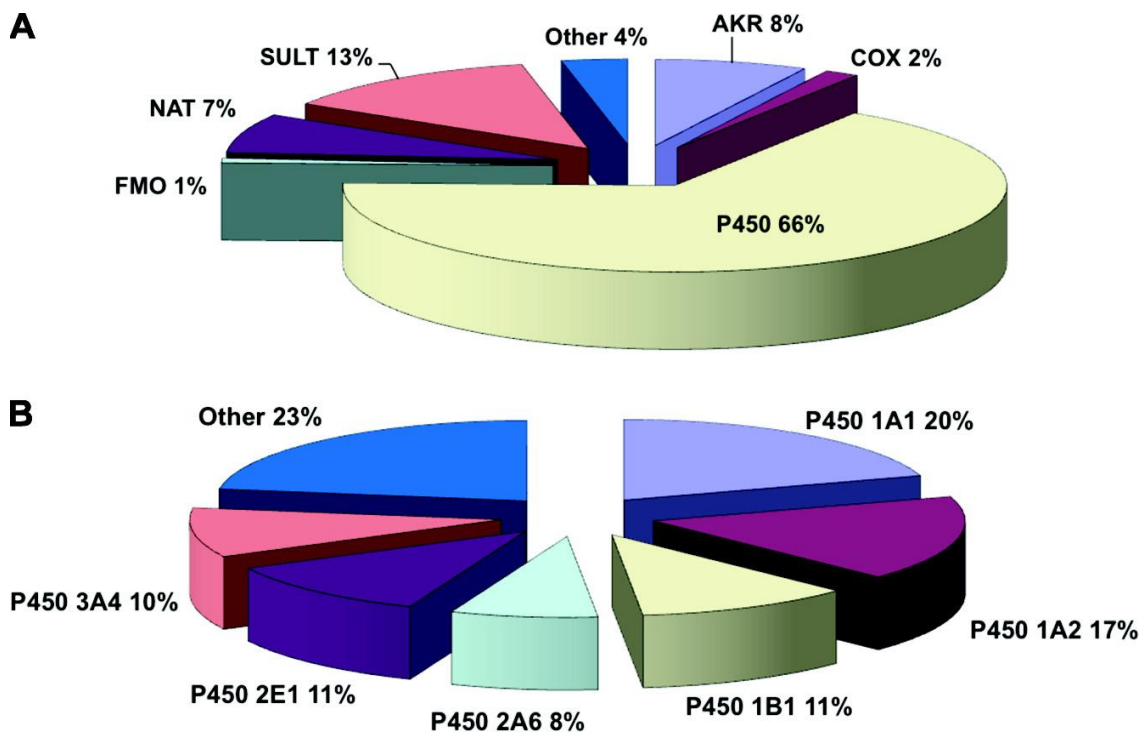


Figure 3.6 Contributions towards the Generation of Reactive Species by Various Human Enzymes (A). Distribution of P450 Mediated Activation Reactions among Human P450 Enzymes (B).

Tightly controlled production of reactive oxygen species is an important constitutive process with critical roles ranging from cellular development to cellular toxicity. At low concentrations, reactive oxygen species are very well recognized to serve the role of secondary messenger in signal transduction pathways. Contrary to this, reactive oxygen species also serve as one of the central elements of cellular toxicity leading to the pathogenesis of many diseases. Another complication arising from cytochrome P450 enzymes is bioactivation or metabolic activation results from the conversion of physiologically inert substrates or xenobiotics to potentially deleterious

metabolically reactive and toxic compounds. Certain xenobiotics capable of undergoing redox cycling during the course of metabolism produce reactive oxygen metabolites. The mechanisms of toxicities precipitated from metabolites formed through bioactivation are very similar to the toxicities associated with reactive oxygen species. The reactive intermediates can also interact with molecular oxygen to produce reactive oxygen species. In addition, cytochrome P450 enzymes are highly sensitive to the chemical exposure resulting in the induction or inhibition of their expression.

3.1.3. Cytochrome P450 2A6

CYP2A6 is a human cytochrome P450 from family 2, sub-family A and polypeptide 6. It is predominantly found in liver but is also expressed in extrahepatic tissues such as lung, trachea and nasal mucosa. CYP2A6 comprises only about 4% of the total hepatic cytochrome P450 and metabolizes 3% of drugs. It metabolizes low molecular weight nonplanar compounds and is widely recognized as the major enzyme responsible for the metabolism of psychoactive tobacco ingredient, nicotine to inactive cotinine and subsequently to trans-3'-hydroxycotinine. In fact, CYP2A6 has been proposed a novel therapeutic target for smoking cessation owing to its major contribution to nicotine metabolism. It is, however, involved in the bioactivation of tobacco-related N-nitrosamines and other carcinogens, which leads to the induction of oxidative stress resulting in cancer, cardiovascular and respiratory diseases⁵³. The metabolic activation of alkylnitrosamines with bulky chains is predominantly carried out by CYP2A6. It is also involved in the metabolic activation of environmental toxicants such as aflatoxin B1,

naphthalene, hexamethylphosphoramide, methyl-t-butyl ether^{54, 55}. Thus, CYP2A6 inhibition presents a potential strategy for protecting the cell from unwanted exposure to reactive metabolites thereby reducing the related cellular stress. Nonetheless, the conversion of anticancer prodrug tegafur to 5-fluorouracil is a clinically significant result of metabolic activation, thus unwanted inhibition of CYP2A6 may have pharmacological implications.

3.1.4. Cytochrome P450 2E1

CYP2E1 is expressed in both hepatic and extrahepatic tissues and is responsible for the metabolism of 3% of drugs. Low molecular weight compounds that are generally neutral and hydrophilic with planar configuration represent common substrates for this isoform. It usually metabolizes compounds such as aliphatic alcohols, ethers, halogenated alkanes, endogenous acetone and other ketone bodies⁵¹. Elimination of endogenous acetone is largely carried out by CYP2E1. In fact, increased CYP2E1 activity has been observed in hyperketonemia as a cellular adaptive response for ketone bodies elimination. Substrates of CYP2E1 also include many industrial chemicals, occupational toxicants and environmental pollutants in addition to procarcinogens.

CYP2E1 can directly form free radicals through disruption of its catalytic cycle leading to the leakage of activated oxygen as reactive species or by generating reactive metabolites through the activation of the xenobiotics. It is a potent generator of superoxide in aerobic environment and its tendency to generate reactive oxygen species through the leaky catalytic cycle makes it toxicologically important^{49, 56}. CYP2E1 is also

responsive to a variety of factors such as exposure to xenobiotics, metabolic and endocrine disorders, and several other pathophysiological conditions. Alcohol induces CYP2E1 and its abuse results is largely responsible for hepatocellular damage causing inflammation, steatosis and cirrhosis. For example, reversible induction of the enzyme through moderate alcohol consumption and its subsequent involvement in ethanol oxidation generates reactive oxygen species. Another important feature arises from the significant localization of CYP2E1 within the mitochondria, which further precipitates its deleterious effects. CYP2E1 also generates toxic and carcinogenic compounds from environmental pollutants such as nitrosamines in cigarette smoke, and has been implicated in drug-induced cytotoxicity⁵³. The reactive metabolites produced by this enzyme cause drug-induced hepatotoxicity as observed with paracetamol and halothane^{57, 58}.

Moreover, CYP2E1 regulation is complex including inhibition, induction, transcriptional activation and post-translational modifications. The highly inducible nature of this enzyme by small molecular xenobiotics such as acetone, alcohol and isoniazid results in increased vulnerability toward drug-induced cytotoxicity⁵¹. For example, increased toxicity of paracetamol in chronic alcoholics results from CYP2E1 induction by alcohol⁵⁹. Furthermore, environmental pollutants such as azoxymethane, acrylonitrile, benzene, nitrosamines and halogenated hydrocarbons are metabolically activated by CYP2E1 to carcinogenic compounds^{53, 60, 61}.

Inhibition of CYP2E1 by various compounds including natural products has been studied extensively as a measure to reduce the alcohol-induced and acetaminophen-

induced CYP2E1 mediated toxicity and thereby protect the cells *in vitro* and *in vivo*. Organosulfur compounds from cruciferous vegetables such as diallylsulfide, diallyldisulfide sulforaphane, phenylethylisothiocyanates and S-allylmercaptocysteine have been shown to inhibit CYP2E1 enzymatic activity and also protein ⁶²⁻⁶⁵. Lycopene from tomatoes, curcumin from ginger rhizomes, rhein from aloe, and fennel and raspberry leaf extracts has been shown to oppose the adverse effects of CYP2E1 mediated toxicities ⁶⁶⁻⁶⁹. Therefore, inhibition of CYP2E1 with concurrent use of natural products that are safe appears to be viable strategy to mitigate hepatic damage.

Further, in comparison with other CYP enzymes involved in drug metabolism, CYP2A6 and CYP2E1 mediated generation of reactive species is greater relative to its role in drug metabolism. Therefore, inhibition of this enzyme may prove beneficial in certain conditions. The potential benefits of selective inhibition of CYP2A6 and CYP2E1 underscore the need for identification of specific inhibitors of these isoforms. Despite this, very few inhibitors specific to each of these isoforms have been identified. Extending this search to natural products may ultimately lead to alternative strategies for reducing the deleterious effects of exposure to environmental toxicants and lead to effective natural approaches to maintaining good health.

3.1.5. The Açaí Berry

Açaí berries have received tremendous attention in the recent years from general population that it emerged as a novel nutraceutical. The health benefits of açaí are often

obscure with little scientific evidence derived from *in vitro* antioxidant assays where quenching of reactive chemical species by the constituents of açai was the main criteria.

Açai extracts have been shown to ameliorate oxidative stress in various *in vitro* assays^{70, 71}. Low molecular weight compounds belonging to several molecular classes have been found to inhibit CYP2A6 and CYP2E1. Açai is so far found to have compounds belonging to several molecular classes including anthocyanins, proanthocyanidins and flavonoids^{72, 73}. These compounds or other compounds awaiting identification in the açai may have the potential to inhibit CYP2A6 and CYP2E1. The underlying mechanisms responsible for reduced generation of reactive oxygen species, particularly in relation to the involvement of CYPs have never been studied. Therefore, identification of chemical constituents in açai berry extract that inhibit CYP2A6 and CYP2E1 and the mechanism by which the identified inhibitors exert their action is particularly important in evaluating one aspect of the antioxidant potential of the açai berry.

Recently, there has been a growing interest in understanding the effects of phytochemicals on normal drug metabolism. Currently, there is a wide spread use of herbal preparations for various disease conditions as complementary and alternative therapeutic alternative. Therefore, the therapeutic outcomes of the phytochemicals present in the herbal supplements in addition to the adverse effects and also their potential for interactions upon co-administration with various drugs are of increasing interest. Certain phytochemicals are capable of inducing or inhibiting the drug metabolizing cytochrome P450 enzymes. Detoxification is the principal biological

function of cytochrome P450 enzymes and is achieved through the oxidative metabolism of various foreign compounds. There are a lot of variations observed in the pharmacokinetics of various drugs in relation to the consumption of phytochemicals as herbal supplements for health benefits. For example, the furanocoumarins such as bergamontin and 6',7'-dihydroxybergamontin present in grapefruit juice are potent inhibitors of CYP3A4 enzyme. CYP3A4 is involved in the metabolism of approximately one-third of the drugs on market. Inhibition of CYP3A4 can lead to clinically relevant adverse effects that sometimes could lead to life-threatening conditions⁷⁴. An additional goal of this study was to probe the potential for acai products to interfere with normal drug metabolism, and thus it's potential to bring about unwanted drug interactions.

Currently, there is no evidence of the interactions between the constituents of açai berry extracts and various drug metabolizing cytochrome P450 enzymes. The availability of this information is required for assisting the medical community for a better and effective use of açai as herbal supplement. Furthermore, certain CYP isoforms are also involved in oxidative biotransformation of various procarcinogens including polycyclic aromatic hydrocarbons and tobacco-related nitrosamines to highly reactive species that are toxic to cells. In some instances, oxidative stress is biochemically connected to drug metabolism leading to several pathologies as a consequence.

In vitro models using S9 fractions of human liver microsomes and cDNA expressed enzymes are commonly used in the identification of inhibitors of cytochrome P450 enzymes. The data obtained from *in vitro* experiments may prove to be

complementary in identifying probable adverse interactions including drug-herbal interactions.

The goals of the current study were to understand the inhibition of cytochrome P450 enzymes by various crude extracts of açai berry using cDNA expressed enzymes in order to gain new insights into the susceptibility of inhibition of various cytochrome P450 enzymes by açai berry extracts. This forms the basis for the understanding of any potential interactions of açai berry extracts with cytochrome P450 enzymes and possibly the interactions between açai berry extracts with any co-administered drugs. Therefore, a panel of cytochrome P450 enzymes were screened for inhibition by açai berry extracts. In addition, inhibition of two of the toxicologically important CYP isoforms, namely CYP2A6 and CYP2E1 was extensively studied using bioassay-guided fractionation approach in an attempt to establish the basis for use of açai berry constituents for possible health benefits arising from inhibition of these toxicologically important enzymes.

3.2. Materials and Methods

3.2.1. Chemicals and Reagents

All the chemicals for CYP assays and solvents for bioassay-guided fractionations and chromatography were HPLC grade reagents were purchased from Fisher Scientific and reagents were prepared using reagent grade chemicals or highest purity available.

3.2.2. Human Liver Microsomes and cDNA Expressed Supersomes

Pooled human liver microsomes obtained from Molecular Toxicology Inc., (Asheville, NC) and cDNA expressed enzymes obtained from Xenotech LLC., (Lenexa, KS) were made into 100 µl aliquots and stored at -80°C until used. The total protein concentration reported were 23.3 and 10 µg/µl for human liver microsomes and cDNA expressed supersomes, respectively.

3.2.3. Açai Berry Extracts

Freeze-dried açai berry powder was obtained from Optimally Organic Inc., (Westlake Village, CA) and stored at -80°C until used. All the material used in the study arrived from a single lot and a corresponding voucher specimen was deposited on file at the Herbarium of the University of North Carolina at Chapel Hill, NC. The authenticity of the sample was verified by DNA identification testing by Authen Technologies, LLC. (Richmond, CA) that confirmed that the genomic DNA of freeze-dried açai berry powder used in the study is consistent with *Euterpe oleracea* and is divergent from other closely related species as well. All the fractions generated from the bioassay-guided fractionations were carried out by Dr. Nicholas Oberlies research group at University of North Carolina at Greensboro. The fractions generated were conveniently distributed into aliquots and stored at 4°C until used.

3.2.4. Bioassay-guided Fractionation of Açai

Bioassay-guided fractionation offers the opportunity to isolate bioactive constituents from complex natural products and was achieved by practicing standard extraction procedures and chromatographic separation techniques. The general approach towards bioassay-guided fractionation for *in vitro* CYP inhibition is depicted in figure 3.7. Initially, crude extracts were generated and subsequently fractionated based on their potency towards the CYP isoforms and the process was repeated to a series of fractionations until the pure compounds were isolated. The identity of isolated constituents was determined by MS and NMR techniques, which were all carried out in the research laboratory of Dr. Nicholas Oberlies at the University of North Carolina at Greensboro.

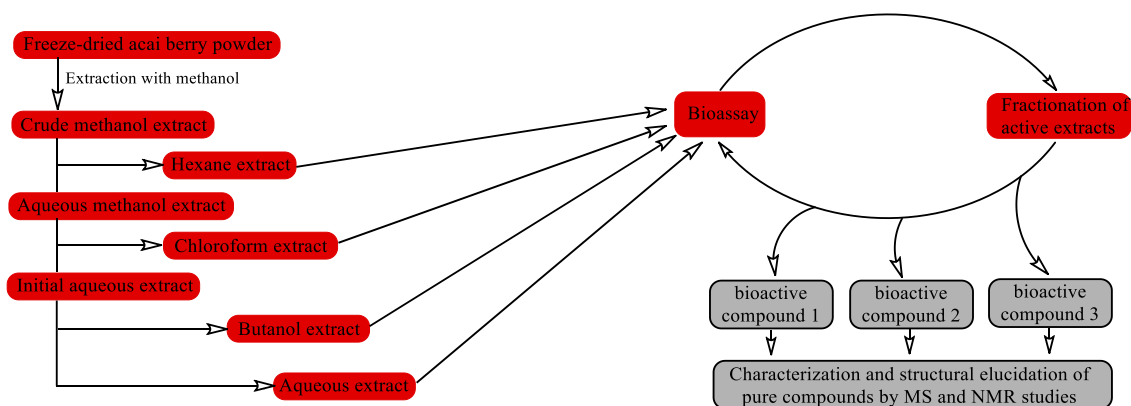


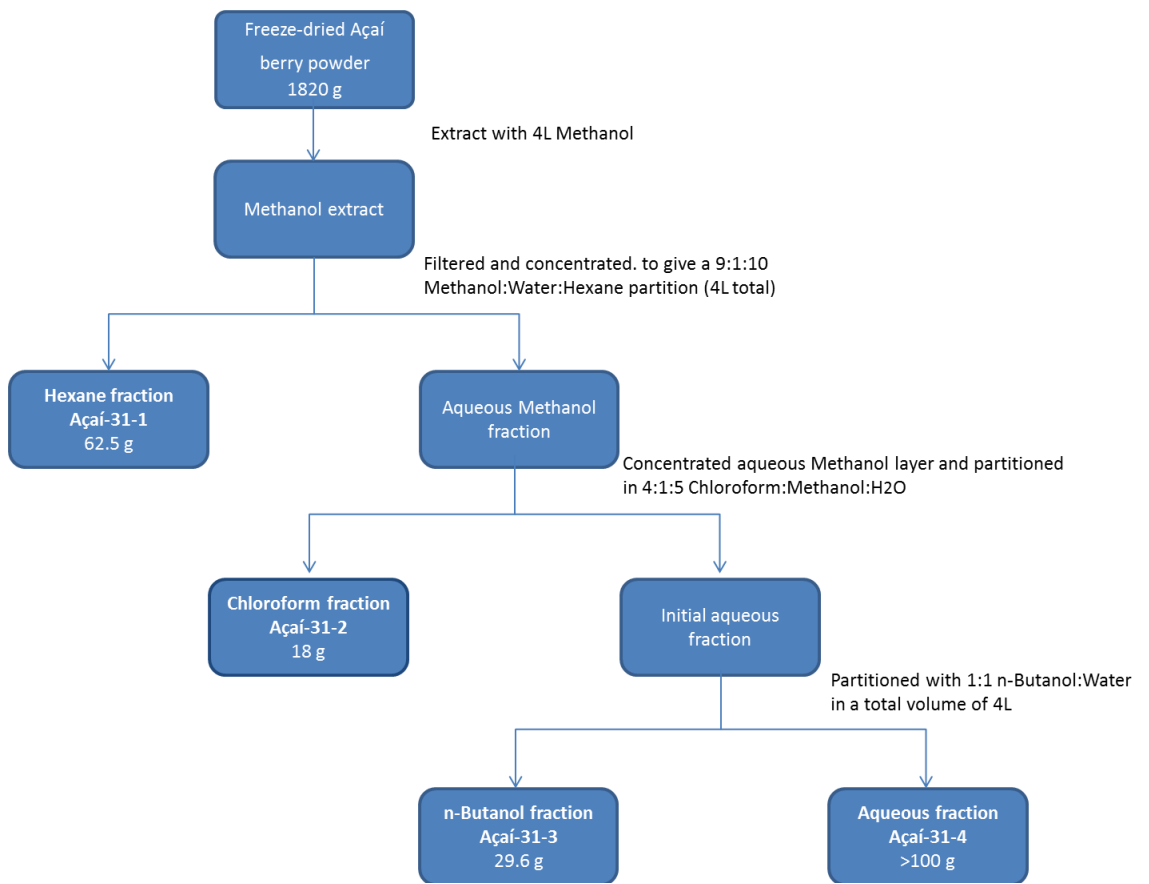
Figure 3.7 Schematic Representation of Bioassay-Guided Fractionation Approach

Briefly, the freeze-dried açai berry powder was extracted with methanol and subsequently partitioned between hexane, chloroform, butanol and aqueous phases,

respectively. The crude extracts were initially tested for CYP inhibition using cDNA expressed enzymes including CYP1A1, CYP1A2, CYP2A6, CYP2B6, CYP2C8, CYP2C9, CYP2D6, CYP2E1 and CYP3A4. The selection of these enzymes was based on their relevance to the metabolism of a vast majority of xenobiotics including drugs and natural product based supplements.

3.2.5. Preparation of Crude Açai Berry Extracts

Bioassay-guided fractionation of freeze dried açai berry powder was initiated by employing solvent partitioning techniques. The freeze dried açai berry powder was initially extracted with methanol. The methanol extract was then subjected to series of partitioning events across the solvents beginning with hexanes, followed by chloroform, butanol and finally water to produce the initial four crude açai berry extracts as illustrated in Scheme 1. These solvents allowed a very good separation of the chemical constituents of açai based on their affinity to the partitioning solvents. For example, partitioning of methanol extract with hexanes allows for the extraction of fats and lipids as hexane extract. The hexane extract was then dried under inert atmosphere such as nitrogen to produce the initial crude hexane extract denoted by Açai-31-1. The aqueous methanol extract was then partitioned with chloroform to produce the crude chloroform extract and dried to produce crude chloroform extract denoted by Açai-31-2. The remaining aqueous methanol extract was subsequently partitioned between n-butanol and water to produce the crude butanol and aqueous extracts and are represented by Açai-31-3 and Açai-31-4, respectively.



Scheme 1. Bioassay-guided Fractionation of Freeze-dried Açai Berry Powder.

The crude extracts that were found to be active in the *in vitro* inhibition of Cytochrome P450 enzymes using human liver microsomes were selected and subjected to a series of fractionations in an attempt to characterize the chemical constituents that were responsible for the observed inhibition. In the current study, two CYP isoforms, namely CYP2A6 and CYP2E1, with established roles in toxicology over metabolism were extensively studied.

3.2.6. Sample Preparation of Açai for CYP Inhibition

All the fractions generated through the bioassay-guided fractionation were partitioned into aliquots for future use. Methanol was used as a co-solvent in the preparation of açai samples for cytochrome P450 inhibition, however as methanol itself can affect cytochrome P450 activity, its concentration in the final reaction mixture was maintained at a low level. For example, each aliquot initially received methanol in an amount that would produce 0.25% final concentration in the incubation mixture.

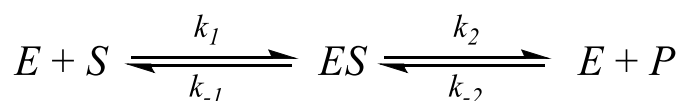
3.2.7. Cytochrome P450 Assays

Açai constituents, like most other drugs might act as substrates or inhibitors of enzymes including cytochrome P450 enzymes. The interactions between the drugs and the açai constituents upon co-administration are better understood using Michaelis-Menten equation. All the enzyme activity assays were developed using substrates that are specific as well as selective to the isoform under test. An initial Michaelis-Menten plot for each of the isoforms tested was generated in order to understand the kinetics of the enzyme function using appropriate probe substrates. Screening of açai berry extracts for the inhibition of CYP isoforms employed only a single substrate concentration. This single substrate concentration for screening experiments was chosen to be close to the observed K_m from the respective Michaelis-Menten plots. The results of enzyme inhibition from screening studies was expressed as percent inhibition with respect to the control reactions. Measurement of inhibition constant, K_I for the açai berry extracts towards CYP isoforms was carried out using the concentrations of açai berry extracts

observed to produce more than 50% inhibition in the initial screening experiments. All the experiments were done in triplicates.

3.2.8. Michaelis-Menten Model of Enzyme Kinetics

Initially, the kinetics of Cytochrome P450 activity was studied using Michaelis-Menten model of enzyme kinetics using probe substrate. An enzyme following a typical Michaelis-Menten kinetics establishes the relationship between the reaction rate and substrate concentration (Figure 3.8). It is characterized by an initial linear increase in rate of reaction where the amount of product [P] formed is proportional to the substrate [S] concentration. Then, the rate of reaction slowly begins to level off and assumes an asymptotic maximum, V_{\max} , at saturating substrate concentration. At low substrate concentrations, the rate of reaction depends on substrate concentration but at high substrate concentrations, the rate of reaction is independent of substrate concentration. The Michaelis constant, K_m , is the substrate concentration at which the active site of the enzyme is half-filled and rate of reaction is half of V_{\max} . It is essentially the concentration at which the reaction rate is half of the predicted V_{\max} . Therefore, K_m is the measure of substrate affinity for the enzyme where low K_m indicates high affinity and vice-versa.



By measuring the rates of catalysis over a range of substrate concentrations, the Michaelis constant, K_m , and maximum rate, V_{\max} , can be readily calculated.

$$V = \frac{d[P]}{dt} = \frac{V_{\max} [S]}{K_m + [S]}$$

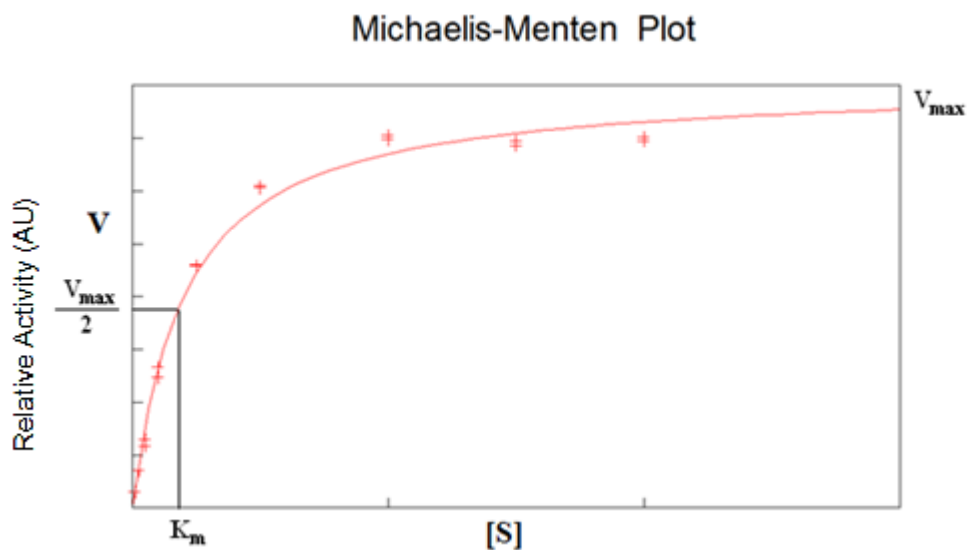


Figure 3.8 A Typical Michaelis-Menten Plot illustrating the Relationship between the Substrate Concentration [S] and the Reaction Rate V and Predicted K_m and V_{\max}

3.2.9. Screening of Açai Extracts

Screening of açai berry extracts for CYP inhibition involved a single probe substrate concentration that was close to the observed K_m as measured from Michaelis-Menten kinetics for each isoform. A concentration close to the K_m is appropriate for inhibition studies as K_m implies that there can be significant competition for the enzyme molecules (Figure 3.9). Use of single probe concentration around K_m also allows for high-through put analysis of various fractions of açai berry extracts generated using bioassay-guided fractionation. All the analyses following the enzymatic incubations were

carried out using appropriate methods for each enzyme isoform. The results of enzyme inhibition were expressed as percent inhibition in comparison to the control reactions.

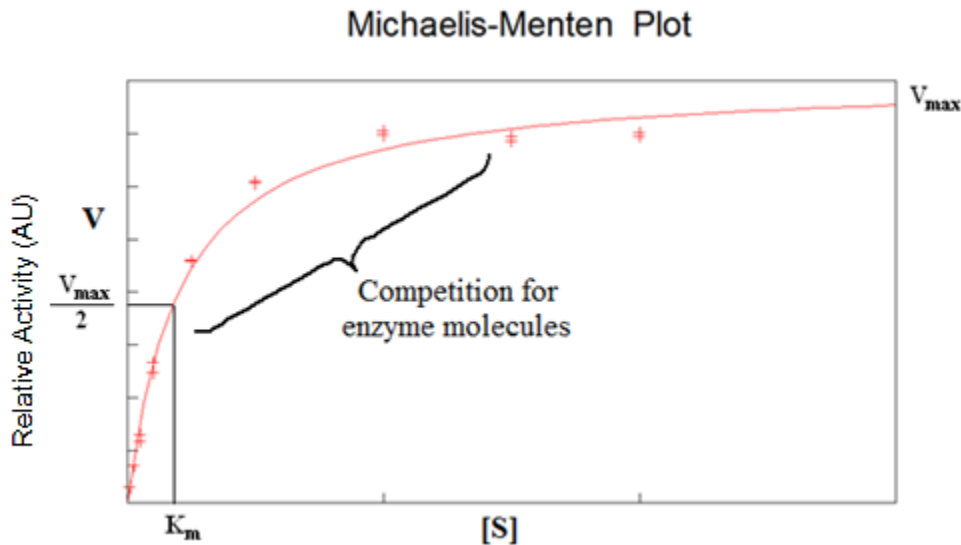


Figure 3.9 A Typical Michaelis-Menten Kinetics Plot illustrating the Concentrations suitable for Inhibition Studies

3.2.10. Determination of Inhibition Constant (K_I)

Inhibition constant K_I for the açai berry extracts towards P450 isoforms was measured using the concentrations of açai berry extracts observed to produce 50% inhibition in the initial screening experiments. The amount of inhibition produced by açai berry extracts was plotted against a Michaelis-Menten plot from control reactions. The inhibition alters the kinetics of the enzyme resulting in a change in K_m or V_{max} or both. During competitive inhibition, the K_m increases while the V_{max} remains unchanged indicating that the substrate concentration required to reach V_{max} in the presence of inhibitor is greater compared to that of the absence of the inhibitor. Competitive

inhibition can be superseded by an increase in substrate concentration. Any change observed with regard to K_m is referred to as K_m^{app} .

$$\frac{K_m^{app}}{K_m} = 1 + \frac{[I]}{K_I}$$

where K_I is the inhibitor's dissociation constant or inhibition constant, and $[I]$ is the inhibitor concentration. By rearranging the equation, K_I for the inhibitor can be calculated.

$$K_I = \frac{[I] * K_m}{K_m^{app} - K_m}$$

In case of noncompetitive inhibition, V_{max} decreases while the K_m remains unchanged and any change in V_{max} is referred to as V_{max}^{app} .

$$\frac{V_{max}}{V_{max}^{app}} = 1 + \frac{[I]}{K_I}$$

$$K_I = \frac{[I] * V_{max}^{app}}{V_{max} - V_{max}^{app}}$$

3.2.11. Isoform Specific Assay Conditions and Modes of Analyses

All the kinetic studies were conducted using specific probe substrates selective for each of the enzyme isoforms in both S9 fractions of human liver microsomes and cDNA expressed supersomes as needed. Enzymatic incubations were performed in a total

volume of 200 μ l containing appropriate probe substrates and enzyme isoforms in 100 mM phosphate buffer (pH 7.4). Enzymatic reactions were initiated by the addition of final concentration of 1 mM NADPH and incubated on water bath for 10-30 minutes. The reactions were quenched by the addition of ice-cold 7% perchloric acid and placed on ice for 10 min followed by centrifugation at 16,000 rpm. The clear supernatant was then transferred to a clean vial for analysis using HPLC using UV detector or liquid chromatography tandem mass spectrometry for measurement of enzymatic activities.

The probe substrates and the products formed in various CYP assays together with the substrate concentrations used for Michaelis-Menten kinetics studies were illustrated in Table 3.1. The observed K_m and the actual substrate concentrations used for screening of açai berry extracts were shown in Table 3.1. The detection parameters for products of the enzymatic reactions of each isoform were summarized in Table 3.2.

Table 3.1 Activity Assay Parameters for CYP isoforms

CYP Isoform	Substrate	Metabolite	Substrate concentration used for Michaelis-Menten Kinetics (μM)	Substrate concentration used for K_m (μM)
1A1	7-ethoxycoumarin	7-hydroxycoumarin	1-200	20
1A2	Naphthalene	1-naphthol	25-300	80
2A6	Coumarin	7-hydroxycoumarin	0.5-10	2
2B6	Bupropion	3-hydroxybupropion	25-400	36
2C8	Amodiaquine	N-desethylamodiaquine	0.5-16	2
2C9	Diclofenac	4'-hydroxydiclofenac	20-100	50
2D6	Dextromethorphan	Dextrorphan	2.5-120	2
2E1	<i>p</i> -nitrophenol	<i>p</i> -nitrocatechol	20-200	50
3A4	Nifedipine	Dehydronifedipine	20-500	30

Table 3.2 Chromatographic Separation Parameters of CYP Activity Assays

CYP Isoform	Mobile Phase A:Acetonitrile with 0.1% Trifluoroacetic acid and B:Water with 0.1% Trifluoroacetic acid (% A/minutes)	Substrate (Retention Time in minutes)	Metabolite (Retention Time in minutes)
1A1	30/0:00; 30/10:00; 100/10:05; 100/13:00; 30/13:05; 30/16:00	7-ethoxycoumarin	7-hydroxycoumarin
1A2	25/0:00; 25/5:00; 100/5:05; 100/8:00; 25/8:05; 25/12:00	Naphthalene	1-naphthol
2A6	35/0:00; 35/10:00; 100/10:05; 100/13:00; 35/13:05; 35/16:00	Coumarin	7-hydroxycoumarin
2B6	15/0:00; 15/5:00; 100/5:05; 100/10:00; 15/10:05; 15/14:00	Bupropion	3-hydroxybupropion
2C8	0/0:00; 20/2:00; 30/8:00; 100/8:10; 100/10:10; 0/10:20; 0/10:20	Amodiaquine	N-desethylamodiaquine
2C9	25/0:00; 25/5:00; 100/5:05; 100/8:00; 25/8:05, 25/12:00	Diclofenac	4'-hydroxydiclofenac
2D6	10/0:00; 0/1:00; 100/8:00; 100/8:50; 10/9:00; 10/10:00	Dextromethorphan	Dextrorphan
2E1	25/0:00; 25/12:00; 100/12:05; 100/15:00; 25/15:05, 25/18:00	<i>p</i> -nitrophenol	<i>p</i> -nitrocatechol
3A4	10/0:00; 0/1:00; 100/8:00; 100/8:50; 10/9:00; 10/10:00	Nifedipine	Dehydronifedipine

Table 3.3. Detection Parameters of CYP Activity Assays

CYP Isoform	Substrate	Metabolite	HPLC UV Detection (nm)	LC-MS/MS Mode of Ionization, (m/z)
1A1	7-ethoxycoumarin	7-hydroxycoumarin	320	
1A2	Naphthalene	1-naphthol	250	
2A6	Coumarin	7-hydroxycoumarin	320	
2B6	Bupropion	3-hydroxybupropion	250	
2C8	Amodiaquine	N-desethylamodiaquine	345	
2C9	Diclofenac	4'-hydroxydiclofenac	280	
2D6	Dextromethorphan	Dextrophan		positive, 258
2E1	<i>p</i> -nitrophenol	<i>p</i> -nitrocatechol	340	
3A4	Nifedipine	Dehydronifedipine		positive, 345

Detection of products of enzymatic reactions using a high performance liquid chromatography, HPLC (Shimadzu) involved a C18 column for separation of the products of the enzymatic reactions. Mobile phase to achieve chromatographic separation of enzymatic reaction products to be measured comprised of water and acetonitrile containing 0.1% trifluoroacetic acid at appropriate flow rates with ratios suitable for efficient separation. Detection of metabolites in HPLC analyses was achieved using a UV detector. The mass spectrometric analysis were performed using Ultra Performance Liquid Chromatography, UPLC (Waters) coupled with Q Exactive Hybrid Quadrupole-Orbitrap Mass Spectrometer (Thermo) using appropriate modes of ionization suitable for quantification of metabolites formed in the incubations.

3.2.12. Data Analysis

Results were obtained from three different incubations and were represented as a percent inhibition. The activities were calculated from the mean \pm standard deviation for triplicate measurements. Percent activities were obtained by calculating the ratio of the average activities of the açai fractions to that of the solvent control measurements and expressed in percentage. Percent inhibitions were calculated by deducing the percent

$$\% \text{ Activity} = \left[\frac{\text{Test}}{\text{Control}} \right] * 100$$

$$\% \text{ Inhibition} = 100 - \% \text{ Activity}$$

3. 3. Results

Currently, the extensive use of herbal and dietary supplements as complementary and alternative medicine has increased the human exposure to a wide variety of phytochemicals. The adverse effects together with their potential to interact with drugs upon co-administration for most herbal preparations currently remains unexplored. The information relevant to use of herbal supplements is also beginning to be addressed in a systematic manner. However, investigation of the interactions of drugs with herbal and dietary supplements is a challenging task often requiring methodologies formulated and optimized discretely for the context of study. Since, these interactions results from an array of phytochemicals present in herbal supplements and unraveling the complexity of

phytochemical constituents is fundamental for a greater understanding of such interactions.

The current study begins with identification of individual CYPs that are susceptible to inhibition by crude extracts of açai. It begins with studying *in vitro* inhibition of açai berry extracts at crude level using cDNA expressed enzymes or supersomes in an attempt to dissect the interactions of açai with each of the CYP isoform. CYP inhibition by chemical constituents present in açai berry may lead to the interactions when co-administered with drugs. In addition, the inhibition of cytochrome P450 enzymes is one process by which phytochemicals may impair metabolic activation or bioactivation of certain chemical and procarcinogens. Therefore, inhibition of CYP2A6 and CYP2E1 was studied in greater detail to identify the inhibitors for these enzymes as a useful strategy for decreasing bioactivation process using human liver microsomes by employing bioassay-guided fractionation of açai.

3.3.1. *In vitro* Inhibition of cDNA Expressed Cytochrome P450 Enzymes

As the cDNA expressed enzymes or supersomes contain individual CYP isoforms, its use is devoid of any non-specific interactions that might arise from using human liver microsomes. Understanding of the Michaelis-Menten kinetic models is important for studying inhibition and therefore Michaelis-Menten plots were generated for each of the enzyme isoform using substrates selective for enzymes prior to the inhibition studies. The Michaelis-Menten plots generated for various CYP isoforms using supersomes were as follows.

3.3.2. CYP1A1 Assay

CYP1A1 catalyzes the O-demethylation of 7-ethoxycoumarin to 7-hydroxycoumarin or umbelliferone (Figure 3.10). The assay procedure for all CYP assays was generalized in section 3.2.11 and the activity assay and analytical parameters for the measurement of enzymatic activities were summarized in Table 3.1 and Table 3.2, respectively.

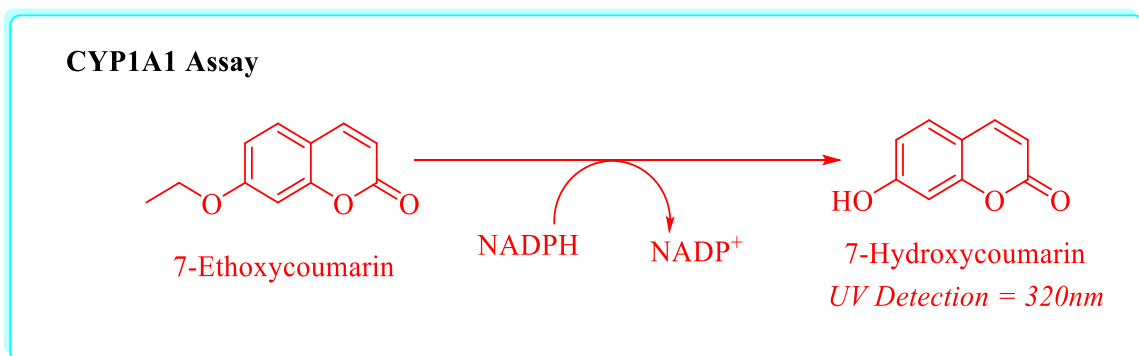


Figure 3.10 CYP1A1 Mediated Catalysis of 7-Ethoxycoumarin to 7-Hydroxycoumarin

Michaelis-Menten plots for CYP1A1 supersomes were generated using SlideWrite software (Advanced Graphics Software Inc.) by plotting the substrate 7-ethoxycoumarin concentrations against the amounts of metabolite 7-hydroxycoumarin formed in the incubation (Figure 3.11). The amount of metabolite, 7-hydroxycoumarin produced in the incubations were quantified relative to substrate concentrations using HPLC with UV detector at 320 nm and expressed as arbitrary area units (AU). The Michaelis-Menten kinetics plot indicated a K_m of 20 μM for O-demethylation of 7-ethoxycoumarin by CYP1A1 supersomes. Therefore, a substrate concentration of 20 μM

7-ethoxycoumarin was used in the subsequent experiments for screening of açai extracts for CYP1A1 inhibition. In a manner similar to Michaelis-Menten kinetics model, a range of substrate concentrations from 1-200 μM 7-ethoxycoumarin were used for K_i determinations of açai berry extracts.

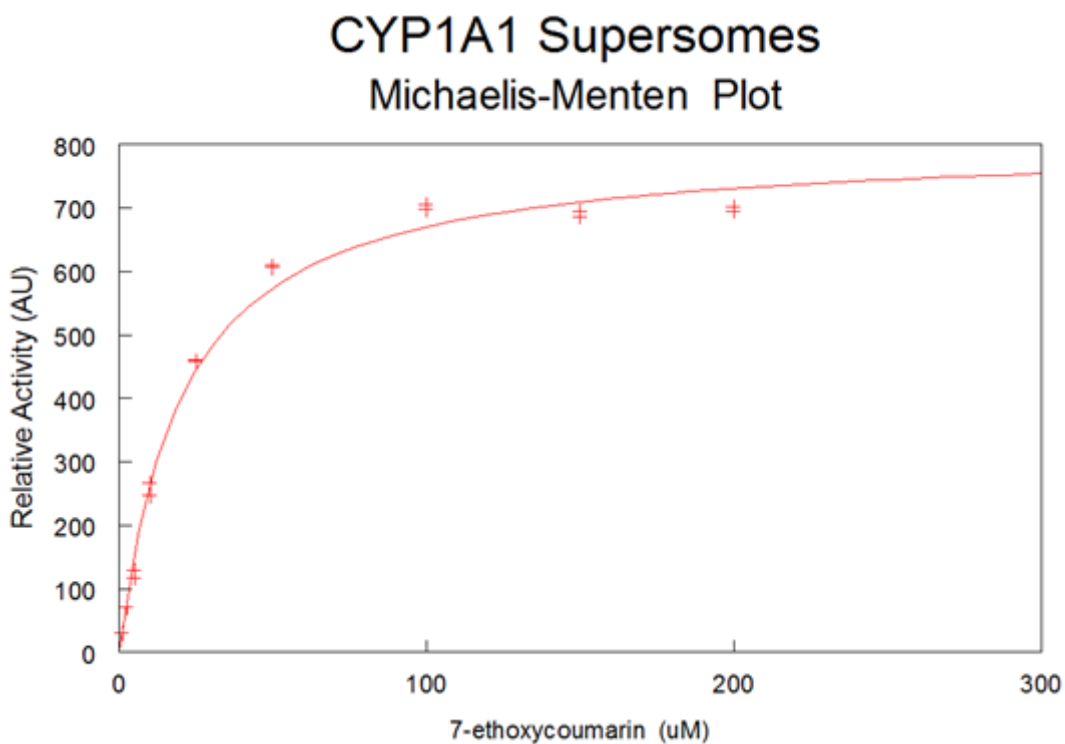


Figure 3.11 Michaelis-Menten Kinetics Plot for O-Demethylation of 7-Ethoxycoumarin by CYP1A1 Supersomes

3.3.3. CYP1A2 Assay

CYP1A2 assay using supersomes involved oxidation of naphthalene to 1-naphthol as shown in Figure 3.12.

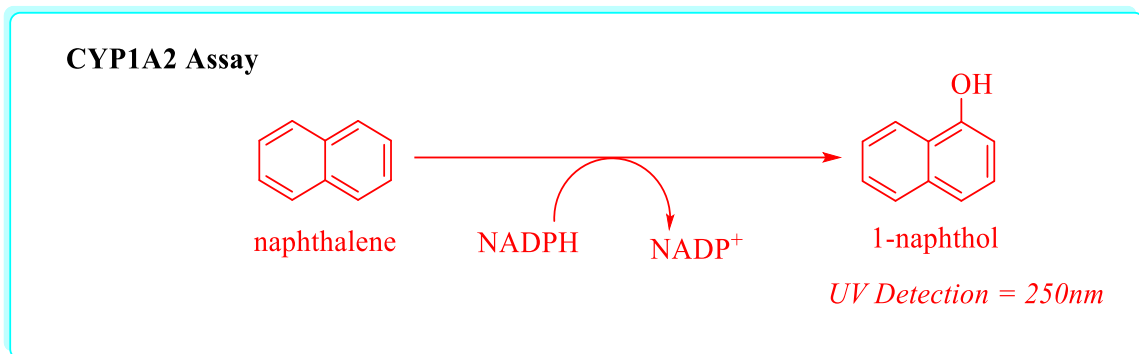


Figure 3.12 CYP1A2 Mediated Hydroxylation of Naphthalene to 1-Naphthol

Michaelis-Menten kinetics for hydroxylation of naphthalene to 1-naphthol by CYP1A2 supersomes were generated using SlideWrite software in a similar manner to that described under CYP1A1 assay (Figure 3.13). The K_m for CYP1A2 supersomes was found to be 35 μM naphthalene based on Michaelis-Menten kinetic study. Therefore, screening of açai extracts for CYP1A2 inhibition utilized a substrate concentration of 70 μM naphthalene.

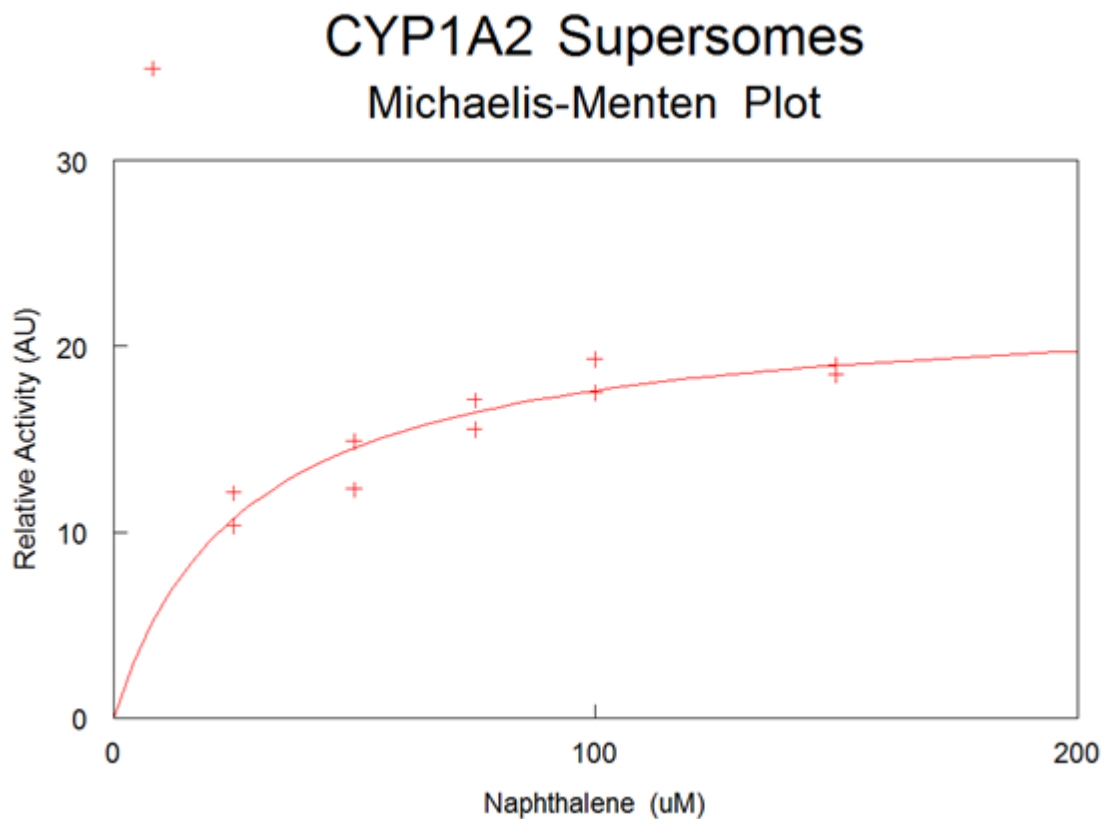


Figure 3.13 Michaelis-Menten Kinetics Plot for Hydroxylation of Naphthalene to 1-Naphthol by CYP1A2 Supersomes

3.3.4. CYP2A6 Assay

CYP2A6 assay was carried by studying coumarin-7-hydroxylation of coumarin to form 7-hydroxycoumarin or umbelliferone as illustrated in Figure 3.14.

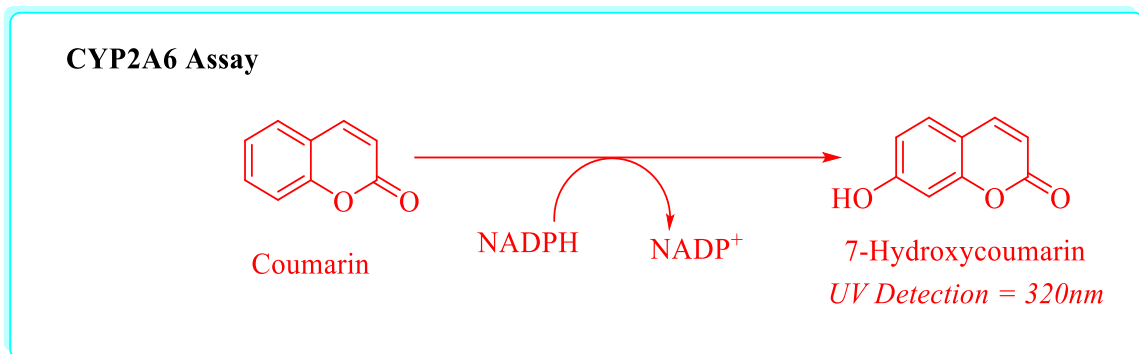


Figure 3.14 CYP2A6 Mediated Hydroxylation of Coumarin to 7-Hydroxycoumarin

Michaelis-Menten kinetics plots were generated using SlideWrite for coumarin-7-hydroxylation by CYP2A6 supersomes established the K_m to be 2.1 μM coumarin (Figure 3.15). Therefore, further studies into screening of açai extracts for CYP2A6 inhibition used a substrate concentration of 3 μM coumarin.

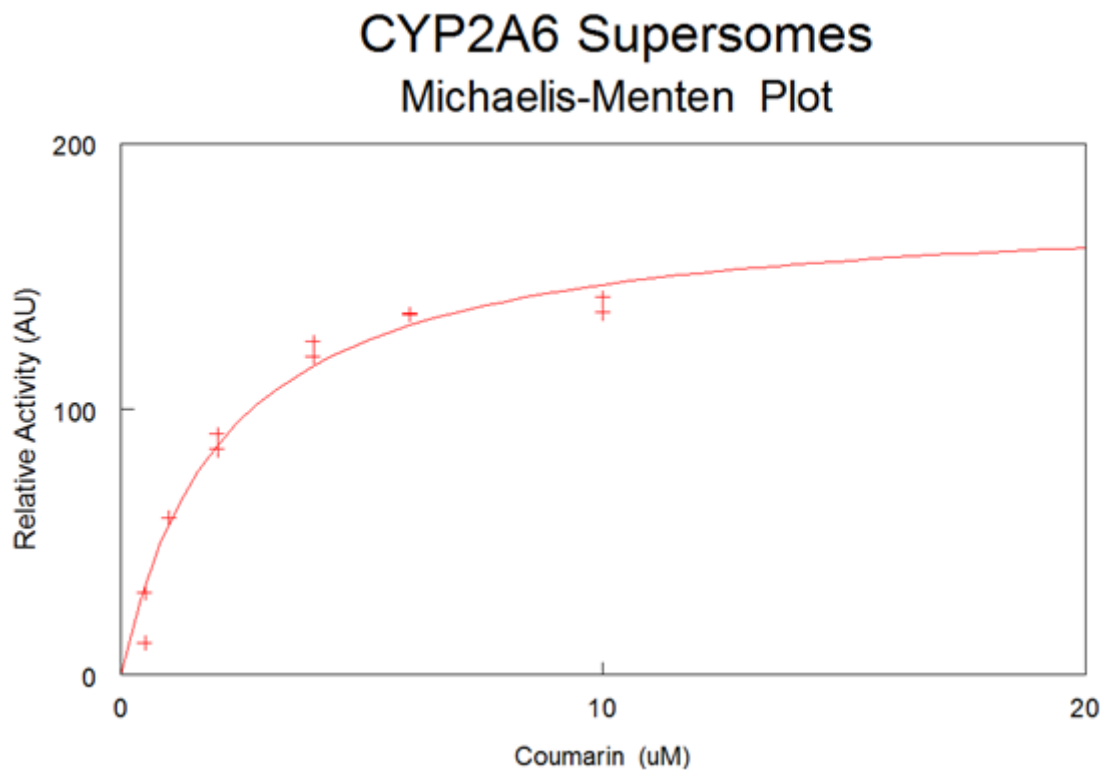


Figure 3.15 Michaelis-Menten Kinetics Plot for Hydroxylation of Coumarin to 7-Hydroxycoumarin by CYP2A6 Supersomes

3.3.5. CYP2B6 Assay

CYP2B6 catalyzes the hydroxylation of bupropion to (2S,3S)-hydroxybupropion, a major metabolite as depicted in figure 3.16. Bupropion is a drug used for treating depression and also smoking cessation and is metabolized by CYP2B6.

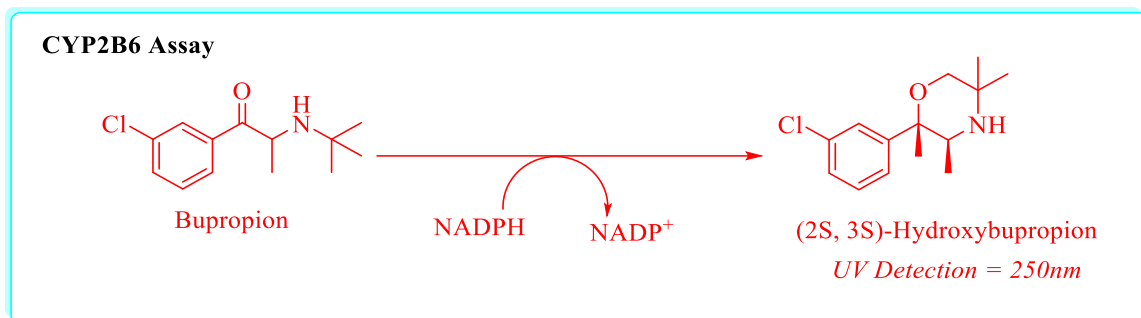


Figure 3.16 CYP2B6 Mediated Catalysis of Bupropion to (2S,3S)-Hydroxybupropion

The kinetic parameters were determined by developing a Michaelis-Menten kinetics plot for CYP2B6 mediated hydroxylation of bupropion to (2S,3S)-hydroxybupropion indicated the K_m of 36 μM bupropion and therefore 40 μM bupropion was utilized for screening of açai extracts for CYP2B6 inhibition (Figure 3.17). A range of substrate concentrations from 25-300 μM were employed for calculating K_I values for açai berry extracts as described for Michaelis-Menten kinetic model.

CYP2B6 Supersomes Michaelis-Menten Plot

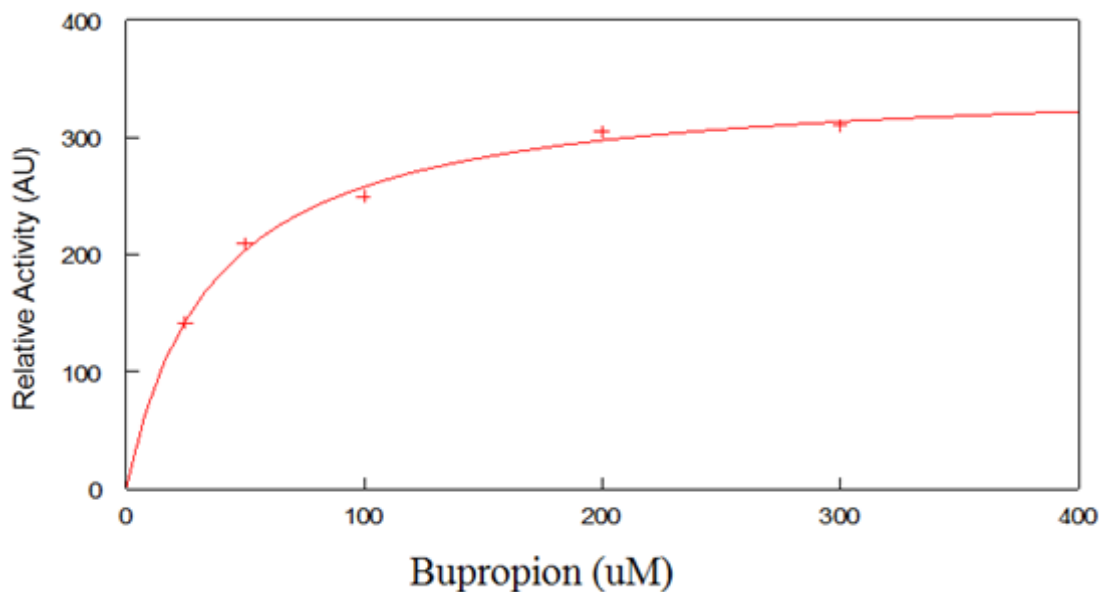


Figure 3.17 Michaelis-Menten Kinetics Plot for Hydroxylation of Bupropion to (2S,3S)-Hydroxybupropion by CYP2B6 Supersomes

3.3.6. CYP2C8 Assay

CYP2C8 mediated catalysis of N-deethylation of an antimalarial drug, amodiaquine to N-desethylamodiaquine was carried out for assessing the enzymatic activity of CYP2C8 as illustrated in figure 3.18.

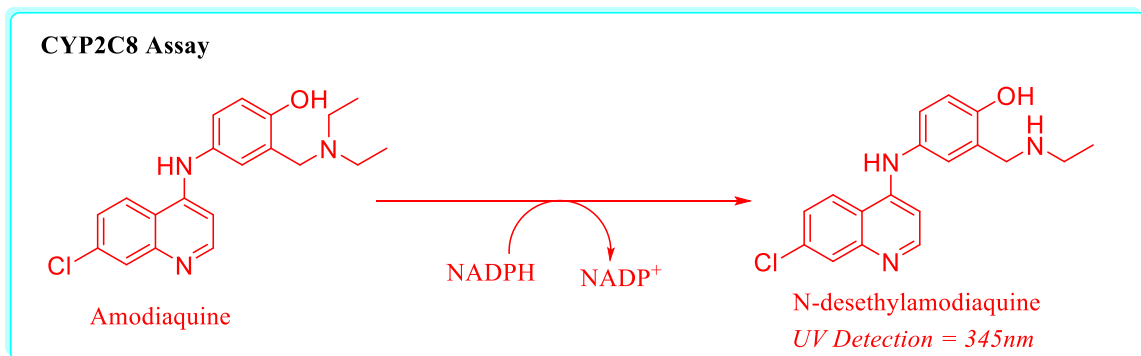


Figure 3.18 CYP2C8 Mediated N-Deethylation of Amodiaquine to N-Desethylamodiaquine

The K_m for CYP2C8 mediated N-deethylation of amodiaquine to N-desethylamodiaquine was found to be 2 μM (Figure 3.19). Subsequent experiments for screening of açai extracts for CYP2C8 inhibition were carried out at 2 μM amodiaquine whereas amodiaquine concentrations ranging from 0.5 to 16 μM were used for K_i determinations.

CYP2C8 Supersomes Michaelis-Menten Plot

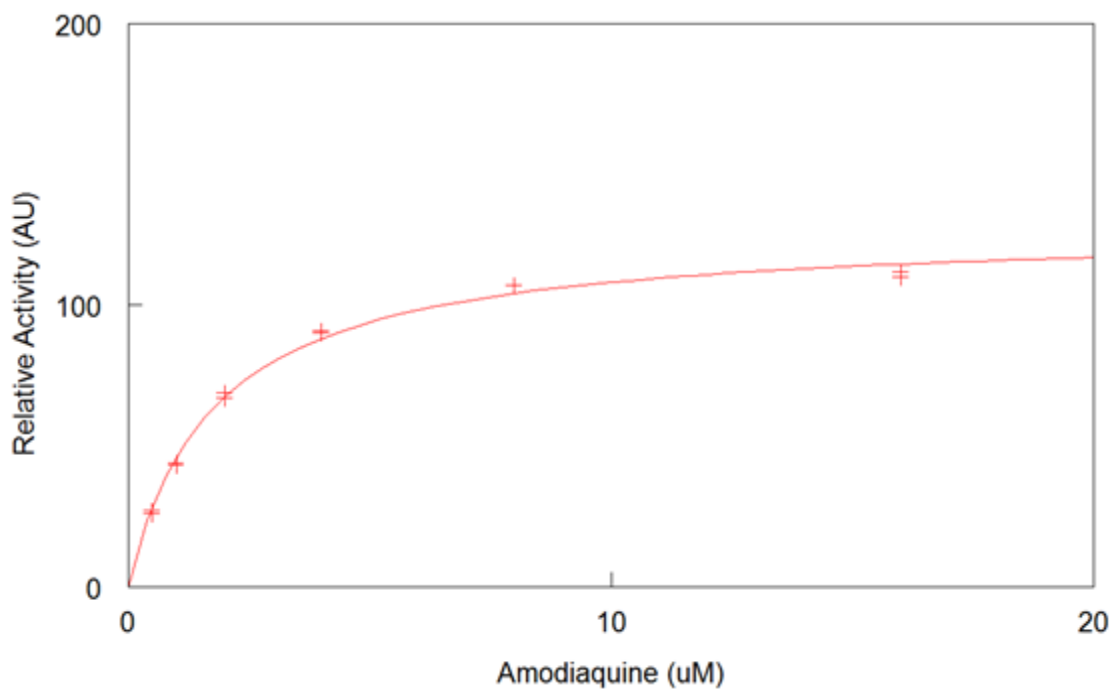


Figure 3.19 Michaelis-Menten Kinetics Plot for N-Deethylation of Amodiaquine to N-Desethylamodiaquine by CYP2C8 Supersomes

3.3.7. CYP2C9 Assay

CYP2C9 catalyzes the hydroxylation of a non-steroidal anti-inflammatory drug, diclofenac to 4'-hydroxydiclofenac as shown in figure 3.20. The K_m observed for CYP2C9 supersomes was found to be 55 μM and this concentration was used for screening of açai extracts for CYP2C9 inhibition (Figure 3.21).

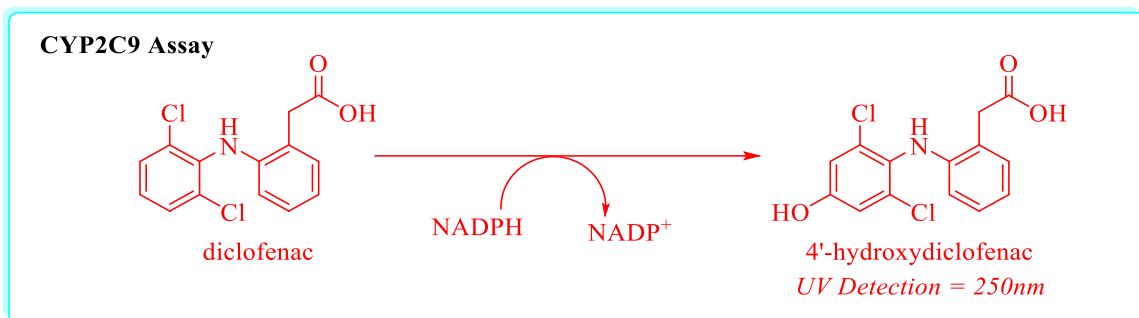


Figure 3.20 CYP2C9 Mediated Catalysis of Diclofenac to 4'-Hydroxydiclofenac

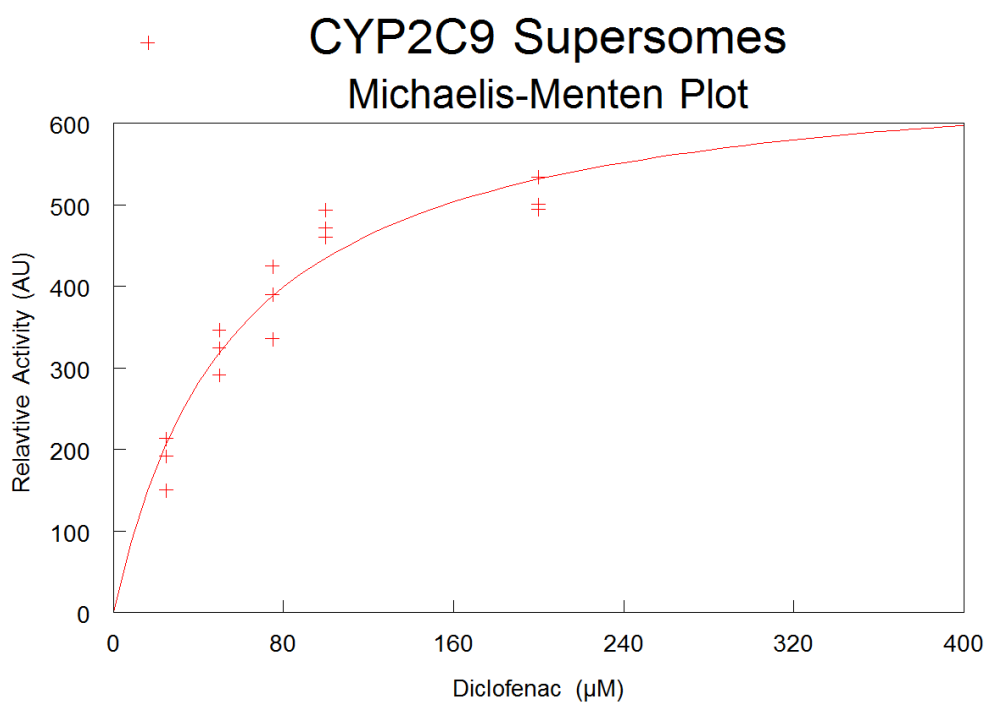


Figure 3.21 Michaelis-Menten Kinetics Plot for Hydroxylation of Diclofenac to 4'-Hydroxydiclofenac by CYP2C9 Supersomes

3.3.8. CYP2D6 Assay

CYP2D6 catalyzes O-demethylation of dextromethorphan to dextrorphan as depicted in figure 3.22.

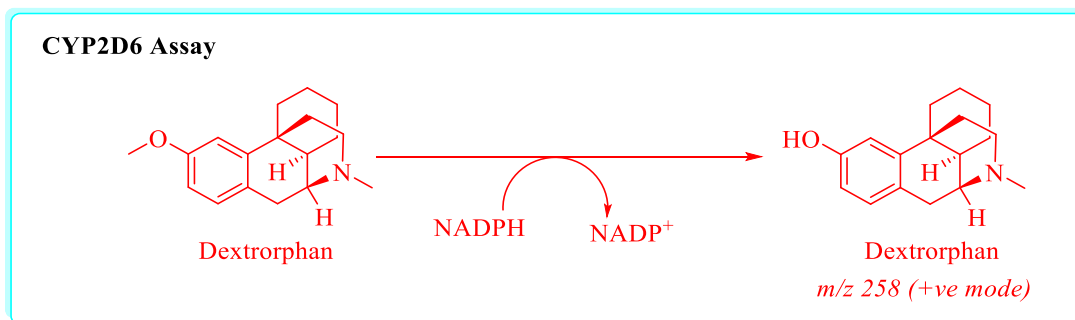


Figure 3.22 CYP2D6 Mediated O-Demethylation of Dextromethorphan to Dextrorphan

The K_m for CYP2D6 supersomes found to be 2 μM and a concentration of 5 μM was used for subsequent screening of açai extracts for CYP2D6 (Figure 3.23).

Dextromethorphan concentrations from 2-25 μM were used for K_I determinations.

CYP2D6 Supersomes Michaelis-Menten Plot

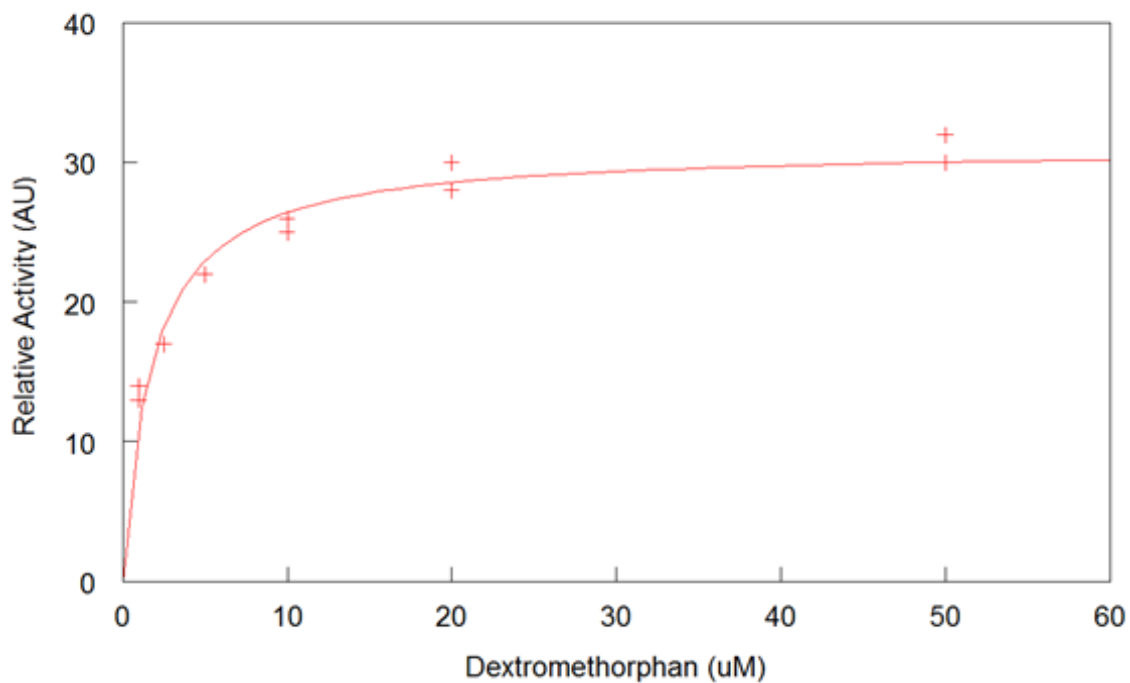


Figure 3.23 Michaelis-Menten Kinetics Plot for O-Demethylation of Dextromethorphan to Dextrorphan by CYP2D6 Supersomes

3.3.9. CYP2E1 Assay

CYP2E1 catalyzes the hydroxylation of *p*-nitrophenol to *p*-nitrocatechol as depicted in figure 3.24.

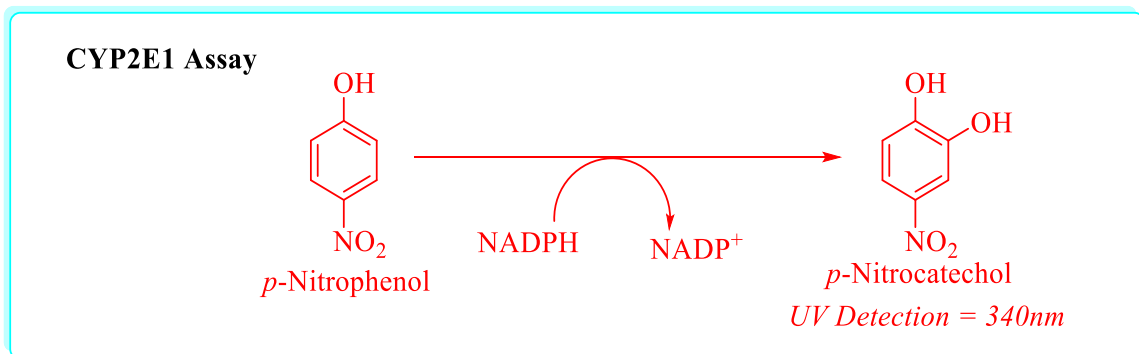


Figure 3.24 CYP2E1 Mediated Hydroxylation of *p*-Nitrophenol to *p*-Nitrocatechol

Michaelis-Menten kinetics plot for the hydroxylation of *p*-nitrophenol to *p*-nitrocatechol by CYP2E1 supersomes generated using SlideWrite indicated the K_m for CYP2E1 supersomes as 50 μM (Figure 3.25). Therefore, further studies included a substrate concentration of 50 μM *p*-nitrophenol for screening of açai extracts for CYP2E1 inhibition used.

CYP2E1 Supersomes Michaelis-Menten Plot

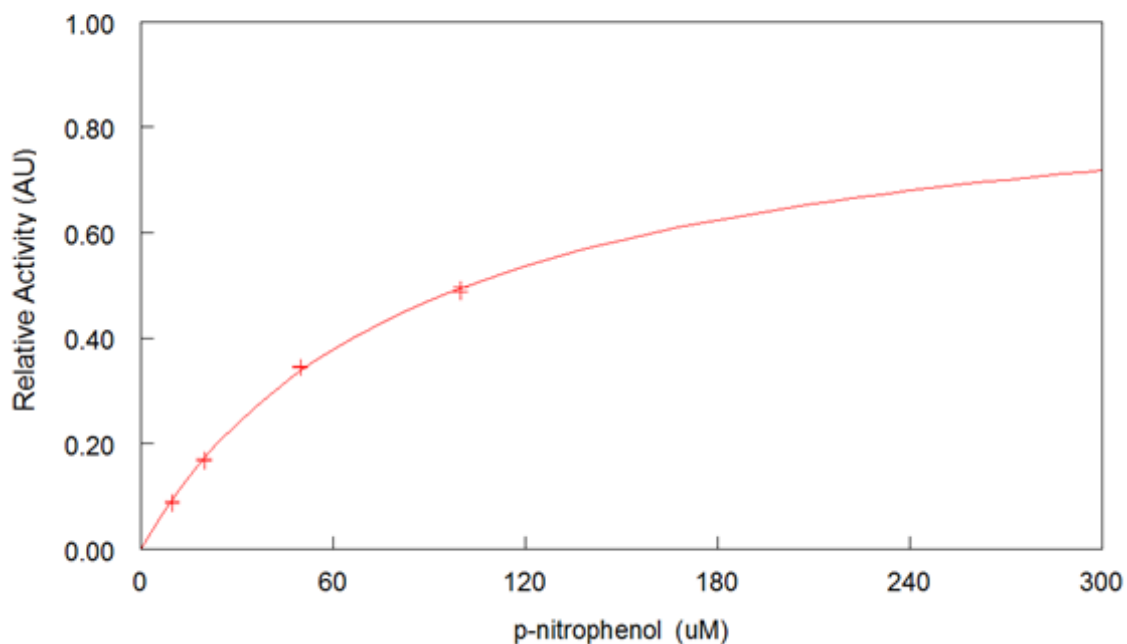


Figure 3.25 Michaelis-Menten Kinetics Plot for Hydroxylation of *p*-Nitrophenol to *p*-Nitrocatechol by CYP2E1 Supersomes

3.3.10. CYP3A4 Assay

CYP3A4 catalyzes the oxidation of nifedipine to dehydronifedipine as depicted in figure 3.26. CYP3A4 enzymatic activities were determined by achieving the separation and quantification of oxidized nifedipine using UPLC coupled to mass spectrometer. The detection and quantification of metabolite, dextrorphan was achieved for m/z of 345 under positive ion mode.

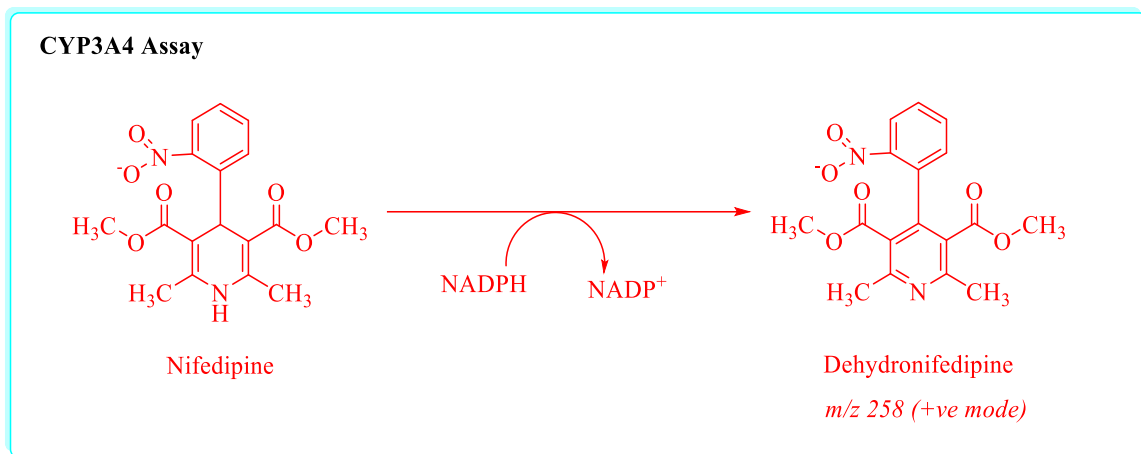


Figure 3.26 CYP3A4 Mediated Oxidation of Nifedipine to Dehydronifedipine

The K_m for CYP3A4 mediated oxidation of nifedipine to dehydronifedipine was found to be 30 μM and the same concentration was used for screening of açai extracts for CYP3A4 inhibition and for K_i determinations, 20-500 μM nifedipine were used (Figure 3.27).

CYP3A4 Supersomes Michaelis-Menten Plot

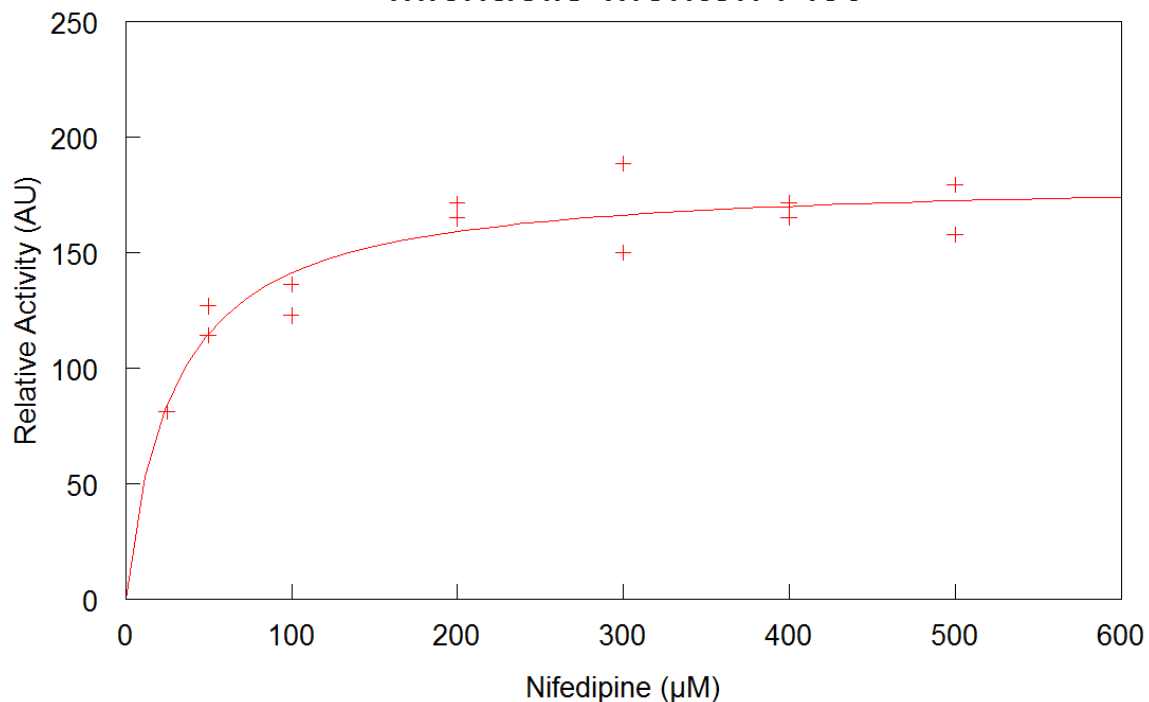


Figure 3.27 Michaelis-Menten Kinetics Plot for Conversion of Nifedipine to Dehydronifedipine by CYP3A4 Supersomes.

3.3.11. Screening of Crude Açai Berry Extracts for *In vitro* Inhibition of cDNA Expressed Cytochrome P450 Enzymes

Michaelis-Menten models provided the kinetic parameters required for CYP inhibition studies. Inhibition studies involved a single concentration that is close to the observed K_m for each CYP isoform. The initial four crude fraction obtained from the bioassay-guided fractionation of freeze-dried açai berry powder as illustrated in the Scheme 1 were screened for their ability to inhibit individually cDNA expressed

cytochrome P450 enzymes at a concentration of 50 µg/ml concentration. The selection of supersomes used in the screening of crude açai berry extracts was based on the involvement of these enzymes in xenobiotic metabolism. The crude extracts were tested across a panel of CYP enzymes that includes isoforms CYP1A1, CYP1A2, CYP2A6, CYP2B6, CYP2C8, CYP2C9, CYP2D6, CYP2E1 and CYP3A4. These isoforms account for the metabolism of approximately 80% of drugs. Among the initial crude extracts, chloroform extract was found to be the most potent inhibitor across the P450 panel tested. The chloroform extract at a concentration of 50 µg/ml showed inhibition of the isoforms CYP1A1, CYP2B6, CYP2C8 and CYP2D6 to a great extent by more than 90% inhibition. Other enzymes that showed significant inhibition included CYP1A2, CYP2A6, CYP2E1 and CYP3A4 (Figure 3.28).

In addition, the crude hexane extract was also found to inhibit CYP1A1 and CYP2C8 to great extent showing more than 95% inhibition for both the isoforms. The isoforms CYP2A6 and CYP2E1 were found to be inhibited moderately by approximately 70% at 50 µg/ml concentration. Moderate levels of inhibition were observed with CYP2A6 and CYP2E1 at 50 µg/ml concentration. The crude butanol extract was found to have moderate to mild inhibition of CYP1A1, CYP2B6 and CYP2C8 isoforms while the other isoforms were found to be unaffected by the crude butanol extract. The aqueous extract appears to have very little effect on the CYP isoforms tested in our study.

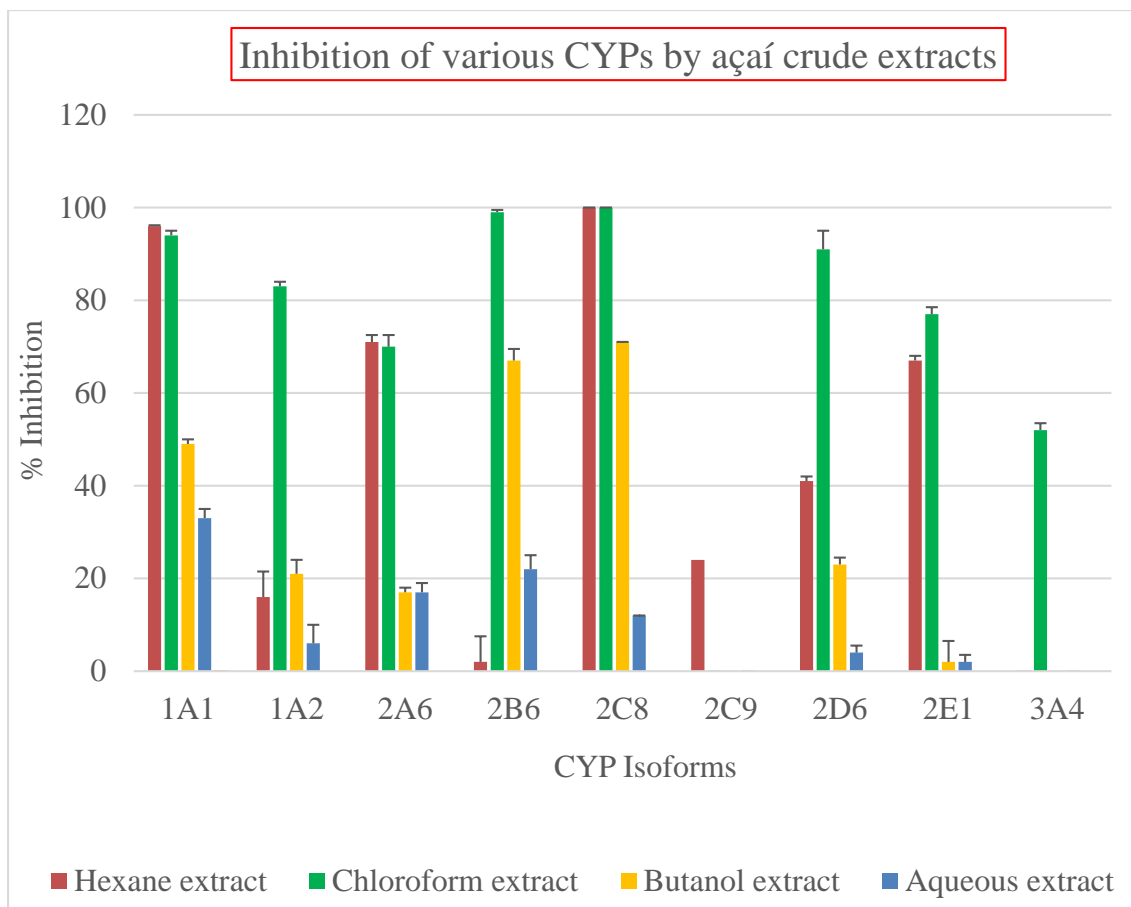


Figure 3.28 Inhibition of Various cDNA Expressed Cytochrome P450 Enzymes by Açai Crude Extracts. Concentration of the Extracts used for Screening was 50 µg/ml. Red, Green, Yellow and Blue Bars represent Crude Hexane, Chloroform, Butanol and Aqueous Extracts of Açai, respectively. † indicates the values were not determined.

In order to determine the extent of inhibition by crude chloroform on these enzyme isoforms, a dose response study was carried out ranging the concentrations from 5 to 50 µg/ml (Figure 3.29).

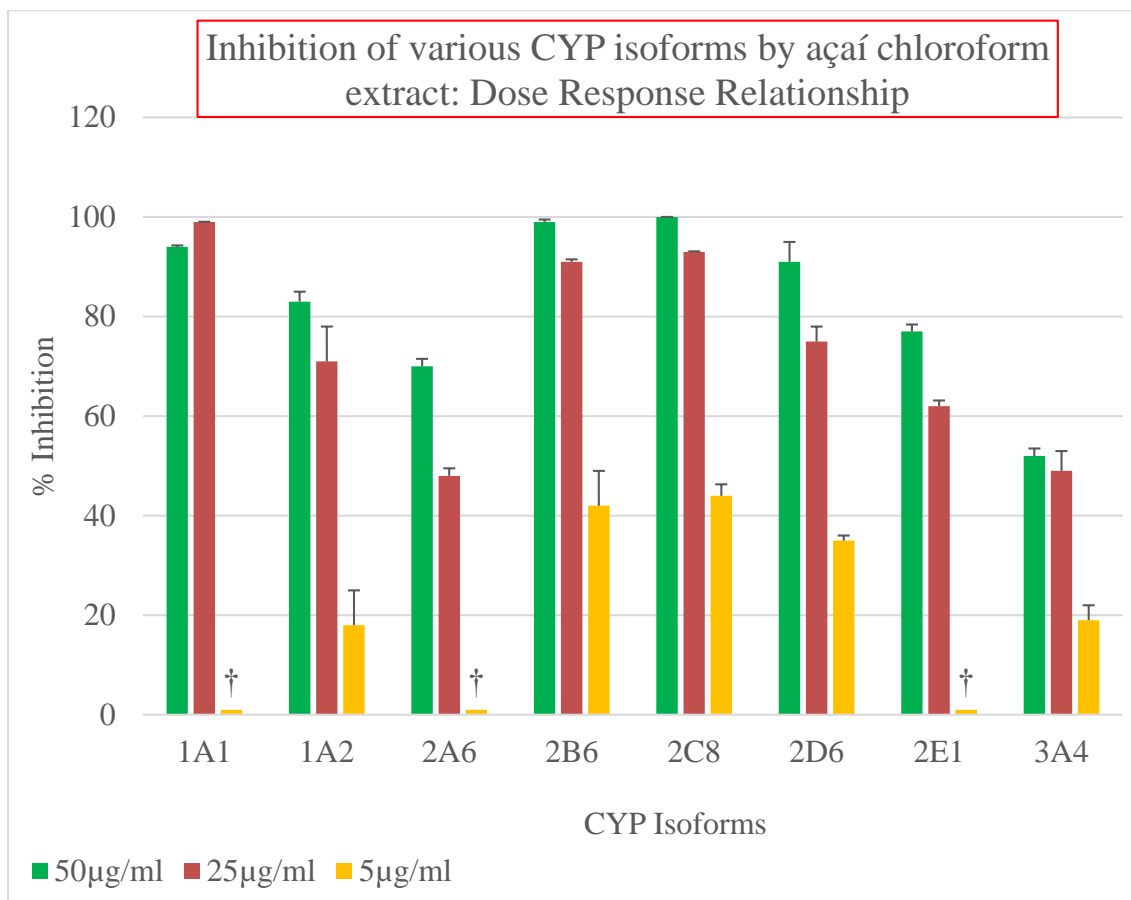


Figure 3.29 Dose Response Relationship for the Inhibition of Various cDNA Expressed Cytochrome P450 Enzymes by Açai Crude Chloroform Extract. Green, Red and Yellow Bars represent Crude Hexane, Chloroform, Butanol and Aqueous Extracts of Açai, respectively. † indicates the values were not determined.

The crude chloroform extract exhibited a clear dose response relationship across all the CYP isoforms. The isoforms CYP1A1, CYP2B6, CYP2C8 and CYP2D6 that were greatly inhibited at 200 µg/ml concentration were also found to be inhibited significantly at the lowest concentration tested. At 5 µg/ml concentration, CYP2B6 and CYP2C8 were found to be inhibited by nearly 50% while CYP2D6 was inhibited by ~30%. Other

isoforms, CYP1A2, CYP2A6, CYP2E1 and CYP3A4 were also found to be inhibited by approximately 50% at 25 µg/ml concentration. CYP1A1, based on its nearly 100% inhibition at 25 g/mL is also likely to be very strongly inhibited at 5 µg/mL, although this dose was not examined for this isoform.

Michaelis-Menten kinetics studies were carried out using substrate concentrations described earlier in Table 3.1 for the CYP isoforms namely CYP1A1, CYP2B6 and CYP2C8 that were shown to be inhibited by chloroform extract in a dose dependent manner. The Michaelis-Menten kinetics studies carried out at a concentration of 10 µg/ml chloroform extract indicated a mixed mode of inhibition for CYP1A1, CYP2B6 and CYP2C8 enzymes (Table 3.4). Furthermore, the K_I and K_I' values obtained for CYP1A1, CYP2B6 and CYP2C8 were found to be in the low µg/ml range, suggesting further studies are warranted to identify specific inhibitors via the activity guided fractionation approach.

Table 3.4 Inhibition constants, K_I and K_I' for inhibition of CYP1A1, CYP2B6 and CYP2C8 by crude chloroform extract of açai at 10µg/ml concentration

CYP Isoform	K_I (µg/ml)	K_I' (µg/ml)	Mode of Inhibition
CYP1A1	4.2	47.4	Mixed
CYP2B6	7.1	18.2	Mixed
CYP2C8	1.0	4.6	Mixed

The results of *in vitro* inhibition of CYP enzymes using supersomes identified individual CYPs that are susceptible to inhibition by chloroform extract of açai. It indicated the potential for interactions of the chemical constituents present in chloroform extracts of açai with CYP enzymes. As a consequence, these interactions may alter the rates of metabolism of several xenobiotics including drugs leading to pharmacokinetic interactions with the drugs in addition to altered endobiotic biotransformation. However, it is also possible that the chemical constituents from chloroform extract of açai might elicit even more complex effects on CYP enzymes through other mechanisms such as induction of CYP enzymes following regulatory effects on CYP gene expression further complicating therapeutic applications.

3.3.12. *In vitro* Inhibition of CYP2A6 and CYP2E1 using Human Liver Microsomes

Metabolism and detoxification processes are the primary roles of CYP enzymes but generation of toxic metabolites during the course of metabolism is also often mediated by CYP enzymes. Interestingly, CYP enzymes also play an important role in the generation of biologically reactive intermediates through the process of bioactivation or metabolic activation. The chemical toxicity arising from CYP enzymes includes toxic metabolites that are electrophilic compounds, free radicals and activated oxygen species. More specifically, certain CYP isoforms are involved in the bioactivation of procarcinogens to ultimate carcinogens. Both CYP2A6 and CYP2E1 were shown to metabolize a greater number of compounds bearing toxicological relevance and are only minor contributors towards drug metabolism. In contrast to other major metabolizing

CYP enzymes such as CYP2C8/9, CYP2D6 and CYP3A4, CYP2A6 has never been implicated for any significant role in clinically significant drug interactions. CYP2A6 with a clearer role in nicotine metabolism linked to decreased risk of tobacco-related cancers and nicotine addiction. The pursuit of finding chemical inhibitors for CYP2A6 is intriguing with a potential for use as adjuvant drugs in nicotine replacement therapy. Similarly, CYP2E1 has been studied extensively for its role in metabolism as well as metabolic activation of wide of variety of drugs, environmental toxicants, carcinogens and procarcinogens. Ethanol oxidation was originally believed to be the primary function of CYP2E1 but is now shown to be involved in metabolism of a wide variety of xenobiotics, with a majority of them having relatively low molecular compounds. A majority of these xenobiotics constitute protoxicants such benzene, carbon tetrachloride, pyridine, nitrosamine and acetaminophen that following the metabolism by CYP2E1 deplete cellular levels of glutathione thus resulting in increased oxidative stress or damage through covalent binding to the proteins to the cells expressing CYP2E1. Inhibition of CYP2E1 by diallylsulfide was shown to decrease the toxicity associated with protoxicants. Similarly, over expression of CYP2E1 increased toxicity and oxidative stress with toxicants such as carbon tetrachloride. Consequently, inhibition of CYP2A6 and CYP2E1 presents one useful strategy to decrease bioactivation processes and subsequent production of toxic metabolites. In the current research, inhibition of CYP2A6 and CYP2E1 using human liver microsomes by the constituents of açai berry extracts was studied extensively using bioassay-guided fractionation. The goal is to identify specific inhibitors for CYP2A6 and CYP2E1 in açai berry extracts. A major

change from the previous section is the choice of human liver microsomes over supersomes for the study and is justified for following reasons. First, the study is more comprehensive and was expected to consume huge amounts of CYP enzymes, human liver microsomes serves as relatively inexpensive option. Second, the availability of specific probe substrates, for example, coumarin and p-nitrophenol for CYP2A6 and CYP2E1 enzymes, respectively.

3.3.13. Bioassay-guided Fractionation of Açai Berry Extracts for CYP2A6 Inhibition ***In vitro* using Human Liver Microsomes**

Coumarin is a very selective substrate for CYP2A6 enzyme and the enzyme does the hydroxylation of coumarin specifically at the 7-position resulting in the production of 7-hydroxycoumarin as illustrated in Figure 3.14. An initial Michaelis-Menten kinetics plot was developed using coumarin as a substrate for CYP2A6 enzymes in human liver S9 fractions in a similar described for CYP2A6 supersomes and plotted using SlideWrite (Figure 3.30). The Michaelis-Menten kinetics plot indicated a K_m of 1.0 μM for human liver microsomes and was found to be smaller compared to the K_m of 1.0 μM observed for CYP2A6 supersomes (figure 3.15). The assay conditions and the detection parameters for CYP2A6 assay were described earlier.

Michaelis-Menten Plot for human CYP2A6

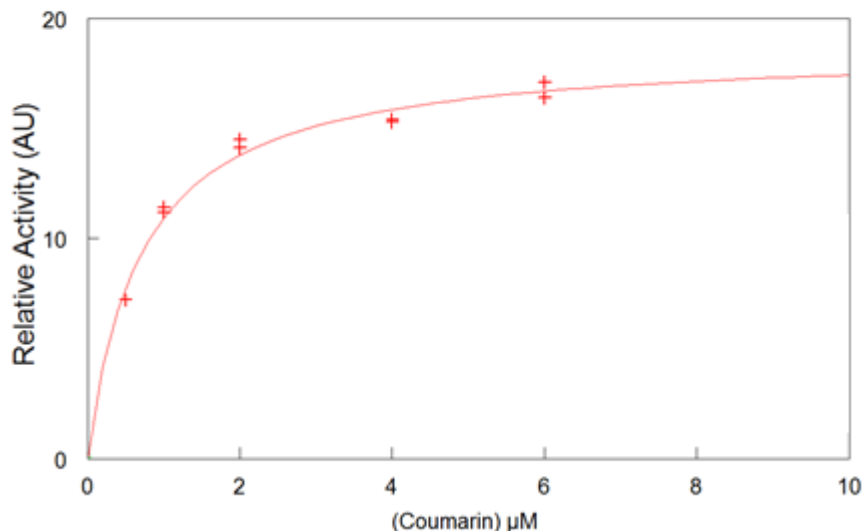
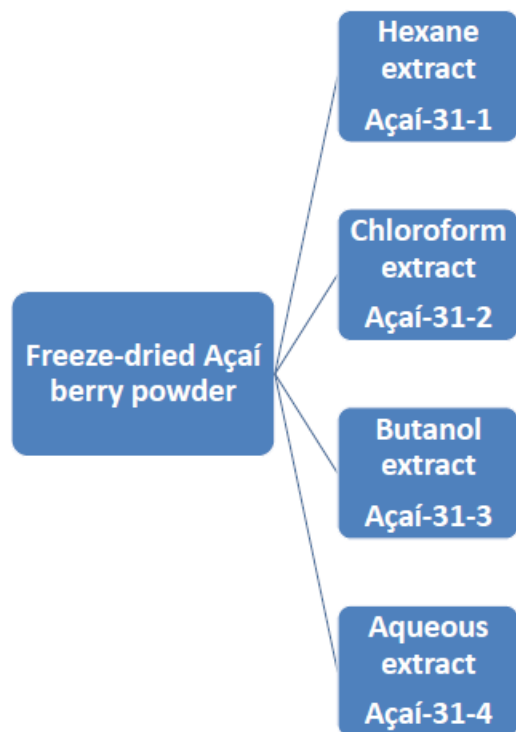


Figure 3.30 Michaelis-Menten Kinetics Plot for Hydroxylation of Coumarin to 7-Hydroxycoumarin by CYP2A6 Enzymes in Human Liver S9 Fraction

Initially, crude açai berry extracts were generated through the process of bioassay-guided fractionation as previously described earlier in scheme 1 were depicted in scheme 2. A preliminary dose response using human liver S9 fractions was carried out for CYP2A6 inhibition by crude açai berry extracts over a range of concentrations at 25, 50, 100 and 200 $\mu\text{g/ml}$ concentrations. All the initial crude extracts inhibited CYP2A6 in a dose dependent manner except for the aqueous extract (Açai-31-4) with which no significant inhibition was observed at concentrations $\leq 100 \mu\text{g/ml}$ (Figure 3.31). The dose response plot revealed that the crude chloroform extract (Açai-31-2) was the most potent of all the extracts followed by the crude hexane extract (Açai-31-1) and crude butanol extract (Açai-31-3), respectively. Both crude chloroform extract (Açai-31-2) and crude

hexane extract (Açaí-31-1) have shown significant inhibition of approximately 50% at 50 $\mu\text{g/ml}$ concentration while the crude butanol extract (Açaí-31-3) showed significant inhibition only at concentrations above 100 $\mu\text{g/ml}$ concentration.



Scheme 2. Initial Crude Extracts of Açaí Berry.

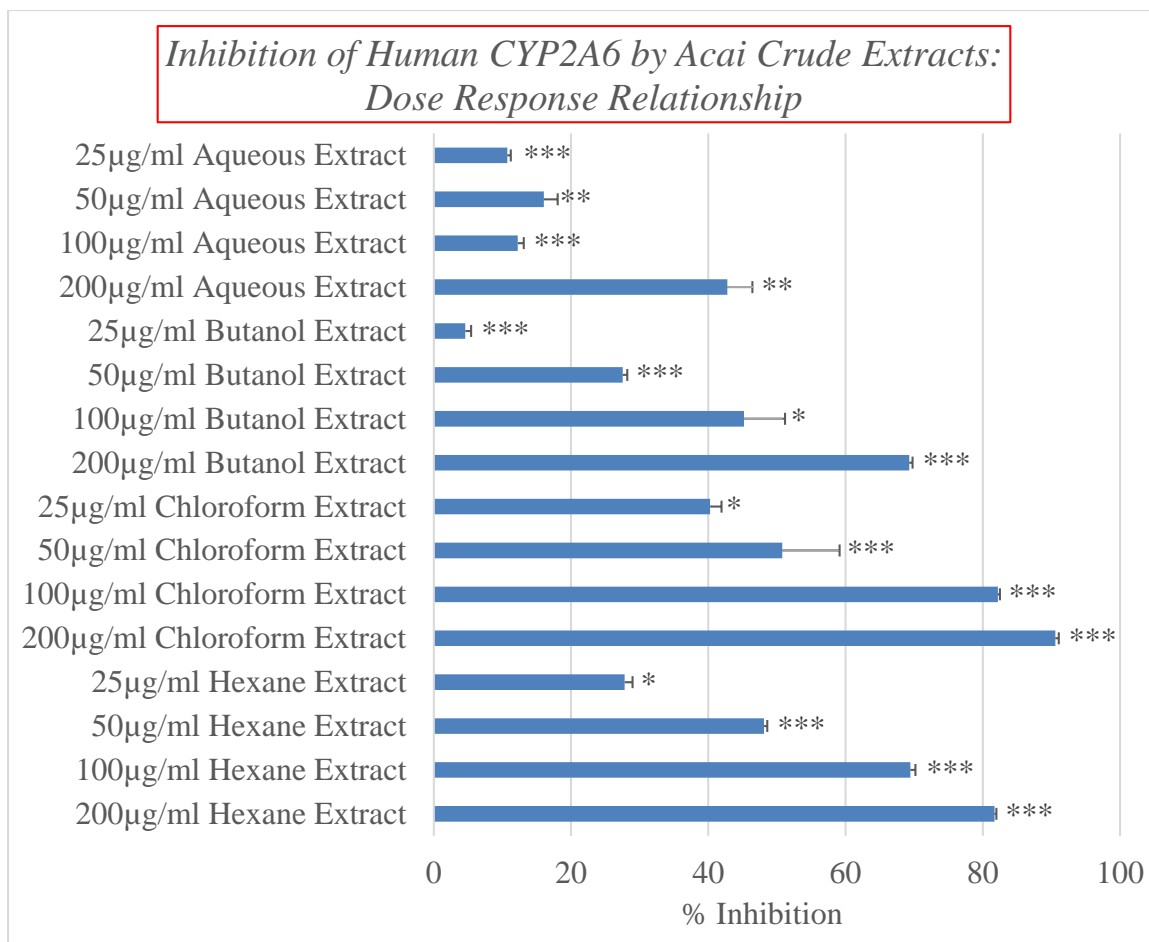
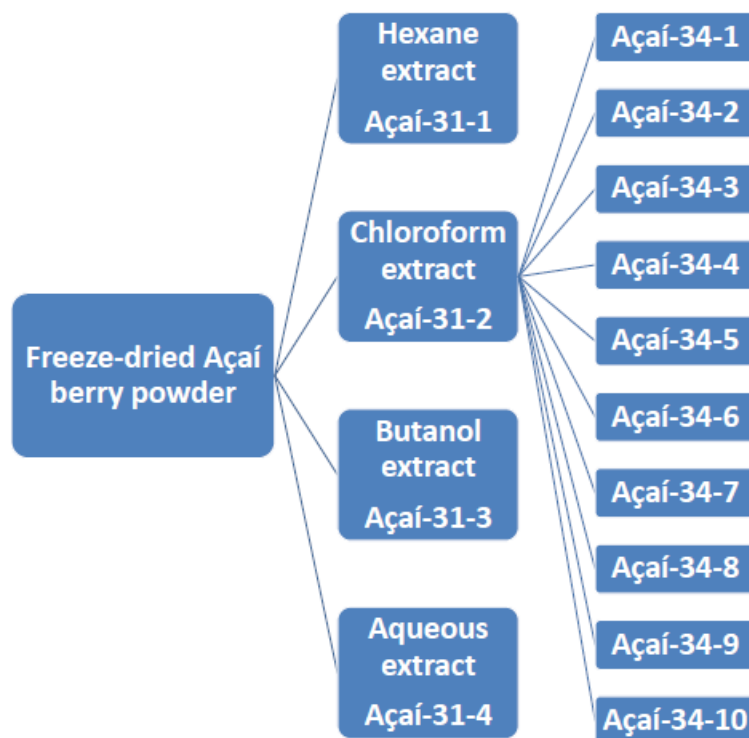


Figure 3.31 Inhibition of Human CYP2A6 by Açai Crude Extracts

The most potent chloroform extract (Açai-31-2) among all the crude extracts was fractionated using column chromatography to produce 10 fractions, Açai-34-1 through Açai-34-10 (Scheme 3).



Scheme 3. Fractionation of Crude Chloroform Extract of Açai (Açai-31-2).

The extent of inhibition observed with chloroform extract, Açai-31-2 provided the rationale for testing the fractions at a reduced concentration. So, a reduced concentration of 50 µg/ml was used for studying CYP2A6 inhibition. Among the 10 fractions, Açai-34-7, Açai-34-8 and Açai-34-9 showed inhibition of 81%, 80% and 61%, respectively (Figure 3.32).

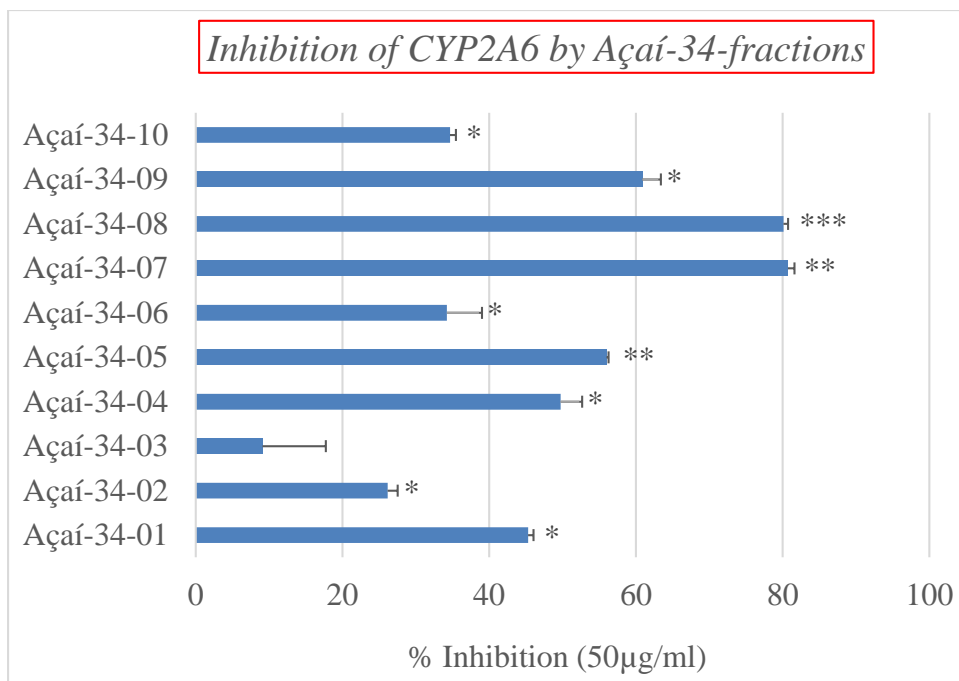
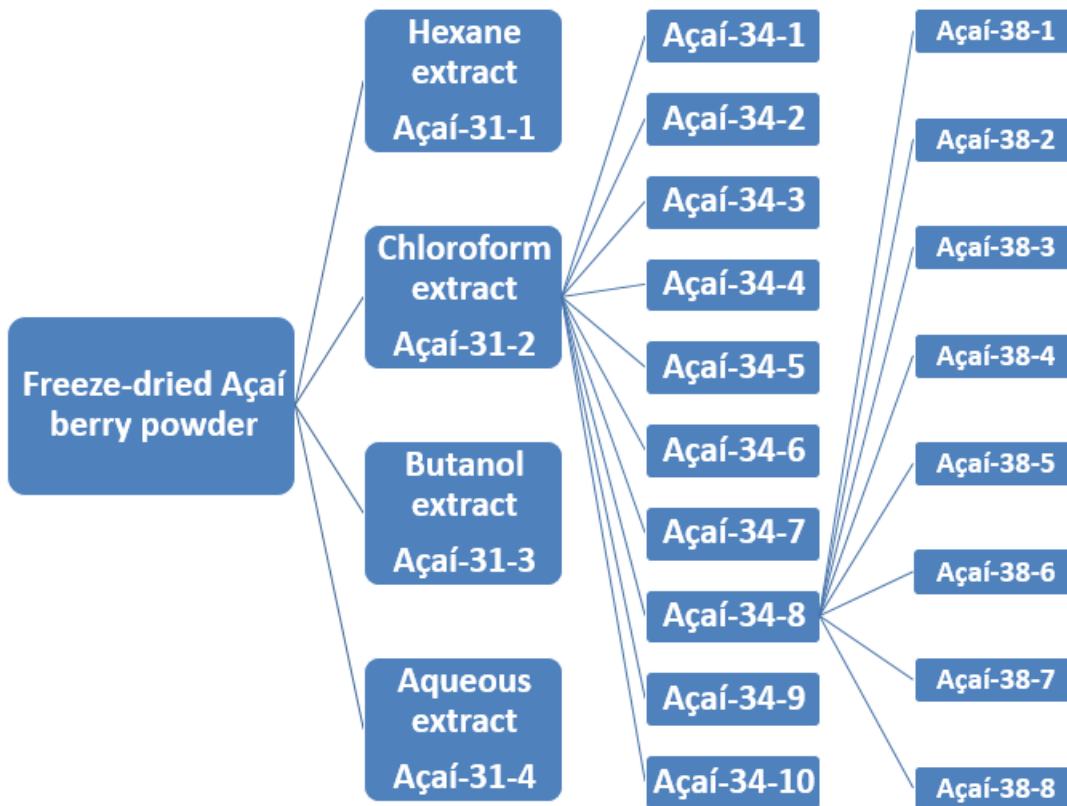


Figure 3.32 Inhibition of Human CYP2A6 by Açai-34-series

Although Açai-34-7 and Açai-34-8 showed similar levels of inhibition, low sample size of Açai-34-7 limited its fractionation and therefore, the largest fraction Açai-34-8 was chosen for further fractionation. Sub-fractionation of Açai-34-8 by gel permeation chromatography resulted in 8 fractions, Açai-38-1 through Açai-38-8 (Scheme 4).



Scheme 4. Fractionation of Açai-34-8.

Among these fractions, Açai-38-1 and Açai-38-2 showed greatest inhibition towards CYP2A6 by 76% and 86% at 50µg/ml concentration, respectively (Figure 3.33). While fraction, Açai-38-3 inhibited CYP2A6 by 61%, Açai-38-4 did not affect the activity of the enzyme significantly. The remaining fractions, Açai-38-5 through Açai-38-8 showed moderate inhibition that appeared to be similar in extent in these fractions.

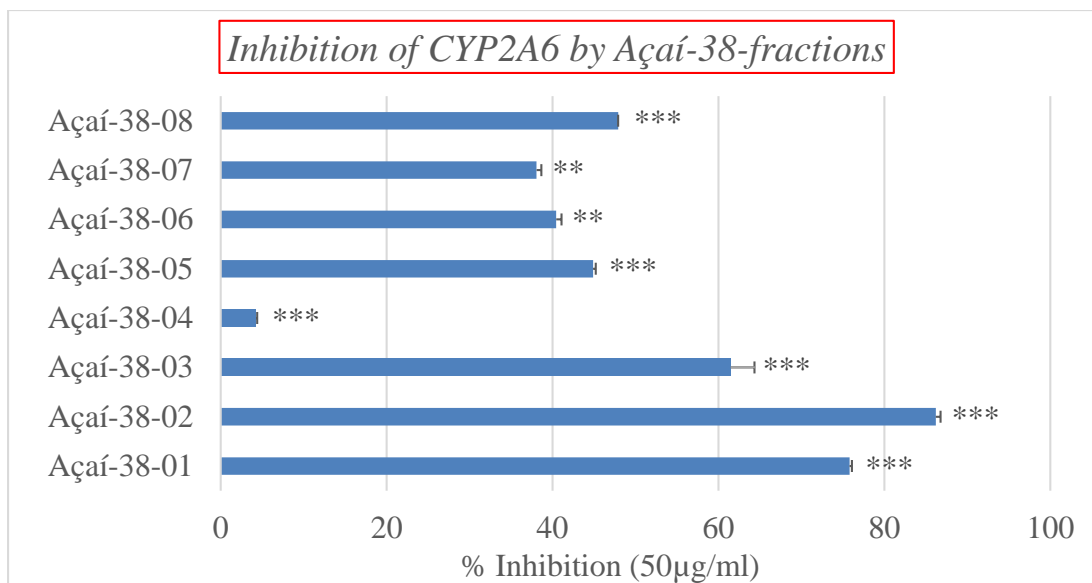
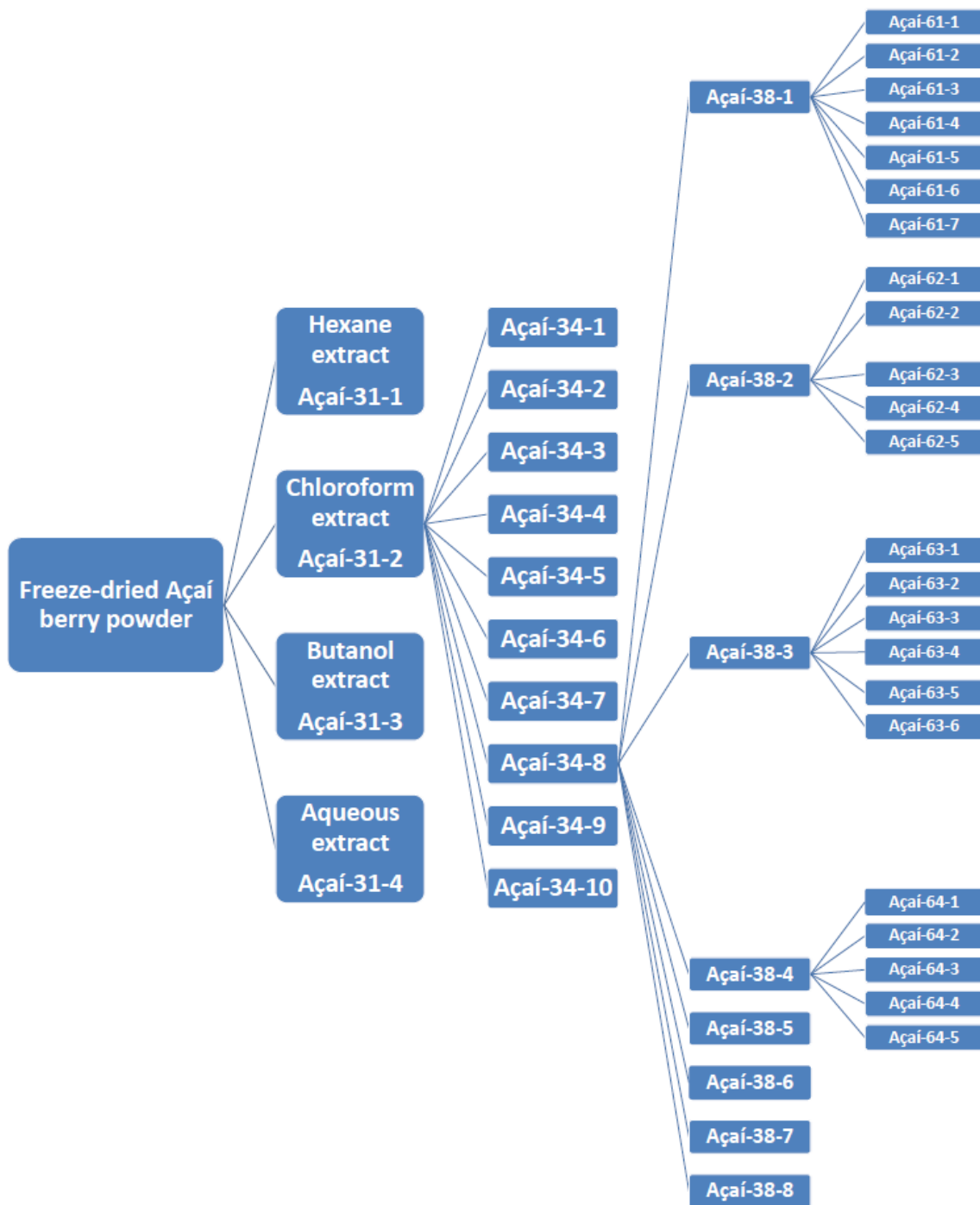


Figure 3.33 Inhibition of Human CYP2A6 by Açai-38-series

Further fractionation was carried out on the active fractions, Açai-38-1 and Açai-38-2 along with two other fractions, a moderately active fraction, Açai-38-3 and an inactive fraction, Açai-38-4. The criterion for proceeding into fractionations for Açai-38-4 was based on the abundance of the fraction obtained. This resulted in the generation of fractions, Açai-61-1 through Açai-61-7 from Açai-38-1, Açai-62-1 through Açai-62-5 from Açai-38-2, Açai-63-1 through Açai-63-6 from Açai-38-3 and Açai-64-1 through Açai-64-5 from Açai-38-4 fractions (Scheme 5).



Scheme 5. Fractionation of Açai-38-1, Açai-38-2, Açai-38-3 and Açai-38-4.

As the fractionations proceeded, significant drop in the amounts generated for some of the fractions was observed. The diminishing amounts of the fractions generated over the course of fractionations, along with the expectation that as constituents were refined, their potency should increase, prompted a reduction in concentration of the inhibitor used. Therefore, the resultant fractions from this stage were tested at a reduced concentration of 25 µg/ml.

Among the 7 fractions generated from Açai-38-1, Açai-61-4 and Açai- 61-5 inhibited CYP2A6 by about 53% and 70%, respectively at half-the-concentration of its parent fraction (Figure 3.34). The fraction Açai- 61-5 showed 70% inhibition at 25 µg/ml and is comparable to the 76% inhibition observed with its parent fraction Açai- 38-1 at 50 µg/ml concentration. Among the other fractions, Açai-61-3 and Açai-61-6 showed mild inhibition and all the other fractions showed no or minimal inhibition properties.

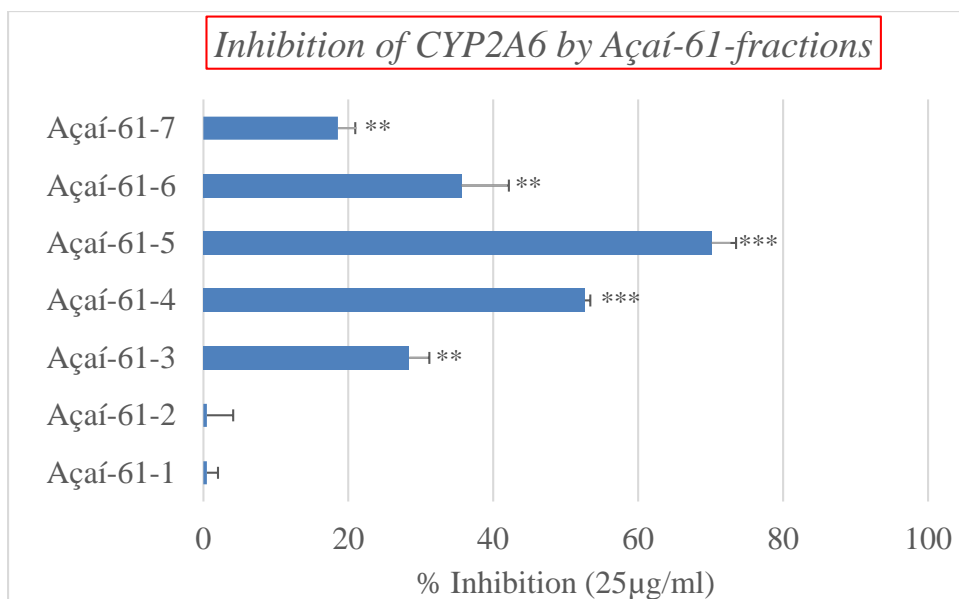


Figure 3.34 Inhibition of Human CYP2A6 by Açai-61-series

A very similar pattern was observed with Açai-38-2 sub-fractions; the fractions Açai-62-2 and Açai-62-3 showed moderate inhibition of about 64% and 53%, respectively at half the concentration of its parent fraction (Figure 3.35). The fractions Açai-62-1 and Açai-62-4 showed mild inhibition while the fraction Açai-62-5 showed minimal inhibition.

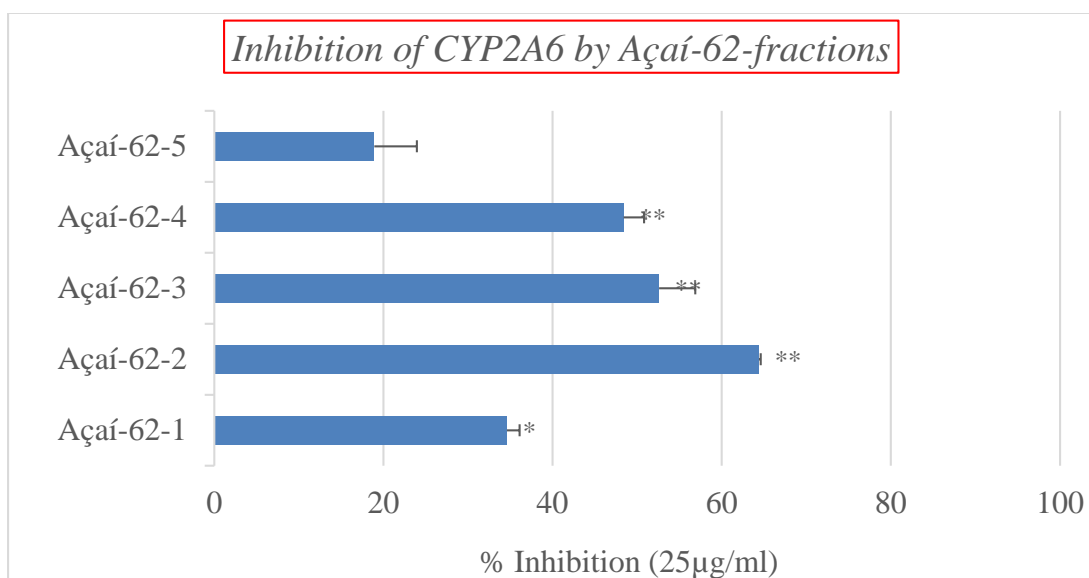


Figure 3.35 Inhibition of Human CYP2A6 by Açai-62-series

The moderately potent fraction Açai-38-3 yielded six fractions among which Açai-63-4 showed 72% inhibition of CYP2A6 at half the concentration of its parent fraction while the other fractions of açai-63-series showed only minimal to no inhibition (Figure 3.36).

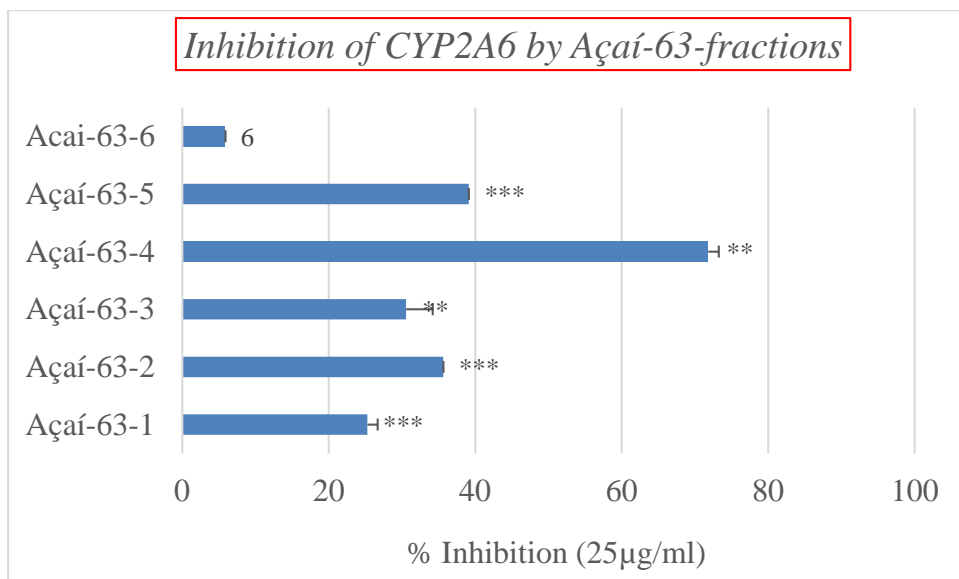


Figure 3.36 Inhibition of Human CYP2A6 by Açai-63-series

As expected, the inactive fraction Açai-34-4 produced five fractions with inhibition ranging from minimal to no inhibition (Figure 3.37).

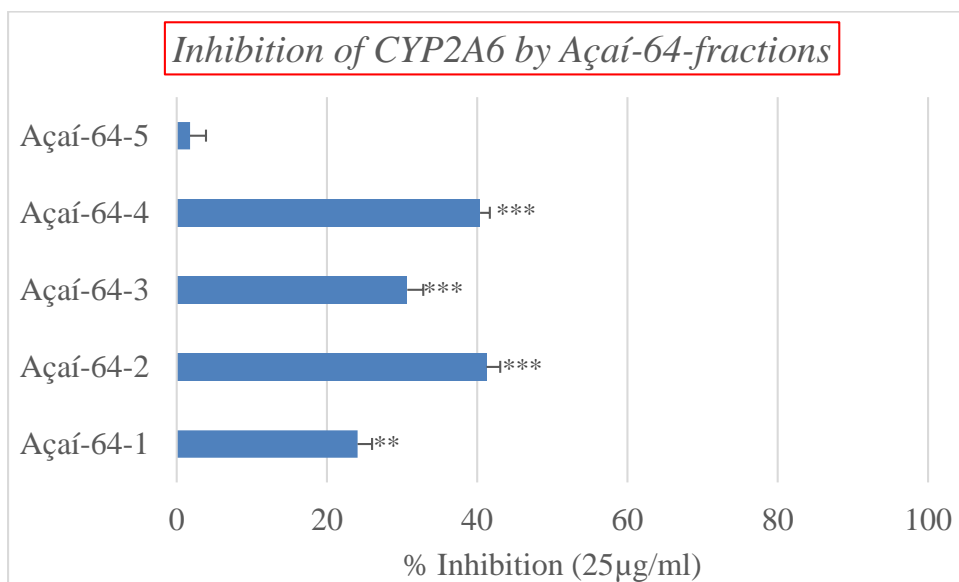
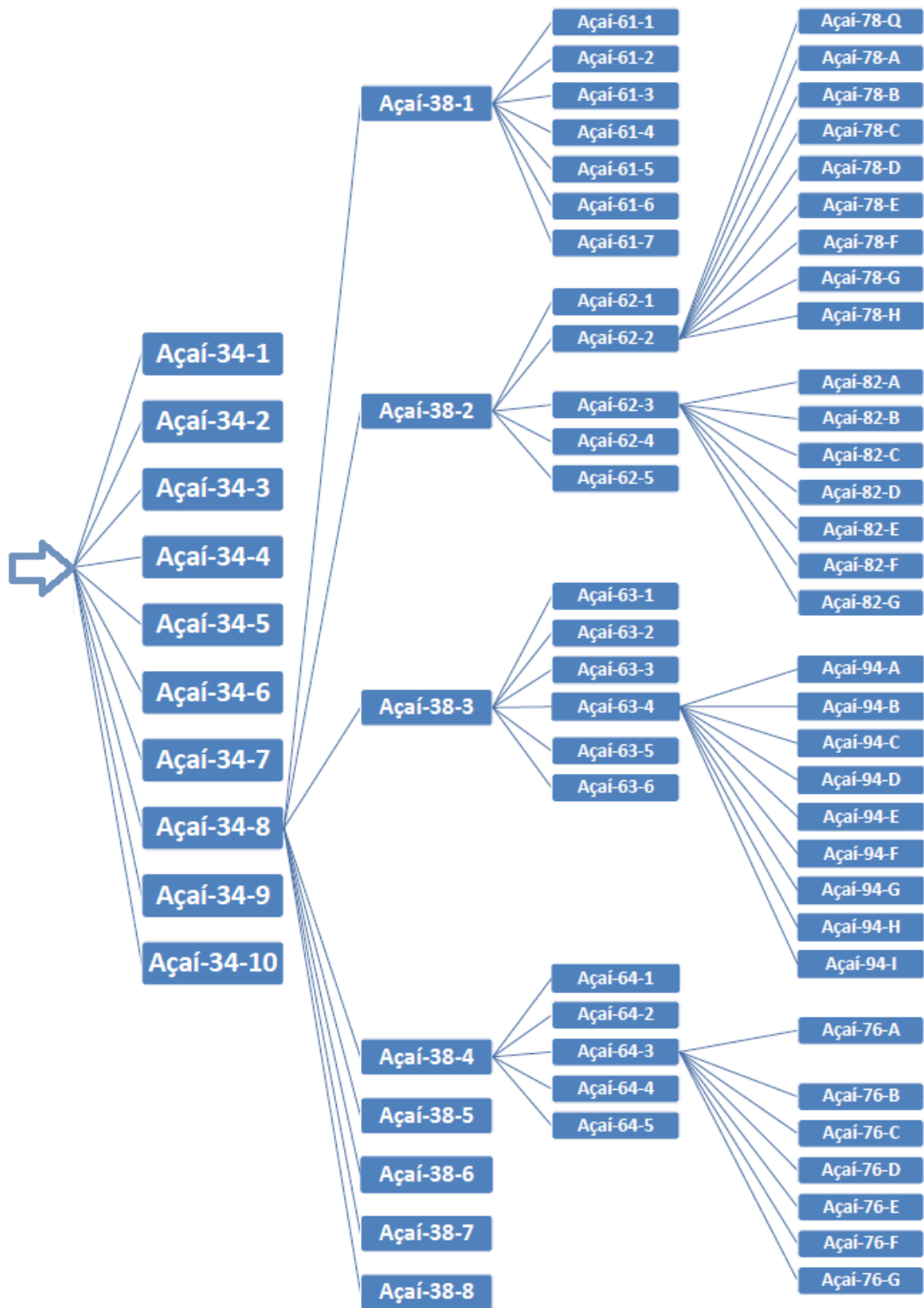


Figure 3.37 Inhibition of Human CYP2A6 by Açai-64-series

The potent fractions belonging to Açai-62-series, namely, Açai-62-2 and Açai-62-3 were further fractionated to produce Açai-78-series and Açai-82-series, respectively (Scheme 6).



Scheme 6. Fractionation of Açai-62-2, Açai-62-3, Açai-63-4 and Açai-64-3.

The process of bioassay-guided fractionation using chromatographic separation techniques is expected to increase the potency of the fractions as the procedure continues. It showed promise in narrowing the activity presumably by concentrating the inhibitory constituents into fewer extracts. However, the bioassay-guided fractionation approach appeared to have lost the pattern of generating potent fractions at this stage. For example, none of the fractions belonging to Açai-78-series that were generated from a moderately potent fraction Açai-62-2 at 25 µg/ml concentration showed any increase in potency (Figure 3.38). On the contrary, the potency was lost across all the fractions generated.

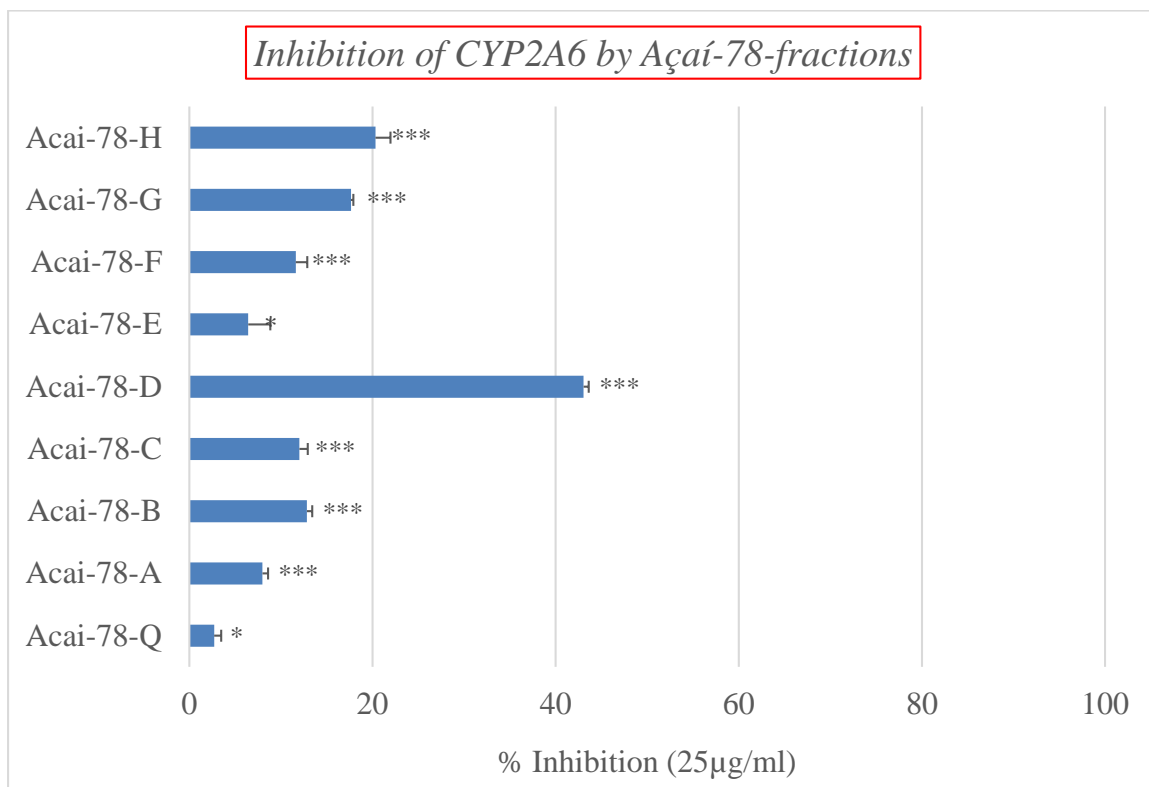


Figure 3.38 Inhibition of Human CYP2A6 by Açai-78-series

Another moderately potent fraction Açai-62-3 produced seven fractions belonging to Açai-82-series (Scheme 6). These fractions also failed to attain further increase in potency instead more than half of the fractions showed potency similar or slightly higher than their parent fraction Açai-62-3 (Figure 3.39). Four of the seven fractions namely, Açai-82-B, Açai-82-C, Açai-82-D and Açai-82-F showed CYP2A6 inhibition comparable to their parent fraction.

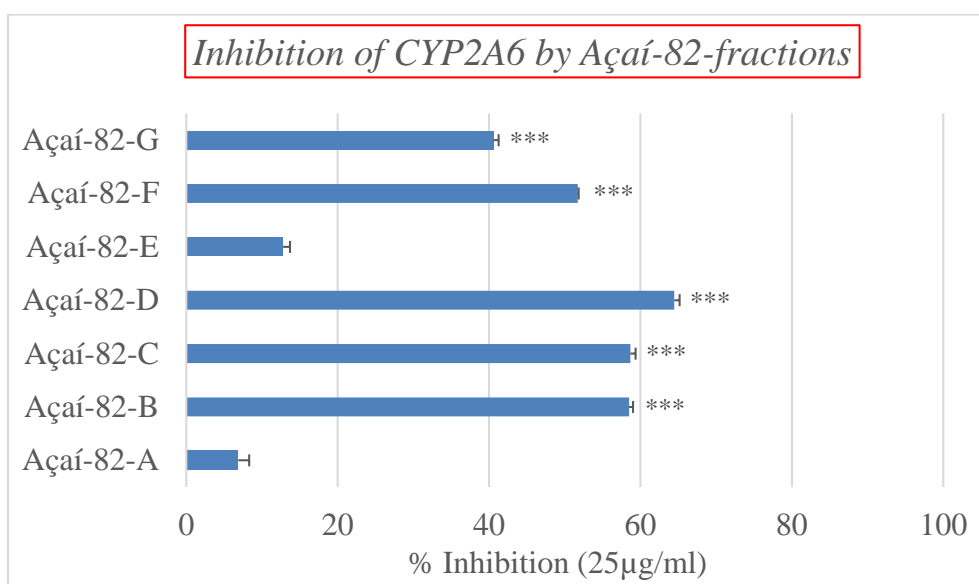


Figure 3.39 Inhibition of Human CYP2A6 by Açai-82-series

A moderately potent fraction Açai-63-4 produced 9 fractions belonging to Açai-94-series (Scheme 6). All of these fractions were found to have lost the potency compared to its parent fraction Açai-63-4 (Figure 3.40). In fact, none of the fractions retained the ability to inhibit CYP2A6 enzyme.

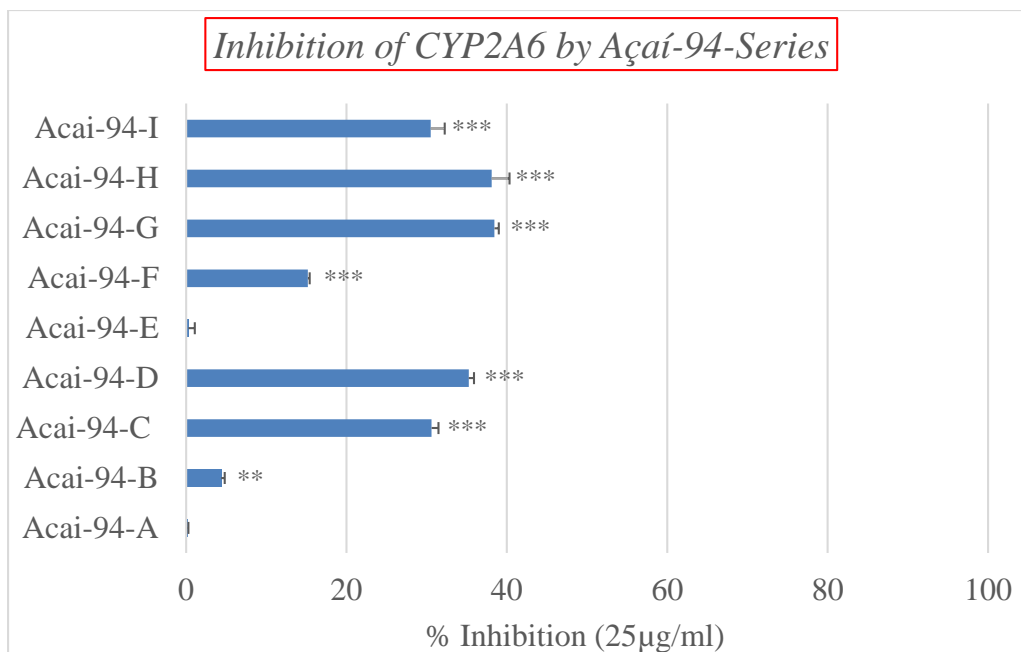


Figure 3.40 Inhibition of Human CYP2A6 by Açai-94-series

Açai-76-series fractions were obtained from a moderately potent fraction Açai-64-3 for CYP2A6 inhibition. However, two fractions namely Açai-76-A and Açai-76-B were found to greatly inhibit CYP2A6 enzyme while two other fractions Açai-76-C and Açai-76-D showed mild inhibition of CYP2A6 and the remaining three fractions had no effect on CYP2A6 enzyme (Figure 3.41).

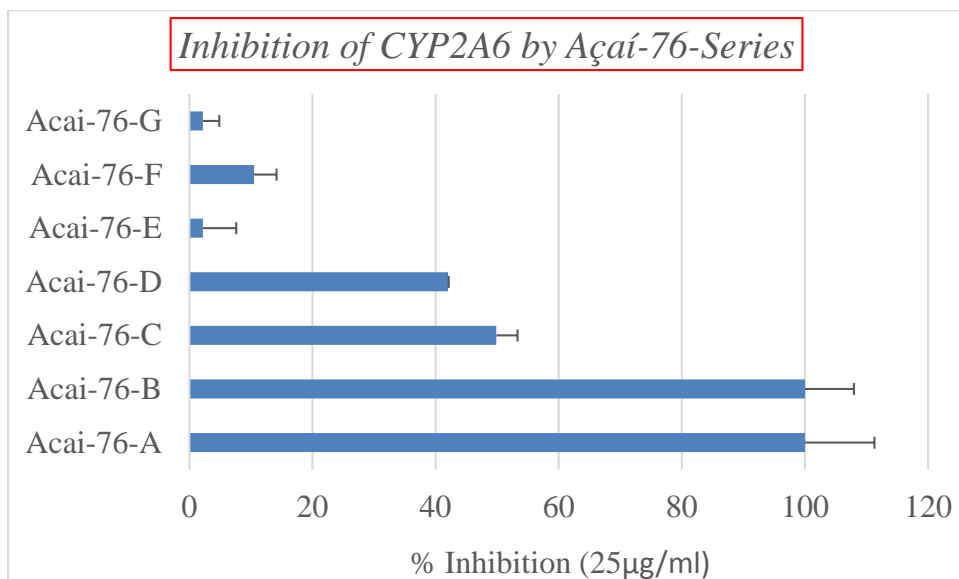
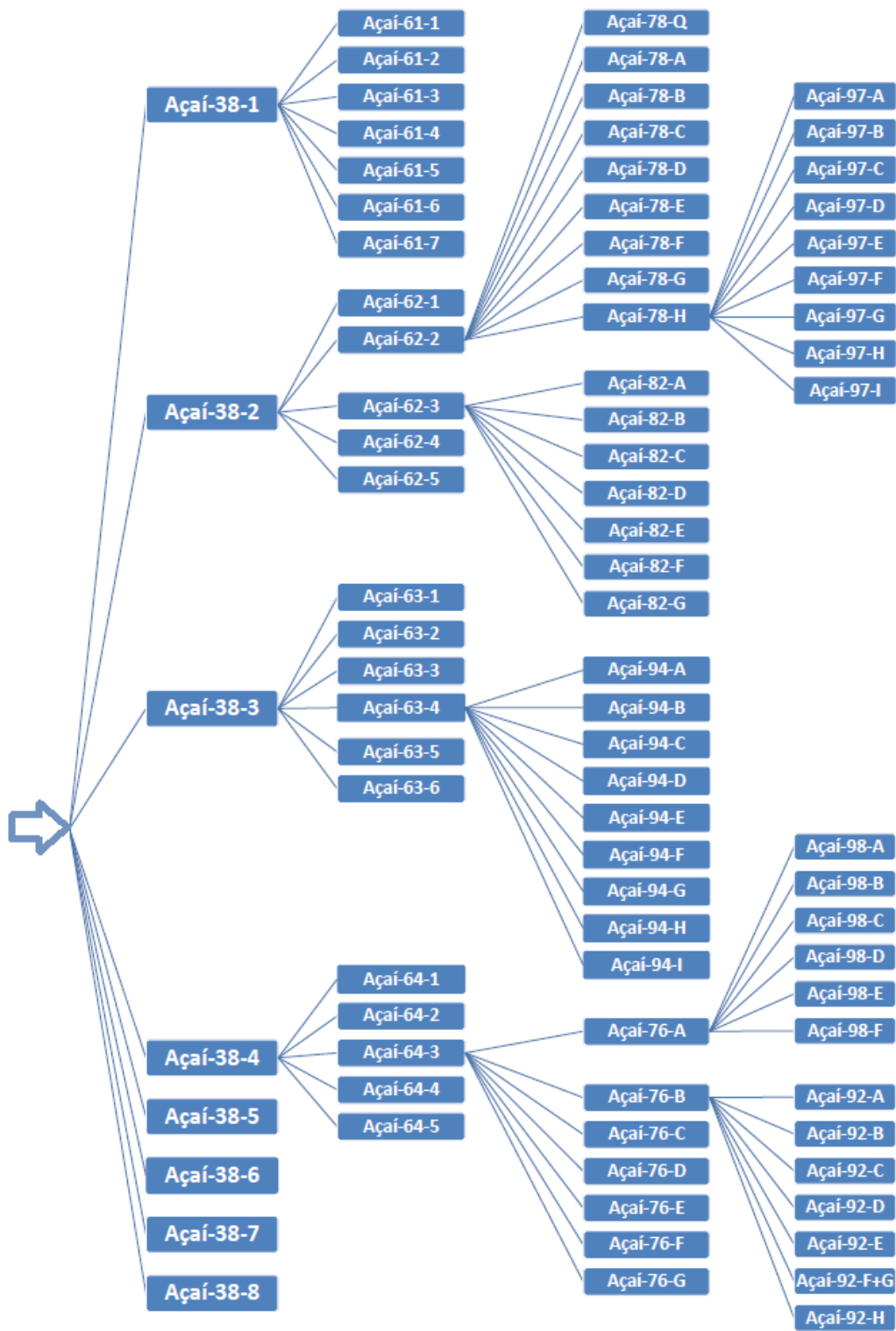


Figure 3.41 Inhibition of Human CYP2A6 by Açai-76-series

Although Açai-78-H was found to be an inactive fraction towards CYP2A6 inhibition, it was fractionated for other purposes described in subsequent chapters. Nine fractions belonging to Açai-97-series were produced from Açai-78-H and the fractions Açai-97-B and Açai-97-D were found to be pure compounds belonging to the chemical class of compounds called pheophorbides (Scheme 6). Açai-97-B and Açai-97-D were characterized by mass spectrometry and NMR spectroscopy to be Pheophorbide-a methyl ester ($C_{36}H_{38}N_4O_5$) and Pheophorbide-a ethyl ester ($C_{37}H_{40}N_4O_5$), respectively (Figure 4.20 and Table 4.1).

The two potent fractions Açai-76-A and Açai-76-B belonging to the Açai-76-series were further fractionated to produce Açai-98-series and Açai-92-series, respectively (Scheme 7).



Scheme 7. Fractionation of Açai-78-H, Açai-76-A and Açai-76-B.

The fractions belonging to Açai-97-series yielded a relatively potent fraction Açai-97-I while all other fractions belonging to the series were found to be inactive or demonstrated moderate inhibition potential towards CYP2A6 enzyme (Figure 3.42). Although Açai-97-I appears to be potent at 25 µg/ml concentration, it must be noted that the concentration appears to be high and may not be achieved in physiological concentrations to be able to cause CYP2A6 inhibition.

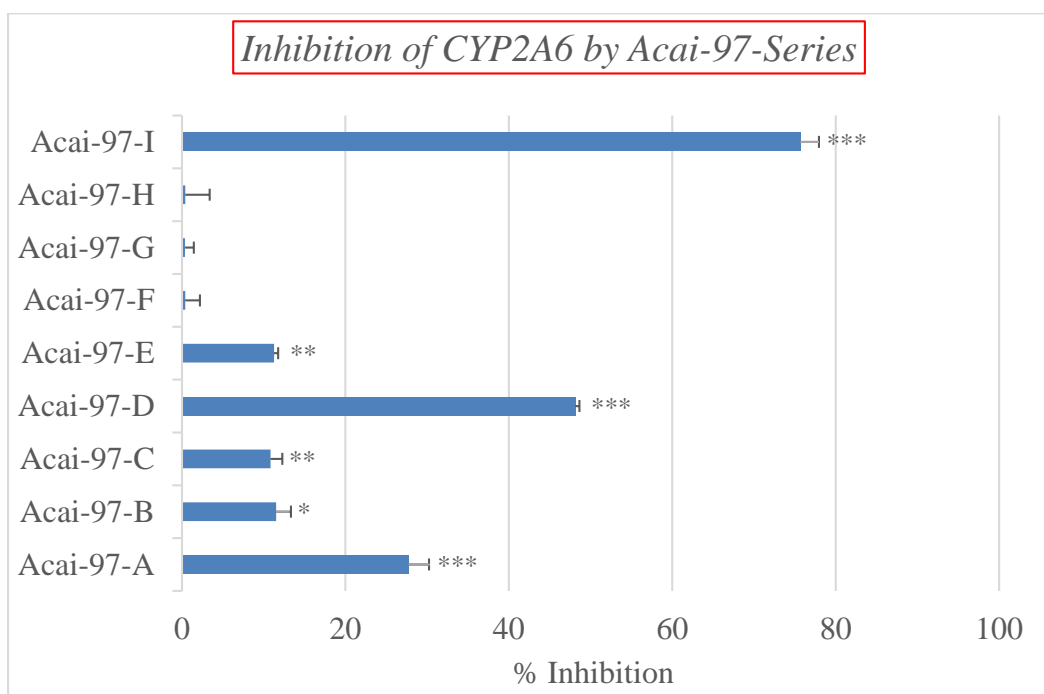


Figure 3.42 Inhibition of Human CYP2A6 by Açai-97-series

The potent fraction Açai-76-A produced Açai-98-series and all the fractions were found to have lost the activity even at 50 µg/ml except for Açai-98-F that showed moderate inhibition of CYP2A6 (Figure 3.43). Similar trend was observed with Açai-92-

series that was generated from yet another potent fraction Açai-76-B. None of the fractions were found to have any inhibitory potential towards CYP2A6 (Data not shown).

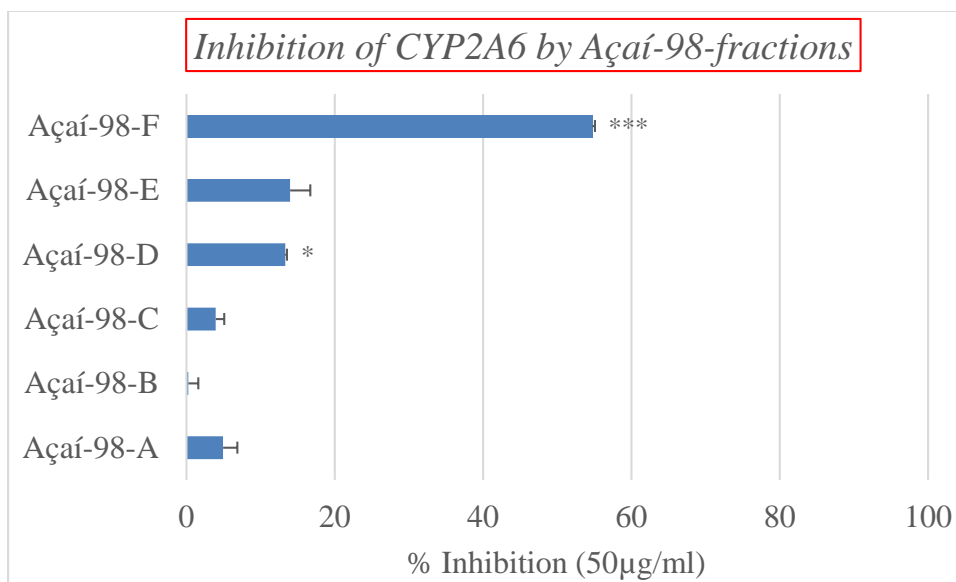


Figure 3.43 Inhibition of Human CYP2A6 by Açai-98-series

3.3.14 Summary of CYP2A6 Inhibition

Despite a minor functional role of CYP2A6 in xenobiotic metabolism, its role in the metabolism of nicotine and carcinogenic nitrosamines generated a lot of interest. The relation between CYP2A6 inhibition and decreased incidence of tobacco related cancers, the relation between CYP2A6 polymorphism and smoking habits contributed to an intriguing area of research. The current study aimed at identifying the inhibitors of CYP2A6 from açai berry extracts as there were only a handful of inhibitors identified so far. Results from initial screening of crude extracts of açai started on a promising note from bioassay-guided fractionation with the chloroform extract showing moderate

inhibition of CYP2A6 at 50 µg/ml concentration. The chloroform extract was then fractionated to yield 10 fractions that produced 2 fractions namely Açai-34-7 and Açai-34-8. The most abundant Açai-34-8 was fractionated to generate 8 fractions with 3 fractions namely Açai-38-1, Açai-38-2 being potent followed by Açai-38-3. However, contrary to what was expected, further fractionations beginning at this stage indicated a decrease in inhibitory potential towards CYP2A6. A couple of rounds of fractionations further utilizing active fractions indicated a common trend leading to a loss of activity. Altogether, 5 rounds of fractionations were carried out in the process of bioassay-guided fractionation. The result that no significant inhibition was observed can be explained as follows. The loss of activity over the course of fractionations may be the result that there were no specific inhibitors present in chloroform extract of açai. It is also conceivable that the shelf-life, treatments during fractionations might have modified or adversely affected the chemical constituents leading to the loss of integrity contained in the crude extract. Further, CYP2A6 with restricted substrate specificities as demonstrated from its role in the metabolism of xenobiotics and endobiotics might have the demand for increased selectivity for its substrates.

3.3.15. Bioassay-guided Fractionation of Açai Berry Extracts for CYP2E1 Inhibition

***In vitro* using Human Liver Microsomes**

The initial crude extracts obtained by fractionation of the freeze-dried açai berry powder as described earlier were tested for CYP2E1 inhibition in a very similar manner using human liver microsomes. The assay employed for the study involved hydroxylation

of *p*-nitrophenol to *p*-nitrocatechol as described earlier and the overall design of the assay was summarized earlier in figure 3.23. An initial Michaelis-Menten kinetics plot generated using *p*-nitrophenol as a substrate for CYP2E1 enzymes in human liver S9 fractions is illustrated in Figure 3.44.

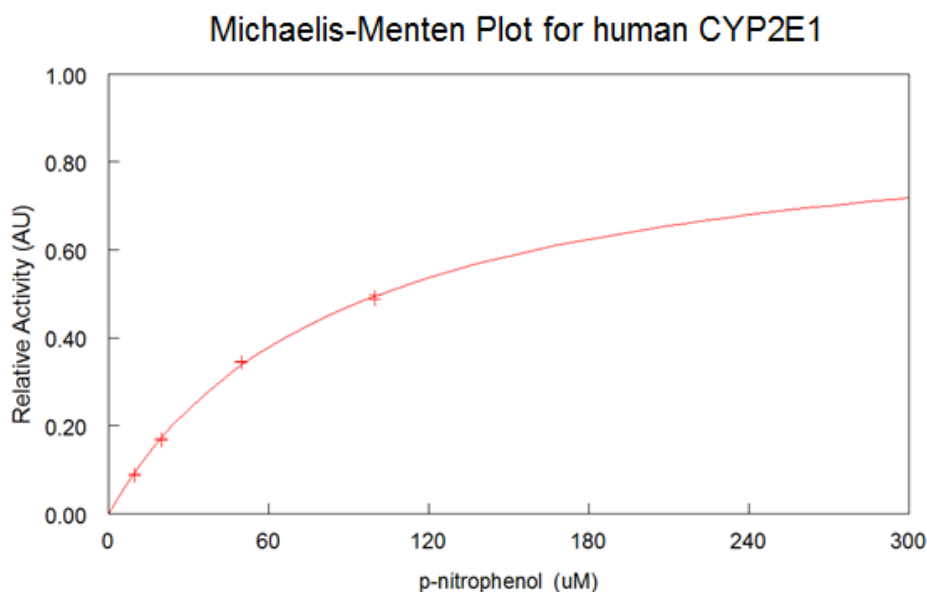


Figure 3.44 Michaelis-Menten Kinetics Plot for Hydroxylation of *p*-Nitrophenol to *p*-Nitrocatechol by CYP2E1 Enzymes in Human Liver S9 Fractions

The process of bioassay-guided fractionation as described in scheme 1 initially produced crude açai berry extracts as illustrated in scheme 2. A preliminary dose response for crude açai berry extracts towards CYP2E1 inhibition was carried out using human liver S9 fractions over a range of concentrations at 25, 50, 100 and 200 µg/ml. Among all the crude extracts, chloroform extract (Açai-31-2) showed significant inhibition of CYP2E1 enzyme in a dose dependent manner (Figure 3.45). Although

hexane extract (Açaí-31-1) showed a dose response, moderate inhibition of CYP2E1 was observed at only higher concentration such as 200 µg/ml. Both butanol extract (Açaí-31-3) and aqueous extract (Açaí-31-4) were found have no effect on CYP2E1 inhibition.

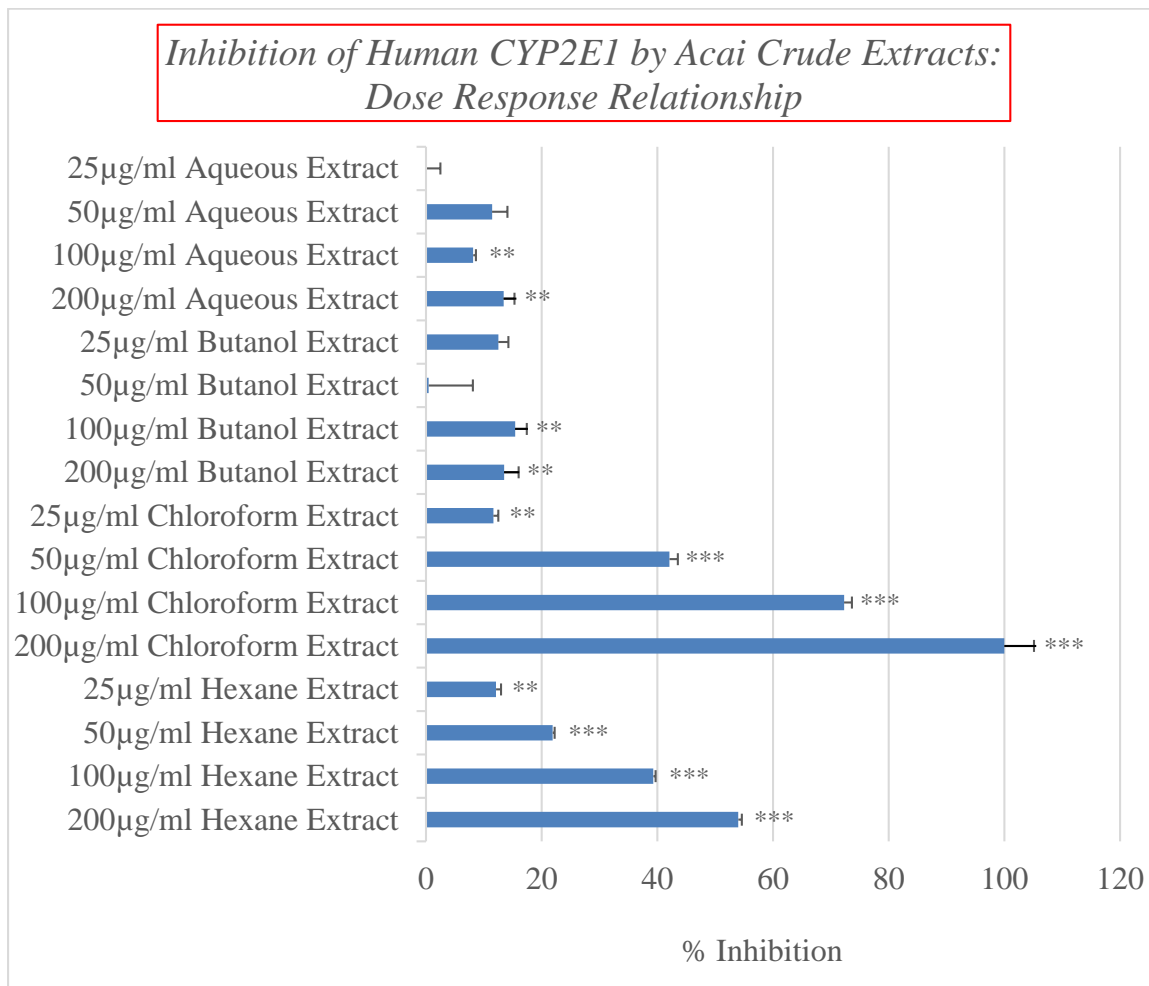


Figure 3.45 Inhibition of Human CYP2E1 by Açaí crude extracts

The chloroform extract (Açaí-31-2) was the more potent extract for CYP2A6 inhibition and therefore was already fractionated using column chromatography resulting in 10 fractions, Açaí-34-1 through Açaí-34-10 as described in scheme 3 were tested at

50µg/ml concentration. Amongst 10 fractions, Açai-34-7 and Açai-34-8 showed moderate inhibition of 53% and 61%, respectively (Figure 3.46). The fractions Açai-34-1 and Açai-34-4 showed mild inhibition of CYP2E1 and the remaining fractions showed no effect on CYP2E1.

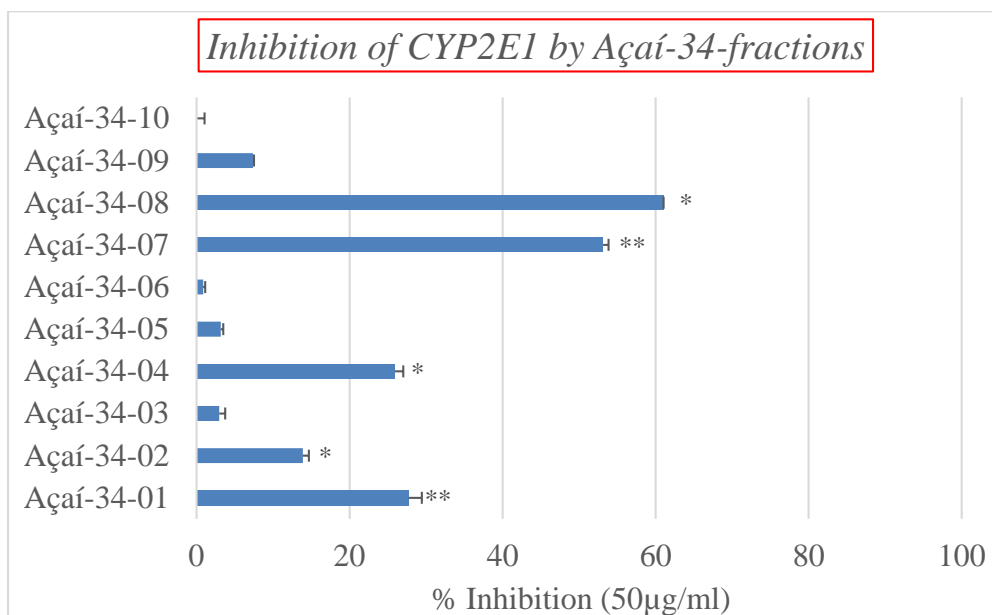


Figure 3.46 Inhibition of Human CYP2E1 by Açai-34-series

While the fraction Açai-34-8 was proceeded for further fractionations, low sample size of Açai-34-7 limited its fractionation (Scheme 4). Almost all the resultant 8 fractions of Açai-34-08 were found to inhibit CYP2E1 as the inhibitory action was observed to be distributed among these fractions except for Açai-38-04 (Figure 3.47). The 3 fractions preceding the inactive fraction Açai-38-04 were slightly less active than the later 4 fractions.

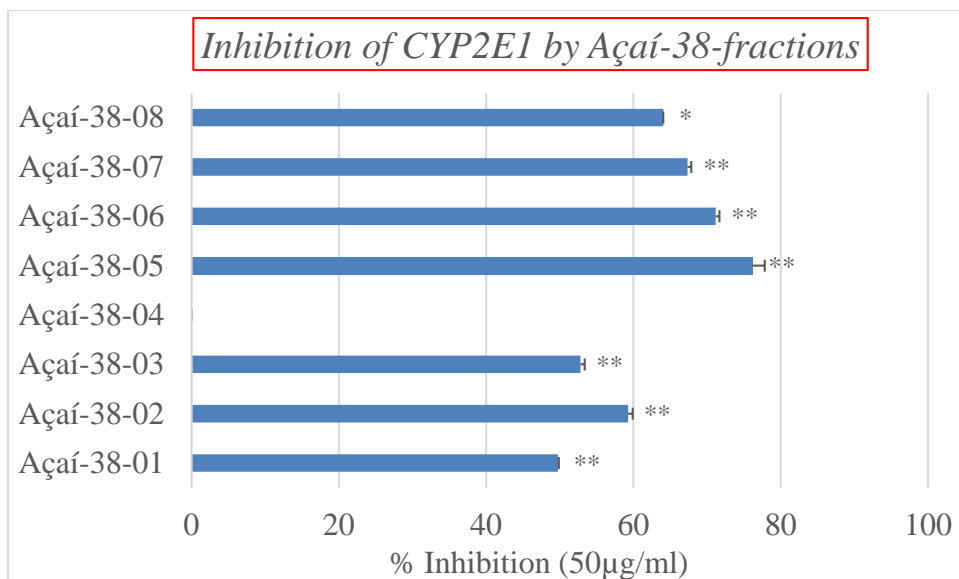


Figure 3.47 Inhibition of Human CYP2A6 by Açai-38-series

While most of the fractions belonging to Açai-38-series showed similar levels of inhibition for CYP2E1, further fractionations of Açai-38-series fractions was limited by the sample size generated. The first four fractions, Açai-38-1 to Açai-38-4 were the most abundant and were further fractionated. This resulted in the generation of fractions belonging to Açai-61-series from Açai-38-1, Açai-62-series from Açai-38-2, Açai-63-series from Açai-38-3, and Açai-64-series from Açai-38-4 fractions as described earlier (Scheme 5). All the fractions here onwards were tested at 25 µg/ml concentration.

Açai-38-1 produced 7 fractions belonging to Açai-61-series which were tested at 25 µg/ml (Scheme 5). However, the inhibitory activity was observed to be spread out across most of the fractions except for Açai-61-1 and Açai-61-7 (Figure 3.48). The extracts Açai-61-4, Açai-61-5 and Açai-61-6 showed moderate inhibition of CYP2E1 at

25 µg/ml concentration. The fractions Açai-61-2 and Açai-61-3 showed mild inhibition of CYP2E1 at this concentration.

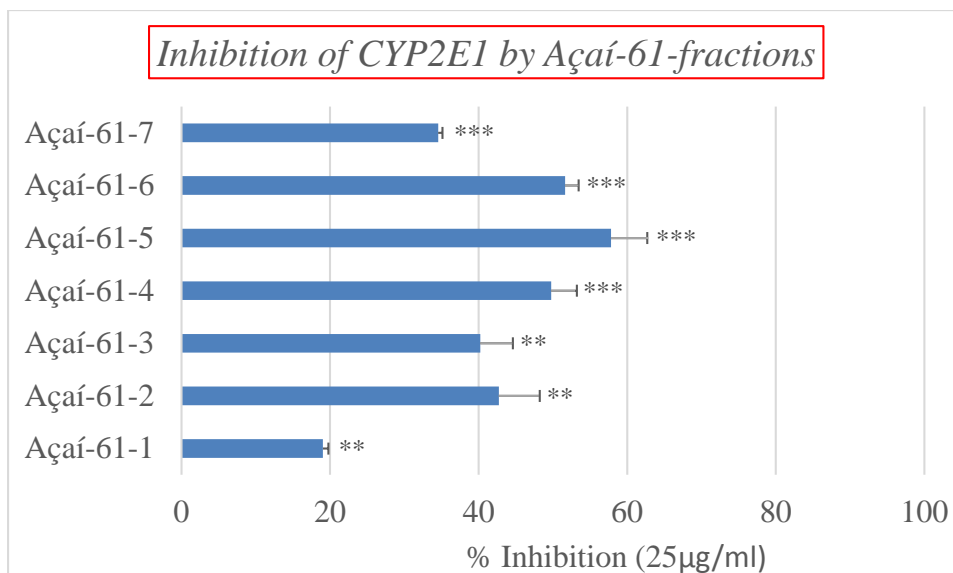


Figure 3.48 Inhibition of Human CYP2E1 by Açai-61-series

Similar results were obtained with the fractions generated from Açai-38-2 that yielded 5 fractions belonging to Açai-62-series (Scheme 5). These fractions were tested for CYP2E1 inhibition at 25 µg/ml concentration. Among these extracts, Açai-62-2 and Açai-62-3 showed inhibition greater than 50% and the rest of the fractions Açai-62-1, Açai-62-4 and Açai-62-5 showed CYP2E1 inhibition that was slightly less potent (Figure 3.49).

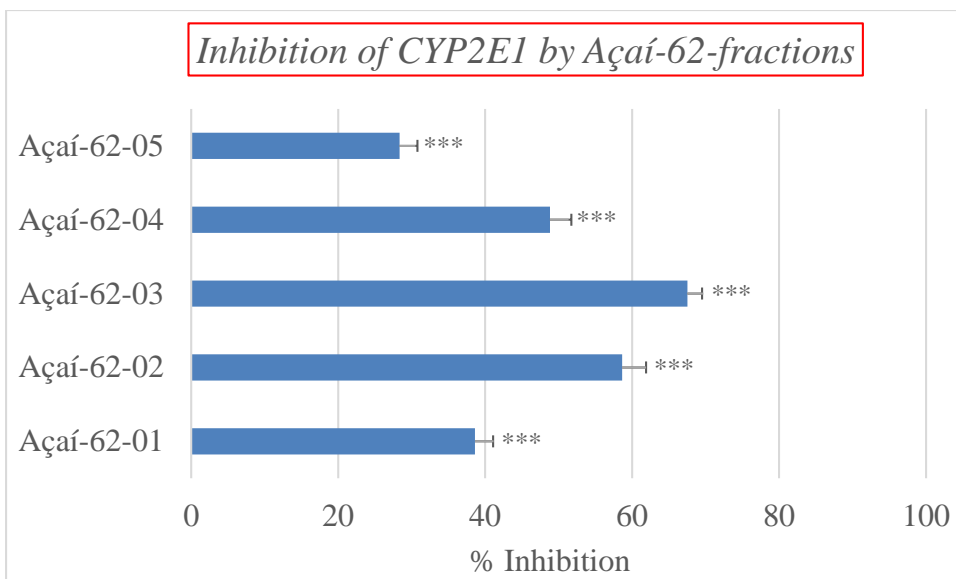


Figure 3.49 Inhibition of Human CYP2E1 by Açai-62-series

Similarly, Açai-38-3 produced 6 fractions belonging to Açai-63-series and these fractions too followed the same trend observed with Açai-61-series and Açai-62-series for CYP2E1 inhibition (Scheme 5). All six inhibited with Açai-63-2 to Açai-63-5 giving more than 50% reduction of CYP2E1 activity (Figure 3.50).

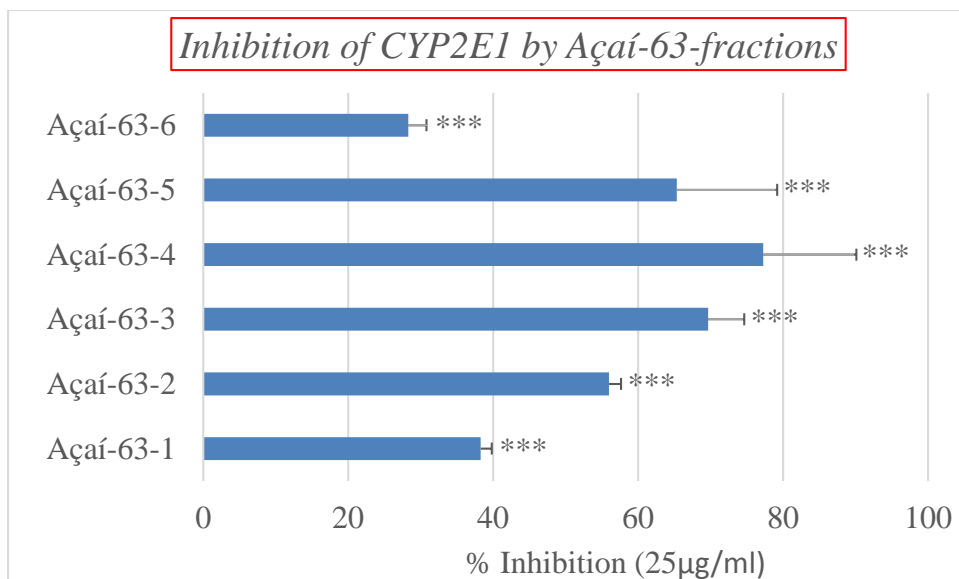


Figure 3.50 Inhibition of Human CYP2E1 by Açai-63-series

The fraction Açai-38-4 produced 5 fractions belonging to Açai-64-series (Scheme 5). These fractions also were found to be active towards CYP2E1 inhibition with the exception of Açai-64-5 (Figure 3.51).

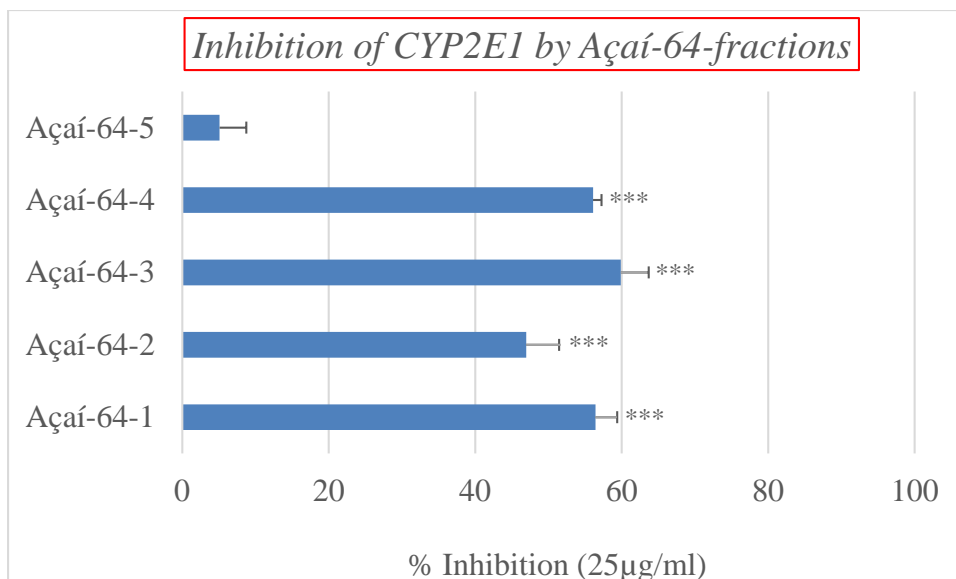


Figure 3.51 Inhibition of Human CYP2E1 by Açai-64-series

The process of bioassay-guided fractionation pursued so far by employing various chromatographic separation techniques was aimed to increase the inhibitory action by narrowing the activity towards fewer fractions as the procedure progresses. However, inhibitory action against CYP2E1 seemed to be spread-out over a very large proportion of all fractions collected.

Further fractionations of two inhibitory fractions of Açai-62-series, Açai-62-2 and Açai-62-3 produced Açai-78-series and Açai-82-series, respectively (Scheme 6).

Unexpectedly, subsequent fractions at these late stages began to lose potency rather than increase in potency. For example, only one fraction belonging to Açai-78-series namely Açai-78-D generated from a moderately potent fraction Açai-62-2 showed inhibition but at 50µg/ml concentration. It should be noted that this concentration is twice the concentration of its parent fraction indicating a clear loss of activity. A majority of

remaining fractions showed only mild inhibition with the exception of Açai-78-E and Açai-78-G, which did not show any increase in potency (Figure 3.52).

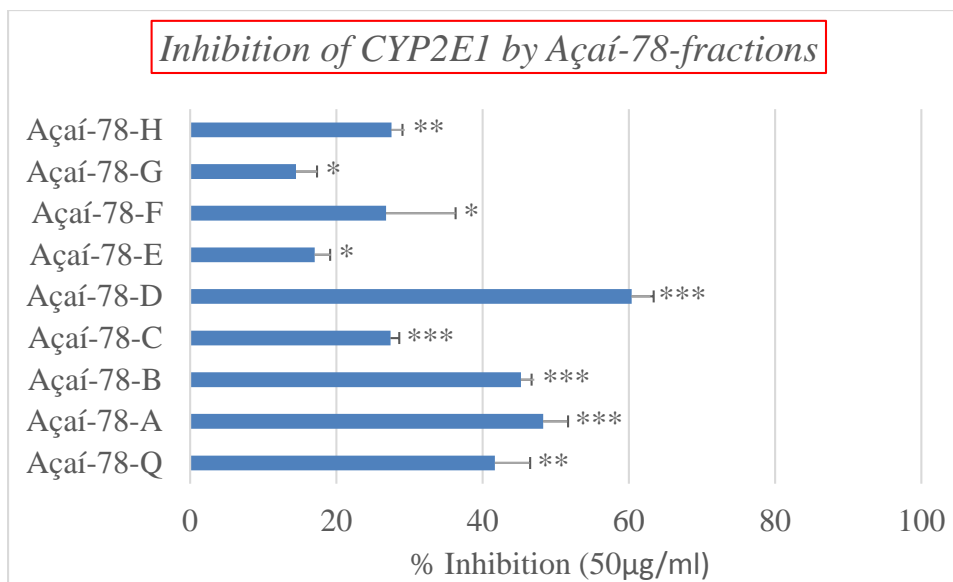


Figure 3.52 Inhibition of Human CYP2E1 by Açai-78-series

Similarly, a moderately potent fraction Açai-62-3 was fractionated to produce seven fractions belonging to Açai-82-series (Scheme 6). All the fractions belonging to Açai-82-series were found to be less potent than the parent fraction indicating loss of potency (Figure 3.53).

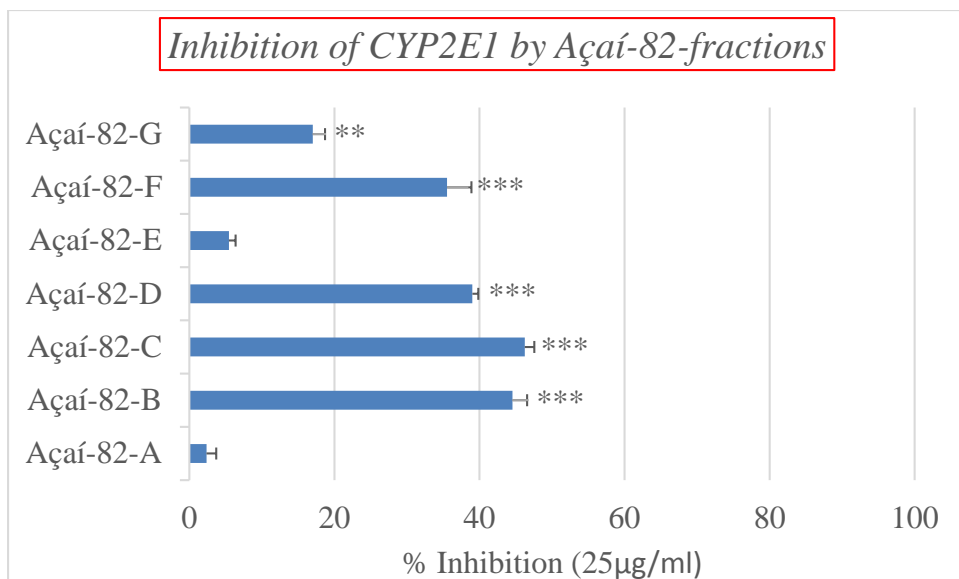


Figure 3.53 Inhibition of Human CYP2E1 by Açai-82-series

This trend was also observed with Açai-94-series comprising of 9 fractions that were generated from a potent fraction Açai-63-4 (Scheme 6). All the fractions belonging to Açai-94-series were found to have lost the potency compared to its parent fraction Açai-63-4 (Figure 3.54). For example, the parent fraction gave 70% inhibition at a concentration of 25 µg/ml, while the most potent fraction Açai-94-H from Açai-94-series only inhibited by 64% at the same dose.

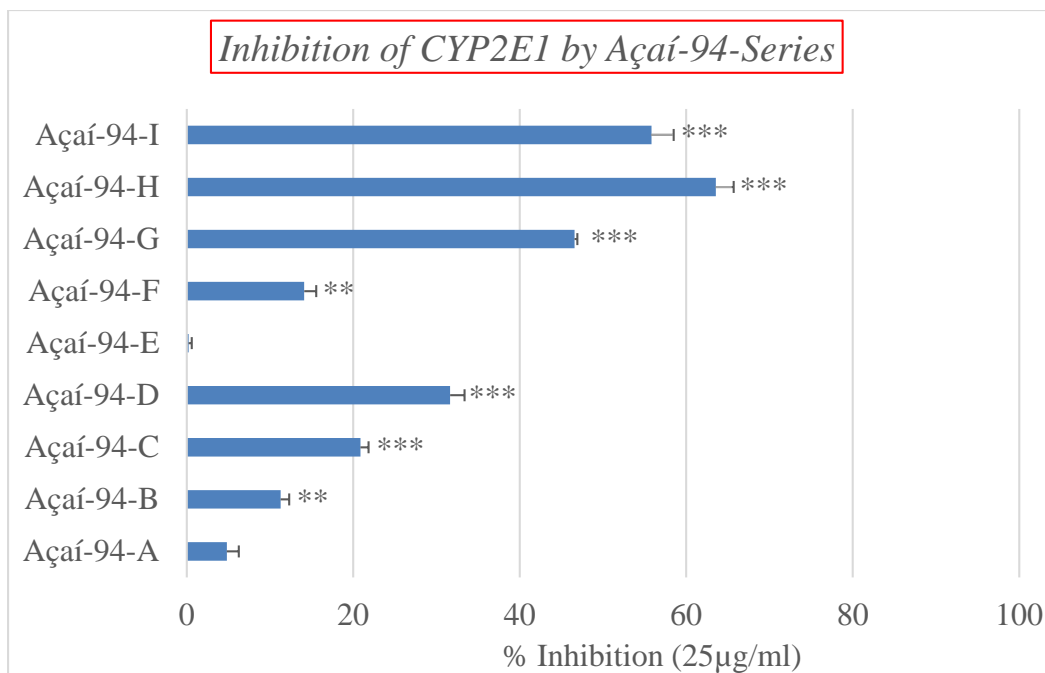


Figure 3.54 Inhibition of Human CYP2E1 by Açai-94-series

Yet another moderately potent fraction Açai-64-3 produced 7 fractions belonging to Açai-76-series fractions (Scheme 6). Again, none of these fractions were found to show significant improvement potency. It produced two fractions, Açai-76-C and Açai-76-D with potencies slightly higher than their parent fraction for CYP2E1 inhibition and all other fraction were found to have minimal inhibitory potential towards CYP2E1 inhibition (Figure 3.55).

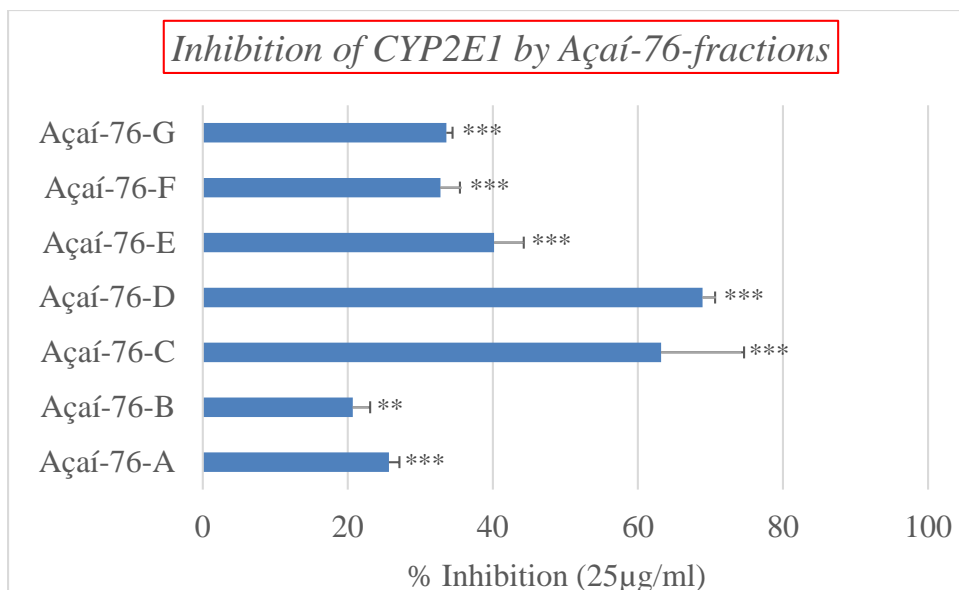


Figure 3.55 Inhibition of Human CYP2E1 by Açai-76-series

Açai-78-H was also fractionated and 9 fractions were produced belonging to Açai-97-series as described under scheme 7. Fractions Açai-97-B and Açai-97-D were found to be pure compounds belonging to the chemical class of compounds called pheophorbides. Açai-97-B and Açai-97-D were characterized by mass spectrometry and NMR spectroscopy to be Pheophorbide-a methyl ester ($C_{36}H_{38}N_4O_5$) and Pheophorbide-a ethyl ester ($C_{37}H_{40}N_4O_5$), respectively (Figure 4.20 and Table 4.1). Although Açai-97-D was an inhibitor, its potency was very low, suggesting very little physiological significance (Figure 3.56).

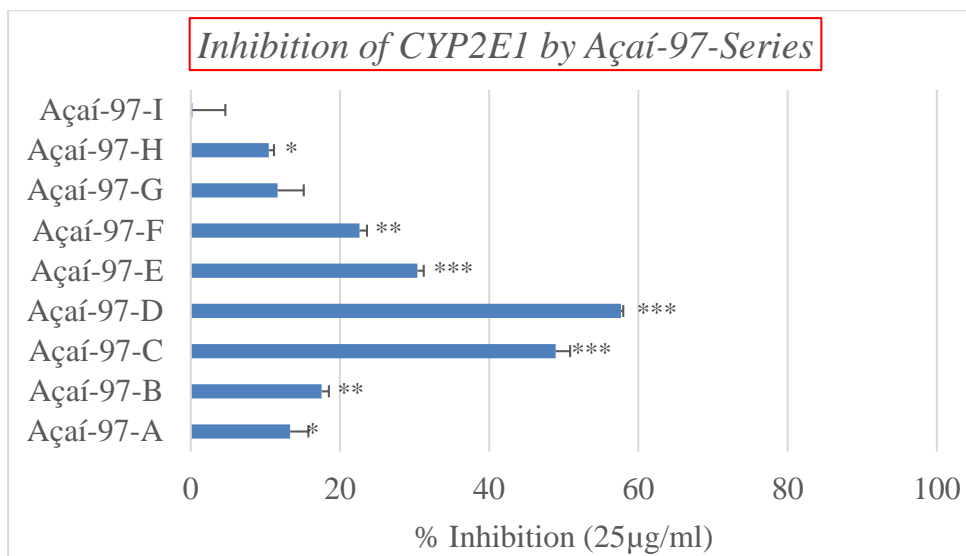


Figure 3.56 Inhibition of Human CYP2E1 by Açai-97-series

Similarly, the two fractions Açai-76-A and Açai-76-B originally identified as promising candidates for further fractionations for CYP2A6 inhibition were further fractionated to produce Açai-98-series and Açai-92-series, respectively (Scheme 7). Neither the Açai-92-series nor the 98 series contained fractions with inhibitory activity toward CYP2E1 (Data was not shown).

3.3.16. Summary of CYP2E1 Inhibition

Inhibition of CYP2E1 by various crude extracts of açai was studied using human liver microsomes. Among all the crude extracts, chloroform extract of açai was found to inhibit CYP2E1 in a dose dependent manner while the hexane extract showed a weak inhibition of CYP2E1 only at high concentrations and the aqueous and butanol extract showed no inhibition. The chloroform extract when fractionated further produced two active fractions, Açai-34-07 and Açai-34-08 with the latter being more potent. Among the

eight fractions that were derived from Açai-34-08, all the fractions except Açai-38-04 produced moderate inhibition of CYP2E1. This trend was most likely the result of a very broad substrate specificity. A very similar trend was observed with the fractions belonging to Açai-61-series, Açai-62-series, Açai-63-series and Açai-64-series that were generated from Açai-38-1, Açai-38-2, Açai-38-3 and Açai-38-4 fractions, respectively. This confirms our earlier finding with aldehydes that the active site of CYP2E1 is flexible with phenylalanine rich active site and extended π -system allowing for the expansion of its own active site. However, the trend failed to continue towards the generation of later fractions as most fractions appear to have lost the activity. The loss of activity can be attributed probably to the decreased stability of the constituents present in those fractions.

3.4. Discussion

The current research demonstrated the *in vitro* inhibition of several Cytochrome P450 enzymes involved in drug metabolism by crude açai berry extracts in an attempt to understand potential drug-herbal interactions involving açai berry and possible physiological significance. Among all the crude extracts, the chloroform extract inhibited most of the cDNA expressed CYP isoforms with variable potency. Additionally, a dose-response relationship established the inhibition of isoforms such as CYP1A1, CYP2B6, CYP2C8 and CYP2D6 at low concentrations of 5 $\mu\text{g}/\text{ml}$. Finally, the K_I values obtained for these enzymes indicates that crude chloroform extract of açai berry might have clinical relevance with its possible role arising from drug-herbal interactions. The fractionation procedure initially isolated the fatty constituents into hexane fraction, then

isolated the water soluble constituents into aqueous fraction leaving the constituents with a good balance between the hydrophilic and lipophilic nature. This balance is critical for chemical constituents to bear any physiological relevance as these constituents are required to cross several biological membranes including gastrointestinal tract for oral absorption before they can even elicit any actions over its target receptors. The physiological significance of chloroform extract can further be rationalized by the apparent lack of inhibition of CYP enzymes by aqueous extract of açai berry and also the lack of inhibition of most CYP enzymes by butanol and hexane extracts. Although, much of the recognition for açai is touted to the presence of high levels of polyphenolic compounds such as anthocyanins and flavonoids, it is to be noted that the butanol and aqueous fractions rich in polyphenolic compounds showed least inhibition of various CYP isoforms tested.

The study was extended towards the identification of inhibitors of the toxicologically important Cytochrome P450 enzymes. CYP2A6 and CYP2E1 were identified for the current study as the candidates of toxicological significance and inhibition of these enzymes may confer protection against their potential detrimental effects. There are several instances where the presence of small quantities of chemical constituents capable of inhibiting these enzymes resulted in protective effects. The bioassay-guided fractionation of freeze-dried açai berry extracts started on a promising note of obtaining inhibitors of CYP2A6 and CYP2E1 enzymes. Overall bioassay-guided fractionation was pursued to produce six different stages of fractions. The promising potential was retained until the first four stages and then over the latter two stages this

potential lost its pattern. This result suggests that the açai berry lacks specific chemical constituents capable of inhibiting CYP2A6 and CYP2E1 enzymes. The fact that earlier crude fractions possess inhibitory potential towards these enzymes can be partly explained by the nature of these enzymes. For example, the evolutionary role of cytochrome P450 enzymes in metabolism conferred these enzymes the key attribute of broad substrate selectivity. Multiple constituents present at crude level might have modulated the activities of CYP2A6 and CYP2E1 resulting in observed inhibition at crude levels better than the latter fractions that are presumed to have a less complexity. Simultaneous binding of several substrate molecules among the fractions at crude level results in the formation of different enzyme-substrate complexes with differing stoichiometry and differing functional properties. Understanding these complex kinetic behaviors however provide insights into the mechanisms worthwhile to predict interactions, the complexity however associated with crude extracts or certain fractions makes the process difficult to pursue. Additionally, the fractions might have lost the inhibitory chemical constituents because of stability issues arising from external factors such as time, temperature and light or through modifications of constituents itself through its exposure to fractionation procedures.

The crude hexane extract of açai produced response similar to the chloroform extract towards CYP2A6 and CYP2E1 inhibition. However, the presumption that the hexane extract is rich in fats and oils renders the extract to be poorly absorbed, metabolically less stable and kinetically short acting in nature in physiological environment. These factors together with chromatographic challenges for separation of

bioactive constituents limited further fractionation of hexane extract. Likewise, the high anthocyanin content that is presumed in butanol and aqueous extract did not affect the CYP enzymes as much at test concentrations and therefore the bioassay-guided fractionation of these was not pursued.

All our findings from *in vitro* inhibition of cytochrome P450 enzymes collectively indicate the presence of chemical constituents in chloroform extract of açai capable of modulating the enzymatic activities of certain CYP isoforms such as CYP1A1, CYP2B6, CYP2C8 and CYP2D6 as demonstrated by the low K_i values. The potential for the pharmacokinetic interactions cannot be undermined and further studies are warranted for our understanding of the physiological, toxicological and clinical significance arising from drug- açai interactions.

CHAPTER IV

**INDUCTION OF ARE-DEPENDENT GENE EXPRESSION IN CULTURED
HEPG2 CELLS BY CONSTITUENTS OF AÇAÍ**

4.1. Introduction

Oxidative assaults are inevitable in the biological systems. Normal physiological processes ranging from mitochondrial metabolism to certain enzymatic reactions and various adverse environmental factors can produce reactive oxygen species as byproducts. Under normal physiological conditions, these reactive oxygen species are efficiently antagonized by various antioxidant defense components confined to particular compartments of the cell. However, a rapid increase in reactive oxygen species results in an oxidative burst that culminates into oxidative stress if it is not managed in a controlled manner. The burden of oxidative stress is largely counteracted by an intricate antioxidant defense system controlled, in part, by Nrf2/ARE signaling pathway. Activation of Nrf2/ARE signaling pathway deploys a battery of antioxidant enzymes that respond adequately to the oxidative stress, which is critical for the maintenance of life. Inadequate response elevates the risk for a variety of oxidative stress related diseases.

The Nrf2/ARE signaling pathway mediates the induction of phase II antioxidant enzymes through the activation of nuclear transcription factors and protects the cells against the damaging effects of oxidants and electrophiles ^{13, 14}. The damaging effects of reactive oxygen species are largely counteracted by cytoprotective antioxidant enzymes,

many of which are part of the phase II drug metabolism system. These enzymes are generally under hormonal control but are also inducible by foreign chemicals. Induction of cytoprotective genes represents a highly effective strategy for protecting cells against oxidants and other reactive species. The activity of phase II enzymes is stimulated by a wide range of chemicals, bioactive agents and environmental conditions ¹³. This stimulation results in an increased expression of genes such as heme oxygenase (HO-1), NAD(P)H:quinone oxidoreductase (NQO1), glutathione-S-transferase (GST), glutamate cysteine ligase (GCL) and Thioredoxin (TXN), conferring protection against oxidative damage to the cell. The expressed enzymes catalyze a wide variety of reactions that neutralize reactive oxygen species and other reactive electrophiles. Numerous studies showed the induction of phase II enzymes such as HO-1 by synthetic and natural compounds, including polyphenolic compounds, is sufficient for the acquisition of antioxidant and cytoprotective activities in a variety of pathological models ⁷⁵.

4.1.1. The Nrf2/ARE Signaling Pathway

Nrf2/ARE signaling pathway mediates expression of phase II antioxidant enzymes as depicted in figure 4.1. A *cis*-acting enhancer sequence in the promoter region of target genes known as the antioxidant response element (ARE). The consensus ARE sequence was initially identified and characterized to have 5'-rTGACnnnGC-3', where "r" represents a purine ^{76, 77}. The consensus ARE motif was subsequently revised and extended to 5'-TMAnnRTGAYnnnGCRwww-3', where "R" is adenosine or guanine and "Y" represents cytosine or thymine "w" is adenine or adenine or thymine ⁷⁸. The

ARE sequence is recognized mainly by a key transcription factor called nuclear factor erythroid 2 related factor 2 (Nrf2)⁷⁹. Nrf2 is known to regulate basal and inducible expression of cytoprotective enzymes. Under basal homeostatic conditions, Nrf2 is repressed by a cysteine-rich protein, Kelch-like ECH associated protein1 (Keap1) in the cytosol⁸⁰. Keap1 bridges Nrf2 to Cullin3-based E3 ligase (Cul3), a ubiquitin ligase that ubiquitinates Nrf2, which marks it for degradation at the proteasome⁸¹. Keap1 and Cul3 collectively sequester Nrf2 and prevent the activation of Nrf2 target genes. The disruption of the interaction between Keap1 and Nrf2 results in the activation and subsequent nuclear localization of Nrf2. Nrf2 then forms heterodimers with other transcription factors such as small Maf proteins and binds to AREs, resulting in transactivation of ARE-driven genes. Therefore, the Nrf2/ARE pathway serves as a defense system in higher organisms to protect them against a wide range of chemical assaults. Nrf2 has a relatively short half-life as it is phosphorylated by the enzyme Fyn kinase. The phosphorylated Nrf2 then translocates back into the cytosol for further degradation (Figure 4.1).

Nrf2/ARE Signaling Pathway

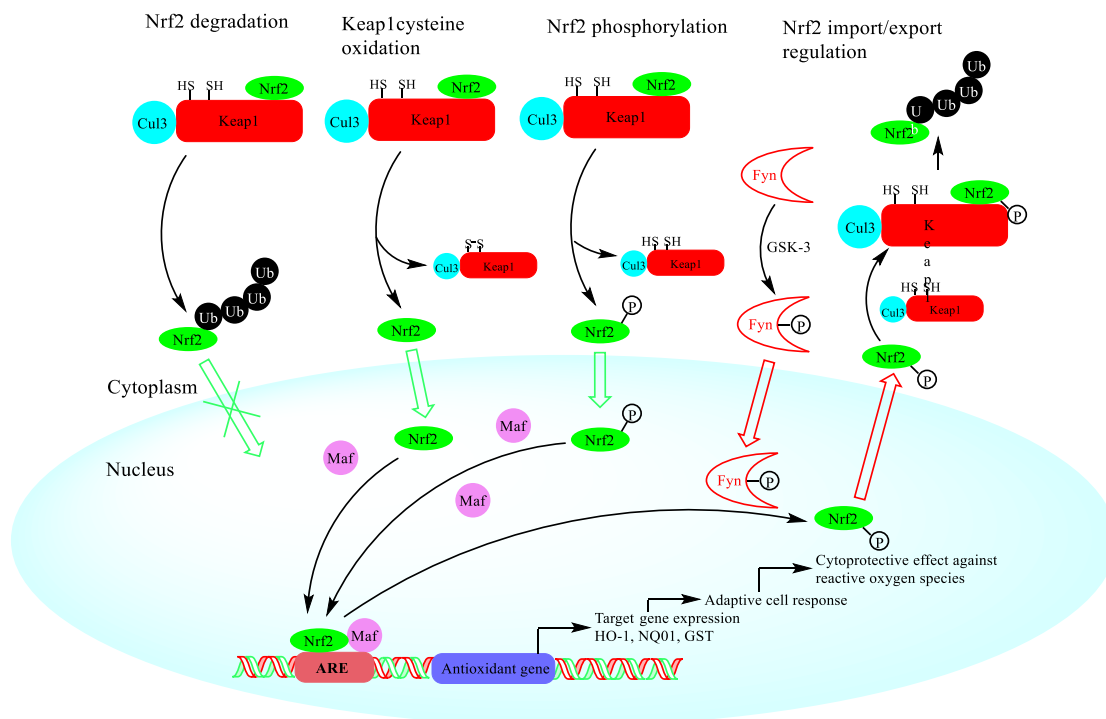


Figure 4.1 Nrf2/ARE Signaling Pathway

The general strategy used in the current study was to examine the effects of constituents of the açai berry on Nrf2-mediated antioxidant gene expression. To do this, an ARE of human thioredoxin (hTXN) was cloned into an experimental luciferase reporter vector, transiently transfected in human hepatocarcinoma (HepG2) cells, and then the cells were treated with açai fractions. The increases in the transcriptional activity of the reporter luciferase that is under the control of thioredoxin ARE upon treatment with açai extracts was studied to identify specific chemical constituents in the açai that stimulate the Nrf2/ARE antioxidant pathway. A bioassay-guided fractionation approach

was done on the freeze-dried açai berry extracts to identify the activators of Nrf2/ARE signaling pathway.

4.1.2. Açai Berries in Relation to Nrf2 Antioxidant Pathway

The widely acclaimed health benefits of açai are thought to be related to high levels of antioxidants including anthocyanins, flavonoids and polyphenolic compounds^{70, 71, 82, 83}. The major anthocyanins identified in açai are cyanidin-3-glucooside, cyanidin-3-rutinoside and cyanidin-3-diglycoside but only accounted for 10 % its overall antioxidant capacity of açai^{70, 73}. Several of the physiological effects of açai can be related to the modulation of Nrf2 antioxidant pathway. For example, pretreatment of açai prior to hydrogen peroxide-induced oxidative stress greatly reduced ROS generation in freshly prepared neutrophils⁷¹. Açai modulated ROS production by neutrophils and favored a healthy oxidant balance in rats by inducing antioxidant gene expression⁸⁴. Açai supplementation in rats improved serum biomarkers of protein oxidation and also reduced the need for protective responses by reducing stress⁸⁵. Also, a systemic evaluation of açai in healthy human volunteers resulted in a significant increase in antioxidant activity of plasma, as demonstrated by ORAC assay⁸⁶. Proanthocyanidins of açai ameliorated acute lung inflammation and emphysema induced by cigarette smoke in mice probably by reducing oxidative stress through modulation of antioxidant gene expression and inflammatory reactions^{87, 88}. In addition, the compounds related to chemical classes found in açai are shown to induce various phase II antioxidant enzymes through Nrf2 and various other signal transduction pathways. For example, anthocyanin

fractions of purple sweet potato reduced dimethylaminonitrosamine- induced oxidative stress in rats by inducing HO-1, NQO1 and also Nrf2, in addition to the enzymes involved in the glutathione system. Induction of HO-1, NQO1 and Nrf2, all of which possess an ARE sequence in their promoter region, demonstrates involvement of the Nrf2/ARE pathway ⁸⁹. Also, induction of antioxidant enzymes such as HO-1 by flavonoid compounds was shown to involve activation of protein kinase and mitogen activated kinase pathways, which is linked to the Nrf2 signal transduction pathway in human umbilical vein epithelial cells ⁹⁰.

Several studies demonstrated a positive relationship between the antioxidant capacities of açai with the observed physiological activities. Inhibition of lipid peroxidation as a result of inhibition of glutathione peroxidase and glutathione reductase, in addition to inhibition of NF-κB activation through the regulation of inflammatory mediators contributed to the athero-protective effect by flavonoids of açai ^{83, 91}. A strong correlation between the antioxidant status and anti-inflammatory activity through inhibition of cyclooxygenase was observed in purified human neutrophils ^{71, 92}. Furthermore, dietary açai reduced N-nitrosomethylbenzylamine-induced esophageal tumorigenesis in rats through the regulation of cytokines ⁹³. Other studies demonstrated the relationship between antioxidant capacity of anthocyanins and oxidative stress-induced apoptosis by correlating the induction of phase II antioxidant enzymes to the inhibition of caspase-3 in rat liver epithelial cell line ⁹⁴.

All the above studies collectively indicate the involvement of signaling pathways modulating the expression patterns of cytoprotective genes by the extracts of açai.

Despite the evidence that açai protects the cell in conditions of oxidative stress, the studies related to its antioxidant potential are limited with regard to generalized regulation of phase II enzymes and the related molecular mechanisms associated with the protective effects of açai products are not clearly understood. The recent refutation of ORAC assay by USDA`s NDL further emphasizes the need to identify mechanisms associated with the antioxidant activity of açai that could possibly involve transcriptional regulatory pathways, like the Nrf2 pathway, or any other mechanism unrelated to direct quenching of reactive species. This forms the long range goal of the current project whose short term aims are to identify the chemical constituents that may take part in the complex process of Nrf2-dependent gene induction.

4.2. Materials and Methods

4.2.1. Chemicals and Reagents

All the chemicals and reagents were purchased as molecular biology grade from Fisher Scientific and Promega.

4.2.2. Cell Culture

The human hepatocellular carcinoma (HepG2) cells, were obtained from American Type Culture Collection (ATCC) were grown in cell culture treated plates. The growth medium for HepG2 cells comprised of high glucose Dulbecco Modified Eagle Medium (DMEM) supplemented with 10% fetal bovine serum (FBS), 100 U/ml

penicillin, and 100 µg/ml streptomycin and incubated at 37C in a 5% carbon dioxide atmosphere.

4.2.3. Oligonucleotides, Vectors and Enzymes

Custom synthesized oligonucleotides used in the construction of plasmid vectors and in PCR were purchased from Integrated DNA Technologies, Inc. All the enzymes for cloning purposes such as restriction digestion, phosphorylation and ligations were from New England Biolabs. The luciferase reporter plasmids, pGL3 promoter vector containing firefly luciferase and pRL vector containing renilla luciferase, and the dual-luciferase assay system were from Promega. Sequencing service for both the wt-ARE and mARE containing pGL3 plasmid vectors was verified by SeqWright Genomic Services.

4.2.4. Construction of ARE Reporter Vectors

A *cis*-acting DNA sequence called ARE is now widely recognized to be involved in the transcriptional activation of phase II antioxidant enzymes following Nrf2/ARE signaling pathway. The pGL3 promoter vector containing genetically engineered firefly luciferase from *Photinus pyralis* was used for monitoring of transcriptional activity in transfected eukaryotic cells. The pGL3-promoter vector is driven by a simian virus 40 (SV40) minimum promoter with upstream restriction sites including *KpnI* and *NheI*. The sequences of sense and antisense strands of oligonucleotides corresponding to wild-type ARE of Thioredoxin and its mutant containing overhangs complementary to *KpnI* and *NheI* sticky ends were initially phosphorylated and subsequently annealed to form

double-stranded oligonucleotides as illustrated in figure 4.2. The double-stranded oligonucleotides were then subcloned between *KpnI* and *NheI* restriction sites of a pGL3 promoter vector. A wild-type and a mutant version of ARE-luciferase plasmid vector were generated using pGL3 promoter vector (Figure 4.3). Amplification of the ligated recombinant DNA was then carried out separately for pGL3 plasmid and the two plasmid constructs, pGL3-*wtARE* and pGL3-*mARE*, in competent *Escherichia coli* cells. Verification of the sequences for the inserts in the plasmid constructs was confirmed by SeqWright Genomic Services. Successful constructs of both the wild-type and the mutant ARE-containing plasmid vectors were amplified in large scale and transfection-grade plasmid purification was achieved using QIAGEN plasmid Maxi Kit.

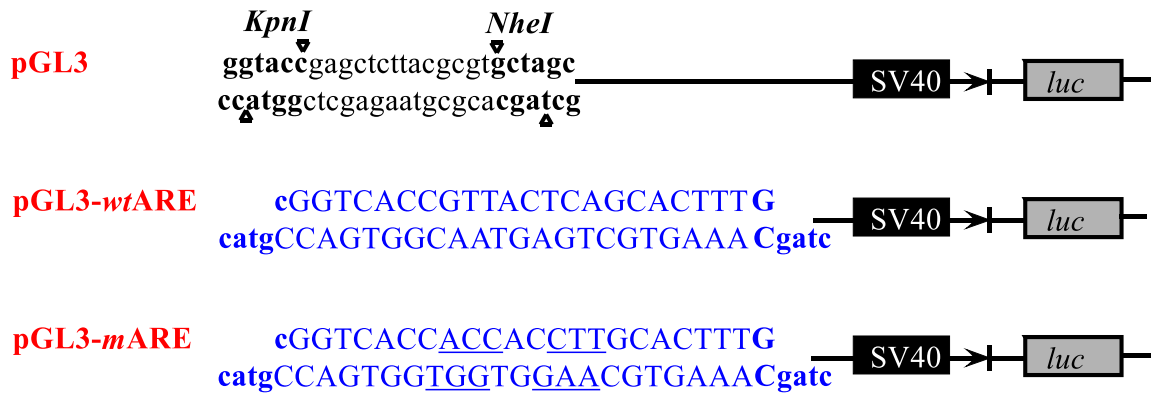


Figure 4.2 Schematic Illustration of Promoter Region of pGL3 Plasmid Vector, Wild-type and Mutant ARE Constructs

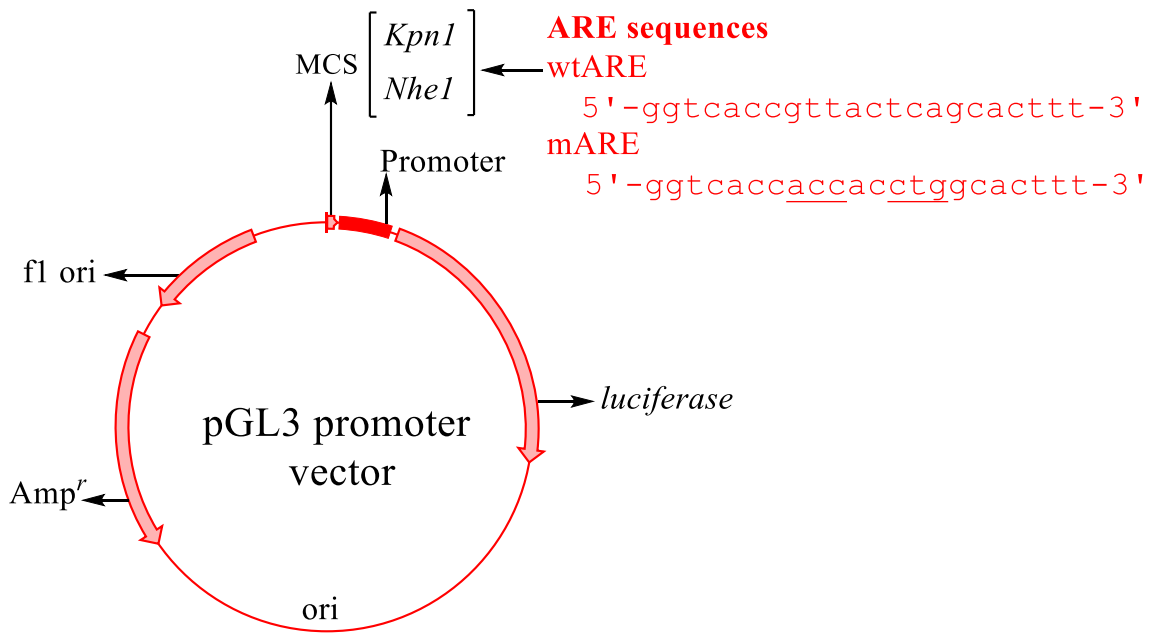


Figure 4.3 Construction of ARE-luciferase containing Plasmid Vectors

4.2.5. Bioassay-guided Fractionation of Açai

All the bioassay-guided fractionations on freeze-dried açai berry powder for identification of inducers of Nrf2/ARE signaling pathway were carried out by Dr. Oberlies research group as described earlier.

4.2.6. Sample Preparation of Açai

Procurement of freeze-dried açai berry powder, storage and its authentication were discussed earlier in Chapter 3. All the fractions generated through the bioassay-guided fractionation of freeze-dried açai berry powder were partitioned into aliquots for future use. Dimethyl sulfoxide at 0.2% was used as a co-solvent in the preparation of açai samples for all cell culture experiments. Each sample initially received dimethyl

sulfoxide required to produce 0.2% final concentration in the incubation mixture followed by slow addition of the medium while vortexing.

4.2.7. Induction of ARE-luciferase

The general experimental approach for the identification of inducers of Nrf2/ARE signaling pathway is illustrated in figure 4.4. Bioassays involved cultured HepG2 cells that were transfected with ARE-containing luciferase vector prior to the treatment with the fractions being tested. HepG2 cells were grown up to 50-60% confluence were transiently transfected with appropriate expression plasmid vectors and then treated with various extracts of açai.

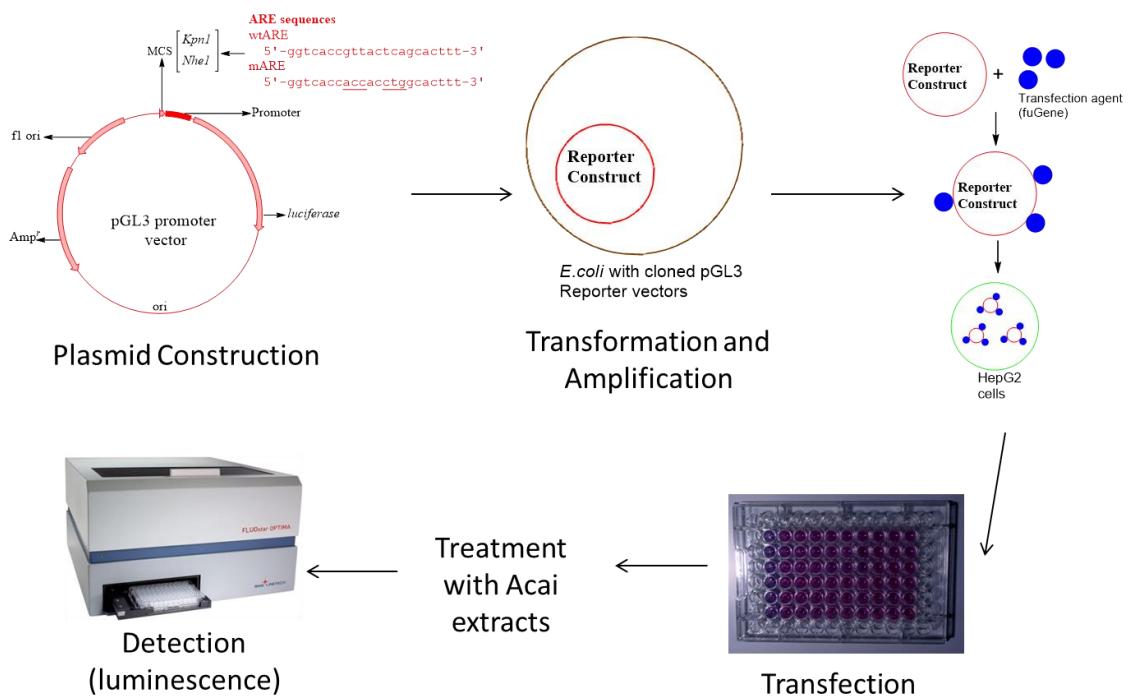


Figure 4.4 Schematic Illustration of ARE-luciferase Induction by Açai Berry in Cultured HepG2 Cells.

4.2.8. Transfection

Reporter gene assays serve as an excellent tool for studying the transcriptional activation of mammalian gene expression. The quantitative analysis of synthesized pGL3 plasmid constructs in transfected HepG2 cells was used to screen a series of fractions generated through bioassay-guided fractionation of freeze-dried açai berry powder. Transient transfection of HepG2 cells grown up to 60% confluence in 96 well plates with the plasmid vectors was facilitated by FuGENE[®] HD transfection reagent (Promega). Briefly, the plasmid vectors were initially incubated with FuGENE[®] HD transfection reagent for 15 minutes in plasmid to transfection reagent ratio of 200 ng:0.6 µl per well to generate the transfection complex. Then serum-free DMEM devoid of antibiotics was prepared and incubated for another 15 minutes to generate transfection medium. To account for the variability in the transfection efficiency, a control plasmid vector pRL-CMV encoding for renilla luciferase combined with transfection medium was prepared simultaneously and combined with pGL3 containing transfection medium. Transfection medium was added such that each well of a 96 well plate received 200ng of appropriate pGL3 plasmid luciferase vector and 20ng of renilla luciferase vector in a serum-free DMEM medium for a period of 24 hours.

4.2.9. Treatment

After 24 hours of transfection, the cells were treated for 24 hours with the appropriate controls and the fractions generated through bioassay-guided fractionation. After the treatments were completed, the cells were washed twice with phosphate

buffered saline (PBS). Each well then received 40 μ l of passive lysis buffer and was sonicated with 5 pulses of 5 seconds each on a water bath sonicator.

4.2.10. Measurement of ARE-luciferase Activity

Transcriptional activity of the firefly luciferase was determined and normalized to the renilla luciferase expression using Dual-Glo luciferase reporter assay kit (Promega) on a PolarStar Optima Microtiter Plate Reader (BMG LabTech). All the measurements were carried out in triplicates and the results were expressed as fold induction with standard deviations compared to the 0.2% DMSO solvent control. In all the experiments, 100 μ M *t*-butylhydroquinone, which is a known inducer of Nrf2/ARE signaling pathway was used as a positive control. The concentration of the açai fractions was maintained at 50 μ g/ml in all the experiments. A dose response study was carried out whenever a fraction warranted for it. Figure 4.5 illustrates the assay principle for measuring luminescence from the enzymatic activities of firefly and renilla luciferase enzymes expressed in HepG2 cells.

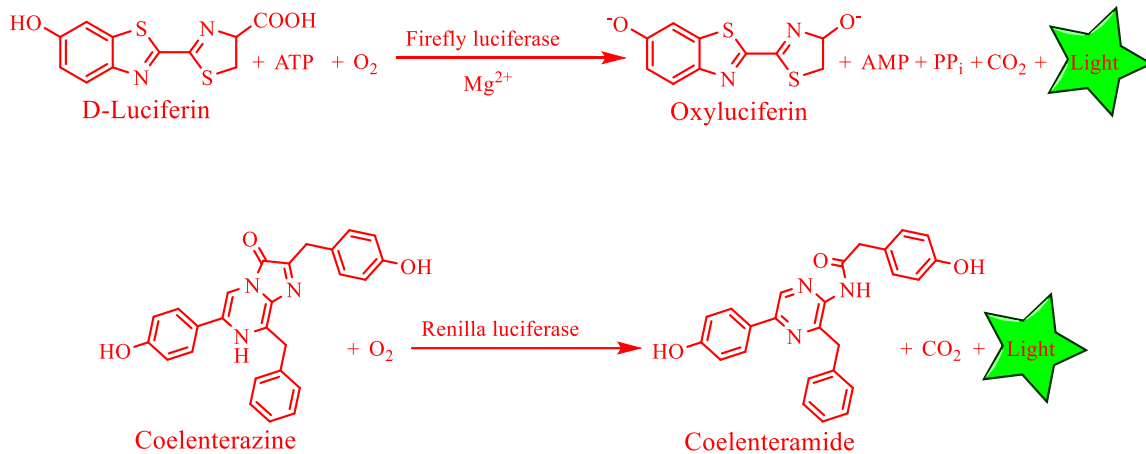


Figure 4.5 Bioluminescence Reactions Catalyzed by Firefly and Renilla Luciferases

Firefly luciferase converts D-luciferin to oxyluciferin and renilla luciferase converts coelenterazine to coelenteramide. Both oxyluciferin and coelenteramide were luminescent products and the amounts produced as a result of enzymatic reaction were measured using a luminometer. The expression of firefly luciferase was normalized to the expression of renilla luciferase, an internal control vector used in transfection. The luminescence produced in the cell lysates were correlated to the luciferase expression that is dependent on the promoter activity. An increase in the expression of firefly luciferase in HepG2 cells receiving pGL3-wtARE reporter plasmid in response to positive control and açai extracts was quantified as induction mediated by Nrf2/ARE signaling pathway. A strong transcriptional activation and therefore luciferase expression observed with wtARE-pGL3 luciferase vector was completely abolished in mARE-pGL3 vector.

4.3. Results

An Antioxidant Response Element (ARE) sequence is an evolutionarily conserved consensus sequence present in the promoter region of the antioxidant genes. The ARE element modulates the expression of Nrf2/ARE signaling pathway and is responsive to various internal and external factors. Inducers of Nrf2/ARE signaling pathway act through the modulation of several factors called transcription factors involved in the process. However, the direct measurement of involvement of Nrf2/ARE signaling pathway is often cumbersome requiring experimental setups such as large amounts of cells, large volumes of reagents and tedious purification processes. Therefore, an indirect measurement for the involvement of the Nrf2/ARE signaling pathway was employed in the study in order to identify chemical constituents with potential ARE activating and therefore antioxidant properties. It involved the construction of luciferase containing promoter vectors and transfection of the promoter vector into cultured HepG2 cells. The promoter containing plasmid vectors work in a manner similar to the expression of antioxidant genes. The plasmid vectors are luminogenic, so their activities were measured by the expression of luciferase enzyme. The detection of ARE-dependent luciferase enzyme is much more sensitive than the actual ARE-dependent antioxidant genes, thus enabling a convenient and sensitive high through put analysis that can be correlated to the involvement of Nrf2/ARE signaling pathway.

In the current research, an ARE sequence corresponding to the human Thioredoxin (hTXN) was successfully cloned into the promoter region of luciferase containing pGL3 plasmid vector to produce pGL3-*wt*ARE plasmid vector. An ARE

sequence present in pGL3-wtARE promoter plasmid vector when stimulated induces the expression of downstream luciferase whose activities were measured using luminometer. Similarly, a mutated ARE sequence containing plasmid was constructed to produce pGL3-mARE plasmid vector. The pGL3-mARE plasmid owing to the presence of non-functional ARE is expected to return the expression of luciferase to the basal level and is expected to be similar to the luciferase expression by pGL3 vector. The success of plasmid construction was verified with SeqWright Genomic Services and the working of the plasmid constructs was verified by conducting a preliminary experiment using *tert*-butylhydroquinone (*t*BHQ) at 100 μ M as a positive control. The results from preliminary experiment corroborated the success of plasmid construction (Figure 4.6). The pGL3-wtARE vector in controls showed basal expression of luciferase that was normalized to one and the expression of all other vectors and all other treatments were shown as fold induction compared to the expression pGL3-wtARE expression from controls. Both the pGL3 and pGL3-mARE vectors showed minimal expression of luciferase because pGL3 lacked the promoter sequence and pGL3-mARE contained a non-functional ARE promoter. The presence of functional ARE in pGL3-wtARE induced the expression of luciferase enzyme by about 2.5 times upon treatment with 100 μ M *t*-butylhydroquinone compared to that of 0.2% DMSO solvent control.

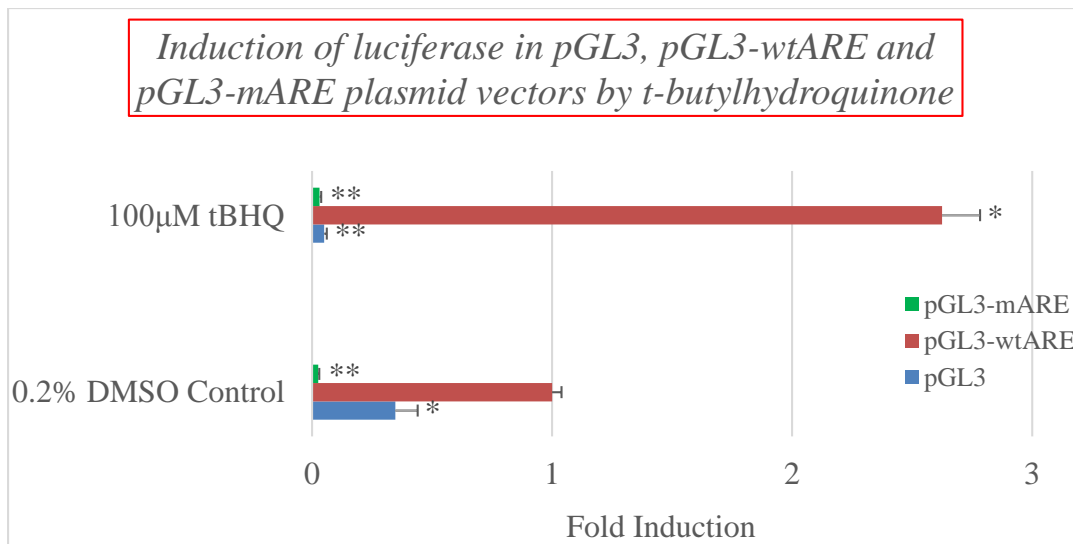


Figure 4.6 Induction of ARE-driven Luciferase Expression pGL3, pGL3-wtARE and pGL3-mARE containing Plasmids in Cultured HepG2 Cells by *t*-Butylhydroquinone

The generation of the initial four crude extracts through partitioning of methanol extract of freeze-dried açai berry powder into various solvents is described earlier in Chapter 3. All the initial four extracts of açai were tested for their ability to induce ARE-driven luciferase expression in cultured HepG2 cells transfected pGL3, pGL3-wtARE and pGL3-mARE plasmid vectors (Figure 4.7). Any increase in the expression of luciferase in cells transfected with pGL3-wtARE vector in response to various treatments compared were compared to the 0.2% DMSO control and is considered as induction. The results from crude extracts indicated that the crude chloroform extract induced the expression of ARE-dependent luciferase in HepG2 cells transfected with pGL3-wtARE plasmid vector by more than 3.5 times at 200 μg/ml concentration. Both butanol and aqueous extracts showed only a slight induction of pGL3-wtARE luciferase at 200 μg/ml concentration while the hexane extract was found to be inactive. In all treatment groups,

the expression of luciferase in cells treated with pGL3 vector remained at the basal level and the expression of luciferase in cells treated with pGL3-mARE was at the basal level.

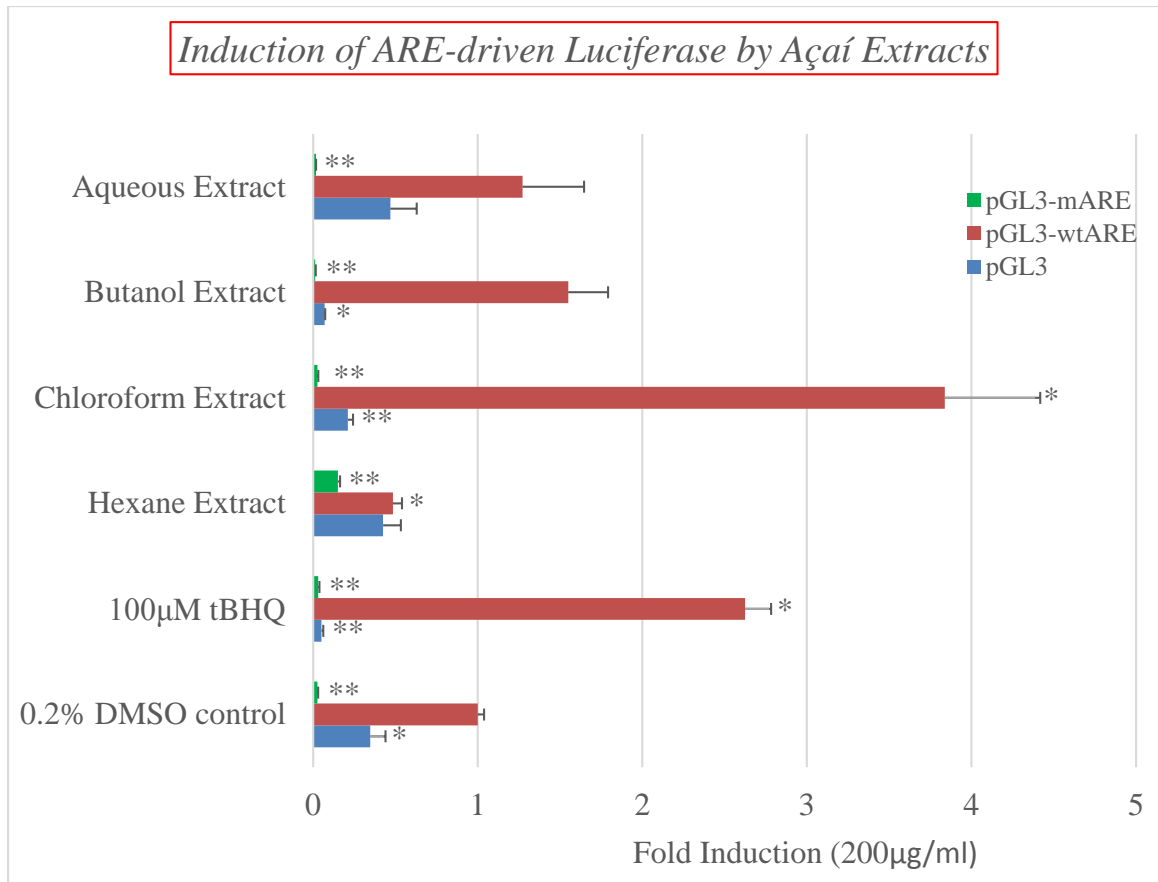


Figure 4.7 Induction of ARE-driven Luciferase Expression in Cultured HepG2 Cells by Crude Açai Berry Extracts

Further, transfection of pGL3-wtARE plasmid produced induction of ARE-driven luciferase expression with positive control in all experiments and the transfection of pGL3 and pGL3-mARE plasmids failed to produce luciferase expression. It indicates that the ARE sequence present in the promoter of pGL3-wtARE plasmid essentially mediates the increased expression of luciferase and is consistent with the involvement of

Nrf2/ARE signaling pathway. The results were reproduced on several occasions and therefore the transfection experiments from this stage onward were limited to the pGL3-wtARE plasmid vectors.

A dose response relationship was established for chloroform extract of açai including 50, 100 and 200 µg/ml concentration and the results indicated the induction of luciferase in cells treated with pGL3-wtARE vector in a dose dependent manner (Figure 4.8).

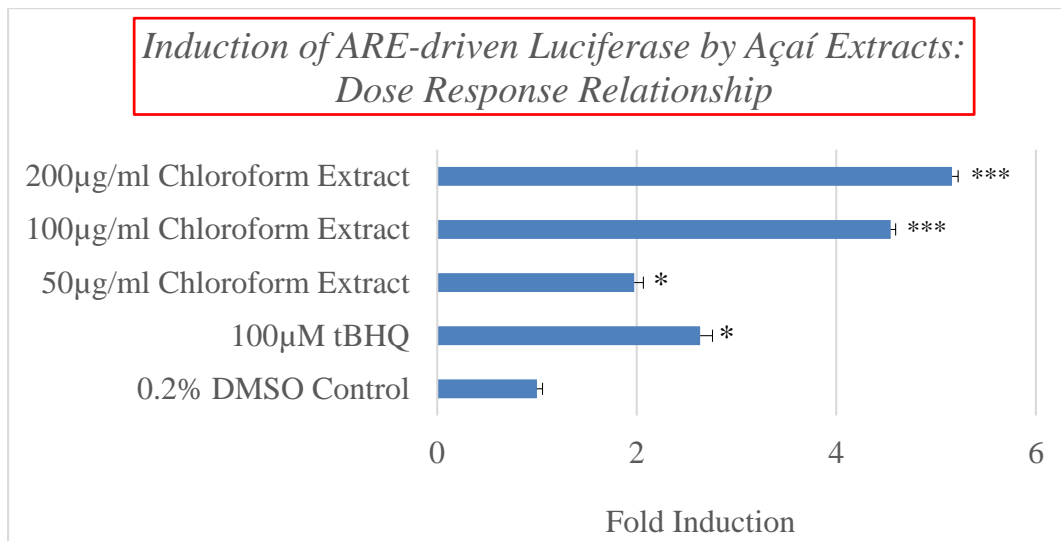
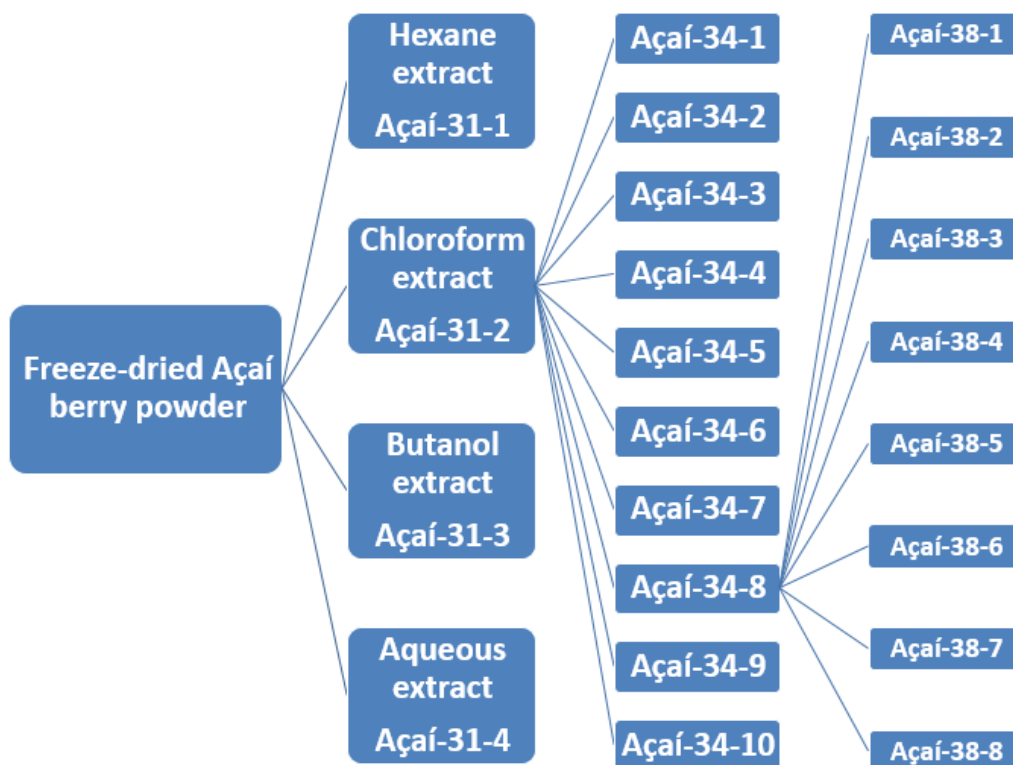


Figure 4.8 Induction of ARE-driven Luciferase Expression in Cultured HepG2 cells by Crude Chloroform Extract Of Açai

Although the crude chloroform extract (Açai-31-2) showed a mild induction of ARE-luciferase at 50 µg/ml concentration, this concentration was chosen for all the ARE-luciferase assays as the bioassay-guided fractionation process was presumed to produce fractions with increased potency. Therefore, all the fractions from this stage were tested

for the induction of ARE-dependent luciferase expression at 50 µg/ml concentration. For qualitative and quantitative purposes, any induction of ARE-luciferase that was less than 2 fold was considered to be no different from basal levels of expression of ARE-luciferase and therefore considered as inactive fraction. Any induction of ARE-luciferase induction between 2 and 4 folds was considered as mild induction. Likewise, any level of induction between 4 and 6 folds was considered as moderate and induction beyond 6 folds was considered as strong induction. The crude chloroform extract (Açaí-31-2) of açai was fractionated using column chromatography to produce 10 fractions, Açaí-34-1 through Açaí-34-10 as illustrated in Scheme 8.



Scheme 8. Bioassay-guided Fractionation of Açaí-31-2 and Açaí-34-8.

Among these fractions, Açai-34-8 was found to be a strong inducer of ARE-luciferase expression showing a 6 fold induction while the remaining 9 fractions were considered to be inactive as these fractions showed less than a 2 fold induction of ARE-luciferase (Figure 4.9). Incidentally, Açai-34-8 happened to be the potent fraction towards CYP2A6 and CYP2E1 inhibition as well and was already fractionated to 8 fractions belonging to Açai-38-Series (Scheme 8).

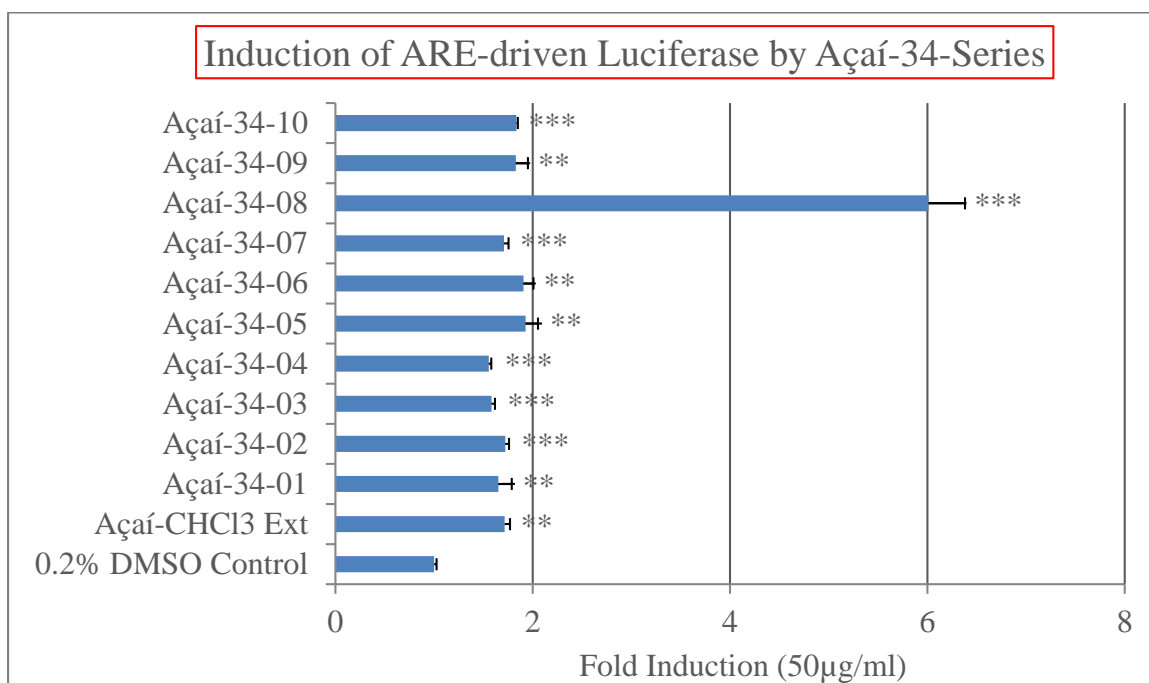


Figure 4.9 Induction of ARE-driven Luciferase Expression in Cultured HepG2 cells by Açai-34-Series.

Among the fractions of Açai-38-Series, induction of ARE-luciferase by Açai-38-7 and Açai-38-8 presented difficulties with the measurement of luminescence resulting from the enzymatic activity of luciferase enzyme. Therefore, the activities of these

fractions were measured at a reduced concentration of 25 $\mu\text{g}/\text{ml}$ and were represented in Figure 4.10. Overall, the fractions Açai-38-7 and Açai-38-8 appeared to have potencies greater than their preceding fractions Açai-38-1 through Açai-38-5. Açai-38-1 showed a moderate induction of ARE-luciferase whereas the fractions Açai-38-2, Açai-38-3 and Açai-38-4 fractions showed mild induction of ARE-luciferase (Figure 4.10).

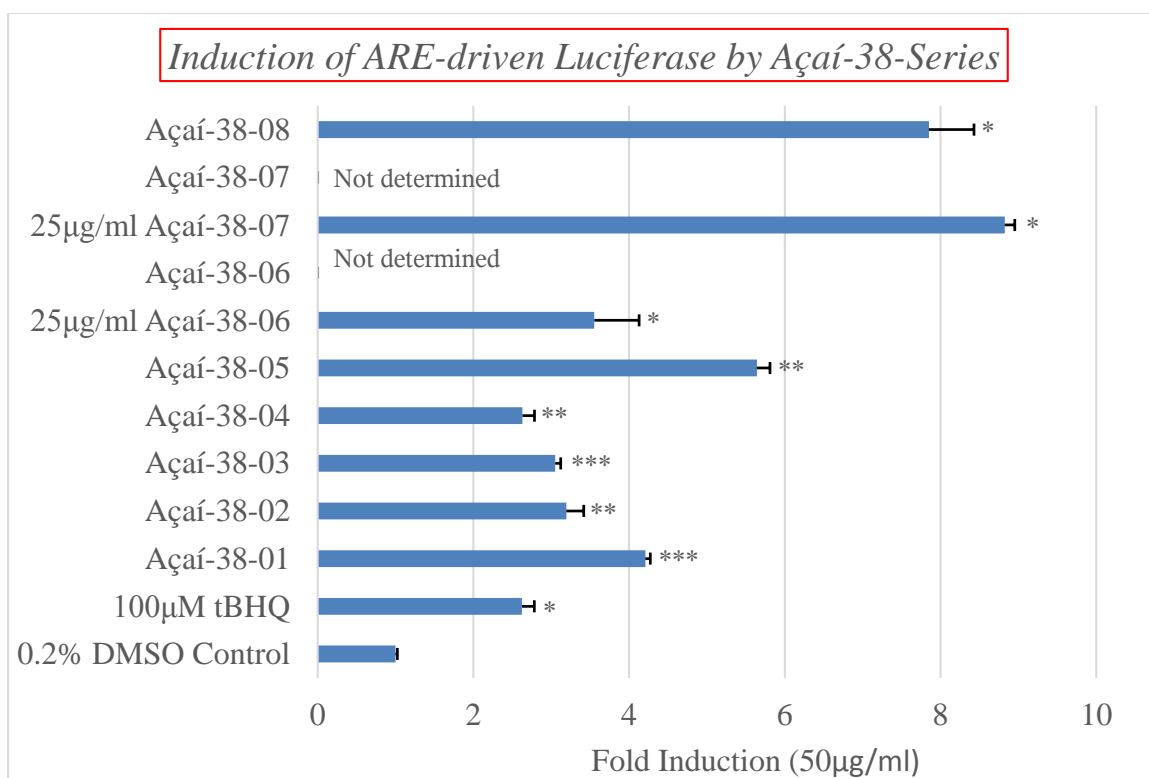
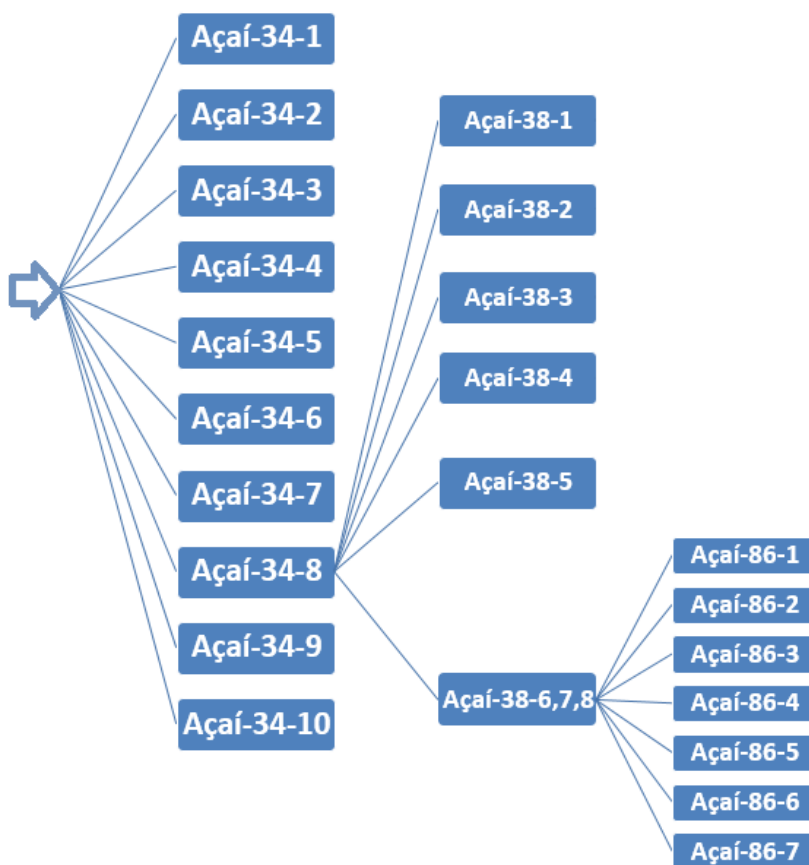


Figure 4.10 Induction of ARE-driven Luciferase Expression in Cultured HepG2 Cells by Açai-38-Series.

Although the fractions Açai-38-7 and Açai-38-8 were found to be more potent fractions, their limited sample size hindered their further processing via bioassay-guided fractionation. Consequently, Açai-38-6, Açai-38-7 and Açai-38-8 were pooled together

and subsequently re-fractionated to produce 7 fractions belonging to Açai-86-Series (Scheme 9).



Scheme 9. Fractionation of Pooled Extracts Açai-38-6, Açai-38-7 and Açai-38-8.

No further increase in the induction of ARE-luciferase was observed with any of the fractions among Açai-86-Series. In fact, none of the fractions were found to retain the ARE-luciferase expression showed by the individual fractions Açai-38-6, Açai-38-7 and Açai-38-8 that contributed to the generation of the Açai-86-Series (Figure 4.11). Moreover, the activities of Açai-86-Series fractions was spread out across all the fractions and was within the range of minimal to mild induction of ARE-luciferase.

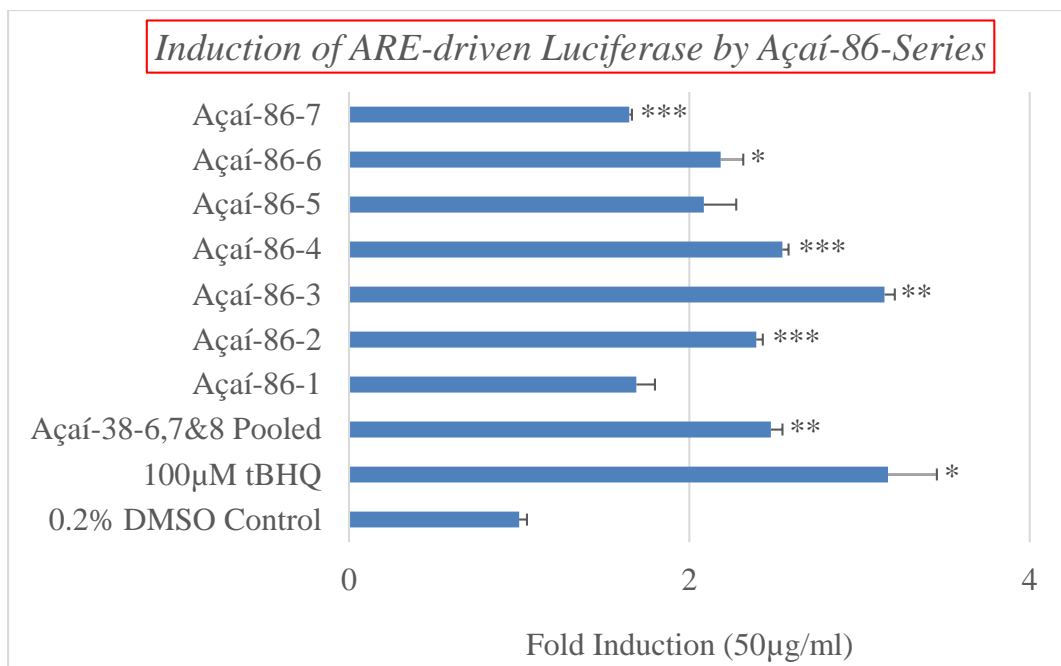
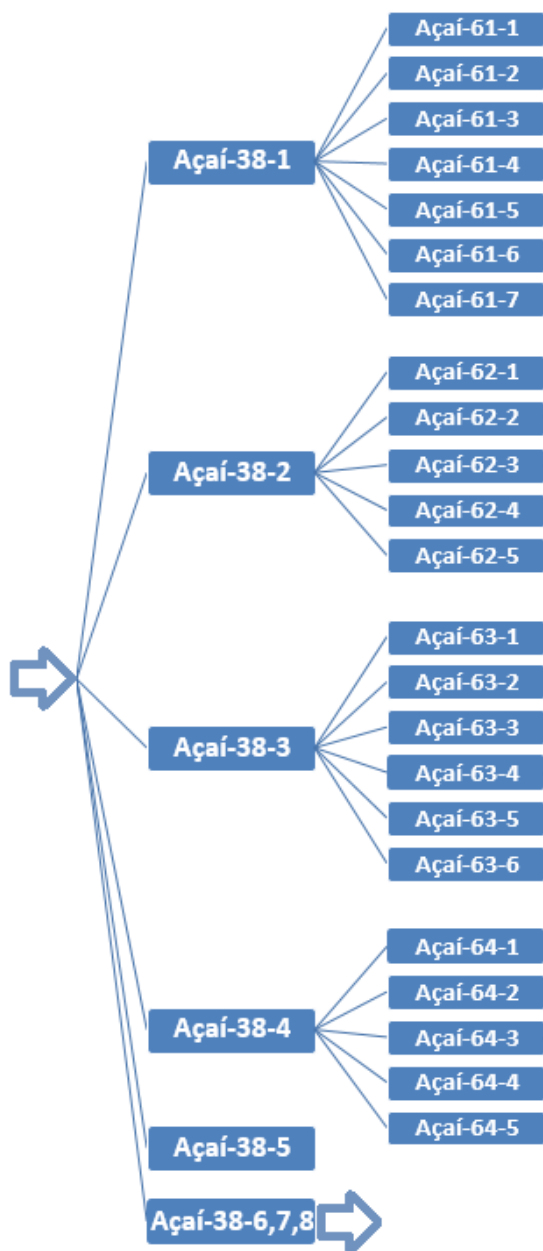


Figure 4.11 Induction of ARE-driven Luciferase Expression in Cultured HepG2 Cells by Açai-86-Series.

The early 4 fractions Açai-38-1, Açai-38-2, Açai-38-3 and Açai-38-4 belonging to the Açai-38-Series were also fractionated because these are the abundant fractions. The fractions namely Açai-61-Series, Açai-62-Series, Açai-63-Series and Açai-64-Series generated from Açai-38-1, Açai-38-2, Açai-38-3 and Açai-38-4 were readily available (Scheme 10). These fractions were also studied for induction of ARE-luciferase in HepG2 cells, given their observed mild induction, and abundance.



Scheme 10. Fractionation of Açai-38-1, Açai-38-2, Açai-38-3 and Açai-38-4.

The Açai-61-Series was comprised of 7 fractions that were generated from a moderately potent fraction Açai-38-1 (Scheme 10). Among these fractions, Açai-61-6 was found to be the fraction with a moderate induction of ARE-luciferase while the

fractions Açai-61-1 and Açai-61-2 were found to be inactive and remaining fractions showed mild induction of ARE-luciferase (Figure 4.12).

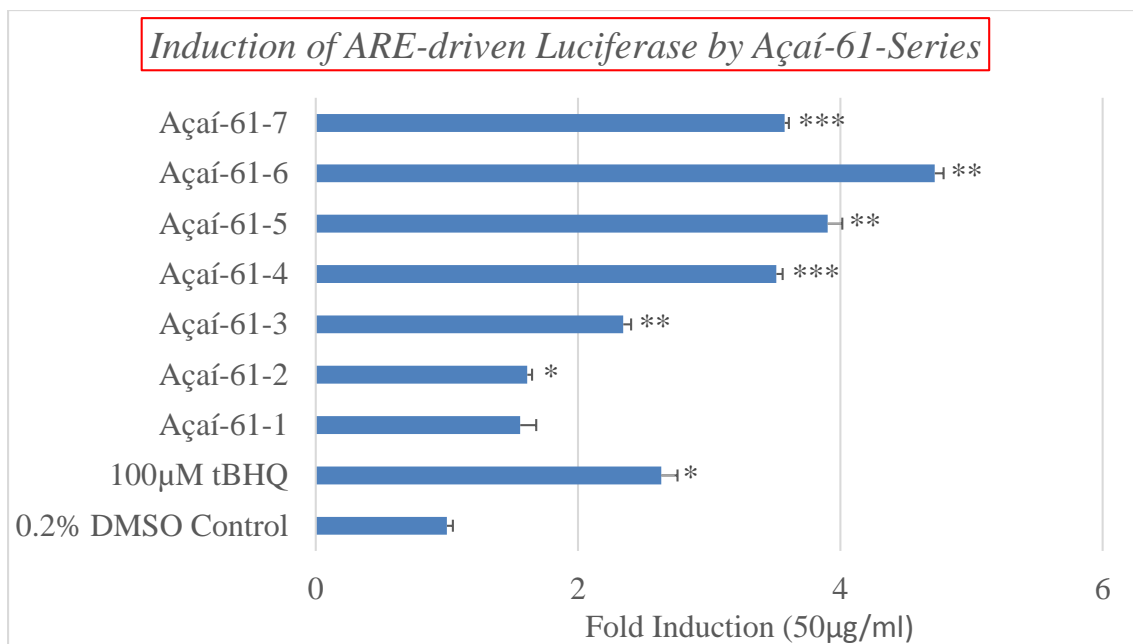


Figure 4.12 Induction of ARE-driven Luciferase Expression in Cultured HepG2 Cells by Açai-61-Series.

Açai-38-2 showed only a mild induction of ARE-luciferase but was already fractionated for studying CYP inhibition to yield Açai-62-Series consisting of 5 fractions (Scheme 10). These available fractions were tested for ARE-luciferase induction and again, all the fractions were found to be mild inducers of ARE-luciferase except one fraction Açai-62-5 that was found to be an inactive fraction (Figure 4.13).

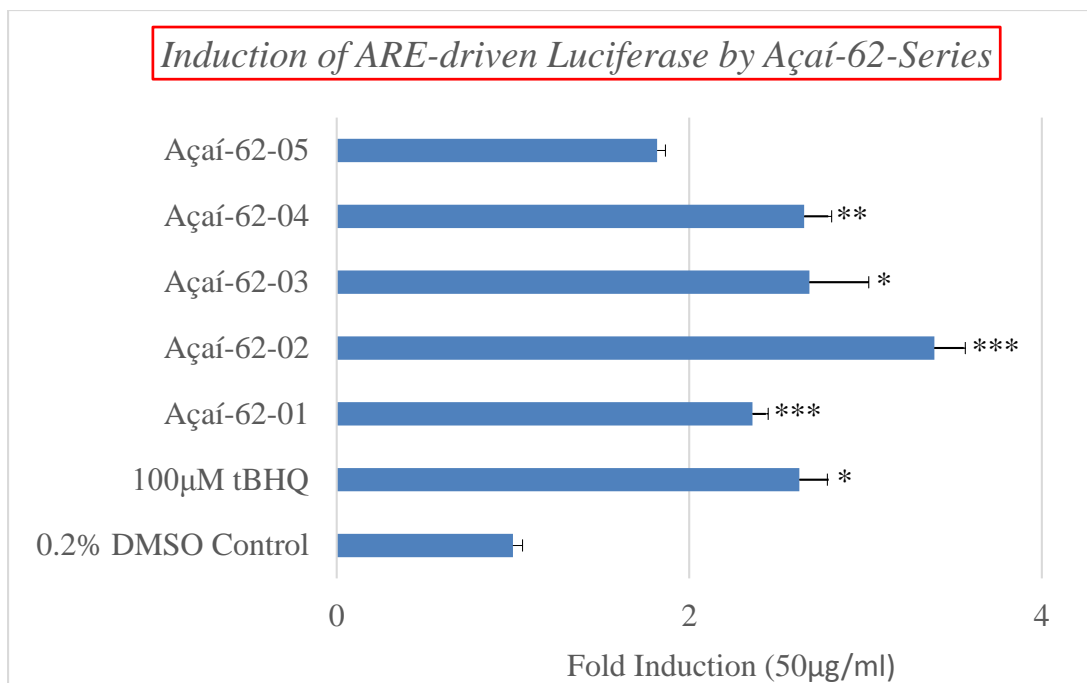


Figure 4.13 Induction of ARE-driven Luciferase Expression in Cultured HepG2 Cells by Açai-62-Series.

Another fraction Açai-38-3 that showed mild induction of ARE-luciferase produced 6 fractions of Açai-63-Series and each of these fractions were tested at 50µg/ml (Scheme 10). Among these fractions Açai-63-04 was found to be a strong inducer of ARE-luciferase, and the fractions Açai-63-3 and Açai-63-6 were found to be moderate inducers of ARE-luciferase. The remaining fractions were found to be mild inducers of ARE-luciferase (Figure 4.14).

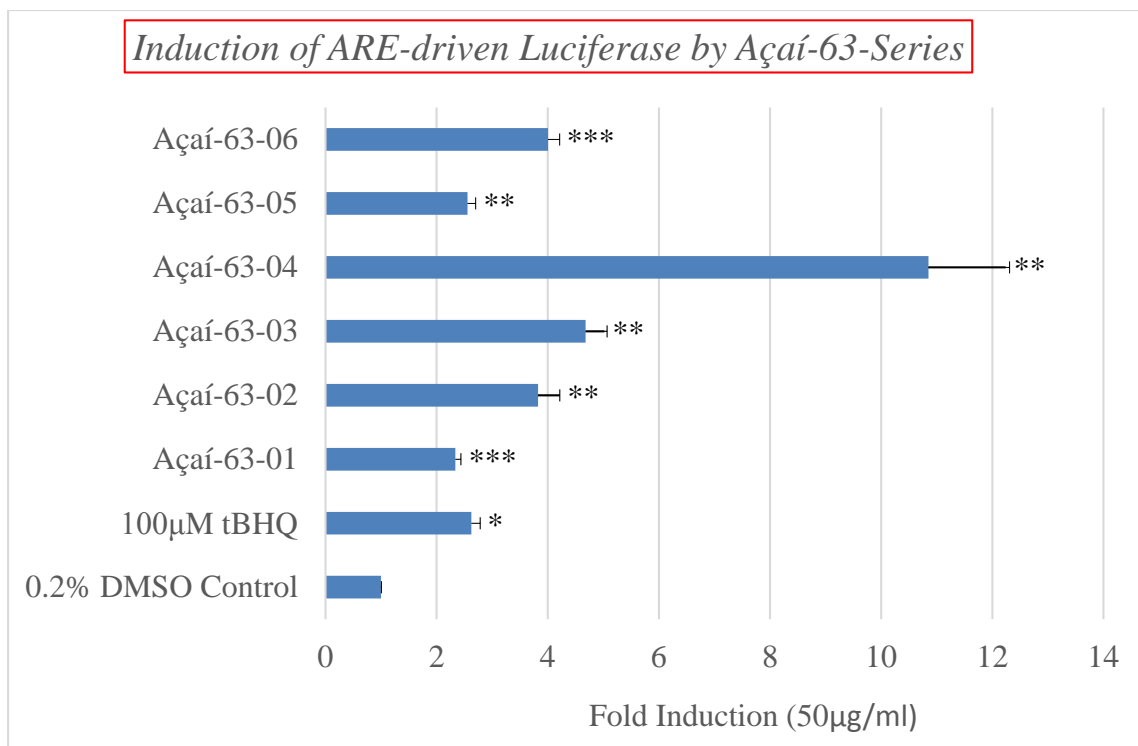


Figure 4.14 Induction of ARE-driven Luciferase Expression in Cultured HepG2 Cells by Açai-63-Series.

The Açai-64-Series comprised of 5 fractions and was generated from Açai-38-4, which was also a mild inducer of ARE-luciferase activity. Among these fractions, Açai-64-1 was found to be a strong inducer of ARE-luciferase while the other 4 fractions were mild inducers of ARE-luciferase (Figure 4.15).

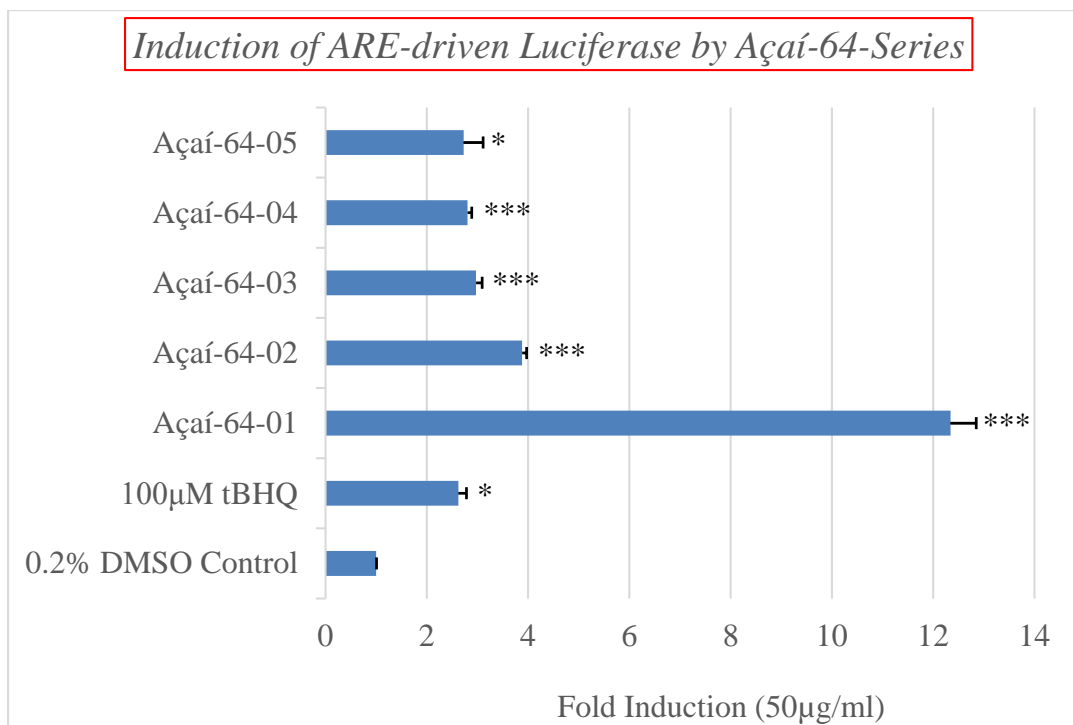
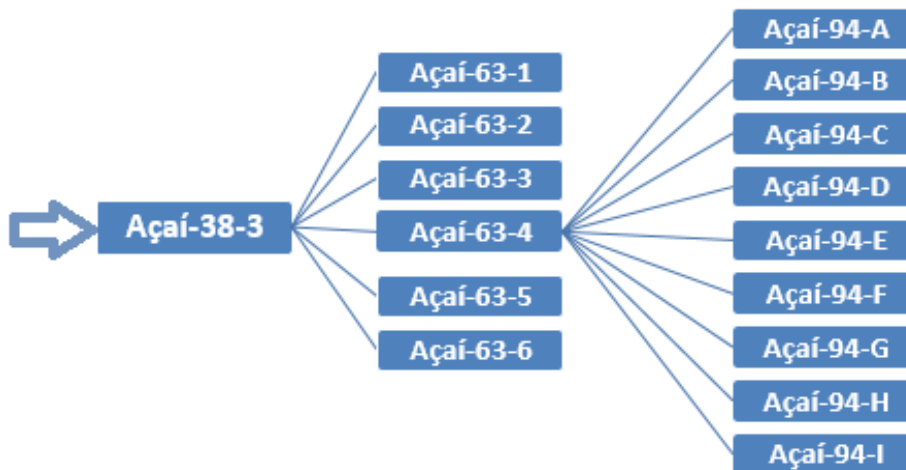


Figure 4.15 Induction of ARE-driven Luciferase Expression in Cultured HepG2 Cells by Açai-64-Series.

Açai-63-4 and Açai-64-1 were found to be the potent inducers of ARE-luciferase (Figure 4.14 and Figure 4.15). Açai-63-4 was fractionated to generate Açai-94-Series and the limited sample size halted the fractionation of Açai-64-1 despite the results indicate that it is most potent fraction so far (Scheme 11). The potent fraction Açai-63-4 that showed strong induction was fractionated to produce Açai-94-Series comprising of 10 fractions. Contrary to what was expected, the potencies across all the fractions of Açai-94-series was noticed to be lower their parent fraction Açai-63-4 (Figure 4.16). Only Açai-94-F and Açai-94-G were found to be moderate inducers of ARE-luciferase and all

the other fractions showed mild induction except for Açai-94-C that was found to be inactive fraction.



Scheme 11. Fractionation of Açai-63-4.

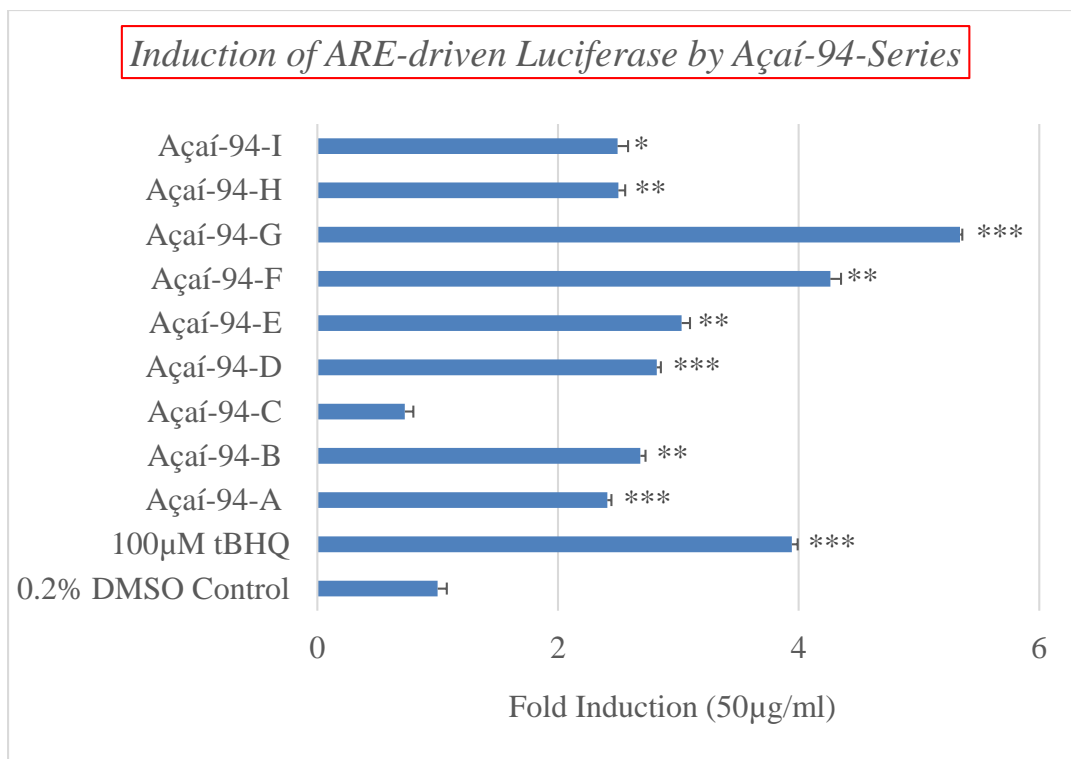
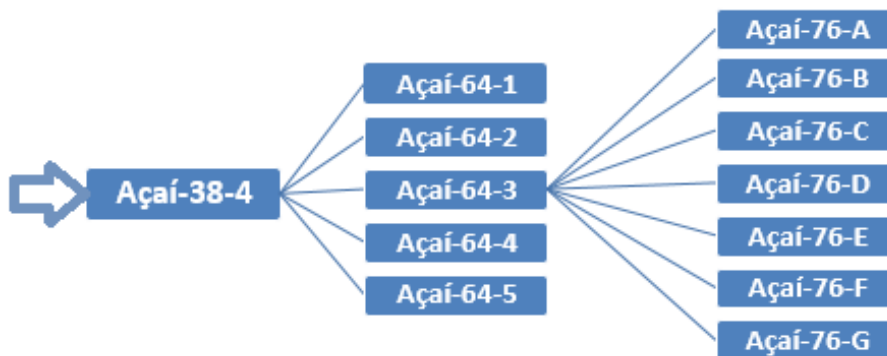


Figure 4.16 Induction of ARE-driven Luciferase Expression in Cultured HepG2 Cells by Açai-94-Series.

Although Açai-64-1 was more potent it was not fractionated further because of limited sample size but another abundant fraction from the same series Açai-64-3 was fractionated for studying ARE-luciferase activity to produce Açai-76-series comprising of 7 fractions (Scheme 12). All the 7 fractions were found to be mild inducers of ARE-luciferase, as expected (Figure 4.17).



Scheme 12. Fractionation of Açai-64-3.

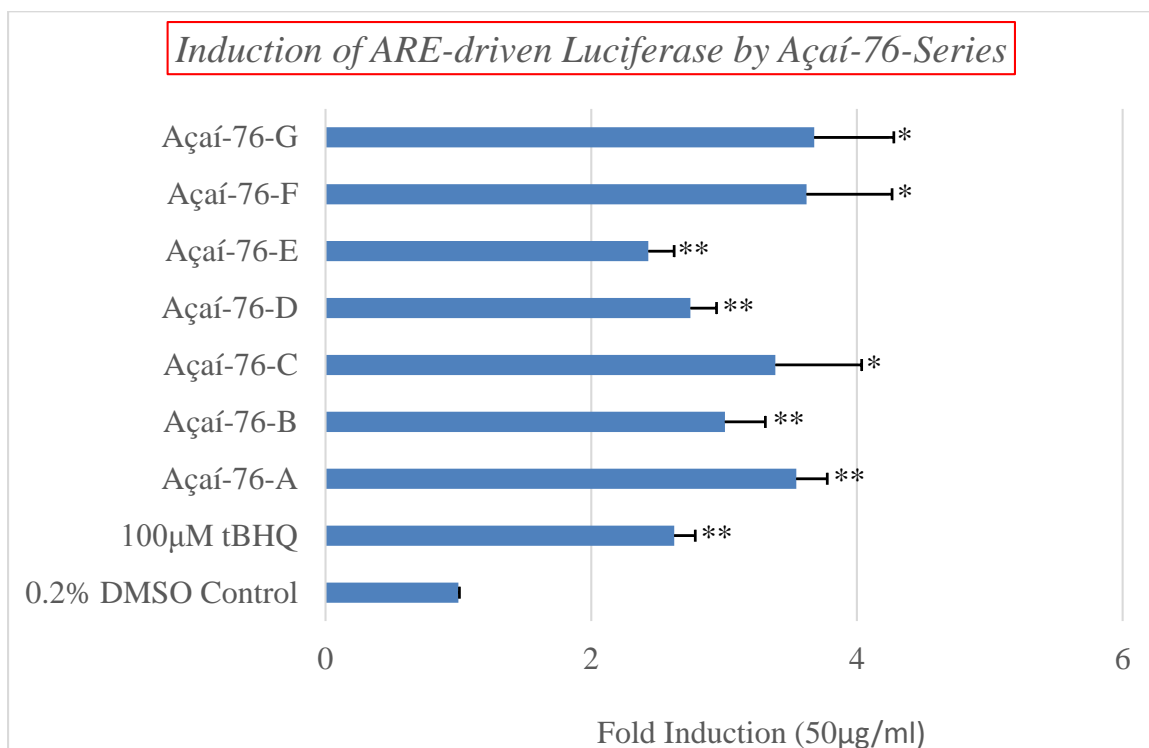
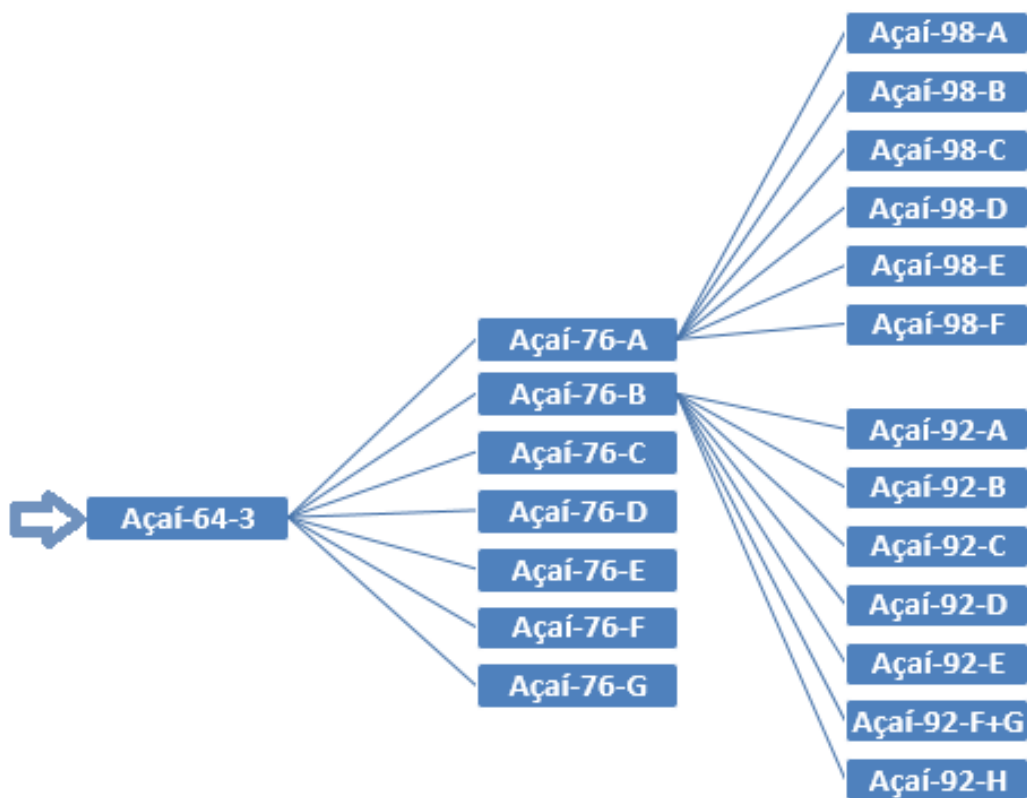


Figure 4.17 Induction of ARE-driven Luciferase Expression in Cultured HepG2 Cells by Açai-76-Series.

The most abundant fractions from Açai-76-series, Açai-76-A and Açai-76-B were fractionated to produce Açai-98-Series and Açai-92-Series, respectively (Scheme 13).



Scheme 13. Fractionation of Açaí-76-A and Açaí-76-B.

Among the 6 fractions from Açaí-98-Series, all the fractions were found to be inactive except for Açaí-98-F that only showed mild induction of ARE-luciferase (Figure 4.18). Other available fractions belonging to Açaí-98-Series produced from Açaí-76-A did not yield any increase in potency. In fact, all the fractions lost the activity except for Açaí-98-F that barely retained the potency similar to its parent fraction.

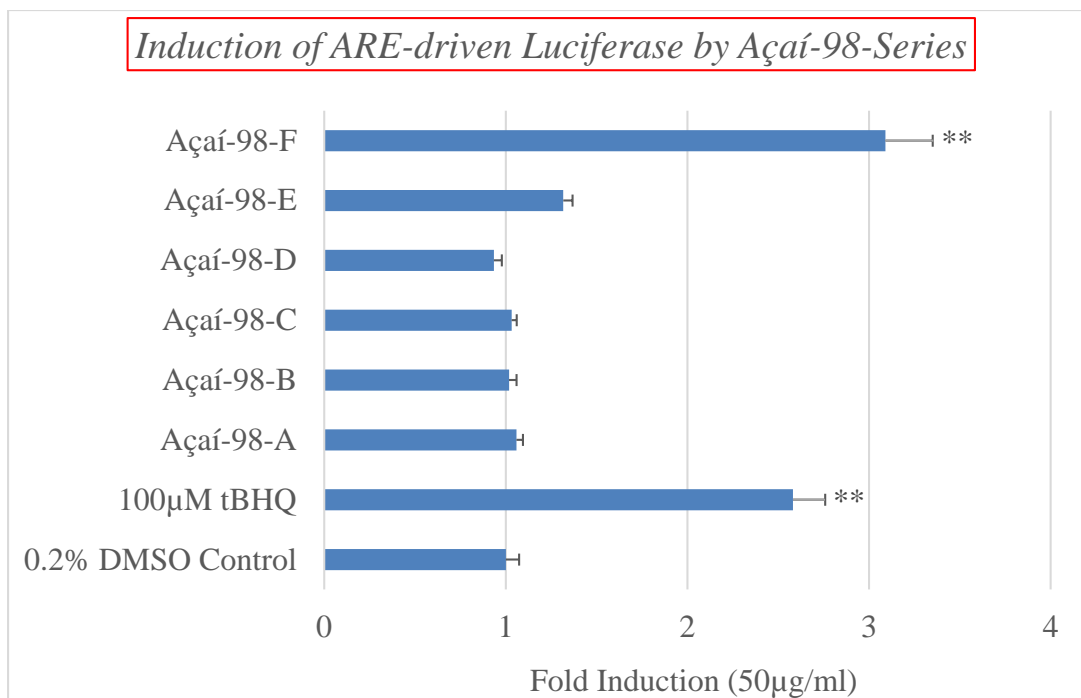


Figure 4.18 Induction of ARE-driven Luciferase Expression in Cultured HepG2 Cells by Açai-98-Series.

Interestingly, Açai-92-H that was produced from Açai-76-B showed remarkable induction of ARE-luciferase activity (Figure 4.19). All the remaining fractions in the series showed mild to no effect on ARE-luciferase activity. Subsequent fractionation of Açai-92-H produced 11 fractions and contrary to what was expected, all the 11 fractions produced from Açai-92-H have lost the activity. This also includes Açai-92-H that was recovered after sample preparation for fractionations indicating that the constituents of Açai-92-H responsible for ARE-induction might be unstable in nature (Data not shown).

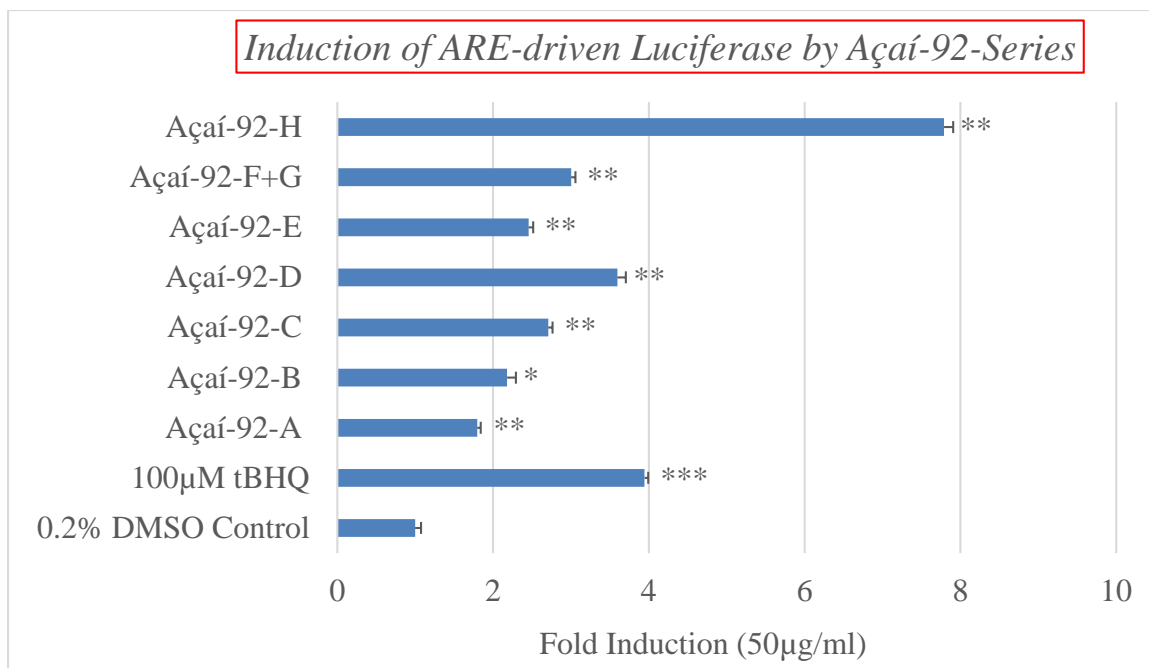
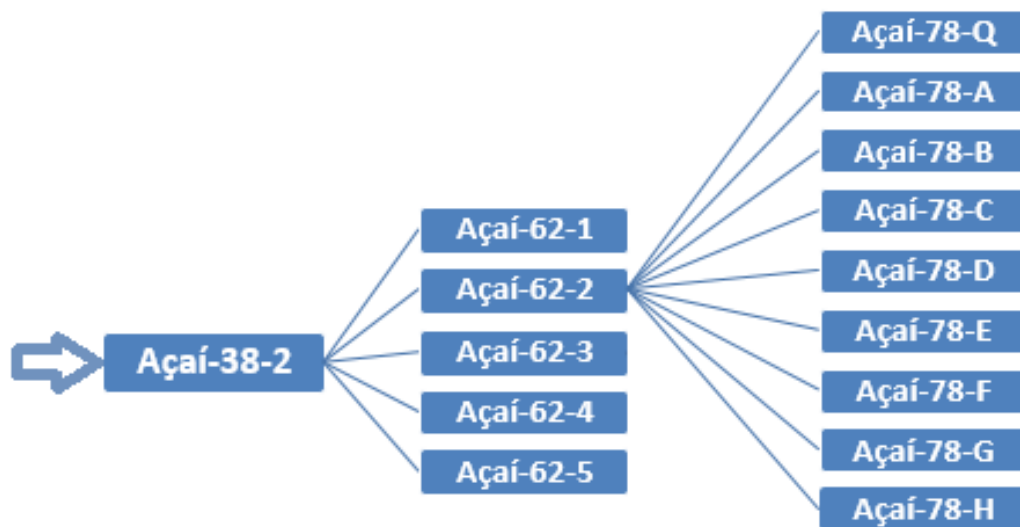


Figure 4.19 Induction of ARE-driven Luciferase Expression in Cultured HepG2 Cells by Açai-92-Series.

Although, the fractions Açai-62-2 and Açai-62-3 were shown to be mild inducers of ARE-luciferase, they were moved forward for studying ARE-luciferase activity since these two fractions were the most abundant and active fractions. Açai-62-2 and Açai-62-3 produced Açai-78-series and Açai-82-series, respectively (Scheme 14).



Scheme 14. Fractionation of Açaí-62-2.

Açaí-78-Series comprising of 8 fractions were produced from Açaí-62-2 that was shown to be a mild inducer of ARE-luciferase. These results indicated the presence of a potent inducer in the form of Açaí-78-H in addition to two other moderate inducers Açaí-78-B and Açaí-78-C. The remaining fractions were found be mild inducers except for one inactive fraction in form of Açaí-78-F (Figure 4.20).

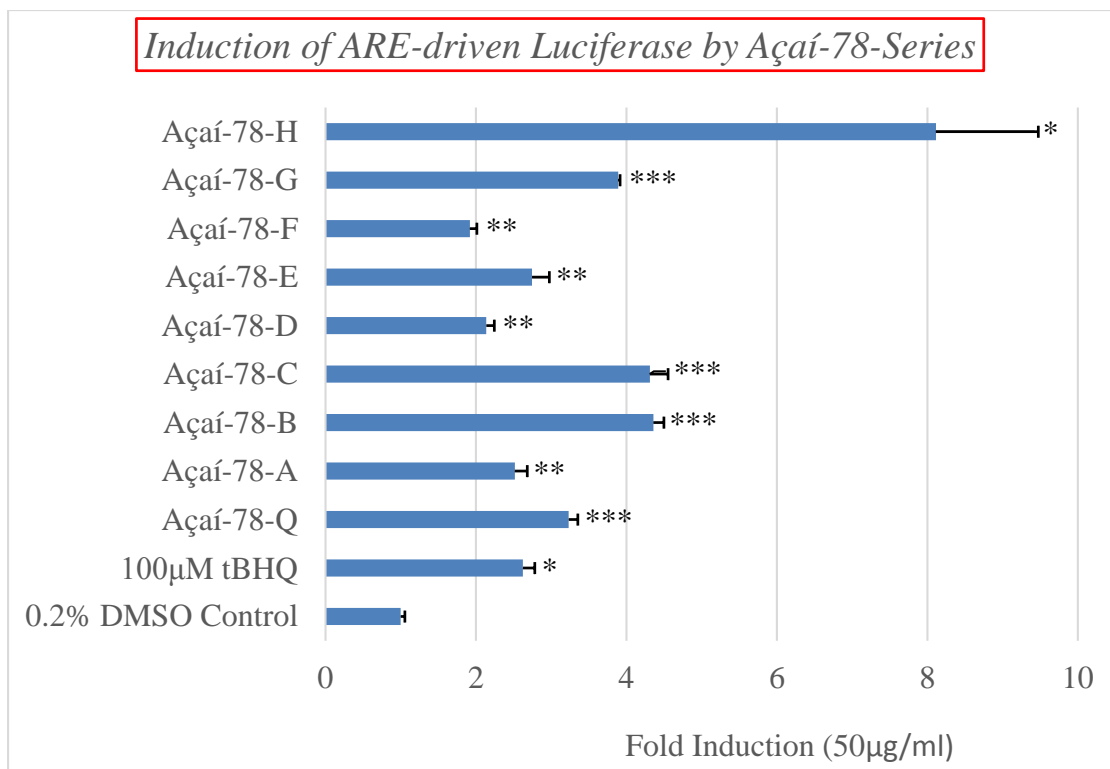
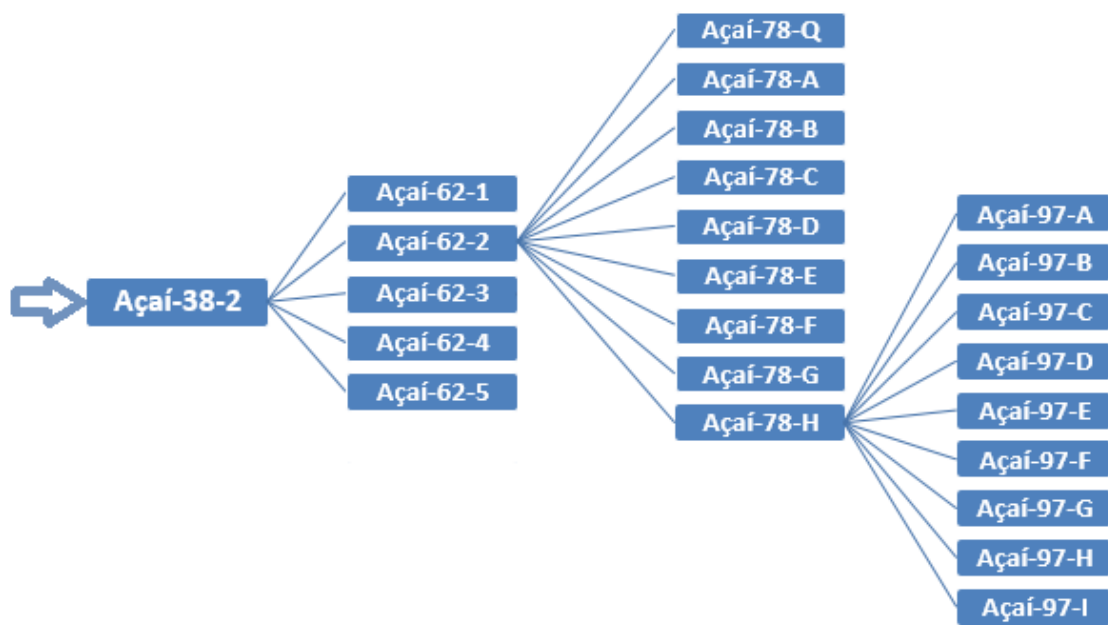


Figure 4.20 Induction of ARE-driven Luciferase Expression in Cultured HepG2 Cells by Açai-78-Series.

The potent fraction Açai-78-H that was shown to be a strong inducer of ARE-luciferase was fractionated to generate 9 fractions belonging to Açai-97-Series (Scheme 15). Açai-78-H was found to be a strong inducer and it convincingly produced three fractions namely Açai-97-B, Açai-97-C and Açai-97-D (Figure 4.21). Both Açai-97-B and Açai-97-D together with Açai-97-C which is a mixture of Açai-97-B and Açai-97-D showed similar potency. The remaining fractions were found to be mild inducers of ARE-luciferase except for Açai-97-F that showed minimal induction of ARE-luciferase.



Scheme 15. Fractionation of Açai-78-H.

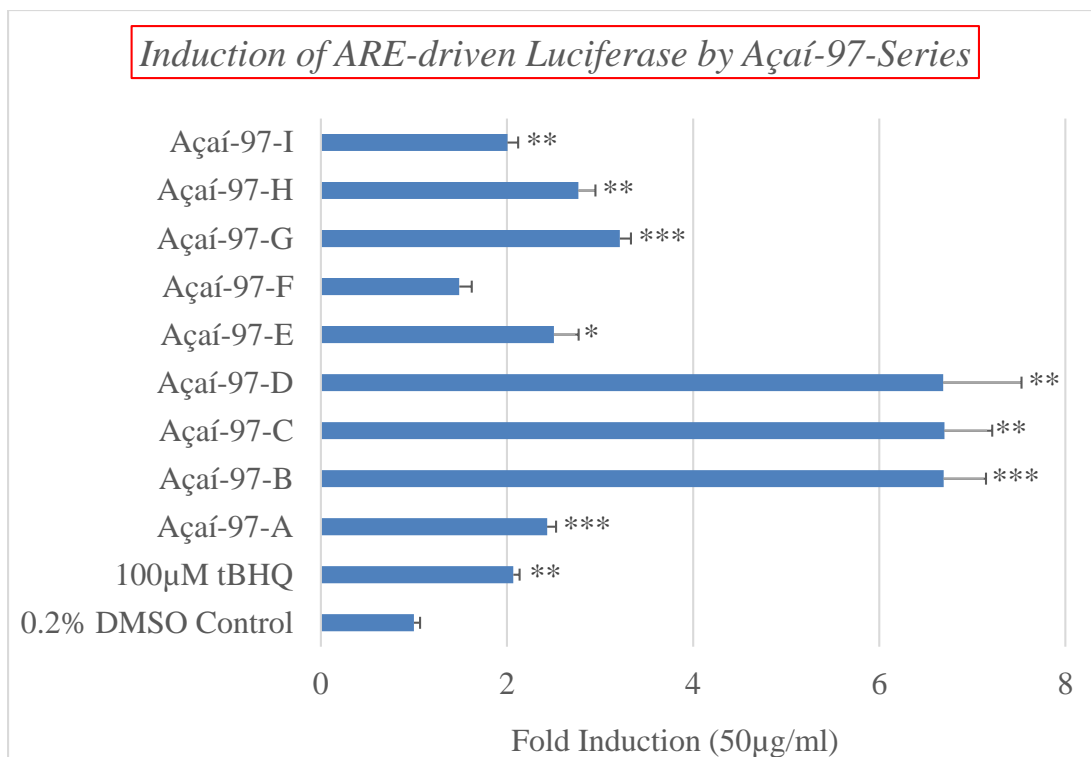


Figure 4.21 Induction of ARE-driven Luciferase Expression in Cultured HepG2 Cells by Açai-97-Series.

Interestingly, Açai-97-B and Açai-97-D were determined to be pure compounds by chromatography, mass spectrometry and NMR techniques and were identified to be and grouped into a class of compounds called pheophorbides (Figure 4.22). Açai-97-B was characterized as pheophorbide-a methyl ester and Açai-97-D was characterized as pheophorbide-a ethyl ester (Table 4.1).

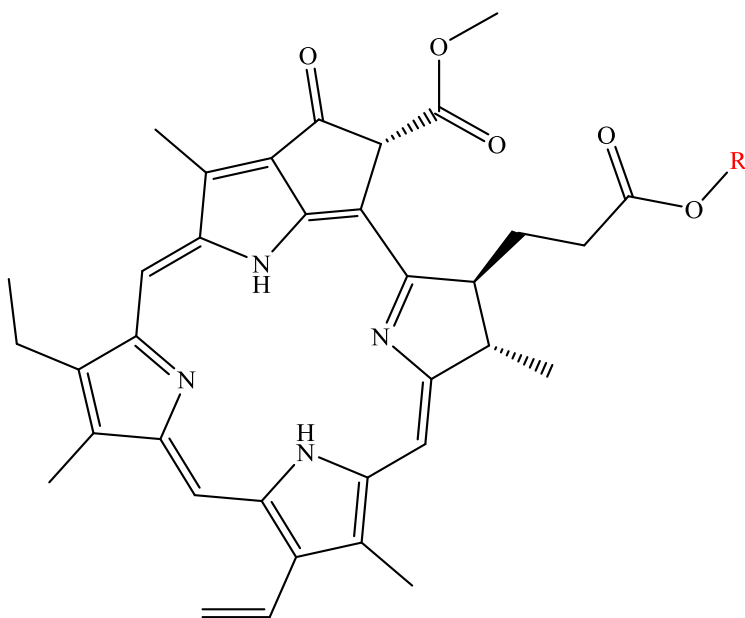


Figure 4.22 Chemical Structure of Pheophorbide-A Derivatives. The substituent R=H refers to Pheophorbide a.

Table 4.1 Chemical Structure of Pheophorbide-a Derivatives.

	R	Molecular formula	Molecular weight
Pheophorbide a	H	C ₃₅ H ₃₆ N ₄ O ₅	592.70gm
Pheophorbide a methyl ester (Açaí-97-B)	CH ₃	C ₃₆ H ₃₈ N ₄ O ₅	606.72g
Pheophorbide a ethyl ester (Açaí-97-D)	C ₂ H ₅	C ₃₇ H ₄₀ N ₄ O ₅	618.74g

Further, availability of pure standards for Açaí-97-B which is Pheophorbide-a methyl ester together with the basic chemical entity Pheophorbide-a allowed for a dose response relationship on these compounds. Both Pheophorbide-a methyl ester and Pheophorbide-a showed a dose dependent induction of ARE-luciferase (Figure 4.23). A

two-fold induction of ARE-luciferase was observed with Pheophorbide-a methyl ester and Pheophorbide-a at lower concentrations of 5 and 10 $\mu\text{g/ml}$, respectively. Induction at this concentration would translate to 8.2 μM and 16.9 μM for Pheophorbide-a methyl ester and Pheophorbide a, respectively.

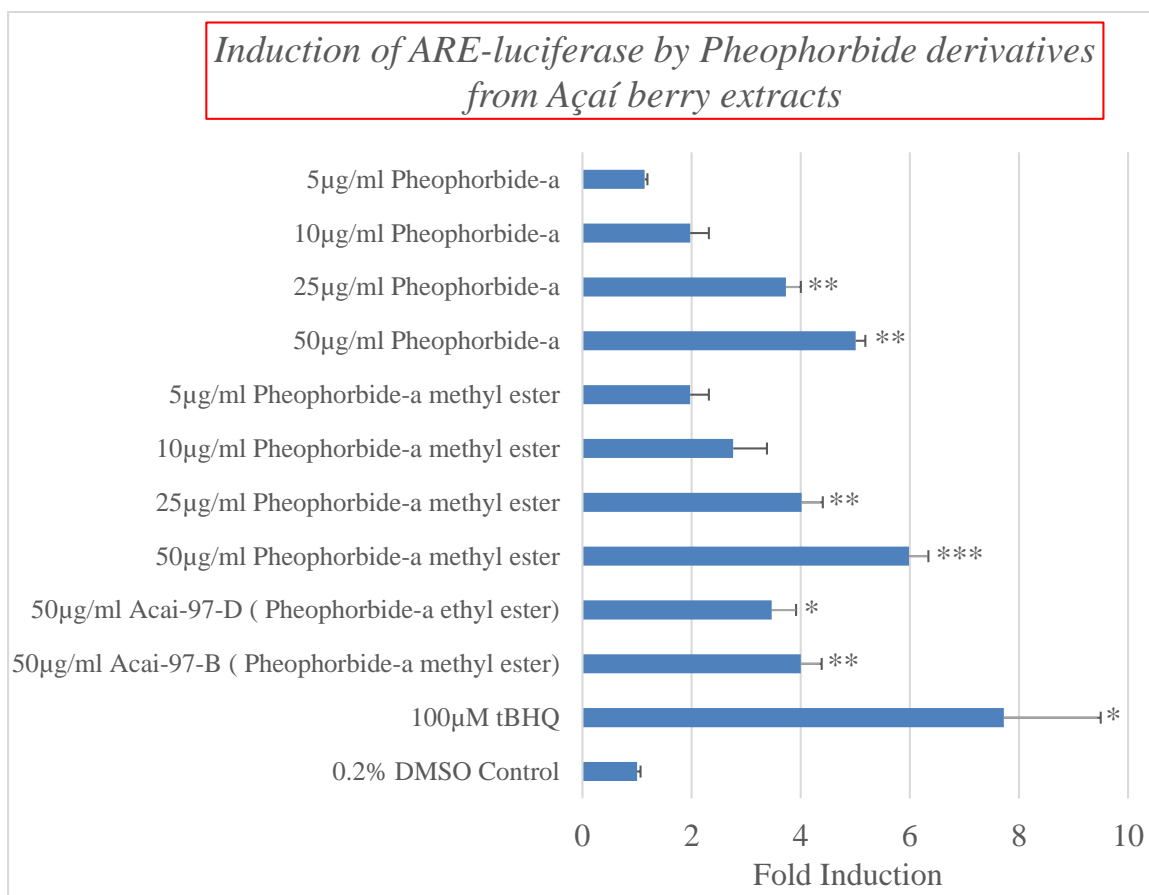
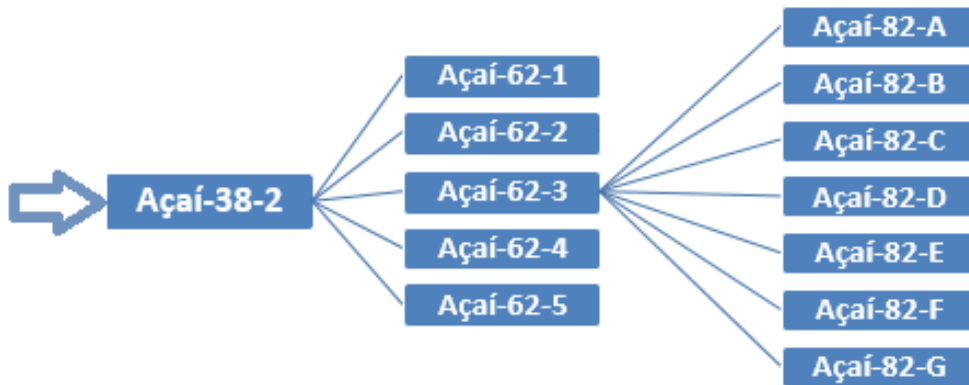


Figure 4.23 Induction of ARE-driven Luciferase Expression in Cultured HepG2 cells by Pheophorbide-a Methyl Ester and Pheophorbide-a

Similarly, another mild inducer of ARE-luciferase Açai-62-3 produced 7 fractions belonging to Açai-82-Series (Scheme 16). Among the 7 fractions, Açai-82-A was found

to be strong inducer while the remaining fractions were found to be mild inducers of ARE-luciferase (Figure 4.24).



Scheme 16. Fractionation of Açai-62-3.

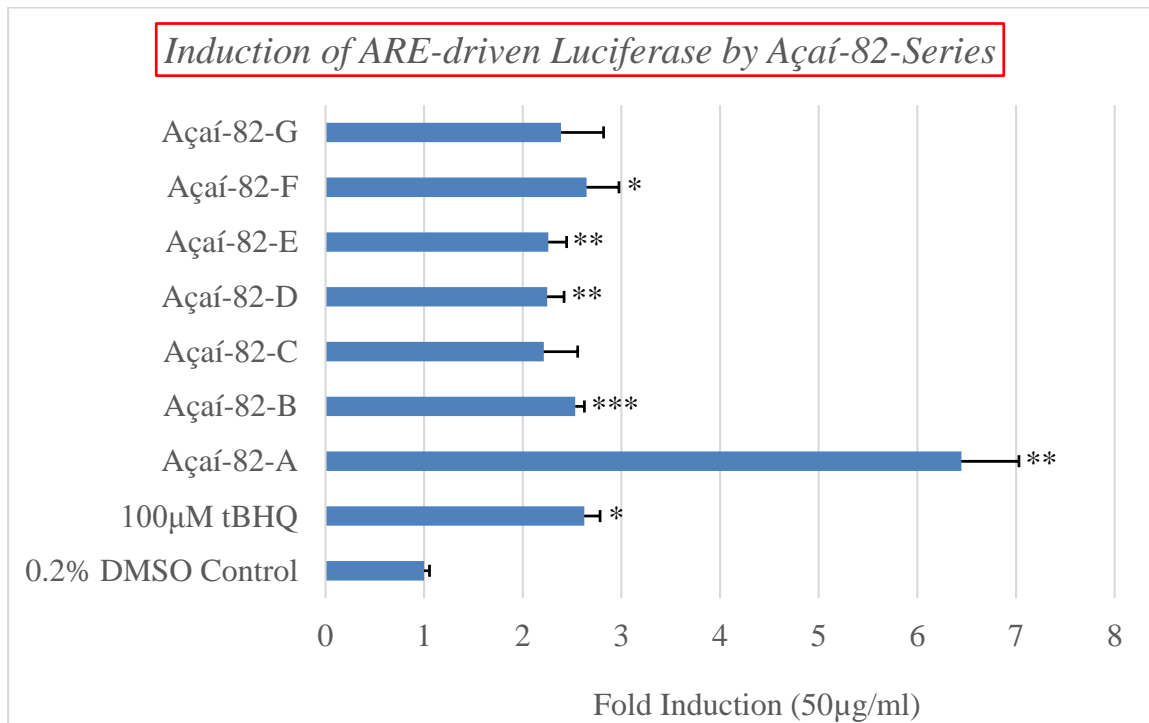


Figure 4.24 Induction of ARE-driven Luciferase Expression in Cultured HepG2 Cells by Açai-82-Series.

4.4. Discussion

The current research attempts to fill the gap about the notion among the general population regarding the purported health benefits of açai. To address this, an ARE-luciferase plasmid vector, as a synthetic model of Nrf2/ARE signaling in the cell, was employed in combination with activity guided fractionation of crude acai powder. In this study, crude chloroform extract of açai berry showed a moderate induction of ARE-luciferase in HepG2 cells and a series of fractionations were pursued further on the chloroform extract with convincing results. Interestingly, a class of compounds called pheophorbides were isolated in their pure form and were showed to be effective inducers of ARE-luciferase. A concentration of 8.2 μM and 16.9 μM for Pheophorbide-a methyl ester and Pheophorbide a, respectively showed a 2 fold induction of ARE-luciferase and is considered to be conceivable in human plasma and therefore has the potential to produce physiological effects. The pheophorbides that were tested in the study included pheophorbide a methyl ester and pheophorbide a ethyl ester along with the commercially available pheophorbide a. A dose response using pheophorbide a and pheophorbide a methyl ester indicated differences in potency probably resulting from structure activity relationship from within pheophorbide class of molecules.

Pheophorbides are compounds that are closely related to chlorophyll-like compounds previously identified as a bioactive constituent in spinach, green seaweed and green algae⁹⁵. Pheophorbide a was shown to have strong *in vitro* antioxidant activities as demonstrated by DPPH radical scavenging assay and hydroxyl radical scavenging

assay⁹⁶. However, much of the recognition for pheophorbides come from their potential photosensitizing nature and was studied for photodynamic therapeutic effects in a variety of cancer models. Photodynamic therapy is a relatively new modality of treatment developed against cancer where the photosensitizing compounds trigger the generation of reactive oxygen species leading to toxic events including cell death. Reactive oxygen species was detected in photodynamic therapy with pheophorbides in cancer models.

Photoactivation of pheophorbide a presented an oxidative challenge in HepG2 cells, subsequently induced heme oxygenase-01 in a Nrf2-dependent manner and such induction was related to the inactivation of Bach1, a repressor protein of Nrf2/ARE signaling pathway⁹⁷. Nrf2 is a key transcription factor and is highly responsive to oxidative stress. It is constitutively over expressed in cancer cells conferring resistance to anticancer drugs. Therefore, the silencing of Nrf2 increased cellular levels of singlet oxygen and other reactive oxygen species resulting in cell death in breast and colon cancer cell lines following pheophorbide a based photodynamic therapy⁹⁸. Further, pheophorbides were also shown to have immunomodulatory activities through the ERK and MAP kinase pathways in a dose dependent manner⁹⁹. Further, pheophorbides when illuminated even by the light from the microscope showed profound antiproliferative properties through induction of photocytotoxic properties leading to apoptosis and cell death¹⁰⁰. Pheophorbide was shown to have antitumor properties and was shown to induce apoptosis in Hep3b cells, a viral induced hepatoma cell line¹⁰¹. The bioavailability of pheophorbides is likely to be low because of its highly hydrophobic nature and therefore several forms have been derived to improve the pharmacokinetic properties of

pheophorbides such as pegylation with polyethylene glycols such that these agents reach the target sites of action such as cancer cells¹⁰². Another study found that pheophorbide protected from diabetic kidney failure as a consequence of streptozotocin induced oxidative stress in rat models by decreasing lipid peroxidation and increasing reactive oxygen species scavenging enzymes such as catalase¹⁰³. However, it must be noted that precise molecular mechanisms underlying the observed effects were not clear and some studies also identified individual differences in some models⁹⁷.

In addition to pheophorbides, there were a couple of other fractions namely, Açai-82-A and Açai-92-H capable of producing inducers of ARE-luciferase. Açai-82-A appears to be a promising candidate to pursue upon further fractionation as it happens to be a fraction close to Açai-78-H that produced pheophorbides. It is also possible that Açai-82-A may contain molecules that are related to pheophorbides as it is the closest neighbor of Açai-78-H. Another potent fraction Açai-92-H upon further fractionation lost the activity and the quest to identify similarly looking constituents in a related fractions is targeted to identify possible inducers in ARE-luciferase in those fractions.

In summary, the process of bioassay-guided fractionation of açai was successfully carried out resulting in the identification of pheophorbides as putative inducers of Nrf2/ARE signaling pathway as demonstrated by the induction of ARE-luciferase.

REFERENCES

1. Semenza, G. L. (2007) Life with oxygen, *Science* 318, 62-64.
2. Lindahl, S. G. (2008) Oxygen and life on earth: an anesthesiologist's views on oxygen evolution, discovery, sensing, and utilization, *Anesthesiology* 109, 7-13.
3. Valentine, J. S., Wertz, D. L., Lyons, T. J., Liou, L. L., Goto, J. J., and Gralla, E. B. (1998) The dark side of dioxygen biochemistry, *Curr Opin Chem Biol* 2, 253-262.
4. Bergendi, L., Benes, L., Duracková, Z., and Ferencik, M. (1999) Chemistry, physiology and pathology of free radicals, *Life Sci* 65, 1865-1874.
5. Nohl, H., Kozlov, A. V., Gille, L., and Staniek, K. (2003) Cell respiration and formation of reactive oxygen species: facts and artefacts, *Biochem Soc Trans* 31, 1308-1311.
6. Dickinson, B. C., and Chang, C. J. (2011) Chemistry and biology of reactive oxygen species in signaling or stress responses, *Nat Chem Biol* 7, 504-511.
7. Slauch, J. M. (2011) How does the oxidative burst of macrophages kill bacteria? Still an open question, *Mol Microbiol* 80, 580-583.
8. Kuhns, D. B., Alvord, W. G., Heller, T., Feld, J. J., Pike, K. M., Marciano, B. E., Uzel, G., DeRavin, S. S., Priel, D. A., Soule, B. P., Zarembek, K. A., Malech, H. L., Holland, S. M., and Gallin, J. I. (2010) Residual NADPH oxidase and survival in chronic granulomatous disease, *N Engl J Med* 363, 2600-2610.
9. Go, Y. M., and Jones, D. P. (2010) Redox control systems in the nucleus: mechanisms and functions, *Antioxid Redox Signal* 13, 489-509.
10. Ray, P. D., Huang, B. W., and Tsuji, Y. (2012) Reactive oxygen species (ROS) homeostasis and redox regulation in cellular signaling, *Cell Signal* 24, 981-990.
11. Jones, D. P., and Sies, H. (2015) The Redox Code, *Antioxid Redox Signal*.
12. Sies, H. (1985) 1 - Oxidative Stress: Introductory Remarks, In *Oxidative Stress* (Sies, H., Ed.), pp 1-8, Academic Press, London.
13. Magesh, S., Chen, Y., and Hu, L. (2012) Small molecule modulators of Keap1-Nrf2-ARE pathway as potential preventive and therapeutic agents, *Med Res Rev* 32, 687-726.
14. Dinkova-Kostova, A. T., and Talalay, P. (2008) Direct and indirect antioxidant properties of inducers of cytoprotective proteins, *Mol Nutr Food Res* 52 Suppl 1, S128-138.
15. Ulbricht, C. (2012) An Evidence-Based Systematic Review of Acai (*Euterpe oleracea*) by the Natural Standard Research Collaboration, *Journal of Dietary Supplements* 9, 128-147.
16. Guengerich, F. P., Kim, D. H., and Iwasaki, M. (1991) Role of human cytochrome P-450 IIE1 in the oxidation of many low molecular weight cancer suspects, *Chem Res Toxicol* 4, 168-179.
17. Chowdhury, G., Calcutt, M. W., and Guengerich, F. P. (2010) Oxidation of N-Nitrosoalkylamines by human cytochrome P450 2A6: sequential oxidation to aldehydes and carboxylic acids and analysis of reaction steps, *J Biol Chem* 285, 8031-8044.
18. Liu, Y., and Glatt, H. (2008) Mutagenicity of N-nitrosodiethanolamine in a V79-derived cell line expressing two human biotransformation enzymes, *Mutat Res* 643, 64-69.

19. Castillo, T., Koop, D. R., Kamimura, S., Triadafilopoulos, G., and Tsukamoto, H. (1992) Role of cytochrome P-450 2E1 in ethanol-, carbon tetrachloride- and iron-dependent microsomal lipid peroxidation, *Hepatology* 16, 992-996.
20. Tung, Y. T., Wu, J. H., Huang, C. C., Peng, H. C., Chen, Y. L., Yang, S. C., and Chang, S. T. (2009) Protective effect of Acacia confusa bark extract and its active compound gallic acid against carbon tetrachloride-induced chronic liver injury in rats, *Food Chem Toxicol* 47, 1385-1392.
21. Karamanakos, P. N., Trafalis, D. T., Geromichalos, G. D., Pappas, P., Harkitis, P., Konstandi, M., and Marselos, M. (2009) Inhibition of rat hepatic CYP2E1 by quinacrine: molecular modeling investigation and effects on 4-(methyl nitrosamino)-1-(3-pyridyl)-1-butanone (NNK)-induced mutagenicity, *Arch Toxicol* 83, 571-580.
22. von Weymarn, L. B., Chun, J. A., and Hollenberg, P. F. (2006) Effects of benzyl and phenethyl isothiocyanate on P450s 2A6 and 2A13: potential for chemoprevention in smokers, *Carcinogenesis* 27, 782-790.
23. Yano, J. K., Denton, T. T., Cerny, M. A., Zhang, X., Johnson, E. F., and Cashman, J. R. (2006) Synthetic inhibitors of cytochrome P-450 2A6: inhibitory activity, difference spectra, mechanism of inhibition, and protein cocrystallization, *J Med Chem* 49, 6987-7001.
24. Porubsky, P. R., Meneely, K. M., and Scott, E. E. (2008) Structures of human cytochrome P-450 2E1. Insights into the binding of inhibitors and both small molecular weight and fatty acid substrates, *J Biol Chem* 283, 33698-33707.
25. Wang, M. H., Wade, D., Chen, L., White, S., and Yang, C. S. (1995) Probing the active sites of rat and human cytochrome P450 2E1 with alcohols and carboxylic acids, *Arch Biochem Biophys* 317, 299-304.
26. Anzenbacherova, E., Hudecek, J., Murgida, D., Hildebrandt, P., Marchal, S., Lange, R., and Anzenbacher, P. (2005) Active sites of two orthologous cytochromes P450 2E1: differences revealed by spectroscopic methods, *Biochem Biophys Res Commun* 338, 477-482.
27. Porubsky, P. R., Battaile, K. P., and Scott, E. E. (2010) Human cytochrome P450 2E1 structures with fatty acid analogs reveal a previously unobserved binding mode, *J Biol Chem* 285, 22282-22290.
28. DeVore, N. M., Meneely, K. M., Bart, A. G., Stephens, E. S., Battaile, K. P., and Scott, E. E. (2012) Structural comparison of cytochromes P450 2A6, 2A13, and 2E1 with pilocarpine, *FEBS J* 279, 1621-1631.
29. Skopalík, J., Anzenbacher, P., and Otyepka, M. (2008) Flexibility of human cytochromes P450: molecular dynamics reveals differences between CYPs 3A4, 2C9, and 2A6, which correlate with their substrate preferences, *J Phys Chem B* 112, 8165-8173.
30. Hendrychova, T., Berka, K., Navratilova, V., Anzenbacher, P., and Otyepka, M. (2012) Dynamics and hydration of the active sites of mammalian cytochromes P450 probed by molecular dynamics simulations, *Curr Drug Metab* 13, 177-189.
31. Ping, J., Wang, Y. J., Wang, J. F., Li, X., Li, Y. X., and Hao, P. (2012) Negatively cooperative binding properties of human cytochrome P450 2E1 with monocyclic substrates, *Curr Drug Metab* 13, 1024-1031.

32. Li, J., Wei, D. Q., Wang, J. F., and Li, Y. X. (2011) A negative cooperativity mechanism of human CYP2E1 inferred from molecular dynamics simulations and free energy calculations, *J Chem Inf Model* 51, 3217-3225.
33. Raner, G. M., Chiang, E. W., Vaz, A. D., and Coon, M. J. (1997) Mechanism-based inactivation of cytochrome P450 2B4 by aldehydes: relationship to aldehyde deformylation via a peroxyhemiacetal intermediate, *Biochemistry* 36, 4895-4902.
34. Yang, S. P., Medling, T., and Raner, G. M. (2003) Cytochrome P450 expression and activities in rat, rabbit and bovine tongue, *Comp Biochem Physiol C Toxicol Pharmacol* 136, 297-308.
35. Waxman, D. J., and Chang, T. K. (2006) Spectrofluorometric analysis of CYP2A6-catalyzed coumarin 7-hydroxylation, *Methods Mol Biol* 320, 91-96.
36. Ortiz de Montellano, P. R., Beilan, H. S., Kunze, K. L., and Mico, B. A. (1981) Destruction of cytochrome P-450 by ethylene. Structure of the resulting prosthetic heme adduct, *J Biol Chem* 256, 4395-4399.
37. Ortiz de Montellano, P. R., Beilan, H. S., and Kunze, K. L. (1981) N-Alkylprotoporphyrin IX formation in 3,5-dicarbethoxy-1,4-dihydrocollidine-treated rats. Transfer of the alkyl group from the substrate to the porphyrin, *J Biol Chem* 256, 6708-6713.
38. Ortiz de Montellano, P. R., Beilan, H. S., and Kunze, K. L. (1981) N-Methylprotoporphyrin IX: chemical synthesis and identification as the green pigment produced by 3,5-diethoxycarbonyl-1,4-dihydrocollidine treatment, *Proc Natl Acad Sci U S A* 78, 1490-1494.
39. Kuo, C. L., Raner, G. M., Vaz, A. D., and Coon, M. J. (1999) Discrete species of activated oxygen yield different cytochrome P450 heme adducts from aldehydes, *Biochemistry* 38, 10511-10518.
40. Vaz, A. D., Pernecky, S. J., Raner, G. M., and Coon, M. J. (1996) Peroxo-iron and oxenoid-iron species as alternative oxygenating agents in cytochrome P450-catalyzed reactions: switching by threonine-302 to alanine mutagenesis of cytochrome P450 2B4, *Proc Natl Acad Sci U S A* 93, 4644-4648.
41. Xu, Y., Shen, Z., Shen, J., Liu, G., Li, W., and Tang, Y. (2011) Computational insights into the different catalytic activities of CYP2A13 and CYP2A6 on NNK, *J Mol Graph Model* 30, 1-9.
42. Yano, J. K., Hsu, M. H., Griffin, K. J., Stout, C. D., and Johnson, E. F. (2005) Structures of human microsomal cytochrome P450 2A6 complexed with coumarin and methoxsalen, *Nat Struct Mol Biol* 12, 822-823.
43. Rendic, S. (2002) Summary of information on human CYP enzymes: human P450 metabolism data, *Drug Metab Rev* 34, 83-448.
44. Ingelman-Sundberg, M. (2004) Human drug metabolising cytochrome P450 enzymes: properties and polymorphisms, *Naunyn Schmiedebergs Arch Pharmacol* 369, 89-104.
45. Nebert, D. W., and Russell, D. W. (2002) Clinical importance of the cytochromes P450, *Lancet* 360, 1155-1162.
46. Williams, J. A., Hyland, R., Jones, B. C., Smith, D. A., Hurst, S., Goosen, T. C., Peterkin, V., Koup, J. R., and Ball, S. E. (2004) Drug-drug interactions for UDP-glucuronosyltransferase substrates: a pharmacokinetic explanation for typically observed low exposure (AUCi/AUC) ratios, *Drug Metab Dispos* 32, 1201-1208.

47. Zanger, U. M., and Schwab, M. (2013) Cytochrome P450 enzymes in drug metabolism: regulation of gene expression, enzyme activities, and impact of genetic variation, *Pharmacol Ther* 138, 103-141.
48. Omura, T., and Sato, R. (1964) The Carbon Monoxide-binding Pigment of Liver Microsomes. II. Solubilization, Purification, and Properties., *J Biol Chem* 239, 2379-2385.
49. Zangar, R. C., Davydov, D. R., and Verma, S. (2004) Mechanisms that regulate production of reactive oxygen species by cytochrome P450, *Toxicol Appl Pharmacol* 199, 316-331.
50. Guengerich, F. P. (2003) Cytochrome P450 oxidations in the generation of reactive electrophiles: epoxidation and related reactions, *Arch Biochem Biophys* 409, 59-71.
51. Ioannides, C., and Lewis, D. F. (2004) Cytochromes P450 in the bioactivation of chemicals, *Curr Top Med Chem* 4, 1767-1788.
52. Rendic, S., and Guengerich, F. P. (2012) Contributions of human enzymes in carcinogen metabolism, *Chem Res Toxicol* 25, 1316-1383.
53. Kushida, H., Fujita, K.-i., Suzuki, A., Yamada, M., Endo, T., Nohmi, T., and Kamataki, T. (2000) Metabolic activation of N-alkylnitrosamines in genetically engineered Salmonella typhimurium expressing CYP2E1 or CYP2A6 together with human NADPH-cytochrome P450 reductase, *Carcinogenesis* 21, 1227-1232.
54. Liu, C., Zhuo, X., Gonzalez, F. J., and Ding, X. (1996) Baculovirus-mediated expression and characterization of rat CYP2A3 and human CYP2a6: role in metabolic activation of nasal toxicants, *Molecular Pharmacology* 50, 781-788.
55. Aoyama, T., Yamano, S., Guzelian, P. S., Gelboin, H. V., and Gonzalez, F. J. (1990) Five of 12 forms of vaccinia virus-expressed human hepatic cytochrome P450 metabolically activate aflatoxin B1, *Proceedings of the National Academy of Sciences* 87, 4790-4793.
56. Davydov, D. R., Petushkova, N. A., Bobrovnikova, E. V., Knyushko, T. V., and Dansette, P. (2001) Association of cytochromes P450 1A2 and 2B4: are the interactions between different P450 species involved in the control of the monooxygenase activity and coupling?, *Adv Exp Med Biol* 500, 335-338.
57. Lee, S. S., Buters, J. T., Pineau, T., Fernandez-Salguero, P., and Gonzalez, F. J. (1996) Role of CYP2E1 in the hepatotoxicity of acetaminophen, *J Biol Chem* 271, 12063-12067.
58. Spracklin, D. K., Hankins, D. C., Fisher, J. M., Thummel, K. E., and Kharasch, E. D. (1997) Cytochrome P450 2E1 is the principal catalyst of human oxidative halothane metabolism in vitro, *J Pharmacol Exp Ther* 281, 400-411.
59. Zimmerman, H. J., and Maddrey, W. C. (1995) Acetaminophen (paracetamol) hepatotoxicity with regular intake of alcohol: analysis of instances of therapeutic misadventure, *Hepatology* 22, 767-773.
60. Sohn, O. S., Fiala, E. S., Requeijo, S. P., Weisburger, J. H., and Gonzalez, F. J. (2001) Differential effects of CYP2E1 status on the metabolic activation of the colon carcinogens azoxymethane and methylazoxymethanol, *Cancer Res* 61, 8435-8440.
61. Wang, H., Chanas, B., and Ghanayem, B. I. (2002) Cytochrome P450 2E1 (CYP2E1) is Essential for Acrylonitrile Metabolism to Cyanide: Comparative Studies Using CYP2E1-Null and Wild-Type Mice, *Drug Metabolism and Disposition* 30, 911-917.
62. Matsumoto, H., Matsubayashi, K., and Fukui, Y. (1996) Evidence that cytochrome P-4502E1 contributes to ethanol elimination at low doses: effects of diallyl sulfide and 4-methyl pyrazole on ethanol elimination in the perfused rat liver, *Alcohol Clin Exp Res* 20, 12A-16A.

63. Sumioka, I., Matsura, T., and Yamada, K. (2001) Therapeutic effect of S-allylmercaptocysteine on acetaminophen-induced liver injury in mice, *Eur J Pharmacol* 433, 177-185.
64. Shimada, M., Liu, L., Nussler, N., Jonas, S., Langrehr, J. M., Ogawa, T., Kaminishi, M., Neuhaus, P., and Nussler, A. K. (2006) Human hepatocytes are protected from ethanol-induced cytotoxicity by DADS via CYP2E1 inhibition, *Toxicol Lett* 163, 242-249.
65. Morris, C. R., Chen, S. C., Zhou, L., Schopfer, L. M., Ding, X., and Mirvish, S. S. (2004) Inhibition by allyl sulfides and phenethyl isothiocyanate of methyl-n-pentyl nitrosamine depropylation by rat esophageal microsomes, human and rat CYP2E1, and Rat CYP2A3, *Nutr Cancer* 48, 54-63.
66. Gui, H. Y., Chen, R. N., Peng, Y., Hu, J. H., Mao, Z., Ning, R., Shang, W., Liu, W., Xiong, J., Hu, G., and Yang, J. (2013) Curcumin Protects against 1-Methyl-4-phenylpyridinium Ion- and Lipopolysaccharide-Induced Cytotoxicities in the Mouse Mesencephalic Astrocyte via Inhibiting the Cytochrome P450 2E1, *Evid Based Complement Alternat Med* 2013, 523484.
67. Xu, Y., Leo, M. A., and Lieber, C. S. (2003) Lycopene attenuates arachidonic acid toxicity in HepG2 cells overexpressing CYP2E1, *Biochem Biophys Res Commun* 303, 745-750.
68. Tang, J. C., Yang, H., Song, X. Y., Song, X. H., Yan, S. L., Shao, J. Q., Zhang, T. L., and Zhang, J. N. (2009) Inhibition of cytochrome P450 enzymes by rhein in rat liver microsomes, *Phytother Res* 23, 159-164.
69. Langhammer, A. J., and Nilsen, O. G. (2014) Fennel and raspberry leaf as possible inhibitors of acetaminophen oxidation, *Phytother Res* 28, 1573-1576.
70. Rodrigues, R. B., Lichtenthäler, R., Zimmermann, B. F., Papagiannopoulos, M., Fabricius, H., Marx, F., Maia, J. G. S., and Almeida, O. (2006) Total oxidant scavenging capacity of Euterpe oleracea Mart. (açai) seeds and identification of their polyphenolic compounds, *Journal of Agricultural and Food Chemistry* 54, 4162-4167.
71. Schauss, A. G., Wu, X., Prior, R. L., Ou, B., Huang, D., Owens, J., Agarwal, A., Jensen, G. S., Hart, A. N., and Shanbrom, E. (2006) Antioxidant Capacity and Other Bioactivities of the Freeze-Dried Amazonian Palm Berry, Euterpe oleracea Mart. (Acai), *Journal of Agricultural and Food Chemistry* 54, 8604-8610.
72. Del Pozo-Insfran, D., Percival, S. S., and Talcott, S. T. (2006) Açai (Euterpe oleracea Mart.) Polyphenolics in Their Glycoside and Aglycone Forms Induce Apoptosis of HL-60 Leukemia Cells, *Journal of Agricultural and Food Chemistry* 54, 1222-1229.
73. Jensen, G. S., Wu, X., Patterson, K. M., Barnes, J., Carter, S. G., Scherwitz, L., Beaman, R., Endres, J. R., and Schauss, A. G. (2008) In vitro and in vivo antioxidant and anti-inflammatory capacities of an antioxidant-rich fruit and berry juice blend. Results of a pilot and randomized, double-blinded, placebo-controlled, crossover study, *J Agric Food Chem* 56, 8326-8333.
74. Dresser, G. K., Spence, J. D., and Bailey, D. G. (2000) Pharmacokinetic-pharmacodynamic consequences and clinical relevance of cytochrome P450 3A4 inhibition, *Clin Pharmacokinet* 38, 41-57.
75. Surh, Y. J., Kundu, J. K., and Na, H. K. (2008) Nrf2 as a master redox switch in turning on the cellular signaling involved in the induction of cytoprotective genes by some chemopreventive phytochemicals, *Planta Med* 74, 1526-1539.

76. Rushmore, T. H., Morton, M. R., and Pickett, C. B. (1991) The antioxidant responsive element. Activation by oxidative stress and identification of the DNA consensus sequence required for functional activity, *Journal of Biological Chemistry* 266, 11632-11639.
77. Friling, R. S., Bensimon, A., Tichauer, Y., and Daniel, V. (1990) Xenobiotic-inducible expression of murine glutathione S-transferase Ya subunit gene is controlled by an electrophile-responsive element, *Proceedings of the National Academy of Sciences* 87, 6258-6262.
78. Wasserman, W. W., and Fahl, W. E. (1997) Functional antioxidant responsive elements, *Proceedings of the National Academy of Sciences* 94, 5361-5366.
79. Itoh, K., Chiba, T., Takahashi, S., Ishii, T., Igarashi, K., Katoh, Y., Oyake, T., Hayashi, N., Satoh, K., Hatayama, I., Yamamoto, M., and Nabeshima, Y.-i. (1997) An Nrf2/Small Maf Heterodimer Mediates the Induction of Phase II Detoxifying Enzyme Genes through Antioxidant Response Elements, *Biochemical and Biophysical Research Communications* 236, 313-322.
80. Itoh, K., Wakabayashi, N., Katoh, Y., Ishii, T., Igarashi, K., Engel, J. D., and Yamamoto, M. (1999) Keap1 represses nuclear activation of antioxidant responsive elements by Nrf2 through binding to the amino-terminal Neh2 domain, *Genes Dev* 13, 76-86.
81. Kobayashi, A., Kang, M. I., Okawa, H., Ohtsuji, M., Zenke, Y., Chiba, T., Igarashi, K., and Yamamoto, M. (2004) Oxidative stress sensor Keap1 functions as an adaptor for Cul3-based E3 ligase to regulate proteasomal degradation of Nrf2, *Mol Cell Biol* 24, 7130-7139.
82. Del Pozo-Insfran, D., Brenes, C. H., and Talcott, S. T. (2004) Phytochemical Composition and Pigment Stability of Açai (*Euterpe oleracea* Mart.), *Journal of Agricultural and Food Chemistry* 52, 1539-1545.
83. Kang, J., Xie, C., Li, Z., Nagarajan, S., Schauss, A. G., Wu, T., and Wu, X. (2011) Flavonoids from acai (*Euterpe oleracea* Mart.) pulp and their antioxidant and anti-inflammatory activities, *Food Chemistry* 128, 152-157.
84. Guerra, J. F. d. C., Magalhães, C., Lopes de, B., Costa, D. C., Silva, M. E., Pedrosa, M. L., and cia. (2011) Dietary açai modulates ROS production by neutrophils and gene expression of liver antioxidant enzymes in rats, *Journal of Clinical Biochemistry and Nutrition* 49, 188-194.
85. Oliveira de Souza, M., Silva, M., Silva, M. E., de Paula Oliveira, R., and Pedrosa, M. L. (2010) Diet supplementation with acai (*Euterpe oleracea* Mart.) pulp improves biomarkers of oxidative stress and the serum lipid profile in rats, *Nutrition* 26, 804-810.
86. Mertens-Talcott, S. U., Rios, J., Jilma-Stohlawetz, P., Pacheco-Palencia, L. A., Meibohm, B., Talcott, S. T., and Derendorf, H. (2008) Pharmacokinetics of anthocyanins and antioxidant effects after the consumption of anthocyanin-rich acai juice and pulp (*Euterpe oleracea* Mart.) in human healthy volunteers, *J Agric Food Chem* 56, 7796-7802.
87. de Moura, R. S., Ferreira, T. S., Lopes, A. A., Pires, K. M. P., Nesi, R. T., Resende, A. C., Souza, P. J. C., da Silva, A. J. R., Borges, R. M., Porto, L. C., and Valença, S. S. (2012) Effects of *Euterpe oleracea* Mart. (AÇAÍ) extract in acute lung inflammation induced by cigarette smoke in the mouse, *Phytomedicine* 19, 262-269.

88. de Moura, R. S., Pires, K. M. P., Ferreira, T. S., Lopes, A. A., Nesi, R. T., Resende, A. C., Sousa, P. J. C., da Silva, A. J. R., Porto, L. C., and Valenca, S. S. (2011) Addition of açai (*Euterpe oleracea*) to cigarettes has a protective effect against emphysema in mice, *Food and Chemical Toxicology* 49, 855-863.
89. Hwang, Y. P., Choi, J. H., Yun, H. J., Han, E. H., Kim, H. G., Kim, J. Y., Park, B. H., Khanal, T., Choi, J. M., Chung, Y. C., and Jeong, H. G. (2011) Anthocyanins from purple sweet potato attenuate dimethylnitrosamine-induced liver injury in rats by inducing Nrf2-mediated antioxidant enzymes and reducing COX-2 and iNOS expression, *Food and Chemical Toxicology* 49, 93-99.
90. Lee, S. E., Jeong, S. I., Yang, H., Park, C.-S., Jin, Y.-H., and Park, Y. S. (2011) Fisetin induces Nrf2-mediated HO-1 expression through PKC- δ and p38 in human umbilical vein endothelial cells, *Journal of Cellular Biochemistry* 112, 2352-2360.
91. Xie, C., Kang, J., Burris, R., Ferguson, M. E., Schauss, A. G., Nagarajan, S., and Wu, X. (2011) Açai juice attenuates atherosclerosis in ApoE deficient mice through antioxidant and anti-inflammatory activities, *Atherosclerosis* 216, 327-333.
92. Jensen, G. S., Ager, D. M., Redman, K. A., Mitzner, M. A., Benson, K. F., and Schauss, A. G. (2011) Pain reduction and improvement in range of motion after daily consumption of an açai (*Euterpe oleracea* Mart.) pulp-fortified polyphenolic-rich fruit and berry juice blend, *J Med Food* 14, 702-711.
93. Stoner, G. D., Wang, L. S., Seguin, C., Rocha, C., Stoner, K., Chiu, S., and Kinghorn, A. D. (2010) Multiple berry types prevent N-nitrosomethylbenzylamine-induced esophageal cancer in rats, *Pharm Res* 27, 1138-1145.
94. Shih, P.-H., Yeh, C.-T., and Yen, G.-C. (2007) Anthocyanins Induce the Activation of Phase II Enzymes through the Antioxidant Response Element Pathway against Oxidative Stress-Induced Apoptosis, *Journal of Agricultural and Food Chemistry* 55, 9427-9435.
95. Jubert, C., and Bailey, G. (2007) Isolation of chlorophylls a and b from spinach by counter-current chromatography, *J Chromatogr A* 1140, 95-100.
96. Cho, M., Lee, H. S., Kang, I. J., Won, M H., and You, S. (2011) Antioxidant properties of extract and fractions from *Enteromorpha prolifera*, a type of green seaweed, *Food Chem* 127, 999-1006.
97. Hagiya, Y., Adachi, T., Ogura, S., An, R., Tamura, A., Nakagawa, H., Okura, I., Mochizuki, T., and Ishikawa, T. (2008) Nrf2-dependent induction of human ABC transporter ABCG2 and heme oxygenase-1 in HepG2 cells by photoactivation of porphyrins: biochemical implications for cancer cell response to photodynamic therapy, *J Exp Ther Oncol* 7, 153-167.
98. Choi, B. H., Ryoo, I. G., Kang, H. C., and Kwak, M. K. (2014) The sensitivity of cancer cells to pheophorbide a-based photodynamic therapy is enhanced by Nrf2 silencing, *PLoS One* 9, e107158.
99. Bui-Xuan, N. H., Tang, P. M., Wong, C. K., Chan, J. Y., Cheung, K. K., Jiang, J. L., and Fung, K. P. (2011) Pheophorbide a: a photosensitizer with immunostimulating activities on mouse macrophage RAW 264.7 cells in the absence of irradiation, *Cell Immunol* 269, 60-67.
100. Lai, C. S., Mas, R. H., Nair, N. K., Mansor, S. M., and Navaratnam, V. (2010) Chemical constituents and in vitro anticancer activity of *Typhonium flagelliforme* (Araceae), *J Ethnopharmacol* 127, 486-494.

101. Chan, J. Y., Tang, P. M., Hon, P. M., Au, S. W., Tsui, S. K., Waye, M. M., Kong, S. K., Mak, T. C., and Fung, K. P. (2006) Pheophorbide a, a major antitumor component purified from *Scutellaria barbata*, induces apoptosis in human hepatocellular carcinoma cells, *Planta Med* 72, 28-33.
102. Rapozzi, V., Zacchigna, M., Biffi, S., Garrovo, C., Cateni, F., Stebel, M., Zorzet, S., Bonora, G. M., Drioli, S., and Xodo, L. E. (2010) Conjugated PDT drug: photosensitizing activity and tissue distribution of PEGylated pheophorbide a, *Cancer Biol Ther* 10, 471-482.
103. Nam, M. H. (2014) In vivo study of the renal protective effects of *Capsosiphon fulvescens* against streptozotocin-induced oxidative stress, *Korean Journal of Food Science and Technology* 46, 641-647.